UNIVERSITY OF TRENTO

Doctoral School in Civil, Environmental and Mechanical Engineering

Curriculum 1. Civil and Environmental Engineering

Serena Petrini

Insight into microalgal-bacterial consortia for sustainable wastewater treatment

Investigations at lab-scale with real wastewater

2020 - Doctoral thesis

UNIVERSITY OF TRENTO - Italy
Department of Civil, Environmental
and Mechanical Engineering

Doctoral School in Civil, Environmental and Mechanical Engineering
Topic 1. Civil and Environmental Engineering - XXXII cycle 2016/2019

Doctoral Thesis - May 2020

Serena Petrini

Insight into microalgal-bacterial consortia for sustainable wastewater treatment

Investigations at lab-scale with real wastewater

Supervisors
Prof. Dr. Eng. Paola Foladori - University of Trento
Prof. Dr. Eng. Gianni Andreottola - University of Trento

University of Trento
Doctoral School in Civil, Environmental and Mechanical Engineering
http://web.unitn.it/en/dricam
Via Mesiano 77, I-38123 Trento
Tel. +39 0461 282670 / 2611 - *dicamphd@unitn.it*

To my family

ABSTRACT

High costs for aeration, greenhouse-gas emissions and excess sludge disposal have entailed a paradigm shift in the wastewater treatment.
Microalgal-bacterial-based wastewater treatments have gained increasing attention because of their potential in energy demand reduction and biomass resource recovery. In particular, photosynthetic oxygenation is combined with bacterial activity to treat wastewater avoiding external artificial aeration.
To optimize the technology in order to become more competitive than activated sludge, an in-depth investigation about the treatment performance and the microbiology interactions under real operational condition is needed.
This work focused on the study of wastewater-borne microalgal-bacterial consortia treating real municipal wastewater. The main objectives were to: (i) Understand the removal mechanisms and the influence of operational conditions to optimize the process; (ii) Analyze the microbial community.
At first, a photo-sequencing batch reactor (PSBR), called Pilot, was started up and continuously monitored for two years to analyze the evolution of the treatment performance and of the biomass composition. At the same time, other two lab-scale PSBRs were installed to evaluate if microalgal inoculation is essential to start up a consortium. Samples of these consortia were collected over a period of one year and analyzed through microscopic observations, flow cytometry and metagenomics, to investigate the microbial structure and diversity.
A second part of the research focused on the optimization of the Pilot to explore its limit in view of the scale-up of the system. In addition, respirometry was adapted to test microalgal-bacterial consortia to estimate the removal kinetic parameters for future modelling.
To conclude, the research project addressed many aspects and lay the foundation to apply a methodological research approach to scale-up this promising technology.

THESIS STRUCTURE

The thesis is structured in 14 chapters. A general introduction on the background of the research is presented in Chapter 1. Chapter 2 provides a brief overview on the state of the art and the research objectives. Chapters from 3 to 13 cover the experimental part of the thesis and are presented as scientific papers, in part published in peer-reviewed scientific journals. For each of these chapters, a preface is included to help link the chapters together according to the research objectives. At the end, Chapter 14 summarizes the main results and future perspectives are discussed.

Where the Chapters refer to published papers insert in the thesis, the references have been changed with the corresponding Chapter.

The term “microalgae” is used as broad term including both eukaryotic microalgae and cyanobacteria. Likewise, the term “bacteria” refers to non-photosynthetic prokaryotic microorganisms, unless stated otherwise.

TABLE OF CONTENTS

CHAPTER 1

GENERAL INTRODUCTION

This Chapter is a general introduction on the background of the research. The evolution of the scientific research in the field of microalgal-based wastewater treatment is briefly described.

1.1 A new paradigm in wastewater treatment

Anthropogenic activity produces large amounts of wastewater rich in nutrients that can cause eutrophication if directly discharged in the environment. At the same time, the increasing population that demand more water, and climate change are moving the planet towards a water crisis; therefore, treatment and reuse of wastewater is becoming imperative. In addition, due to the depletion of natural resources, it has emerged the importance to recover nutrients.

Following the concept of circular economy, there is a need to change the point of view. Waste is no longer something to dispose of, but a resource. Therefore, it arises the necessity to transform wastewater treatment plants (WWTPs) to water resource recovery facilities (WRRFs). Moreover, in the era of climate change, the concept of sustainable development results in a push to rethink the wastewater treatment as an effective treatment with low energy consumption, low carbon production and resource recycling.

To date, activated sludge (AS) process is the most widespread biological treatment method for wastewater. However AS-based technologies are characterized by high energy consumption with related greenhouse gases emission, and excess sludge disposal.

In the last decades, scientific research has been stimulated to develop more sustainable alternatives in order to overcome the drawbacks of AS-based technology. The ideal treatment provides high quality effluents, maximize nutrient recovery and energy production, and at the same time it is economically to operate (low energy consumption) and sustainable (minimum CO_2 footprint).

A promising solution to this challenge is represented by the combination of microalgae and bacteria. The potentiality of this alternative relies on (free) photosynthetic oxygenation to replace mechanical aeration together with carbon dioxide sequestration through photosynthesis. The sustainability of the process derives also from the possibility of energy valorization via anaerobic digestion and nutrient recovery via biomass (Posadas et al., 2017).

1.2 From microalgal cultivation to wastewater treatment

Microalgae are photosynthetic unicellular organisms by definition microscopic (with the size in the order of micrometers). They primarily exploit light energy and inorganic carbon (CO_2) for their metabolism, producing at the same time O_2. Chlorophyll *a* is the photosynthetic pigment present in all the species (Lee, 2008). They contribute to the production of almost 50% of the oxygen in the atmosphere (Andersen, 2005; Chapman, 2013).

Microalgae are a highly diversified group of eukaryotes (Barsanti and Gualtieri, 2014) that also contains cyanobacteria, which are oxygenic photosynthetic prokaryotes (i.e. bacteria). They commonly occur in water (freshwater or marine) but they can also be found in all types of soils (Richmond, 2004; Lee, 2008), where they exist individually or in groups.

The interest in microalgae as a source of food and biofuel date back to the 1950s. At that time, Oswald firstly described the possibilities to treat wastewater with microalgae (Oswald et al., 1953). However, the research on microalgae blooms in the late 1990s, when the problem of increasing energy consumption, fossil fuel depletion and climate change started to arise.

In the last years microalgae have been regarded as a possible substitute in the generation of biofuel alternative to fossil fuels. Thanks to their high content in lipids (20-40%) and carbohydrates (30-60%), microalgae can be used for biodiesel and bioethanol production, respectively (Gupta et al., 2019). Additionally, unlike fossil fuels, microalgae cultivation releases oxygen and fix CO_2 (Khan et al., 2018).

Microalgae are considered third generation biofuel, since are devoid of the major drawbacks of the first (terrestrial crops) and second (residues of lignocellulosic agriculture and forest, non-food crop feedstocks) generation biofuels: (i) competition with food market for land and water use and (ii) land use changes (deforestation) (Brennan and Owende, 2009). In addition, microalgae are characterized by higher productivity compared to terrestrial crops and need less

water since they grow in aqueous media (Brennan and Owende, 2009).

Following a biorefinery concept, to increase the economic feasibility, residual biomass could be further processed into valuable co-products (Chew et al., 2017). Microalgal biomass include different biomolecules (such as lipids, proteins, carbohydrates, pigments, vitamins and polyunsaturated fatty acids) that have potential applications in industrial products (de Jesús Martínez-Roldán and Ibarra-Berumen, 2019) as described in Table 1.1.

Sector	**Application/Compounds**	**Reference**
Human nutrition	Food additive; Food supplement (high-protein content)	Bernaerts et al., 2019
Pharmaceuticals	Antioxidant, anti-inflammatory, antitumor, anticancer, antimicrobial, antiviral and antiallergic	Deniz et al., 2017
Cosmetics	Thickening, water-binding and antioxidants agents	Ariede et al., 2017
Animal feed and aquaculture	Feed	Dineshbabu et al., 2019
Agriculture	Biofertilizer, plant growth promoter	Renuka et al., 2018
Energy production	Methane Hydrogen Ethanol	Brennan and Owende, 2009
Environment remediation	Wastewater treatment	Judd et al., 2015
	CO_2 mitigation	Gonçalves et al., 2017

Table 1.1 *Potential applications of microalgae and microalgal biomolecules.*

Despite microalgal potential as biofuel resource, the commercial viability presents many challenges. In particular, microalgal cultivation is still not economically competitive with fossil fuel production. The use of wastewater as growth medium enables to lower the cost of microalgal cultivation (Christenson and Sims, 2011). In this way it is possible to reduce the requirement of fresh-

water and the addition of nutrients (Gupta et al., 2019). Wastewaters have high amount of nitrogen and phosphorous that are essential biomass constituents (de Jesús Martínez-Roldán and Ibarra-Berumen, 2019). It is worth noting that microalgae cultivated with wastewater cannot be processed for human use (Molinuevo-Salces et al., 2019).

The utilization of wastewater as growth medium results not only in biomass production, but also in carbon dioxide mitigation and bioremediation (Cai et al., 2013). Therefore, researchers have been increasing their attention in the suitability of microalgae for wastewater treatment (Cai et al., 2013; Wang L. et al., 2016). In particular, municipal wastewater represents an excellent option for microalgal remediation, because the content of nitrogen and phosphorous is sufficient to sustain the growth and, at the same time, the concentration of other contaminants (especially heavy metals) does not reach inhibitory levels (de Jesús Martínez-Roldán and Ibarra-Berumen, 2019).

After the successful preliminary results in biodiesel production, part of the research started to focus on the possibility to treat wastewater (Posadas et al., 2017). Microalgae have proved to be effective in the treatment of different types of wastewater. At the beginning, microalgae were tested as tertiary treatment of wastewaters rich in nutrients, such as agro-based industries (Gupta et al., 2019), or as post-treatment after anaerobic units. Then, research has shown that microalgae can be applied also for secondary wastewater treatment, especially if combined with bacteria.
Microalgae alone are characterized by low settleability due to negatively charged surface and colloidal stability in suspension (Barros et al., 2015). The co-existence with bacteria results in spontaneous bio-flocculation. Therefore, it is easier and more sustainable to separate the biomass from the liquid phase.

As wastewater itself contains different microorganisms (especially bacteria), microalgal based wastewater treatment results in a consortium of different microbes (He et al., 2013; Saunders et al., 2016). Microalgae inevitably coexist with bacteria unless wastewater is sterilized or filtrated, but with huge costs (He et al., 2013).

If the presence of bacteria may be a problem under the point of view of microalgal cultivation (contamination), it represents a resource for wastewater treatment mainly thanks to the symbiotic relationship between microalgae and bacteria that is related to gas exchange. Microalgae in presence of light, produce oxygen that bacteria use for respiration and in the oxidation process of compounds, releasing at the same time CO_2 that is essential for microalgae to perform photosynthesis. In addition, the microorganisms variety is beneficial for the robustness of the treatment process (Muñoz and Guieysee, 2006). Since the consortia is characterized by different metabolic pathways it is more adaptable to operating condition (especially, environmental conditions and influent wastewater characteristics).

In conclusion, microalgal-bacterial consortia for wastewater treatment have received increasing attention in the recent years as a sustainable alternative to activated sludge process. The advantages are the avoidance of mechanical aeration (and thus energy savings), replaced by photosynthetic oxygenation, and the production of valuable biomass for energy recovery and valuable compound extraction. However, there are still some challenges to overcome before this promising technology can be implemented at real-scale.

CHAPTER 2

MICROALGAL-BACTERIAL CONSORTIA FOR WASTEWATER TREATMENT

In this Chapter, a brief overview on the state of art about microalgal-bacterial consortia for wastewater treatment is presented.
The chapter is not intended to provide a complete review on the topic: only the aspects related to the research work are presented. Each of the following Chapters, contains a more focused introduction on the topic addressed and a critical discussion of the results.
At the end, the research needs for the development of microalgal-bacterial systems are highlighted and the objectives of this research work are stated.

The most widespread biological treatment for wastewater is based on activated sludge (AS). Activated sludge is a consortium of heterotrophic and nitrifying bacteria that undergoes different working conditions (i.e. aerobic, anoxic, anaerobic), able to ensure satisfactory levels of pollutant removal. However, AS-based processes are characterized by high-energy consumption (largely associated to mechanical aeration to sustain bacterial activity; WRF and EPRI, 2013) and environmental impacts (high CO_2 footprint and excess sludge disposal) (Figure 2.1).
More stringent discharge regulations, increasing of process costs due to energy input and sludge disposal, coupled with environmental impacts, have pushed the scientific research to explore sustainable alternatives (Gonçalves et al. 2017). In a context of climate change and sustainable development, next generation processes should overcome the drawbacks of AS-based technology and, at the same time, providing an efficient and reliable treatment. This entails a paradigm shift in wastewater treatment.

A promising solution for a sustainable and low-cost wastewater treatment is represented by the combination of microalgae and bacteria.
If properly exploited, the presence of microalgae means: (i) cost-free oxygenation, (ii) CO_2 sequestration and (iii) production of valuable biomass (Figure 2.1). To enhance CO_2 sequestration, flue gas treatment can be combined with wastewater treatment. As far as the biomass produced is concerned, it can be transformed into biofuels, biofertilizer or to extract high-valuable compounds, such as pigments or vitamins (Ferreira et al., 2019). If compared to conventional wastewater treatment plants, microalgal-bacterial based treatment may significantly reduce oxygenation costs with respect to activated sludge and may enhance nutrient recovery with respect to anaerobic digestion of excess sludge (Muñoz and Guieysse, 2006).

Many different review papers have attempted to synthetize the knowledge and the research gap in microalgal-bacterial consortia applied to wastewater treatment. In this Chapter are introduce some basic concept to sustain the research work, referring to the main literature for more detailed discussions.

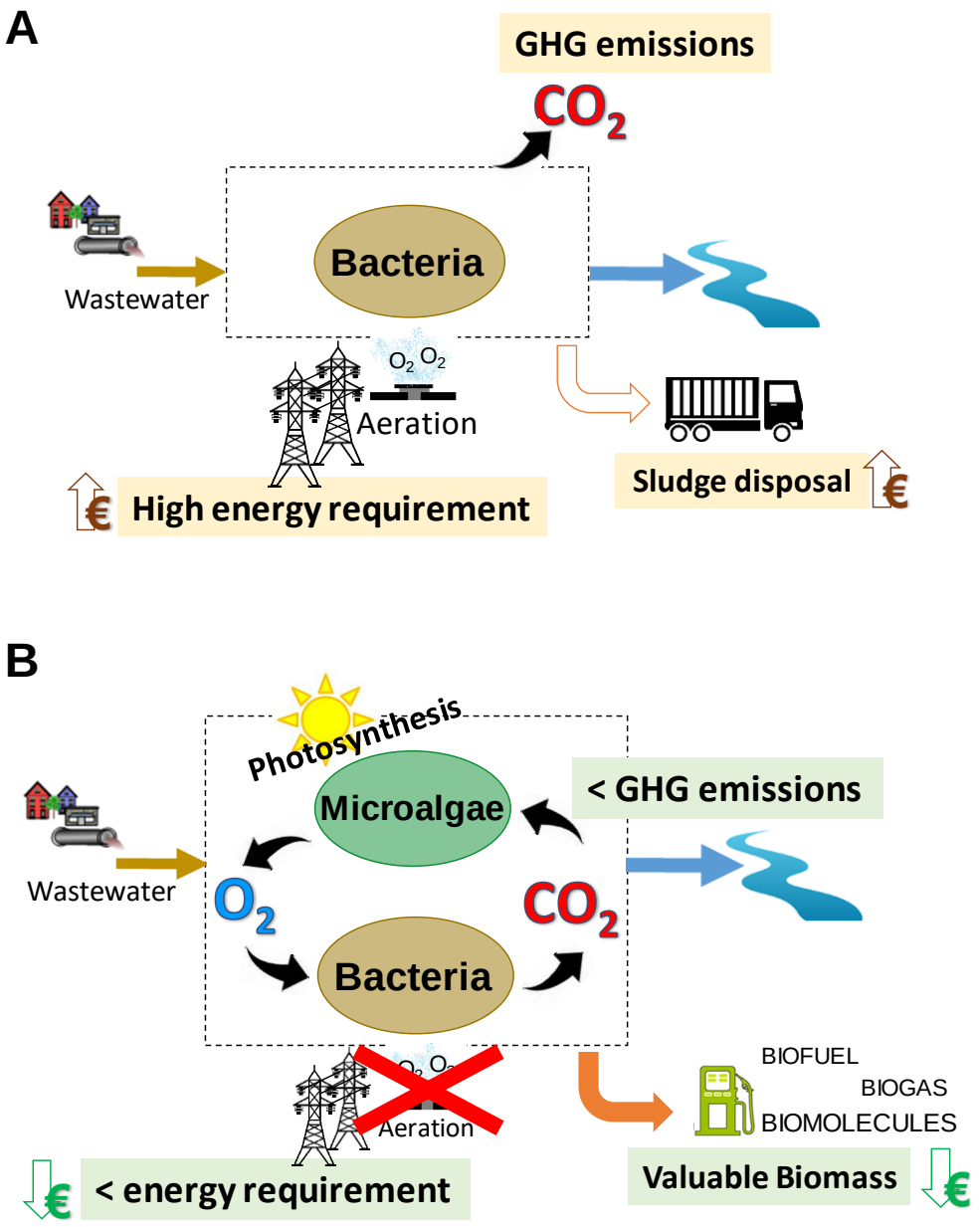

Figure 2.1 *Comparison between (A) Conventional wastewater treatment based on activated sludge, and (B) Microalgal-bacterial-based treatment*

2.1 Interactions between microalgae and bacteria

Spontaneous consortia of microalgae grow as biofilms on submerged surfaces (usually tank walls) of conventional wastewater treatment plants (Ferreira et al., 2019; references therein). However, their bloom is prevented by non-suitable conditions as for example turbidity and the presence of dense flocs of activated sludge (Albertano et al., 1999). These biofilms of microalgae are characterized by high diversity. In particular, cyanobacteria, diatoms, and green algae are the dominant groups (Ferreira et al., 2019). In the late 1990s, Craggs et al. (1996) started to firstly assess the potential of these native microalgal consortia.

Different selected microalgal species have been tested in the treatment of wastewater (Wang Y. et al., 2016; Li et al., 2019); in particular *Chlorella* and *Scenedesmus spp.* that have shown to be effective in the removal of nitrogen and phosphorous from different wastewater types (Cai et al., 2013). However, these species have been mostly tested using synthetic wastewater (Cuellar-Bermudez et al., 2017; Li et al., 2019), at a lab- and pilot-scale. *Chlorella* and *Scenedesmus spp.* naturally dominate algal-ponds (Muñoz and Guieysse, 2006), but these systems are not efficient and cannot compete against activated sludge as sustainable alternative and cost-effective solutions. Moreover, mixed strains can perform functions difficult for single species (Subashchandrabose et al., 2011). Native consortia of microalgae may spontaneously establish during wastewater treatment (Olguin et al., 2012). Therefore, systems with pure microalgae are difficult to maintain permanently (Xu et al., 2009; Cuellar-Bermudez et al., 2017) unless the influent wastewater is sterilized, but with huge costs (He et al., 2013).

Microalgae and bacteria naturally co-habit and interact in the environment (Subashchandrabose et al., 2011). Likewise, in wastewater treatment microalgae co-exist with other microorganisms (mainly bacteria) that enter the system through the influent wastewater (He et al., 2013; Saunders et al., 2016) and the air (Cuellar-Bermudez et al., 2017), or that are specifically inoculated (e.g. activated sludge). Anyway, microalgae and bacteria result in a complex consortium.

Their main symbiotic relationship is based on exchange of oxygen and

carbon dioxide. In the treatment of wastewater this means that in presence of light, microalgae through photosynthesis may produce the oxygen to sustain bacterial activity (i.e. oxidation of compounds and respiration) and at the same time bacteria release CO_2 that is essential for microalgae to perform photosynthesis. Therefore, the exploitation of this symbiotic relation results in a wastewater treatment that avoid artificial aeration, lowering energy consumption and greenhouse gas (GHG) emissions. In addition, photo-oxygenation limits the risks of pollutant volatilization unlike intensive mechanical aeration (Muñoz and Guieysse, 2006).
The first research group that tried to engineer microalgal-bacterial consortia was guided by Prof. William Oswald, who reported for the first time the symbiosis of microalgae and bacteria in the treatment of wastewater in oxidation ponds (Oswald et al.,1953).

Microalgal-bacterial interactions may result in mutualism, parasitism or commensalism, in both natural and biotechnological environments (Amin et al., 2012; Kouzuma and Watanabe, 2015; Ramanan et al., 2016). To date, the interactions between and within microalgae and bacteria during the wastewater treatment are not yet completely understood (Ramanan et al., 2016). Several authors have reported both cooperative (metabolites' exchange) and competitive interactions (Unnithan et al., 2014; Ramanan et al., 2016; Gonçalves et al. 2017; Lee and Lei, 2019). The main interactions known are presented in Table 2.1 (Gonçalves et al. 2019).

Understand the community relationships is crucial to achieve an efficient treatment of wastewater (Subashchandrabose et al., 2011). However, there is still a lack of knowledge about the microalgal-bacterial consortia that established in system treating wastewater; in particular about all the metabolic pathways available. Most studies have focused on the interactions between one or two species not considering the variety of the consortia that establish in wastewater treatment systems and the characteristics of the influent wastewater (Wang et al., 2018).

Microalgal-bacterial consortium presents similar bacterial composition

Interaction	Bacteria ⟶ Microalgae	Microalgae ⟶ Bacteria
Cooperative	Supply of CO_2	Supply of O_2
	Excretion of growth-promoting factors	Supply of organic matter
	Secretion of extracellular polymeric substances that can serve as a habitat	Secretion of extracellular polymeric substances that can serve as a habitat
Competitive	Excretion of substances with algacidal effect	Excretion of substances with bactericidal effect

Table 2.1 *Cooperative and competitive interactions occurring in microalgal-bacterial consortia (Partially adapted from Gonçalves et al. (2019).*

found in conventional activated sludge process (García et al. 2018). However, their metabolisms may differ from the one observed in activated sludge due to different design and operational conditions.

Wastewater composition and operational conditions affect the proportion of microalgae and bacteria and the composition of the consortium (i.e. the dominant species) (Posadas et al., 2017; Ferreira et al., 2019). Despite there are not direct quantification, scientists agree that bacteria predominate in the consortium (Posadas et al., 2017). In addition, changes in environmental conditions may shift the microbial community, affecting the stability of the system (Wang et al., 2018).

Finally, another advantage of the co-existence of microalgae and bacteria is bio-flocculation. Bio-flocculation is flocculation caused by secreted biopolymers (Christenson and Sims, 2011) and it spontaneously occurs quite often in microalgal-bacterial consortia (Molinuevo-Salces et al., 2019). As reported from many authors (Quijano et al., 2017 and references therein), microalgae and bacteria aggregate in flocs or granules resulting in a settleable system that does not require expensive and complex method of separation (such as filtration), reducing biomass recovery costs (Gonçalves et al. 2017).

Microalgal-bacterial flocs or granules settle quicker due to their large size

(Table 2.2) compared with microalgae and bacteria alone.

The success of bio-flocculation depends on the production of EPS (Extracellular polymeric substances) and on the ability of microorganisms to attach to them (Lee et al., 2010). Microalgae and bacteria both produce EPS, but they are indistinguishable from one another (Barros et al., 2015).

Microalgal-bacterial	Size	Reactor type	Reference
Flocs	50 μm-1 mm	SBR	Guitzeit et al., 2005
Flocs	150-300 μm	SBR	van Den Hende et al., 2011
Flocs	300-1000 μm	Raceway pond	van Den Hende et al., 2016
Flocs	200-600 μm	SBR	Chapter 10
Granules	600-2000 μm	SBR	Tiron et al., 2017

Table 2.2 *Size of microalgal-bacterial flocs and granules reported in literature. SBR: Sequencing Batch Reactor*

2.2 Pollutant removal

According to the working conditions, contaminants can be removed through biotic (e.g. biomass uptake, oxidation process, nitrification and denitrification) or abiotic process (e.g. ammonia volatilization and phosphorous precipitation), and one metabolism (microalgal or bacterial) could prevail over the others. However, to date the limiting factors of growth in microalgal-bacterial consortia are still unclear.

2.2.1 Carbon removal

Organic matter Bacteria are the main responsible of organic matter removal. However, microalgae that possess heterotrophic and mixotrophic metabolism, may contribute to the removal of biodegradable organic carbon (Cuellar-Bermudez et al., 2017). Anoxic condition that may occur in dark zone or during dark period, may allow denitrification in presence of nitrate and organic matter.
In the treatment of municipal wastewater, organic matter is not considered

a critical parameter. As shown in Table 2.3, high percentage of removal are usually reported in literature. However, when scaling up the process organic matter removal may decrease (Van den Hende et al., 2014).

Inorganic carbon In presence of light, microalgae use CO_2 as carbon source for growth via photosynthesis (autotrophic growth). At the same time, bacterial respiration and oxidation processes produce carbon dioxide.
At neutral pH, CO_2 is mostly present in the form of HCO_3^- (Figure 2.3), that is assimilated by microalgae and then internally transformed to CO_2 prior to utilization (Cai et al., 2013). At high values of pH (>10), CO_3^{2-} is mostly present (Figure 2.3) and since it is not biogenic, microalgae growth is limited (Solimeno and García, 2017).
CO_2 may also be introduced in the system (exhaust gases) to enhance microalgal growth and control pH (Posadas et al., 2015).

Compared to conventional activated sludge, CO_2 emissions are remarkably lower. In addition, a negative balance may occur if flue gas (rich in CO_2) is injected into the process (Molinuevo-Salces et al., 2019).

2.2.2 Nitrogen removal

Nitrogen is mainly present in wastewater in the form of ammonium. The possible removal mechanisms with microalgal-bacterial consortia are assimilation to form new biomass, nitrification-denitrification, and ammonia volatilization (with pH>9).
For what concern microalgae, ammonium is preferred for biomass production over other inorganic nitrogen forms, and only when it is completely consumed nitrate or nitrite consumption occurs (Cai et al., 2013; He et al., 2013).
According to the treatment condition, the main removal mechanism differs (Wang et al., 2018). Su et al. (2011) treating municipal wastewater reported that algal biomass assimilation was the main removal mechanism, accounting for more than 40% of total nitrogen removal, while nitrification represented only the 17-20%. On the contrary, Karya et al. (2013) treating synthetic wastewater,

showed that nitrification was the main nitrogen removal mechanism, accounting for 80% of total nitrogen removal.
When pH values higher than 9 are reached, ammonia volatilization take place and effectively influence nitrogen removal (Delgadillo-Mirquez et al., 2016). High pH is due to inorganic carbon consumption linked to photosynthetic activity, not counterbalanced by bacterial oxidation. However, pH could be controlled by bubbling CO_2. The simultaneous processes of nitrification and carbon dioxide consumption (photosynthesis) could maintain pH close to neutrality (González-Fernández et al., 2011).
Nitrifiers oxidize ammonium into nitrate. Nitrate could be denitrified in presence of organic matter and anoxic condition by anoxic heterotrophic (denitrifying) bacteria or could be assimilated by microalgae as nitrogen source for biomass production. Anoxic conditions may occur during dark periods, in dark zones of the reactor and inside flocs. Thanks to diffusional gradients between the outer and the inner of microalgal-bacterial aggregates, oxygen may not penetrate in the inner part of the flocs, therefore nitrification and denitrification may occur simultaneously.
When oxygen is supplied only through photosynthesis, low DO may occur in the system; as a result, heterotrophs compete with nitrifiers for oxygen and nitrification may be slow down, resulting in partial nitrification (nitrites accumulation). This phenome could be exploited to obtain a shortcut N removal. Wang et al. (2015) obtained over 80% of N removal through nitritation/denitrification. While Manser et al. (2016) combined the partial nitrification with Anammox instead of heterotrophic denitrification.

Biomass composition, operational conditions and reactors design affect the process. In particular inorganic carbon availability and dissolved oxygen concentration directly control the main nitrogen removal mechanism (Posadas et al., 2017).
The process should be driven towards the most convenient removal process, depending on the sludge final destination and the wastewater treatment goals (Karya et al., 2013). It is crucial to understand the working conditions to apply according to the nitrogen removal mechanism to be exploited.

Ref	Working volume	System	Wastewater	COD in	COD out	%COD	HRT (d)	external air/CO_2	light/ dark
Gutzeit et al.,2005	30 L	CSTR	municipal	471	51	88-93	1.5-2	NO	10/14
	600 L	CSTR			54	88-94	5-7	NO	10/14
Arcila et al., 2016	50 L	HRAP	municipal	593	562	12	2	NO	12/12
					53.6	92	6	NO	12/12
					65	91	10	NO	12/12
Su et al., 2011	14 L	PSBR	municipal	141.9	<3	98	8	NO	12/12

Table 2.3 *Organic matter removal, measured as Chemical Oxygen Demand (COD) removal, reported in different scientific papers studying microalgal-bacterial consortia to treat municipal wastewater. CSTR: completely stirred tank reactor; HRAP: High rate algal pond; PSBR: photo-sequencing batch reactor.*

Of particular concern when considering nitrogen removal pathways is the formation of N_2O, a potent greenhouse gas. However, since the mechanism of N_2O formation have not been yet elucidated, further research is needed (Wang et al., 2018).

2.2.3 Phosphorous removal

Biomass uptake and chemical precipitation are the main phosphorus removal mechanisms.
Chemical precipitation occurs in the presence of Ca^{2+} and Mg^{2+} when pH values higher than 9 are reached (Cai et al., 2013).
Microalgae are capable of luxury phosphorous uptake (Powell et al., 2008). Powell et al. (2008) determined that the key factors influencing luxury uptake are phosphate concentration, light intensity and temperature. Some microalgal species accumulate P in the form of polyphosphate up to 2-3% of their cell dry weight when P supply is high (in the order of 10 mg/L) (Powell et al., 2009). Phosphorus assimilation by microalgae could be a suitable removal mechanism but long HRTs are required to reach high removal efficiency.
To exploit enhanced biological phosphorus removal through polyphosphate-accumulating organisms (PAOs), there is the necessity to guarantee suitable conditions as alternation of anaerobic and aerobic conditions and availability of simple carbon compounds.

2.2.4 Heavy metal and micropollutant removal

Microalgal-bacterial consortia have proved to be effective in the treatment of industrial wastewater containing hazardous compounds (Wang Y. et al., 2016). In particular, microalgal-bacterial consortia could potentially remove compounds that are receiving increasing attention such as heavy metals (Muñoz et al., 2006) and pharmaceuticals (Matamoros et al., 2015). However, the efficiency of the process depends on the concentration of the toxic compounds, because they may inhibit the microorganisms (Molinuevo-Salces et al., 2019).

2.3 Valorization of produced biomass

Since the valorization of the produced biomass is not a research topic of my doctoral Thesis, a briefly discussion is provided.

The presence of microalgae represents an added value of the biomass produced that opens new possibilities of exploitation as mentioned in Chapter 1. Since the biomass is obtained after wastewater treatment, the most suitable uses are energy production, biofertilizer and animal food production (Acien et al. 2017).
There is still a lack of knowledge on the best valorization pathway to improve the economic outlook of the process. For example, Vulsteke et al. (2017) assessed the economic viability of four pathways to valorize microalgal-bacterial biomass. They founded that biomass as shrimp feed supplement and extraction of phycobiliproteins are the most profitable solutions while the revenues with biogas production are negligible.

2.4 Parameters affecting microalgal-bacterial activities

Physical, chemical, biological and operational factors may affect microalgal and bacterial activity and so the treatment removal efficiency. The parameters that have a stronger effect are discussed below.

2.4.1 Temperature

The optimal temperature for growth is species related, however most of the microalgae in wastewater treatment, as bacteria, tolerate temperatures between 16 and 27°C (Barsanti and Gualtieri, 2014). Under 16°C biomass growth slows down while temperature over 35°C can be lethal (Barsanti and Gualtieri, 2014). Attention at temperature values should be paid under outdoor conditions especially in temperate zones, where temperatures fluctuate throughout the year.

2.4.2 Light

Light is the key parameter since is the energy source for microalgae to perform photosynthesis and thus to produce oxygen. Microalgae absorb the photosynthetic active radiation (PAR, measured as μmol m^{-2} s^{-1}) that is the fraction of irradiance between 400 and 700 nm. For most of the microalgae, the photosynthetic apparatus gets saturated at light irradiances of about 200-250 μmol m^{-2} s^{-1} (Richmond, 2004). It is worth noting that only the 40% of the direct solar irradiance reaching the Earth surface is photosynthetically active (Richmond, 2004). On a sunny day, the maximum solar irradiance suitable for photosynthesis is 1800 μmol m^{-2} s^{-1} (Richmond, 2004).

In presence of microalgae, light penetration inside the system is paramount to ensure photo-oxygenation, therefore self-shading effect due to biomass concentration and photobioreactor design (shape, materials) should be properly considered. Biomass represent a limitation for light irradiance, in fact a high concentration reduces light penetration and results in mutual shading (self-shading) creating dark zones inside the system and thus reducing photosynthetic activity. Therefore, during light period microalgae are expose to light and dark with a certain frequency that is linked to the mixing condition.
Turbidity of the influent wastewater is another factor to consider because it affects light penetration.

The rate of photosynthesis (P) is strictly correlated to light intensity (I), and this relationship can be depicted in three stages, as shown in Figure 2.2 (Béchet et al., 2013): (i) Light-limited: at low irradiance there is proportionality between P and I; (ii) Light-saturated: after a certain light intensity the photosynthetic apparatus become light-saturated. P is maximum independently from the light intensity; (iii) Light-inhibited: if light intensity is beyond an inhibitory threshold, the rate of photosynthesis starts to decrease due to deactivation of the photosynthetic process.
Artificial lamps (e.g. Fluorescent lamp, LED lights) can provide a suitable light energy that is constant and controllable. Therefore, artificial light is useful to exclude the variability of light when studying the effect of other parameters on the

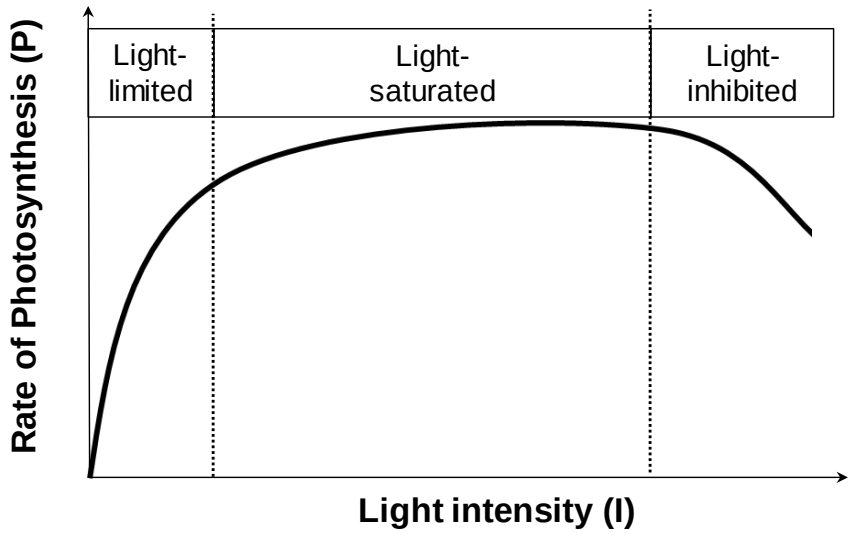

Figure 2.2 *Typical relationship between the Rate of Photosynthesis (P) and Light intensity (I). (Adapted from Béchet et al., 2013)*

treatment process. On the other hand, power consumption affects negatively the energy balance of the process making the use of artificial light not suitable in real scale applications. In literature, the light intensities that are employed more frequently, range between 100 and 200 μmol m^{-2} s^{-1} that correspond to 5-10 % of full daylight (2000 μmol m^{-2} s^{-1}) (Barsanti and Gualtieri, 2014). Sunlight is the more sustainable light source to exploit since it is free and holds the full spectrum of light. However, sunlight is characterized by seasonal variation and daily weather conditions; therefore, it represents a variable difficult to control. Notwithstanding, solar-drive photo-oxygenation is the key towards a cost-effective and sustainable process able to overcome the drawbacks of activate sludge processes (Posadas et al., 2017).

Light intensity can also affect bacterial activity. In particular, nitrifiers can be inhibited by light and Nitrite Oxidizing Bacteria (NOB) are more sensitive than Ammonium Oxidizing Bacteria (AOB) (González-Fernández et al., 2011). Vergara et al. (2016) reported photoinhibition of nitrifiers with irradiance above 500 μmol m^{-2} s^{-1}. The result was a decrease of more than 20% in ammonium removal rates and nitrate production rates. Therefore, particular attention should

be made when exploiting sunlight especially during peak hours when light intensity may reach 2000-3000 μmol m^{-2} s^{-1} (Vergara et al., 2016).

2.4.3 Dissolved Oxygen (DO)

The dissolved oxygen (DO) inside the system is the result of photosynthetic oxygenation, and oxygen consumption by biomass respiration and compounds oxidation (i.e. biomass growth). In microalgal system, DO can reach super-saturation level resulting detrimental (Richmond, 2004) and photorespiration may occur (Kliphuis et al., 2011). However, bacteria oxygen consumption may prevent oxygen saturation condition.

2.4.4 pH

pH depends on metabolic activities of the microorganisms, alkalinity and ionic composition of the influent wastewater (Posadas et al., 2017).
pH fluctuations can inhibit both microalgae and bacteria activity. Microalgae are able to tolerate high pH variations (Razzak et al., 2013), with an optimal value of 8 for the great part of the studied species (Barsanti and Gualtieri, 2014). Most of bacteria do well within pH range from 6.5 to 8.5. Nitrifiers are more sensitive to pH and the optimum value is in neutral and slightly alkaline conditions (Le et al., 2019).
The processes that mainly impact pH are photosynthesis and nitrification. During light period, microalgae perform photosynthesis and thus CO_2 is assimilated and OH^- are released, as a consequence pH tends to increase. At the same time, bacteria respiration and oxidation of substrate produce CO_2 that may attenuate the pH increase.
Nitrification, in particular ammonium oxidation, release H^+ reducing the alkalinity, so the pH tends to decrease. The co-occurrence of photosynthesis and nitrification may be sufficient to balance pH variation and make it stable around neutrality. Alternatively, CO_2 can be added as external flux (i.e. flue gas) to help to control the pH since this parameter can reach values of up to 11 if CO_2 fixation through photosynthesis is not counterbalanced (Posadas et al.,

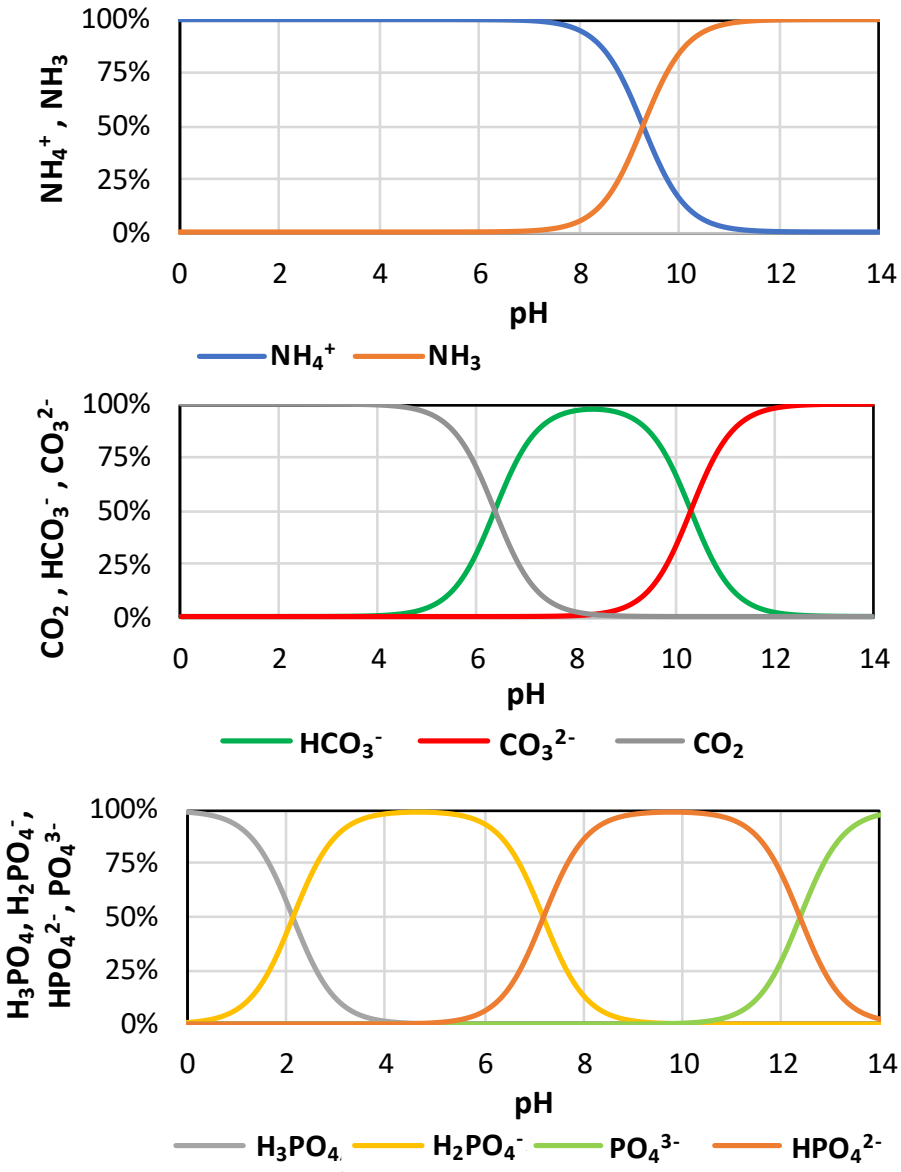

Figure 2.3 *Ammonia, Carbonates and Phosphate equilibria in solution at the temperature of 25°C*

2014).
In dark condition there is not photosynthetic activity therefore, microalgal respiration together with bacterial respiration tend to decrease pH, since CO_2 is only released. At the same time, if anoxic condition occurs, denitrification may take place and part of the alkalinity destroyed during nitrification may be recovered. The alkalinity of the influent wastewater is fundamental to avoid great pH fluctuation.

pH determines the equilibrium of ammonium/ammonia, phosphates and carbonates (Figure 2.3). High pH induces the removal of N and P through ammonium volatilization and phosphorus precipitation. On the other hand, at high pH, CO_2 is available in the form of CO_3^{2-} and cannot be assimilated by microalgae (Solimeno and García, 2017).
High pH value may also affect settleability by causing auto-flocculation (Barros et al., 2015).

2.4.5 Mixing

Ensure good mixing condition in microalgal-bacterial based processes is important for the following reasons :

- To enhance the aggregation of the biomass. However, strong mixing could result in cell damage and shear stress (Quijano et al., 2017; Posadas et al., 2017);
- To prevent the biomass to settle and the formation of nutrient and gas gradients in the mixed liquor (Posadas et al., 2017);
- To promote the exposition of all microalgae to light. In this way, microalgae alternate light and dark conditions (Posadas et al., 2017);
- To increase mass transfer rates between biomass, liquid phase and air (Posadas et al., 2017).

In open systems the mixing is usually provided by a paddle wheel, while in closed system it can be supported by mixers or mechanical aeration (Ting et al., 2017). Sometimes air enriched in CO_2 is supplied to support photosynthesis,

generating also mixing (Ting et al., 2017; Vo et al., 2019).

2.4.6 Hydraulic Retention Time (HRT) and Sludge Retention Time (SRT)

The HRT regulates the contact time between the biomass and the compounds to remove. If the process does not include a settling phase and recirculation of biomass, the HRT corresponds also to the Sludge Retention Time (SRT). This is common in system designed for microalgal cultivation (i.e. open systems).
Uncoupling HRT and SRT enables to retain the biomass in the system for a longer period. In this way, slow growing microorganisms, as nitrifiers (μ_m =0.45 d^{-1}, Ekama and Wentzel, 2008), have the possibility to develop and remain inside the system. SRT affects biomass production and control the biomass concentration inside the system, influencing light availability and penetration. In addition, SRT plays a role in the formation and selection of flocs with good settleability thanks to biomass recirculation (Valigore et al., 2012). With high SRT, inert solids are retained inside the system and this may influence light penetration.

Usually photobioreactors are operated at HRT between 2 and 6 days (Muñoz and Guieysse, 2006). Therefore, large areas are required with respect to activated sludge systems that operate at lower HRTs. To reduce the high footprint, it is necessary to understand how to control microalgal-bacterial systems in order to guarantee high removal efficiency with lower HRTs. However, with shorter HRTs, it is important to avoid biomass wash out.
Different SRTs have been applied to microalgal-bacterial system, but few studies have focused on the effect of this parameter.

Considering the central role of HRT and SRT on defining removal rates, biomass composition and productivity, further investigations are need because there is still a lack of information.

2.5 Microalgal-bacterial reactor configurations

Since this research is not focused on the development or design of suitable reactor configurations for wastewater treatment, a briefly overview is provided.

Systems operated with microalgae are called photobioreactors. Biomass can be suspended in the mixed liquor or attached (biofilm). The main distinction is between open and closed systems.
A schematic comparison of the most tested reactor configurations for wastewater treatment is made in Table 2.4.

Currently, the reactor configurations tested with microalgae and bacteria to treat wastewater were developed firstly with the aim to cultivate microalgae (Ting et al., 2017).
Unfortunately, the few systems specifically proposed to treat wastewater are at lab-scale. For example, the research group of University of Valladolid (de Godos et al., 2014) has been studying a novel anoxic-aerobic algal-bacterial photobioreactor with biomass recycling (to uncoupling HRT and SRT) with a total working volume of about 3.5 L.

Schemes conventional in activated sludge process but based on photosynthetic oxygenation, require a proper design of the treatment unit to effectively exploit light. In fact, the optimization of light supply (high surface/volume ratio) and mixing should be the key elements to take into account in photobioreactor design while applying the concept of sustainable development.

Open reactors are the most used due to low cost of investment and maintenance. In addition, they are easy to scale up (Cai et al., 2013). The most widespread reactors used for wastewater treatment are High Rate Algae Ponds (HRAPs)(de Jesús Martínez-Roldán and Ibarra-Berumen, 2019). Other open systems less efficient are waste stabilization ponds and raceway ponds.
Even if there are few examples of HRAPs tested for wastewater treatment at real scale (De Godos et al., 2016), to date, there is still a lack of long-term studies for providing proper design and operational guidelines (Alcántara et al., 2015).

Closed photobioreactors can be divided according to reactor geometry (e.g. vertical columns, tubular, flat), of which tubular shape is the most commonly implemented. They are characterized by a higher light harvesting and efficient control of operational conditions compared to HRAPs. However, the costs of investment and maintenance are higher (Table 2.4).

	Pros	**Cons**
HRAPs	Low installation, operational and maintenance cost	- High land requirements - Low light photosynthetic efficiency - Evaporation loss - Poor gas transfer
Closed photo-bioreactors	- Easier parameter control (pH, DO, irradiation) - Easier CO_2 supply - High surface/volume ratio	High construction and operational costs

Table 2.4 *Main advantages and disadvantages of HRAPs and Closed photobioreactors*

2.6 Technologies for studing microalgal-bacterial consortia

Microalgal-bacterial consortia can be characterized in different ways. Here, some technologies applied to study the performance of the treatment removal and the biological characterization of the consortia are discussed (Table 2.5).

Removal treatment performance	**Biological characterization**
Chemical analysis	Microscopy
On-line parameters	Flow cytometry
Track studies	Omics technology
Respirometry	

Table 2.5 *Technologies applied to study the performance of the treatment removal and the biological characterization of microalgal-bacterial consortia for wastewater treatment.*

Chemical analysis is the first method applied to monitor the treatment removal by measuring the influent and effluent concentration of the compounds to be removed; mainly organic matter, nitrogen- and phosphorus-forms. Organic matter can be quantified as biological oxygen demand (BOD), chemical oxygen demand (COD) and total carbon content (TOC). The most used parameter is COD so it is easy to compare results from different authors.
Chemical analyses can be exploited to monitor the removal or production of a compound during the treatment process (e.g. Wang et al., 2015; Tiron et al., 2015). However, they are time-consuming and do not guarantee real-time information.

For real-time monitoring, on-line analyzers are a valid alternative. The use of sensors for the measurement of chemical parameters as ammonium, nitrate and phosphorous, is not so common because of high costs and maintenance level (i.e. frequent calibration), while probes that measure indirect parameters have been use more frequently, thanks to their lower price and reliability. In particular, DO and pH meters are the most used as monitoring tools (Su et al., 2011; Karya et al., 2013; Tiron et al., 2015; Wang et al., 2015; Acien et al., 2016; Van den Hende et al., 2017).
The advantage of on-line probes is that the obtained data could be used as a means to control and modified the process but until now, these parameters have been largely overlooked.

Chemical analysis are also useful to estimate removal or production rates of compounds such as ammonium and nitrate, in short batch tests (in the order of hours). The removal rate of a compound can be estimated from the slope of the straight line that interpolates the measured concentrations of the considered compound over time. These tests are short and enable to retrieve useful information. However, few examples are reported in the literature (e.g. Karya et al., 2013). In this research work, this kind of test is called “track study”.

Respirometry is another useful technique to estimate the activity of microorganisms (i.e. heterotrophic bacteria, nitrifiers and photosynthetic microorganisms) through the measurement of oxygen production and consumption rate.

In the literature, various respirometric apparatus have been tested, also in combination with titrimetry (Choi et al., 2010; Decostere et al., 2013; Vargas et al., 2016; Sforza et al., 2018). However, the different experimental protocols developed are not always comparable.
Respirometry is valuable because it enables to estimate the kinetic parameters to be used in mathematical models to predict the behavior of the consortia (Rossi et al., 2020).

Biomass concentration is a parameter that has been estimated in many different ways, such as (i) Content of suspended solids expressed as total or volatile (TSS or VSS) (Su et al., 2011; Karya et al., 2013; Van den Hende et al., 2017; Kang et al., 2018); (ii) Optical density (Cabanelas et a., 2013); (iii) Content of chlorophyll (Kang et al., 2018); (iv) Cell counting (Peniuk et al., 2016). Therefore, it is very difficult to compare the results from different experiments.
Biomass concentration is an essential parameter to refer to, both in the design and operation of the process. To estimate the specific removal rate of a compound or to model the process, biomass concentration is the basic parameter to know. Therefore, it is of paramount importance that scientists agree on an univocal parameter to express biomass concentration.
To quantify the abundance of different microorganisms, microscopy and flow cytometry have been both applied following different standardize methods, mainly developed for natural environments (Hyka et al., 2013; Perera et al., 2019).

To understand the interactions that may occur inside microalgal-bacterial consortia, the identification and the characterization of individual microorganisms are critical. Traditional (microscopy) and innovative techniques have been applied. In Table 2.6 and 2.7 the main advantages and disadvantages of the tools applied more frequently are summarized.

Tools	Advantages	Disadvantages	References
Physical techniques			
Optical and epifluorescence microscopy	- Non-destructive and easy to use; - Suitable for microalgal cell counting; - Distinguishes fluorescence emitting microalgae and cyanobacteria from bacteria.	- Provides basic morphological information of the consortia; - Difficult to separate autofluorescence signal.	Van den Hende et al., 2017; Kang et al., 2018
Scanning electron microscopy	- 3-D imaging of the consortia; - Observation of surface characteristics.	- Crucial sample fixing; - Complex sample preparation; - Expensive.	Zhang et al., 2018; Arcila and Buitrón, 2017
Flow cytometry	- Rapid and precise; - Cells can be quantified; - Individual organisms can be differentiated and separated (the latter only if the instrument is equipped with a cell sorter).	- Demands specialized skills; - Requires method optimization and instrument calibration.	Peniuk et al., 2016

Table 2.6 *Advantages and disadvantages of the Physical techniques tools to characterize the microalgal-bacterial consortia treating wastewater (partially adapted from Perera et al., 2019).*

Tools	Advantages	Disadvantages	References
Molecular techniques			
Metagenomics	- Provides species composition; - Identifies genetic variabilities.	- Expensive; - Complexity in data analysis; - Availability of limited genome libraries; - Limitations in isolation from low abundant species; - Metabolic pathways can only be predicted.	Cho et al., 2017; Meng et al., 2019

Table 2.7 *Advantages and disadvantages of the Molecular techniques tools to characterize the microalgal-bacterial consortia treating wastewater (partially adapted from Perera et al., 2019).*

2.7 Research gaps

Microalgal-bacterial consortia for wastewater treatment have been studied since the 1950s. Thanks to their versatile metabolism, microalgae and bacteria have been applied for the treatment of most types of wastewaters (Ferreira et al., 2019). Different types of reactors and configurations have been tested. Most of the systems have been developed at lab- and pilot-scale and have been usually operated under conditions far from the real ones. In most cases the tests have been performed using synthetic or sterilized wastewater with selected microalgal and/or bacterial strains. The few implementations at real scale (mainly HRAPs) lack of long-term studies. Therefore, there is still a lack of knowledge about treatment performance, design parameters and operational guidelines.

Despite the successful implementations, at the moment, microalgal-bacterial-based processes are not competitive with activated sludge, mainly because they are characterized by high HRTs (in the order of days) and thus by high footprint.

Studies at a lab- and pilot-scale have demonstrated the potential of microalgal-bacterial consortia in the removal of organic compounds, nitrogen and phosphorous. But, to become competitive, microalgal-bacterial based technology should be optimize following the principles of sustainability and low-cost (i.e. low-energy requirements and low costs for biomass recovery).
In view of the large-scale application of this technology, different authors (Molinuevo-Salces et al., 2019; de Jesús Martínez-Roldán and Ibarra-Berumen, 2019) agree that there are still some challenges to overcome.
To engineer the process research should be focused on:

- Understand real wastewater characteristics effects;
- Assess the influence of operational and environmental conditions;
- Reduce the use of land;
- Valorize the produced biomass.

Microalgal-bacterial consortia treating wastewater have not yet been fully characterized, therefore there is not a consolidated knowledge as for activated

sludge. Their composition is still under research due to the huge possible combinations that can occur (naturally or engineered) (Gonçalves et al., 2019), so the diversity of the consortia is still not well-known.

To date, studies exploring the microbial communities are limited, but thanks to the advent of novel molecular biology methods, more information will be retrieved about population dynamics and metabolic pathway availability. Understand the removal mechanisms is crucial to guarantee an effective treatment. Definitively, through the "-Omics techniques", it will be possible to gain deeper insight into the interactions between microorganisms.

Considering the different applications of microalgal-bacterial consortia it is urgent to develop standardized methods of investigation, in order to compare the data obtained worldwide, especially about: (i) biomass concentration; (ii) quantification of microalgae and bacteria; (iii) measure of the kinetic parameters of the microorganisms (heterotrophic bacteria, nitrifiers and photosynthetic microorganisms).
The definition of the above mentioned quantities is crucial in the development and application of mathematical models. In the last years, some progresses have been made specifically for models to describe the behavior of microalgal-bacterial consortia treating wastewater (Solimeno and García, 2017). However, there is still not a reliable model that could help to support the design and the operation of the systems (Gonçalves et al., 2019). The kinetic parameters, which have been used in the recently developed models, are not always representative of microalgal-bacterial consortia because they are retrieved from models developed for microalgal cultivation or activated sludge.

Process parameters consolidated for activated sludge need to be redefined in the microalgal-bacterial consortia; above all biomass concentration due to the central role of light. Exploitation of photo-oxygenation as solely oxygen source is the key aspect for a sustainable process. The most economic light source is sunlight. However, it is a variable that can only be controlled to a limited extent, since it is characterized by daily weather conditions and seasonal variations. Therefore, it emerges the importance to perform outdoor

experiments to understand the influence of sunlight and also of temperature.

The use of real wastewater is the *conditio sine qua non* to study the resilience capacity and stability of microalgal-bacterial consortia under real operational condition. Pollutant concentrations, turbidity, color, pH are the main characteristics of the influent wastewater that may affects the treatment performance.

Once consolidated the knowledge about the optimal operational parameters to obtain the maximum removal rates, it would be possible to reduce the HRT of the system while maintaining high removal efficiency. In this way, the land-use would be lowered and microalgal-bacterial consortia would result more competitive against activated sludge. While, the identification of proper biomass valorization pathways would increase the sustainability of the process.

Finally, to evaluate the applicability of microalgal-bacterial consortia to the treatment of wastewater, the presence of possible drawbacks should be considered. Ones of the major drawbacks to take into account are the emissions in the atmosphere of N_2O and the release of cyanotoxins in the effluent wastewater.

2.8 Objectives

This research work aims to gain insight into wastewater born microalgal-bacterial consortia as an alternative solution to activated sludge in the secondary and tertiary treatment, for the removal of organic compounds and nutrients from municipal wastewater without the support of mechanical aeration.

Following the discussion on the research gaps (Section 2.7), the main objectives of the thesis are:

(i) to understand microalgal-bacterial dynamics, which microorganisms develop and persist in the systems, their evolution and their interactions;
(ii) to understand the removal mechanisms involved, which is the role of microalgae and bacteria in the treatment;
(iii) to investigate the influence of biomass concentration and sunlight, since they are crucial operating parameters that may affect the wastewater treatment;
(iv) to provide methods of investigation that can be applied to any possible declination of microalgal-bacterial consortia.

To reach the objectives and contribute to increase the knowledge on these processes under real operational conditions (in view of the full-scale treatment), all the experiments were conducted using real municipal wastewater collected after primary sedimentation at the wastewater treatment plant of Trento Nord (Trento, Italy). The use of real wastewater led to the development of native microalgal-bacterial consortia.

Due to the lack of knowledge at real-scale, this research work focused on investigations at lab scale. Closed photobioreactors, with a maximum working volume of 2 L, were installed and operated as sequencing-batch reactors. Each cycle was characterized by different phases (feed, react, settle and discharge) and a photoperiod.

The reactors were employed to examine the start-up of the consortia, that is

the development of microalgae and bacteria; then the stability of the process was assessed in the long term. In this phase, many aspects were investigated to shed light on the relationships between system variables and design parameters.
Finally, the limits of the microalgal-bacterial consortia were explored in order to optimize the process.

Part of the work was also dedicated to extend advanced methods of investigation (respirometry and flow cytometry), used in activated sludge, to characterize removal rate of microalgal-bacterial consortia and their composition.

The aim is to help to lay the foundation to apply a methodological research approach in the study of microalgal-bacterial consortia for wastewater treatment and thus scale-up this promising technology.

The research questions addressed are summarized below.

RESEARCH QUESTIONS	**Chapter**
Is microalgal inoculation essential to start-up a system?	3-4-5
Is the removal process stable over time?	6
How to promote nitrogen removal?	7
How to monitor the evolution of the removal process?	8
How far to push the system?	9
What is the influence of biomass concentration on the process?	10
Which are the kinetics of the removal process?	11
How to characterize biomass composition in a time effective way?	12
Is the microbial community stable over time?	13

CHAPTER 3

PHOTOBIOREACTORS START-UP AND INITIAL MICROALGAL INOCULATION: TREATMENT PERFORMANCE

The role of the initial microalgal inoculation on the start-up of photobioreactors was investigated. Pollutant removal efficiency, sludge production and solids settleability were evaluated (This Chapter). Microbial community composition and evolution were monitored through next generation sequencing (Chapter 4) and flow cytometry (Chapter 5).
It emerged that the initial inoculation did not affect in the long-term the system performance; moreover, photosynthetic microorganisms were able to grow spontaneously.

This Chapter is based on:
Petrini S., Foladori P., Beghini F., Armanini F., Segata N., Andreottola G., 2020. *How inoculation affects the development and the performances of microalgal-bacterial consortia treating real municipal wastewater.* Journal of Environmental Management 263, 110427. https://doi.org/10.1016/j.jenvman.2020.110427

Abstract

To date, little is known about the start-up of photobioreactors and the progressive development of stable microalgal-bacterial consortia with a view to the full-scale treatment of real wastewater.

Two photo-sequencing bioreactors, one inoculated with *Chlorella vulgaris* (RC) and one with the absence of inoculum (RW), were fed with real municipal wastewater and run in parallel for 101 days. The influence of the inoculation was evaluated in terms of pollutant removal efficiency, excess sludge production, solids settleability and microbial community characteristics.

No significant differences were observed in the removal of COD (89±4%; 88±3%) and ammonium (99±1%; 99±1%), mainly associated with bacteria activity. During the first weeks of acclimation, *Chlorella vulgaris* in RC promoted better P removal and very high variations of DO and pH. Conversely, under steady-state conditions, no significant differences were observed between the performances of RC and RW, showing good settleability and low effluent solids, 7±8 and 13±10 mg TSS/L respectively. Microbiome analysis via 16S rRNA gene sequencing showed that, despite a different evolution, the microbial community was quite similar in both reactors under steady state conditions. Overall, the results suggested that the inoculation of microalgae is not essential to engender a photobioreactor aimed at treating real municipal wastewater.

3.1 Introduction

Advanced photobioreactors based on microalgae have received closer scientific attention in recent years due to factors such as energy demand reduction and biomass resource recovery (Wang et al., 2018). In the treatment of wastewater, photosynthetic aeration produced by microalgae and cyanobacteria may in the future replace the mechanical aeration that causes, for intensive energy consumption, up to 50% of the operational costs of wastewater treatment plants (WWTPs).

The association between microalgae and bacteria appears to be a powerful alternative for wastewater treatment (Arcila and Buitrón, 2017), considering that: (1) microalgae produce oxygen; (2) nitrifying bacteria use oxygen for the oxida-

tion of ammonium; (3) heterotrophic bacteria use oxygen for organic matter removal, generating CO_2; (4) microalgae use CO_2 for photosynthesis, preventing excessive variation of pH; (5) microalgae can grow under mixotrophic conditions, contributing to the removal of organic matter in wastewater (Gupta et al., 2016).

Several studies in the literature have focused on the application of single microalgal species or monocultures for wastewater treatment (Cuellar-Bermudez et al., 2017). Most of them refer to inoculation with pure algal strains and feeding of synthetic or sterilized wastewater (Cuellar-Bermudez et al., 2017). However, when real municipal wastewater is used as influent substrate, systems based only on pure microalgae (axenic conditions) are difficult to maintain permanently (Xu et al., 2009); indeed, unsterilized wastewater inevitably contains a variety of different microorganisms (He et al., 2013; Saunders et al., 2016). Moreover, in photobioreactors, culture contamination cannot be avoided because of huge costs of sterilization (He et al., 2013) and possible entrance of air in outdoor conditions or scaled-up systems (Cuellar-Bermudez et al., 2017). Hence, bacterial and microalgal cells grow simultaneously in the reactor (Kang et al., 2018) and the initial inoculation with pure microalgae may not persist in the system.

On the other hand, a large body of research has demonstrated that microalgal-bacterial consortia can naturally develop from real wastewater (He et al., 2013; Arango et al., 2016; Tsioptsias et al., 2016; Cho et al., 2017; Kang et al., 2018). In this way the difficulties of inoculating large volumes with pure strains are overcome, and the costs associated with sterilization are avoided (He et al., 2013).

To date, only a few studies have investigated the role of different inoculation ratios and their fate in photobioreactors (Su et al., 2012; Arango et al., 2016; Sun L. et al., 2019). Further research is needed on how the unsterilized conditions may affect the initial inoculation, its development, and the final wastewater treatment performances of the microalgal-bacterial consortium. Moreover, little is known about the evolution of the microalgal-bacterial consortium composition and its dynamics during acclimation (García et al., 2018).

The main objective of this research was to evaluate the influence of inoculation by comparing two photo-sequencing bioreactors (PSBRs) fed with the same real municipal wastewater and run in parallel:

1) the first PSBR was initially inoculated with *Chlorella vulgaris* (henceforth *C. Vulgaris*), a common microalga used in bioprocesses (Ryu et al., 2014), and then fed with wastewater;
2) the second PSBR was not inoculated with any pure strains, but only fed with wastewater.

The two PSBRs were compared during the entire acclimation period until steady-state conditions were reached. Full monitoring was performed during this period, with the aim of evaluating pollutant removal efficiency, excess sludge production, solids settleability and microbial community characteristics. The purpose of the comparison was to evaluate if the inoculum is essential or if only wastewater is sufficient to start up a system, since inoculation on a large scale is not (economically) feasible.

3.2 Materials and Methods

3.2.1 Experimental set-up

Reactors RC and RW - Two identical PSBRs, reactors RC and RW, were installed (Figure 3.1). The reactors consisted of transparent Pyrex glass cylinders (12 cm diameter; 20 cm height) with a working volume of 1.5 L. The systems were not sealed from the atmosphere. No forced aeration was provided. Mechanical stirrers set at 50 rpm provided gentle mixing and promoted microorganism aggregation (Sutherland et al., 2014). The reactors were operated at room temperature (average temperature was 24.8±2.0 °C in RC and 24.0±2.0 °C in RW).

Illumination - The reactors, never exposed to sunlight, were continuously illuminated by a fluorescent lamp (F30W/33, General Electric, UK) placed on one side of the reactors. No dark phase was provided in order to promote microalgal growth. The light intensity at the inner wall of the reactors, in the most exposed

part, was 45 μmol m^{-2} s^{-1}. A SQ-520 quantum sensor (Apogee Instruments, USA) was used to measure light intensity as photosynthetically active radiation (PAR).

Microalgal inoculation in RC and RW - Only RC was initially inoculated with *C. vulgaris*, while RW was started without an external inoculum.

Periodic feeding and discharge - Except for the first week of acclimation without feeding, both reactors were fed 3 times per week (on Monday, Wednesday and Friday) with the same load of municipal wastewater. The volumetric exchange ratio was 50% (0.75 L), resulting in an average hydraulic retention time in the range of 4-4.7 days. At the end of the cycle, before discharge, solids were separated in a 1-hour-sedimenation phase that favored the natural selection of settleable microalgal-bacteria flocs.

3.2.2 Microalgal strain used for inoculation

C. vulgaris was used as microalgal inoculum only in RC. *C. vulgaris* was chosen because it has been widely studied in regard to microalgal-based wastewater treatment (He et al., 2013; Ryu et al. 2014; Gonçalves et al., 2016). Pre-inoculum growth was conducted in Algae Broth medium modified by Allen (1952); the culture was then settled, collected and used as inoculum in RC.

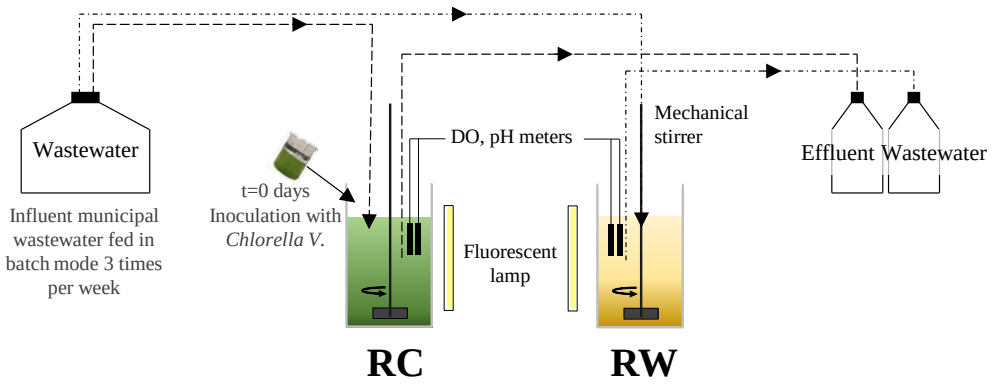

Figure 3.1 *Scheme of the experimental apparatus. At the beginning (t=0 days) RC was inoculated with C. vulgaris, while RW was not inoculated.*

3.2.3 Influent municipal wastewater

Municipal wastewater was used to feed both reactors during the experimental period. Wastewater was collected after the primary sedimentation of the Trento Nord WWTP (Italy). The composition of the influent pre-settled wastewater (Table 3.1) was in accordance with typical values expected for this type of wastewater (Tchobanoglous et al., 2003). Since no filtration of the wastewater was performed, the microorganisms naturally present in wastewater entered the reactors and affected the population dynamics.

3.2.4 Sampling frequency

The experiment lasted 101 days, in order to include the acclimation period in its entirety and to observe steady-state conditions for several weeks.
The treatment performances were monitored by collecting samples of influent and effluent wastewater 2-3 times per week. After collection, samples were immediately transferred to the lab for the chemical analyses.
The evolution of biomass settleability and microbial community was investigated by collecting the mixed liquors in the reactors every 10 days in the first 60 days of experimentation and then every 21 days. For the microbial community analysis, samples were stored at -80°C in the dark, and then they were processed all together at the end of the sampling campaign.

3.2.5 Analytical methods

Total Chemical Oxygen Demand (COD), soluble COD (sCOD), Total Suspended Solid (TSS), Total Kjeldahl Nitrogen (TKN), NH_4^+-N, NO_2^--N, NO_3^--N, total P and PO_4^{3-}-P were analyzed in influent and effluent wastewater according to Standard Methods (APHA, 2012). The parameter sCOD was measured after filtration of the sample on 0.45-μm membrane.
To evaluate settleability, the mixed liquors in RC and RW were settled for 60 minutes in Imhoff cones. Solids concentration in the reactors was quantified as TSS.

Dissolved Oxygen (DO) and pH were recorded every 15 min in both reactors. DO and temperature were measured with OXI340i meters coupled with the sensor CellOx®325 (WTW, Germany). The parameter pH was measured with a pH340i meter and a pH3310 meter, all coupled with the electrode Sentix®41 (WTW, Germany).

3.2.6 Microscopy

Microscopic observations were performed using a Nikon Optiphot EFD-3 Microscope (Nikon, Japan). The floc structure of biomass in RC and RW was observed under bright-field microscopy.

3.2.7 Microbial community analysis

The microbial communities in RC and RW were investigated in depth by means of 16S rRNA gene high-throughput sequencing. DNA was extracted using DNeasy® PowerSoil® Kit (Qiagen, German) with a modified protocol. For all samples, 1 ml of mixed liquor was transferred to the PowerBead and processed according to QIAGEN DNeasy® PowerSoil® Kit instructions, except that the collection tube was centrifuged for 2 minutes, 1 minute and 1 minute after adding Solution C3, C5 and C6, respectively.
Library preparation followed the procedure described by the “Illumina 16S metagenomicc Sequencing library preparation” protocol using the V3-V4 primers (Klindworth et al., 2013) and the Nextera XT Set A indexes (Illumina San Diego). 16S rRNA reads analysis was carried out using QIIME version 1.9.1 (Caporaso et al., 2010). Reads were merged with PANDAseq (Masella et al., 2012) using default parameters and then de-multiplexed with split_libraries_fastq.py. Open reference Operational Taxonomic Unit (OTU) picking was performed with pick_open_reference_otus.py using UCLUST (Edgar, 2010) with a 97% sequence similarity. OTUs with less than 10 reads were discarded. Taxonomy was assigned using SILVA 132 (Pruesse et al., 2007) as reference database. Relative abundances were extracted from the results of summarize_taxa_through_plots.py.

3.2.8 Statistical analysis

Statistical analyses (means and standard errors) were performed using Microsoft Excel. The statistical significance was determined by a Student's t-test and set at $P<0.05$.

3.3 Results and Discussion

3.3.1 How the inoculum affects the treatment performance

COD removal

During the entire experimentation, the removal efficiency of COD was very high in both reactors despite the wide fluctuations of the influent concentrations (Figure 3.2).

Except for the first week of acclimation, the average COD removal was 89±5% in RC and 89±7% in RW. The profiles of effluent sCOD were comparable in the two reactors throughout the experimentation (Figure 3.2). Under steady-state conditions, the average values of the effluent sCOD were 25±9 mg sCOD/L in RC and 22±5 mg sCOD/L in RW (not significantly different, $P>0.05$) as summarized in Table 3.1.

Since the systems exhibited similar COD removal from the beginning, it can be concluded that the inoculum of *C. vulgaris* did not significantly affect the COD removal performance. This result matches the finding of Su et al. (2012), who reported similar COD removals (between 91±2% and 96±1%) in reactors inoculated with different ratios of microalgae and activated sludge treating municipal wastewater. A similar result was reported by García et al. (2018), who found that the microalgae did not influence the Total Organic Carbon removal efficiency in the treatment of piggery wastewater. This can be explained by considering the autotrophic growth of *Chlorella spp.*, which does not use organic matter under light conditions. Therefore, the removal of organic matter was mainly due to bacteria, whilst *C. vulgaris* played a negligible role in this process (Molinuevo-Salces et al., 2010; Lee et al., 2015).

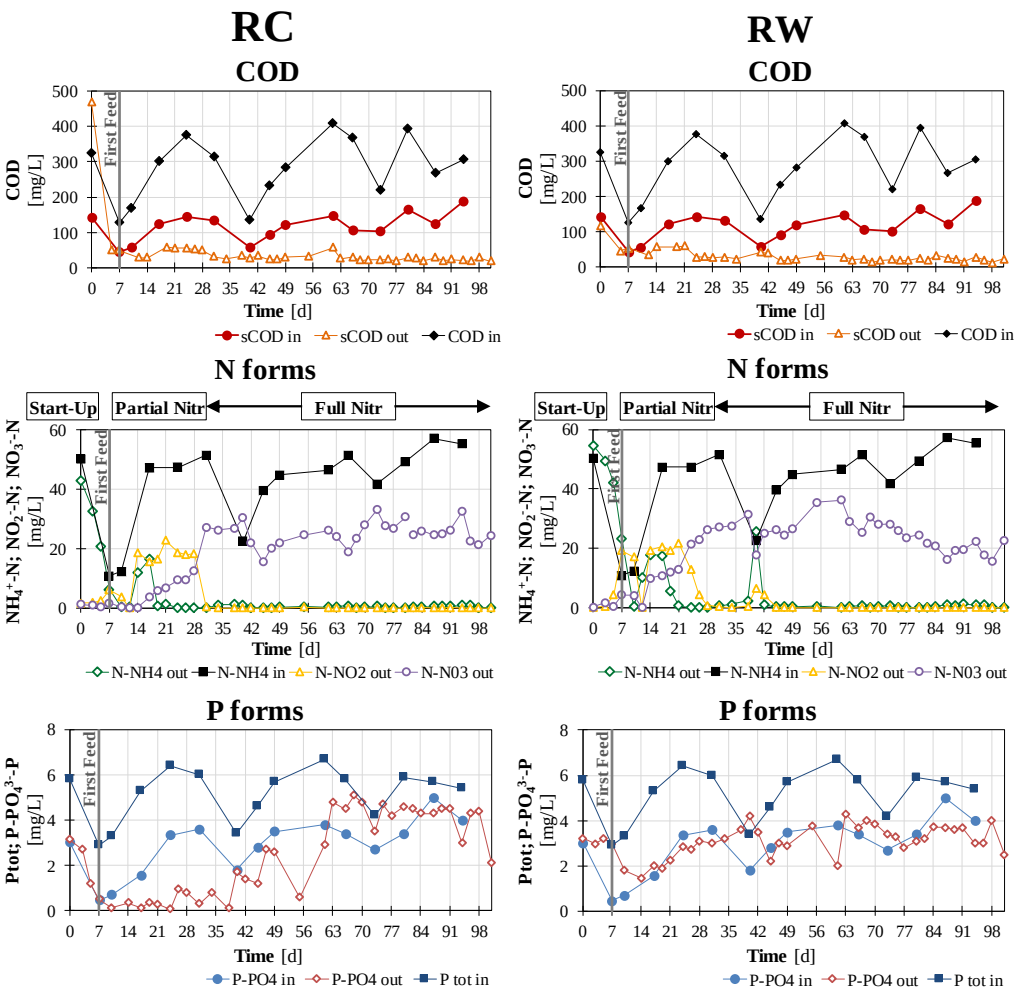

Figure 3.2 *Influent and effluent concentrations of COD, N forms and P forms in RC (with C. vulgaris inoculum) and RW (without inoculum) vs. time.*

N forms removal

Nitrogen forms in the effluents (NH_4^+-N, NO_2^--N, NO_3^--N) are presented in Figure 3.2. In both reactors, the evolution over time of N forms can be described as a sequence of three phases: (1) start-up, during the first week of acclimation; (2) partial nitrification, which lasted 30 days and formed a temporary accumulation of nitrites; and (3) full nitrification, which took place when steady state conditions were reached.

About RC, inoculated with *C. vulgaris*, the removal of NH_4^+ during the start-up (the first 7 days of acclimation) was due to the growth of *C. vulgaris* and ammonia stripping caused by the significant pH increase during the photosynthetic activity (Cai et al., 2013; Figure 3.3). Bacterial nitrification played a minor role as demonstrated by the small effluent nitrites (6.1 mg NO_2^--N /L) and nitrates (1.7 mg NO_3^--N/L) after the first 7 days. Subsequently, from day 7 to day 30, a partial nitrification took place in RC, demonstrated by incomplete removal of NH_4^+ and high concentration of NO_2^- (20 mg NO_2^--N /L) in the RC effluent, while NO_3^- increased progressively from 0 to 30 mg NO_3^--N/L. The presence of nitrites in the effluent indicates that NOB (Nitrite Oxidizing Bacteria) grow more slowly than AOB (Ammonia Oxidizing Bacteria). The lower kinetic of NOB during the period of acclimation was the consequence of certain environmental factors that temporarily affect NOB growth, such as strong variations in pH and high alkaline values (see Section 3.3.2), free ammonia and nitrous acid (Anthonisen et al., 1976) or dissolved oxygen (Blackburne et al., 2008). Full nitrification was achieved after day 30, leading to the complete removal of NH_4^+. Under steady-state conditions in RC, the average effluent concentrations were 0.4±0.3 mg NH_4^+-N/L, negligible NO_2^- and 26.0±3.6 mg NO_3^--N/L (Table 3.1). Removal efficiency of NH_4^+ was 99±1% on average.

In RW, the evolution of N forms was very similar to RC. During steady-state conditions in RW, the effluent concentrations were 0.4±0.4 mg NH_4^+-N/L, 23.7±5.3 mg NO_3^--N/L and negligible NO_2^- (Table 3.1). However, an important difference between RC and RW occurred during the acclimation period, when a faster establishment of bacterial nitrification was observed in RW, which was completed after just 25 days. The finding that complete and stable nitrification is more rapid in RW than in RC may be associated with the moderate pH variations in RW. As shown in Figure 3.3, while the pH in RW did not exceed 9, the pH in RC occasionally reached 10 due to the more intensive photosynthesis generated by *C. vulgaris*. Such high values of pH, as occurred in RC, created a selective pressure on bacteria (Krustok et al., 2015), while *C. vulgaris* was able to grow effectively at alkaline pH around 10 (Khalil et al., 2010). Furthermore, the presence of *C. vulgaris* in RC may have delayed the development of full nitrification

(Choi et al., 2010). Conversely, in RW, without an initial algal inoculum, microalgae needed more time to grow, and nitrifying bacteria growth was uninhibited from the beginning.

P removal

The profiles of P forms in RC and RW are compared in Figure 3.2. During the first 60 days of acclimation, a much higher removal of PO_4^{3-} was observed in RC: it was 66±30% with respect to 3±6% in RW. In fact, RC produced an effluent concentration of 0.8±0.8 mg PO_4^{3-}-P/L in comparison to 2.8±0.8 mg PO_4^{3-}-P/L in RW (Figure 3.2). It was very clear that the inoculum of *C. vulgaris* in RC contributed to considerably improving the P removal. According to Iasimone et al. (2018), the larger removal of phosphates occurring in RC may be due to microalgae uptake and chemical precipitation favored by pH, which may rise towards 10 (see Section 3.3.2). Another reason may be the luxury uptake of phosphorus in microalgae able to absorb more phosphorus than is necessary (Eixler et al., 2006; Powell et al., 2009).

Conversely, in RW the concentration of PO_4^{3-} in the effluent (3.1±0.7 mg PO_4^{3-}-P/L) was essentially comparable with that in the influent (2.9±1.2 mg PO_4^{3-}-P/L), without significant variations of this behavior during the whole experimentation (Figure 3.2), denoting negligible removal of PO_4^{3-}. Furthermore, the pH in RW was not high enough to promote P precipitation (see Section 3.3.2).

As soon as the pH in RC stabilized around 7.5 (after 60 days of operation), PO_4^{3-} in the effluent increased and removal efficiency decreased from 66±30% to 7±14%. This may also be associated with a change from *C. vulgaris* to other types of photosynthetic microorganisms in the RC, remarkably less performant in P removal.

In summary, the inoculum of *C. vulgaris* was able to favor the P removal in RC for the first 60 days, while subsequently, the progressive loss of *C. vulgaris* and the changes in microalgal composition caused a worsening in P removal efficiency that became similar between RC and RW under steady-state conditions.

TSS removal

Strong variations in the concentration of TSS in the effluents occurred in RC

and RW during the experimental period. During the first 30 days of acclimation there were high TSS concentrations in the effluents, while in the subsequent period the floc structure changed in both reactors and the TSS concentration became very good under steady-state conditions (t > 60 days), reaching average values of 7±8 mg/L and 13±10 mg/L in RC and RW, respectively.

The use of pure *Chlorella* or other pure strains is often associated in the literature with difficult sedimentation and separation problems (Christenson and Sims, 2011). Conversely, the development of a mixed microalgal and bacteria consortium can ensure a good separation and low solids in the effluents (Su et al., 2011).

		RC (inoculum)		**RW** (without inoculum)		**Statistically significant difference** (P<0.05)
Parameter	**Influent concentration** [mg/L]	**Effluent concentration** [mg/L]	**Removal efficiency** [%]	**Effluent concentration** [mg/L]	**Removal efficiency** [%]	
Total COD	321±71	34±9	89±4	37±5	88±3	NS
sCOD	136±32	25±9	81±8	22±5	83±5	NS
$\eta_{COD-sCOD}$*	-	-	92±4	-	93±2	
TKN	54±3	1.0±0.3	98±0	1.5±0.4	97±0	S
NH_4^+-N	49.5±5.6	0.4±0.3	99±1	0.4±0.4	99±1	NS
NO_2^--N	0.2±0.2	0.06±0.08	-	0.01±0.03	-	S
NO_3^--N	0.7±0.3	26.0±3.6	-	23.7±5.3	-	NS
Total N	55±3	27±4	52±7	25±5	45±8	NS
PO_4^{3-}-P	3.7±0.7	4.2±0.8	7±14	3.4±0.6	12±16	S
Total P	5.6±0.7	4.4±0.8	20±19	3.7±0.6	33±11	S
TSS	153±53	7±8	94±7	13±10	91±8	NS

* The removal efficiency (η) was calculated according to the expression $\eta = \frac{COD - sCOD}{COD}$

Table 3.1 *Characterization of influent and effluent wastewater (ave.±st.dev.), removal efficiency and significance of difference in RC and RW during steady-state conditions (t > 60 days). S:Statistically significant, NS:No statistically significant*

3.3.2 How the inoculum affects the on-line operational parameters

Just after the first 2 days of acclimation DO rose to 8 mg O_2/L in both systems (Figure 3.3) due to the progressive development of photosynthesis. In RC, *C. vulgaris* well adapted to municipal wastewater leading to an intensive production of oxygen and no lag phase was observed (Iasimone et al., 2018). Since no inoculation with *C. vulgaris* was performed in RW, it was speculated that the small amount of microalgae naturally present in the influent municipal wastewater was able to grow in the PSBR.
DO and pH profiles in microalgal-bacterial consortia appear very complex because the profiles induced by photosynthetic microorganisms overlap with those produced by the bacterial processes: for example, oxygen is consumed by bacteria but simultaneously produced by photosynthesis.
In depth consideration of the profiles of DO and pH in both reactors (Figure 3.3) identifies the following details in each cycle (that is, between two subsequent feeding phases):

i. the feeding, indicated by the vertical dotted lines in the graphs of Figure 3.3, generated an immediate consumption of DO that might drop to zero, due to the huge demand of oxygen for the oxidation of biodegradable COD and NH_4^+. Bacterial nitrification also caused the utilization of alkalinity, which leads to a simultaneous decrease of pH;
ii. DO concentration remained close to zero until the complete removal of external substrates and pH continued to decrease. This phase, called "zero-DO" phase (Chapter 8), reveals that oxygen demand for heterotrophic biodegradation and nitrification is higher than photosynthetic oxygen production;
iii. when biodegradable COD and NH_4^+ were completely depleted, DO was no longer required and rose very rapidly. At the same time pH increased due to the uptake of HCO_3^- by photosynthesis;
iv. the end-point of ammonium was thus identified on the basis of two characteristic points: the flex in the DO curve called "DO breakpoint"

and the simultaneous local minimum in the pH profile called "Ammonia Valley" (see the zoomed-in plot in Figure 3.3). Together they suggest that the nitrification is complete (Chapter 8).

On observing the DO profiles in both reactors during the entire experimentation (Figure 3.3), a progressive decrease of the daily maximum DO concentration was apparent, which was more evident in RC. At the end of the acclimation, the "zero-DO" phases became longer, and the "Ammonia valley" was delayed in both reactors due to: (1) increase of floc size and limited light penetration (self-shading) that reduced the photosynthetic activity and oxygen production, and (2) the slower nitrification rate due to limited oxygen availability.
In regard to pH, the daily variations were moderate in RW during the entire period of acclimation, with values always between 7-8.5, except for the first 15 days. Conversely, pH variations were remarkably sharper in RC, especially during the first 60 days of acclimation. The intense photosynthesis reactions produced by the inoculum of *C. vulgaris* greatly affected the pH profile, leading to rapid variations from 7 to over 9.5 in a few hours. Such high values of pH may cause stripping of free ammonia and difficulties in adaptation of heterotrophic bacteria involved in biodegradation. In the literature, Muñoz and Guieysse (2006) indicated that microalgae can have a detrimental effect on bacterial activity by increasing the pH. In agreement, also Choi et al. (2010) reported that microalgae may inhibit bacterial growth by increasing the pH. High pH values at the end of the cycles may have favored also phosphorus precipitation, contributing to a very effective P removal in RC during the first 60 days of acclimation (see Section 3.3.1). However, after 60 days, pH in RC evolved toward more stable and less fluctuating values. At the end of acclimation, RC matched the profile of RW, with values in the 7-7.5 range in both systems.
In conclusion, the inoculum of *C. vulgaris* in RC produced highly fluctuating profiles of DO and pH during acclimation. Conversely, when steady state conditions were reached (t> 60 d), profiles in RC became more regular and similar to the values observed in RW.

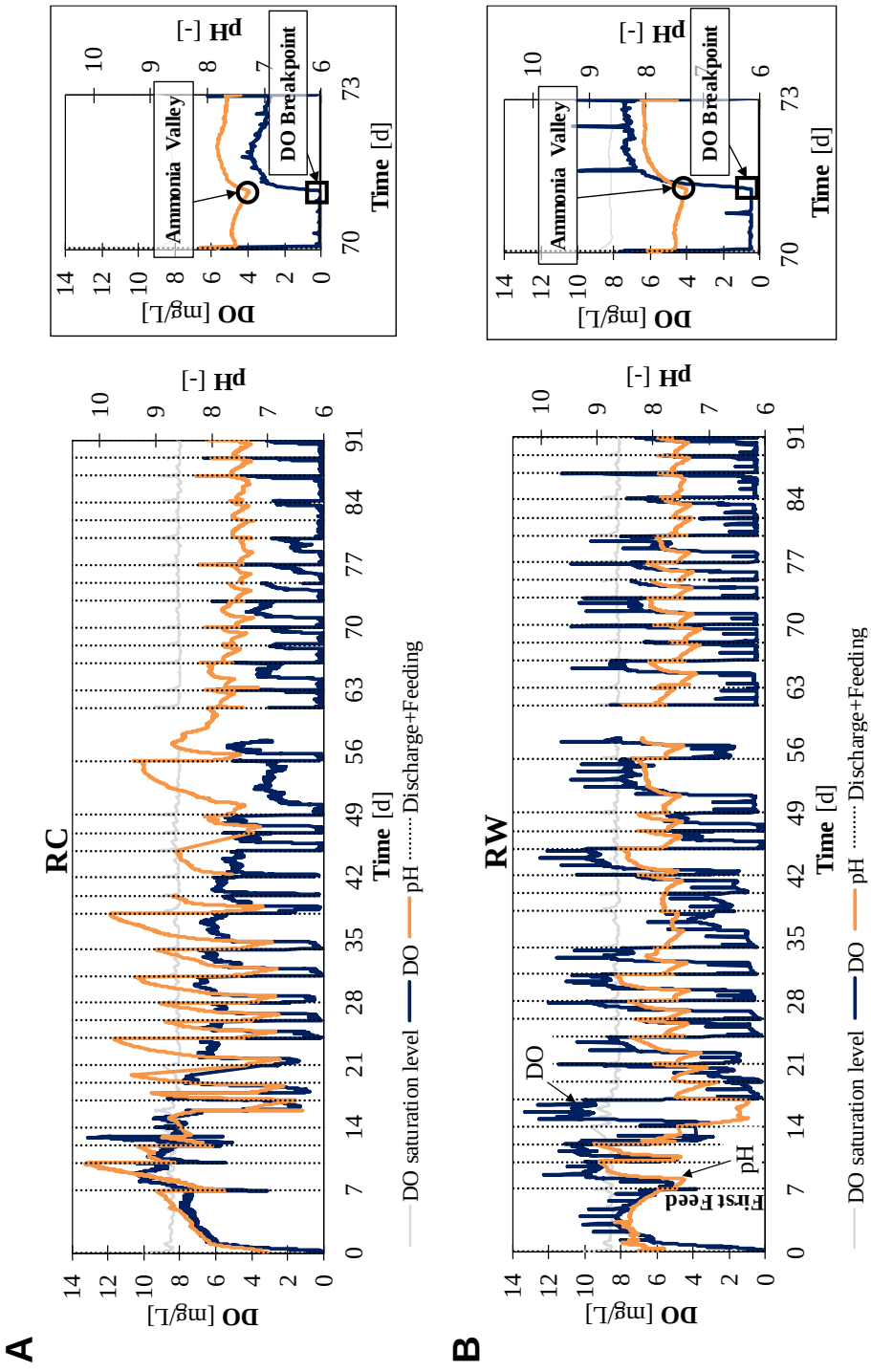

Figure 3.3 *Evolution of DO and pH in (A) RC (with C. vulgaris inoculum) and (B) RW (without inoculum) vs. time.*

3.3.3 How the inoculum affects the TSS production

During the acclimation period, the TSS concentration increased progressively with time in both reactors (Figure 3.4). However, RC inoculated with *C. vulgaris* exhibited TSS concentration always higher than RW. In particular, TSS concentration in RC was often more than double that in RW: for example, in the first 60 days the average concentration was 1.1±0.3 g TSS/L in RC and 0.5±0.1 g TSS/L in RW (significantly different, P<0.05). This suggested that the initial inoculum with *C. vulgaris* might have promoted the biomass growth and a larger initial fraction of microalgae might have favored the photosynthetic productivity.

By contrast, García et al. (2018), on treating piggery wastewater, reported that the highest biomass concentration was reached by the non-inoculated photobioreactor. In particular, García et al. (2018) obtained biomass concentrations of 2610±191, 2569±69 and 2445±222 mg TSS/L in the inoculated reactors and 3265±133 mg TSS/L in the reactor without inoculum. Further investigation is needed to explain these different behaviors and the link with operational conditions. With regard to the productivity rate (that is the slope of curves in Figure 3.4), a negligible rate was observed in the 30-60 days period in both reactors,

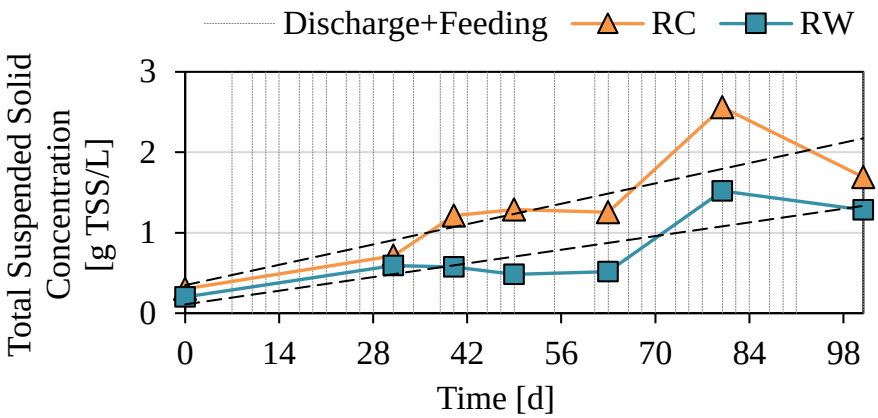

Figure 3.4 *TSS concentration in RC (with C. vulgaris inoculum) and RW (without inoculum) vs. time.*

and TSS concentration remained quite constant in the systems. This behavior was due to the loss of solids in the effluent caused by a progressive modification in the microscopic structure of the flocs and the increased turbidity in the effluents (see Section 3.3.4). Conversely, after 60 days, the microscopic structure transformed significantly and the solids leaving the systems decreased drastically to 7±8 mgTSS/L and to 13±10 mgTSS/L in RC and RW respectively. An effect of a lesser amount of solids leaving with the effluents was the enrichment of TSS in the reactors in the subsequent period (Figure 3.4).

3.3.4 Evolution of floc formation and settleability

At the beginning of acclimation (7-17 days in Figure 3.5A), highly dispersed suspensions were present in both reactors. In RC, the inoculated *C. vulgaris* was dominant, while in RW only the microorganisms naturally present in wastewater were dispersed in the suspension. Despite no inoculation of RW with microalgae, just after the first week a certain microalgal diversity (some *Chlorella*, filamentous green microalgae, unicellular cyanobacteria, diatoms) was observed under optical microscope.

With regard to settleability, the initial suspension rich in *C. vulgaris* in RC entailed a low sedimentation capacity with only a small amount of settleable solids and a bright green effluent (7-17 days in Figure 3.5B). As found by various authors (Muñoz and Guieysse, 2006; Barros et al., 2015), small unicellular microalgae species like *Chlorella sp.* have low flocculation capacity and thus scant settleability. Arango et al. (2016) confirmed that reactors inoculated with microalgae did not settle at all. In fact, microalgae remained in suspension in the liquid with scant aggregation in flocs. As a consequence, the non-settleable microorganisms in RC progressively left the reactor with the effluent wastewater. This produces a selective pressure that favors the growth of flocculent microalgae and bacteria and promotes the formation of dense aggregates. Conversely, microalgae spontaneously formed in RW were better retained in the consortium, in agreement with the findings of Arango et al. (2016), who observed that the microalgae developed in the reactor attached naturally to the flocs.

After 30 days of acclimation, flocs formed in both reactors (Figure 3.5A). The progressive enrichment of extracellular polymeric substances over time, which took several weeks, may be at the origin of flocs formation (Su et al., 2011). In this period, the effluent from RC reduced the green color and turbidity. Conversely, the effluent from RW altered to a very turbid dark brown and green suspension (Figure 3.5B-Day 38).

After 80 days, flocs enriched in filamentous photosynthetic microorganisms (especially cyanobacteria) and the consortia evolved in both reactors in a granular structure, stable under steady state conditions. Filamentous photosynthetic microorganisms were the frame of the flocs where bacteria, diatoms and only a few *Chlorella* were entrapped. In both reactors, the larger structure of granules, also more compact and denser, produced an improvement of biomass settleability. Therefore, the effluents resulted clear in reactor RC and RW, with low TSS concentrations. The final stable consortia were characterized by a high microalgal diversity, difficult to be distinguished morphologically; where *C. vulgaris* was only a minor group, whereas filamentous cyanobacteria predominated together with diatoms. These results were in agreement with García et al. (2018), who confirmed the difficulty of maintaining monoalgal cultures in wastewater treatment and observed that different concentrations of microalgae in the inoculum only affected the time required to reach steady state, but not the evolution to a complex microalgal-bacterial consortium.

In synthesis, despite different evolution of the two consortia, an efficient sedimentation was obtained in both cases after 2 months (under steady-state conditions) due to granular flocs easy to be separated from the effluents. This result was in agreement with Van den Hende et al. (2014), who observed good sedimentation in microalgal-bacterial consortia developed without any inoculum.

3.3.5 Evolution of the bacterial community composition

Figure 3.6 shows the relative abundance (> 1%) of bacterial species at phylum level in the consortia RC and RW over time. The first sample was similar in

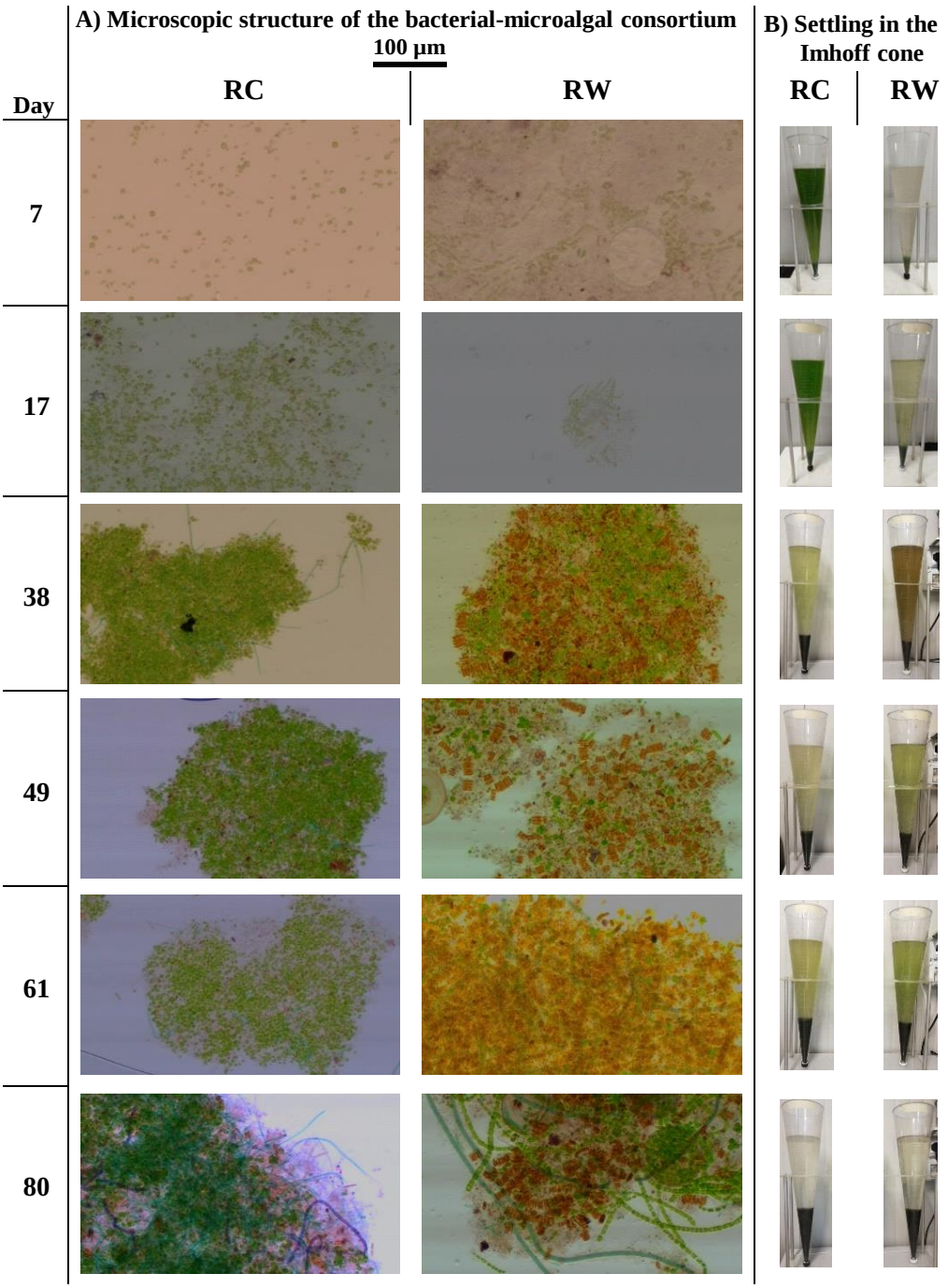

Figure 3.5 *Evolution of the consortia in RC (with C. vulgaris inoculum) and RW (without inoculum: (A) flocculent and granular structure; (B) settling observed after 60 min in the Imhoff cone.*

RC and RW, since the reactors were filled with the same wastewater except for *C. vulgaris*, which are eukaryotic microalgae not revealed by 16s-rRNA.
Initially, the main phylum in both reactors was *Proteobacteria* (a common population in activated sludge system; Zhang et al., 2012), but its proportion progressively decreased with time. *Cyanobacteria* cells grew very quickly in RW: after only 7 days of acclimation, 8% of bacteria were *Cyanobacteria*. By contrast, RC needed approximately 30 days to develop almost 10% of *Cyanobacteria*.
During acclimation, the microbial diversity increased with time in both reactors. Although the modifications of the microbial composition differed in the two reactors, the last samples comprised similar dominant species except for *Chlamydiae* and *Hydrogenedentes*, which were present only in RC, and *Deinococcus*, present only in RW. In particular, under steady-state conditions (t > 60 days), the predominant phyla were *Proteobacteria* (32±4% in RC and 29±2% in RW), commonly found in wastewater treatment, and *Cyanobacteria* (19±7% in RC and 28±2% in RW), which replaced *C. vulgaris* in RC, in agreement with the observations of consortia under microscope (see Section 3.3.3). The phylum *Bacteroidetes*, associated with fecal contamination, progressively reduced its relative abundance in both reactors, reaching 12±2% in RC and 10±4% in RW under steady state conditions.

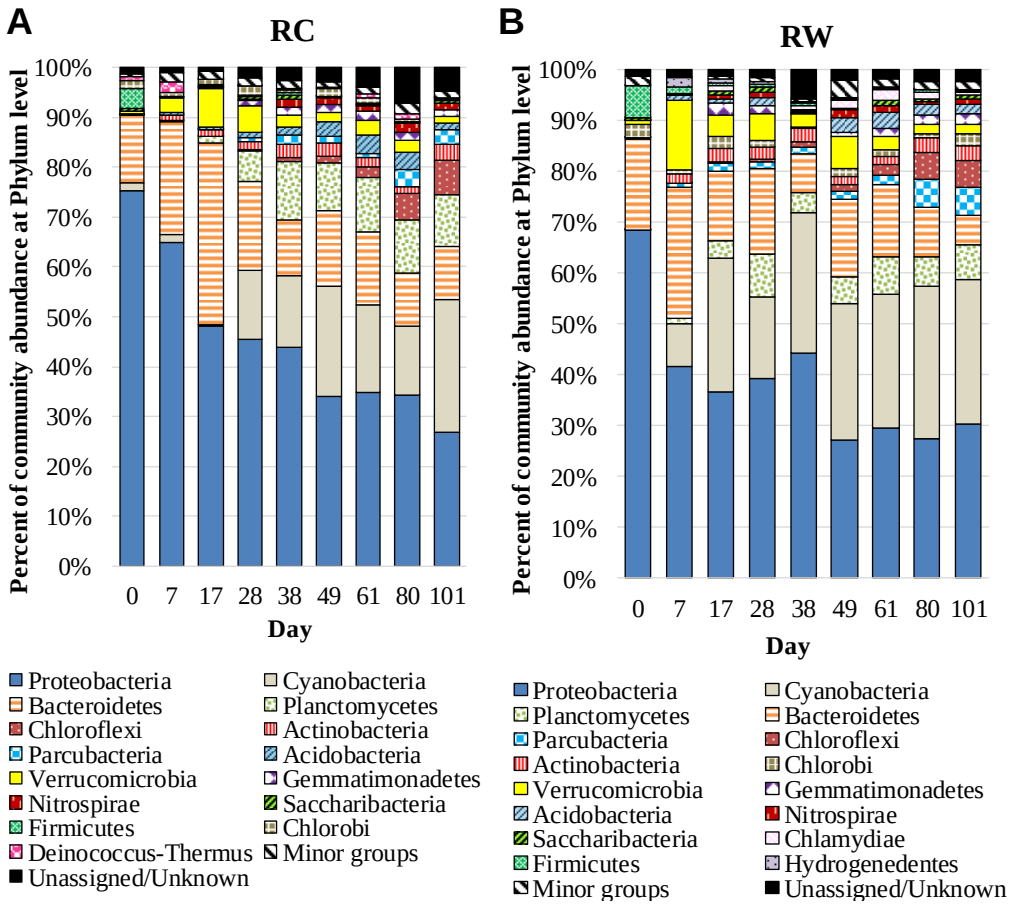

Figure 3.6 *Community bar-plot analysis at phylum level (relative abundance > 1%) in (A) RC (with C. vulgaris inoculum) and (B) RW (without inoculum).*

3.4 Conclusion

The acclimation and steady-state conditions of two microalgal-bacterial consortia developed with or without *C. vulgaris* inoculum were investigated in detail. The main findings are summarized in what follows:

- *Pollutant removal* - COD and ammonium removals were mainly associated with bacteria activity, so the inoculum of *C. vulgaris* played a negligible role. Conversely, the inoculum with *C. vulgaris* improved P removal significantly but only during the first period of acclimation when *C. vulgaris* was dominant;
- *DO and pH profiles* - In the presence of *C. vulgaris* very high variations of DO and pH were observed, while the variations became narrower and profiles more stable when the consortia evolved towards granular flocs under steady state conditions;
- *Productivity and TSS concentration* - They are higher in the reactor inoculated with *C. vulgaris* due to the enhanced photosynthetic productivity;
- *Settleability* - Despite the different evolution of two consortia, good settleability and low effluent solids were obtained in both reactors after 2 months, due to the formation of well-settleable granular flocs;
- *Microbiology* - Despite the different evolution of the microbiota, the composition of the consortia was quite similar in both reactors under steady state conditions, with the dominance of filamentous photosynthetic microorganisms in the granular structure.

These results confirm that the inoculum with pure microalgae strains is not necessary in photobioreactors aimed at treating real wastewater. In fact, no significant differences were observed between the performances of the photobioreactors with or without *C. vulgaris* inoculation. Moreover, the photosynthetic microorganisms were able to grow spontaneously without inoculation, reaching steady state conditions in a couple of months.

Acknowledgements

The authors thank Giovanna Flaim (Research and Innovation Centre, Edmund Mach Fondation, San Michele all'Adige, Italy) for providing *Chlorella Vulgaris*.

CHAPTER 4

PHOTOBIOREACTORS START-UP AND INITIAL MICROALGAL INOCULATION: MICROBIOTA EVOLUTION

This Chapter focuses on the influence of the initial microalgal inoculation on the composition and evolution of the microbial community developed in the experiment presented in Chapter 3.
16S rRNA gene sequencing and shotgun metagenomics revealed that the initial microalgal inoculation did not affect the long-term bacterial community composition. In addition, new environmental species associated to microalgal-bacterial consortia were discovered.

This research was made in collaboration with the Department of Cellular, Computational and Integrative Biology (CIBIO) - University of Trento.

This Chapter is based on:
Petrini S., Masetti G., Foladori P., Beghini F., Armanini F., Segata N., Andreottola G. *Influence of Chlorella vulgaris inoculation on the microbiota evolution of photobioreactors treating real municipal wastewater.* In preparation

Abstract

Microalgal-bacterial consortia have been regarded as a promising alternative for wastewater treatment. However, the role of initial microalgal inoculation is still poorly understood.

In this study, two identical photobioreactors, one inoculated with *Chlorella vulgaris* and the other without inoculum, were fed with real municipal wastewater and run in parallel until steady-state conditions were reached. Biochemical analyses were coupled with next generation sequencing (NGS) to understand the role of initial algal inoculation on the treatment performance and microbiota evolution.

Chemical oxygen demand and ammonium removal (93% and 99%, respectively) were associated to bacterial activity. Inoculum of *Chlorella vulgaris* initially delayed the development of full nitrification. NGS data revealed that the initial inoculation of *Chlorella vulgaris* did not affect the long-term bacterial community evolution. Despite the initial differences, the microbiota of both reactors shifted from the one of the influent wastewater towards a similar community, suggesting an adaptation to the operational conditions.

Collectively, our results show that the initial algal inoculation is not necessary in photobioreactors aimed at treating real wastewater, because microalgal-bacterial consortium can developed spontaneously from the resident-wastewater microorganisms. In view of the full-scale application, this means avoiding high sterilization cost of the wastewater and expensive initial algal inoculation.

4.1 Introduction

The combination of microalgae (both eukaryotic microalgae and prokaryotic cyanobacteria) and bacteria has been regarded as a promising solution for wastewater treatment, alternative to the conventional activated sludge (Ramanan et al., 2016; Arcila and Buitrón 2017; Wang et al., 2018). Microalgae and bacteria symbiosis relies mainly on the oxygen and carbon dioxide exchanges. In the presence of light, microalgae produce the oxygen through photosynthesis to sustain bacterial activity. In return, bacteria produce carbon dioxide essential for photosynthesis.

Microalgal-bacterial consortia proved to be effective in the treatment of different types of wastewater (Wang Y. et al., 2016; Lee and Lei 2019), without artificial aeration that represents up to 50% of the operational energy costs of conventional wastewater treatment plants (WWTPs). In particular, closed photobioreactors may represent a suitable implementation to compete against expensive activated sludge reactors (Posadas et al., 2017).

Microalgal-bacterial consortia have been mainly tested in photobioreactors at lab-scale treating synthetic or sterilized wastewater, with microalgal inoculum in most cases (Cuellar-Bermudez et al., 2017). However, in view of the full-scale application, real wastewater contains inevitably other microorganisms (Saunders et al., 2016; Kang et al., 2018). Hence, inoculation of microalgae does not guarantee their persistence in the system (Xu et al. 2009). Resident-wastewater microorganisms cannot be avoided due to high sterilization costs. In addition, inoculation is not (economically) feasible at large scale (He et al. 2013). On the other hand, microalgal-bacterial consortia can naturally develop from real wastewater (He et al., 2013; Arango et al., 2016; Tsioptsias et al., 2016; Cho et al., 2017; Kang et al., 2018).

To date, the role of the initial inoculation of microalgae on the wastewater treatment performance and consortium development during acclimation is still poorly understood (García et al., 2018; Higgins et al., 2018). In particular, little is known about the bacterial community dynamics and the interactions with the inoculated microalgae.
While some studies have investigated the role of different inoculation ratios in the development of microalgal-bacterial consortia (Su et al., 2012; Arango et al., 2016; Sun L. et al., 2019), comparative studies with consortia spontaneously developed from real wastewater are rare. In general, few studies have investigated the evolution of microalgal-bacterial consortia and their composition through DNA-based analyses (Mishra et al., 2019).

Within this framework, the aim of the study was to determine the role of the initial inoculation of a microalgal strain (1) on the treatment performance and (2) on the development of the microbiota (bacterial composition and diversity)

in photobioreactors treating real municipal wastewater.
Two photobioreactors, fed with the same wastewater, were started-up and run in parallel for 101 days. One reactor (RC) was inoculated with *Chlorella vulgaris* (*C. vulgaris*), and the other (RW) was started without microalgal inoculum. *C. vulgaris* was chosen as model microalgae since it has been widely tested (Safi et al., 2014; Gonçalves et al., 2016). Pollutant removal efficiency and bacterial community characteristics were monitored to assess the influence of the inoculation during the acclimation period until steady-state conditions were reached. Biochemical analyses were coupled with 16S rRNA gene sequencing. In addition, shotgun metagenomics was performed on targeted samples to provide an in-depth evaluation of microalgal-bacterial consortia compositions.

Our study provides valuable information about the start-up of photobioreactors and the development of stable microalgal-bacterial consortia.

4.2 Materials and Methods

4.2.1 Experimental set-up

Two identical photobioreactors, named RW and RC, were operated in parallel as photo-sequencing batch reactors and fed with the same wastewater (Figure 4.1). The reactors (12 cm diameter; 20 cm height; Colaver, Italy) had a working volume of 1.5 L. Initially, the reactors were filled with wastewater and only one was inoculated with *C. vulgaris* (RC). Except for the first week of acclimation (without feeding), the reactors were fed 3 times per week (duration of each cycle 2-3 days). Reactors were continuously illuminated by a fluorescent tube (F30W/33, General Electric, UK) that provided a light intensity of 45 μmol m^{-2} s^{-1} at the inner wall. Stirring was provided by mechanical stirrers set at 50 rpm. The systems, not sealed from the atmosphere, were operated at room temperature (24±2.0 °C). No external aeration was provided and pH was not controlled. At the end of each cycle, effluents were discharged after 1-hour-sedimentation phase.

4.2.2 Microalgal strain inoculated in RC

C. vulgaris culture was a gift of the researcher Giovanna Flaim (Edmund Mach Foundation, Italy). Prior to inoculation, *C. vulgaris* was grown in Algae Broth medium (modified by Allen, 1952). The culture was settled and used as inoculum. The initial concentration of *C. vulgaris* inside RC was measured through flow cytometry (A40 flow cytometer, Apogee Flow Systems, UK), as described in Chapter 5, and resulted of $6.8 \cdot 10^9$ cell/L.

4.2.3 Influent municipal wastewater

Real municipal wastewater after primary sedimentation (WW) was collected in the Trento Nord WWTP. No filtration of wastewater was performed and resident microorganisms entered the reactors. WW characterisation is reported in Table S4.1.

4.2.4 Sampling

The reactors were run for 101 days to observe an acclimation phase and a steady-state phase.
Samples of the microalgal-bacterial biomass were collected for DNA extraction from the reactors at the beginning of the experiment (t=0 days, T0), after the first week of acclimation (t=7 days, T7) and then at regular intervals (every 10 days until day 47 and then every 21 days) (Figure 4.1). WW samples were collected every week (Figure 4.1). Samples were immediately stored at -80 °C until further processing.
To monitor the treatment performance, samples of influent (WW) and effluent wastewater were collected 2-3 times per week and immediately analyzed.

4.2.5 Analytical methods

Influent (WW) and effluent wastewater were analyzed for chemical oxygen demand (COD), soluble COD (sCOD), Total Kjeldahl Nitrogen (TKN), NH_4^+-N, NO_2^--N, NO_3^--N, total P and PO_4^{3-}-P, according to Standard Methods (APHA,

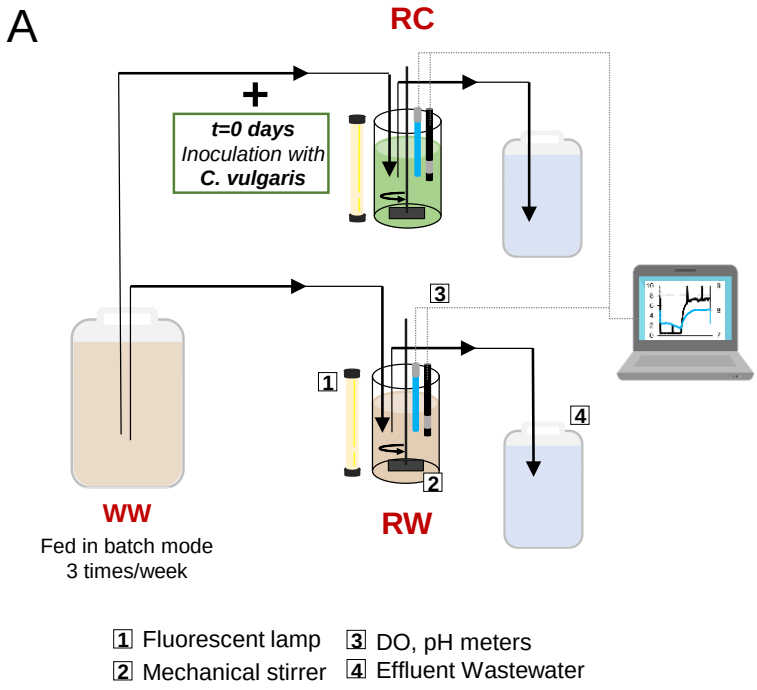

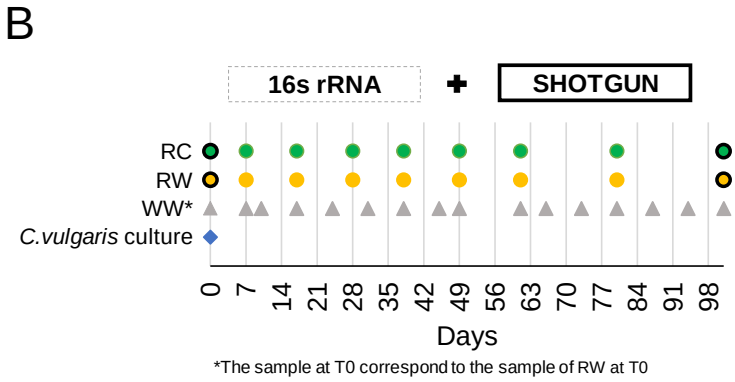

Figure 4.1 *(A) Scheme of the experimental apparatus. RC was inoculated a t=0 days with C. vulgaris (B) Sample collection timepoints for DNA analysis. Samples used for shotgun sequencing are displayed with a thick black border.*

2012). The parameter sCOD was measured after filtration of the sample on 0.45 μm membrane. The light intensity was measured as photosynthetically active radiation (PAR) with a SQ-520 quantum sensor (Apogee Instruments, USA). Dissolved Oxygen (DO), pH and temperature were recorded every 15 minutes with WTW instrumentation (Germany).

4.2.6 DNA extraction and library preparation

DNeasy® PowerSoil® Kit (Qiagen, Germany) was used to extract DNA with a modified protocol. For all samples, the PowerBead was filled with 1 ml of mixed liquor and processed following the QIAGEN DNeasy® PowerSoil® Kit instructions except that the collection tube was centrifuged for 2, 1 and 1 minutes after adding Solution C3, C5 and C6, respectively.
16S rRNA gene sequencing libraries were prepared following the "Illumina 16S metagenomic Sequencing library preparation" slightly modified protocol using the V3-V4 primers (Klindworth et al., 2013) and the Nextera XT Set A indexes (Illumina, San Diego). The first amplification was performed with Q5® High-Fidelity DNA Polymerase kit (New England Biolabs, USA). The samples were sequenced on Illumina MiSeq platform.
Shotgun metagenomics libraries were prepared with "Illumina Nextera XT library preparation" protocol and sequenced on Illumina HiSeq platform (Illumina, San Diego).

4.2.7 16S rRNA gene sequencing processing and analysis

Paired-ends reads were merged with Pandaseq (Masella et al., 2012) using default parameters. Quality-filtering was conducted with Qiime 1.9 (Caporaso et al., 2010) and operational taxonomic units (OTUs) were assigned using the open-reference OTU picking strategy against the 16S reference database SILVA 132 release (Quast et al., 2013). OTUs with less than 10 counts and those assigned to Chloroplast were discarded from the analysis.
Alpha, beta-diversity indices, and phylum-to-genus relative abundances were obtained in Qiime 1.9 (Caporaso et al., 2010). The trend of alpha diversity

indices over-time was calculated through linear regression. Beta-diversity was estimated from the Bray-Curtis dissimilarity matrix and it was represented in a multi-dimensional scaling (MDS) plot. Differences in relative abundances between "pre28" and "post28" days groups were assessed using a pairwise t-test with Benjamini-Hochberg (BH) correction (Benjamini and Hochberg 1995). Correlations between alpha diversity indices and sampling days, and bacteria at the family-level and nitrogen removal compounds were assessed with the Spearman's correlation coefficient.

4.2.8 Shotgun metagenomic analysis, assembly and microbial genome reconstruction

Species-level taxonomic profiling, was performed with MetaPhlAn2 (v2.9.21, database version "mpa_v293_CHOCOPhlAn_201901") , using default parameters (Truong et al., 2015).

To reconstruct microbial genomes from metagenomes (MAGs), the single-sample metagenomic assembly and binning followed the approach of (Pasolli et al., 2019). Briefly, reads were assembled using MEGAHIT v1.2.8 (Li et al., 2015), retaining only contigs longer than 1,000nt. BowTie2 v2.2.9 (Langmead and Salzberg 2012) was used to map reads against contigs with option '–very-sensitive-local' and MetaBAT2 v2.12.1 (Kang et al., 2015) was used for contigs binning, with option '-m 1500'. CheckM v1.0.7 (Parks et al., 2015) was used to quality-control the bins/putative reconstructed genomes. High-quality genomes were defined by >90% CheckM completeness and <5% CheckM contamination and were used for subsequent analysis. Average Nucleotide Identity (ANI) was computed pairwise between putative genomes using FastANI v1.1 (https://github.com/ParBLiSS/FastANI.git).

We next applied a subroutine of PhyloPhlAn2, 'phylophlan2_metagenomic', on our set of MAGs to identify the closest species-level genome bins (SGB), genus-level genome bins (GGB), and family-level genome bins (FGB), additionally to the closest Reference Genome, according to the MASH distance (Ondov et al., 2016). This was computed between the MAGs and a database composed of

162,527 MAGs and 146,186 Reference Genomes. According to these measures, we were able to determine if a specific MAG must be included into an already defined SGB according to the threshold of 5% genetic distance, as defined in (Pasolli et al., 2019). If a MAG results too far in terms of MASH distance to every SGBs, a new SGB must be generated. Thus, we organized the set of "orphan" MAGs applying an average linkage assignment and hierarchical clustering algorithm. The distances for assignment and clustering are based on computing the MASH distances between this subset of MAGs versus themselves. The same procedure has been repeated also for the GGB and FGB level using 15% and 30% of genetic distance, respectively.
Phylogenetic analysis of the high-quality genome bins was performed using PhyloPhlAn2 (version 0.39, repository of Sept 2019) using 400 markers and options: "–accurate –diversity high".

4.3 Results and Discussion

4.3.1 Initial inoculation of *C. vulgaris* does not impact the long-term wastewater treatment performance

The primary goal of the wastewater treatment is the removal of organic compounds and nutrients (nitrogen and phosphorus). To assess the treatment performance of the reactors, COD, sCOD, TKN, NH_4^+-N, NO_2^--N, NO_3^--N, total P and NH_4^+-N, NO_2^--N, NO_3^--N were measured in the influent and effluent wastewater (Table S4.1- S4.3).

Both systems showed a similar COD removal efficiency (Figure 4.2). After one week of acclimation, the reactors had a COD removal efficiency around 88±4% that further increased with time and stabilized after day 60, with average removal efficiency of 92±4% and 93±2% for RC and RW respectively. Despite the fluctuations of COD in the real influent wastewater, RC and RW were characterized by low and stable effluent sCOD concentrations with an average of 31±12 and 29±13 mg COD/L, respectively. COD removal was similar from the beginning and therefore the inoculum of *C. vulgaris* played a negligible role.

These results are in agreement with other works about photobioreactors (Lee et al., 2015; García et al., 2018), in which the organic matter was mainly removed by heterotrophic bacteria.

Nitrogen entered the systems in the form of TKN (average value of 45±15 mg N/L). During the first week of acclimation, both reactors were able to partially remove ammonium (85% and 58%, respectively) but with different removal mechanisms. In RC, ammonium was mainly removed by *C. vulgaris* and ammonia stripping, which was linked to pH increase due to photosynthetic activity (Figure S4.1) (Cai et al., 2013), while nitrification played a minor role. In fact, RC effluent (Table S4.3) contained fewer nitrites (6.1 mg NO_2^--N/L) and nitrates (1.7 mg NO_3^--N/L) compared to RW characterized by effluent concentrations of 19.3 mg NO_2^--N/L and 4.3 mg NO_3^--N/L (Table S4.2). Since RW was not inoculated with *C. vulgaris*, ammonium was partially oxidised into nitrites and nitrates by nitrifying bacteria developed spontaneously from the WW.
In both reactors the ammonium removal efficiency was characterized by a quick evolution after the first 7 days of acclimation with a two-week temporary worsening (Figure 4.2). An accumulation of nitrites was observed in RC and RW until day 28 and 24, respectively. This phenomenon was linked to the development of the Nitrite Oxidizing Bacteria (NOB that included *Nitrospiraceae*, Figure 4.6). At the same time, nitrates increased in the effluent indicating that the main ammonium removal mechanism of both reactors was nitrification. Afterward, ammonium was effectively nitrified during the entire experimentation with removal efficiency of 99±1% and 97±8% in RC and RW, respectively.
Despite a different evolution during the acclimation phase, bacterial nitrification was the main ammonium removal mechanisms in both reactors at T101. Therefore, the inoculation of *C. vulgaris* only delayed the development of full nitrification (Choi et al., 2010).

RC was able to effectively remove P during the first 60 days of acclimation (83±18%) while RW exhibited a low P removal efficiency throughout the entire experimentation (41±13%) (Figure 4.2). The decline observed in RC after 60 days could be due to the progressive loss of *C. vulgaris*. At the end, both reactors showed low total P removal efficiency (25±17% and 39±11% for RC and RW

respectively).

Overall, the effect of *C. vulgaris* inoculation on the pollutant removal was negligible since after an acclimation period the reactors showed similar removal efficiency performances.

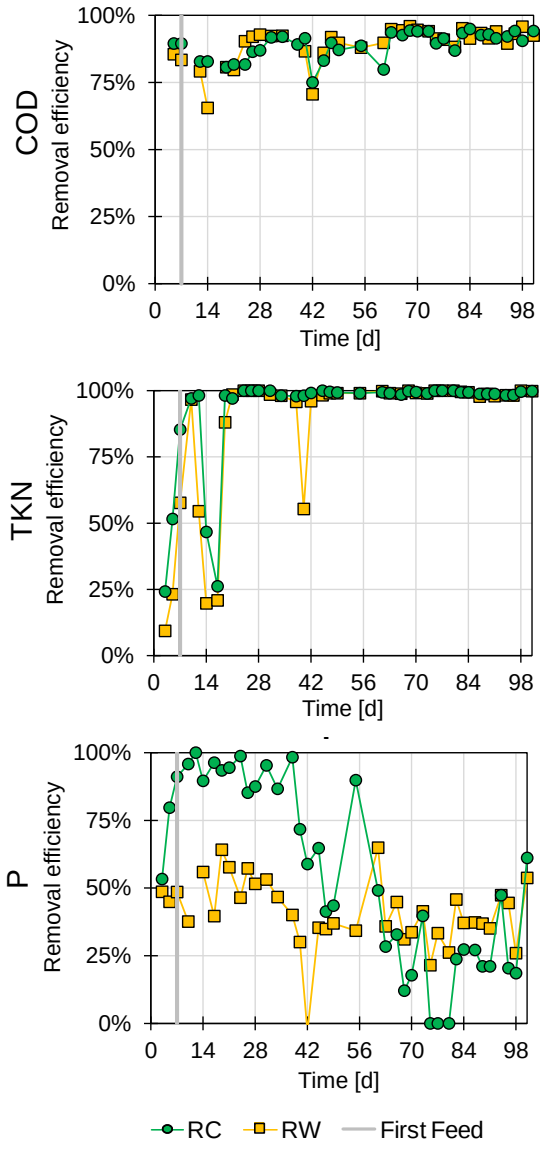

Figure 4.2 *Removal efficiency of COD, TKN and P over time.*

4.3.2 Bacterial communities' evolution towards a similar consortium

16S rRNA gene sequencing was employed to investigate the bacterial composition differences between reactors and WW microbiota. We obtained a total of 3,894,184 reads with a mean 40,564.417±14,627.790 reads/sample, ranging from min 306 (in negative-control sample library) to 71,375 max sample library size.

Alpha diversity indices were calculated to examine the within-group diversity over time. Reactors' indices increased during the experiment. In particular, RC showed a significant correlation between indices and days of sampling (Figure 4.3). From day 49, RC was characterized by a higher richness (i.e. Chao1 and the number of observed OTUs) and a higher evenness of the bacterial communities compared to RW, suggesting that the initial inoculum of *C. vulgaris* may have promoted bacterial growth and adaptation (Ramanan et al., 2016). In the long-term, both reactors tended to higher diversity suggesting a more stable bacterial community (Tang et al., 2018). On the contrary, WW showed a significant decreasing richness (Chao1 R=-0.59, P=0.026) but a more stable evenness over time.

To reveal differences and similarities of bacterial communities over time, beta-diversity was calculated with the Bray-Curtis dissimilarity matrix. The three groups (WW, RC, RW) showed a spatial separation except for T0, in which the microbiota composition of the reactors clustered according to the composition of the WW (Figure 4.3), as they were initially filled with the same wastewater.

Due to the variability of real wastewater, the bacterial communities of WW showed an undefined pattern towards time points, with samples clustering in proximity.

After 7 days of acclimation in batch mode, reactors microbiota radically changed from that of WW. In particular, RC sample was closer to *C. vulgaris* culture. In fact, the culture of *C. vulgaris* was not axenic but had its own associated bacterial community (Figure 4.3). At T7, RC showed a very low Chao1 index and

observed OTUs (Figure 4.3) suggesting that *C. vulgaris* affected the development of bacteria except the one that were present in the inoculum.
Hereafter, the reactors bacterial community experienced a continuous change with time, shifting from WW to a more stabilized community represented by a long-term photobioreactor (pilotPR, i.e. a microalgal-bacterial consortium working from more than 2 years in a similar photobioreactor, (Chapters 6, 13)). The transformation of reactors bacterial communities was more pronounced between 28 days (T28) and 61 days (T61) as shown in the MDS plot (Figure 4.3), where samples moved from left to right. From T61, the distance between reactors samples collected on the same day diminished, indicating that the microbiota was becoming more similar to each other, slowly converging towards the long-term pilotPR.
Taken together, this data indicates that time had a major effect in both reactors. The greater differences between the two groups were at T38, T49 and T61. To note, the operational conditions remained unchanged throughout the experiment, the only variables were the characteristics of the WW.

At the taxonomic level, 52 phyla and 747 genera were identified. *Proteobacteria* was the most abundant phylum in all samples ranging from 29% to more than 50% (Figure 4.4). *Proteobacteria* has been widely found in municipal WWTPs (Cydzik-Kwiatkowska and Zielińska 2016; Zhang et al., 2017). As in our samples, *Proteobacteria* mostly belonged to the class *Betaproteobacteria* (Wu et al., 2019) involved in organic matter degradation and nutrient removal (Nascimento et al., 2018; Cydzik-Kwiatkowska and Zielińska 2016).
In WW samples, the most abundant phylum was *Proteobacteria*, in line with the findings of Ye and Zhang (2013), followed by *Bacteroidetes* (>17%) and *Firmicutes*, representing all together at least 85% of the bacterial community. The microbiota composition of the WW remained stable during the experiment.
The composition of the reactors samples at T0 was similar to that of WW. However, RC at T0 contained also bacteria associated with the *C. vulgaris* inoculum. Even under laboratory cultivation conditions of unialgal cultures, certain bacteria may accompany microalgae (Lee et al., 2015), which in this case were the

genera *Massilia* and *Janthinobacterium* belonging to the phylum *Proteobacteria* (Figure S4.2).

After the acclimation in batch mode at T7, both reactors showed a large shift in the bacterial structure (Figure 4.3, 2C). Out of the most abundant phyla at T0, *Proteobacteria* and *Bacteroidetes* persisted in the reactors while *Firmicutes* dramatically reduced passing from 4% to 0.5% in RC, and from 6% to 1.5% in RW. A similar result was reported by Higgins et al., (2018), testing a wastewater microbial community with microalgae in the treatment of winery wastewater. At the same time, *Cyanobacteria* spontaneously developed in RW (1%) and gradually increase from T38, replacing *Bacteroidetes* as second abundant phyla in the last sample. In RC, *Cyanobacteria* started to establish after T28 at higher abundance than RW, reaching 21% in the last sample.

The shift in bacterial population during the first 7 days suggests an adaptation of the community to the operational conditions of the reactors. Moreover, the development of *Cyanobacteria* in RW demonstrates that a microalgal-bacterial consortium can develop spontaneously from the influent wastewater. In fact, *Cyanobacteria* is the largest and widely distributed group of photosynthetic prokaryotes (Dvořák et al., 2017).

Over time, low abundant phyla present in WW developed in the reactors such as *Planctomycetes* and concomitantly *Cyanobacteria*. From T38, both reactors presented higher relative abundance of *Planctomycetes* (6%-12%), however no genus related to the Anammox (Fuerst and Sagulenko 2011) was here found (data not shown). *Nitrospirae* developed earlier in RW after 17 days and in RC only after 28 days. Even at lower relative abundance (around 1% in the last four timepoints), *Nitrospirae* played a central role in nitrification since it contained dominant NOB, i.e. *Nitrospira spp.*

To note, *Acidobacteria*, *Chlorobi*, *Chloroflexi* and *Gemmatimonadetes* phyla comprise phototrophic bacteria that exploit light as an energy source for the growth without oxygen production (Zeng and Koblížek 2017). As observed in the MDS plot (Figure 4.3), starting from T61, the composition of the reactors became more similar to each other. The above results demonstrated that the initial inoculation of *C. vulgaris* did not affect, in the long-term the bacterial

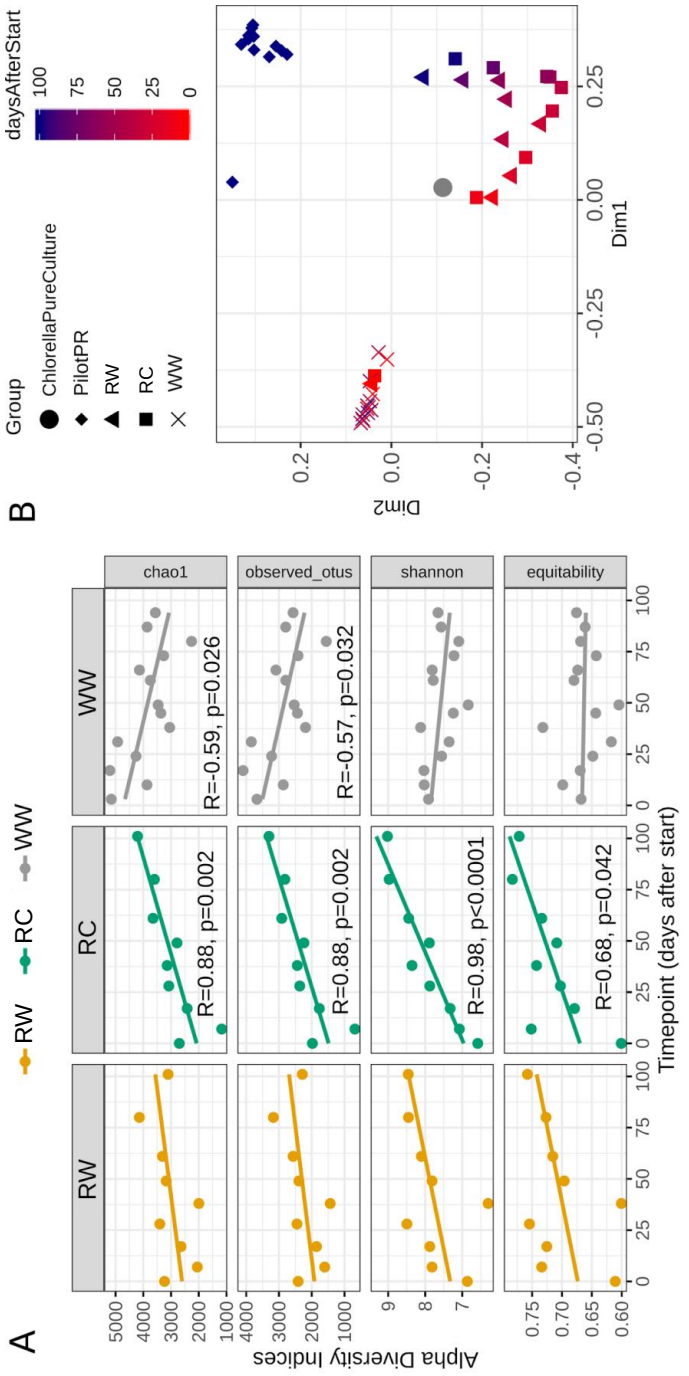

Figure 4.3 *(A) Alpha diversity indices in each group amongst time points (days after start) modelled through a linear regression. (B) Multi-dimensional scaling (MDS) plot based on Bray-Curtis dissimilarity matrix.*

community, which stabilized in the reactors over time.
Interestingly the top-5 most abundant bacterial phyla found in the late reactors timepoints, expect of *Cyanobacteria*, were frequently detected and have been considered typical resident of activated sludge (Gao et al., 2016; Zhang et al., 2017; Zhang et al., 2018; Xu et al., 2018; Kim et al., 2019).

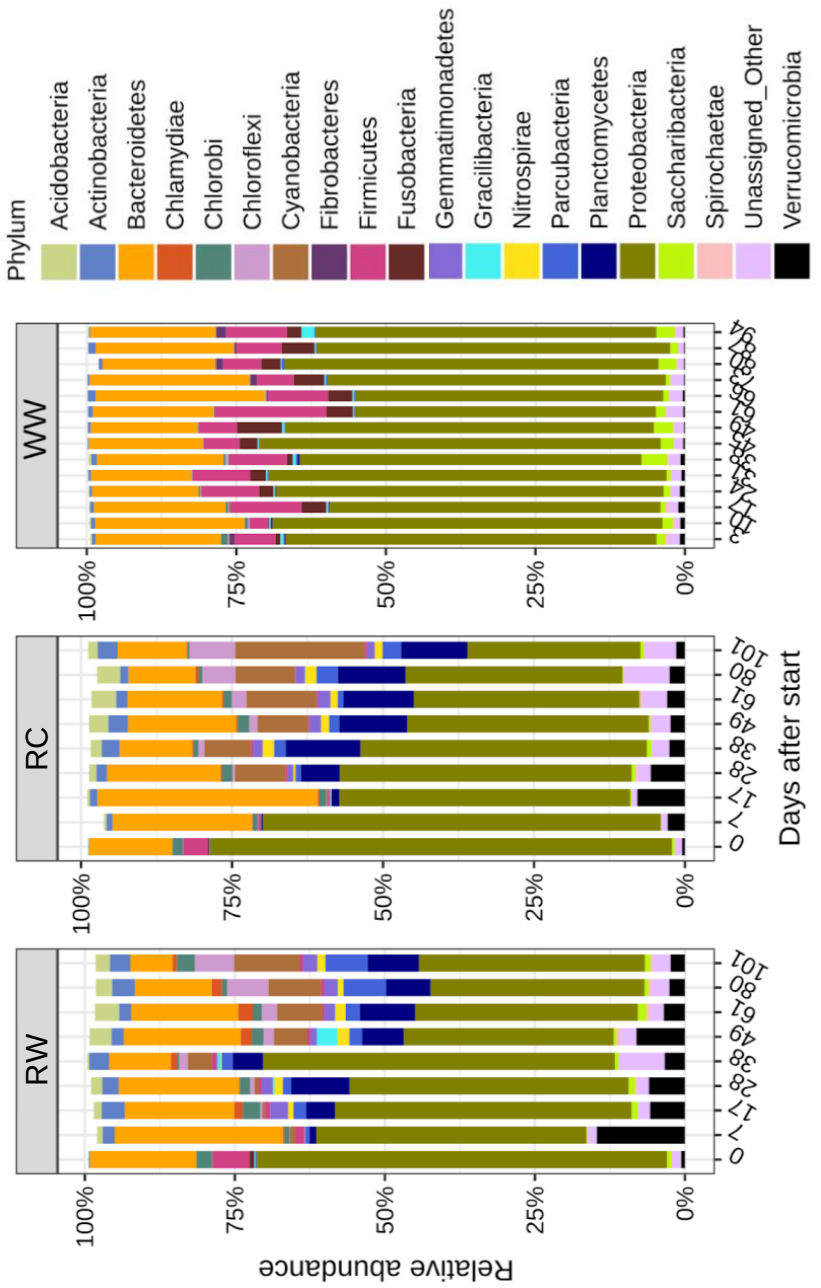

Figure 4.4 *Top-20 most abundant phyla distribution as percentage abundances in each group and per time points sampled. Low-abundant phyla were grouped together.*

4.3.3 Microbiota structure of photobioreactors differs from the influent wastewater microbiota

Consistent with the beta-diversity results, the heat-map at phylum level revealed time-related changes of the bacterial community inside the reactors and its separation from WW.

WW showed a unique clustering compared to the others, while differences in the phylum composition were identified amongst time points in RC and RW groups (Figure 4.5).

The composition of the bacterial community of the reactors varied with time. RC and RW at T0 clustered together with WW. After the first week of acclimation, the microbial composition of both reactors shifted towards a distinct structure with respect to WW. Changes of the bacterial communities can be appreciate in Figure 4.5 where reactors samples cluster form left to right over time.

The most abundant phyla of bacteria that entered the reactors with WW were replaced. The bacterial communities that developed in the reactors were completely different from WW. The microbial communities in the reactors were affected by the operating conditions that created an environment not suitable for the most abundant bacteria that entered the systems.

Reactors' bacterial communities from days 80 and 101 clustered together on the right branch of on-column hierarchical clustering revealing that, with time, the microbial community structures of the two reactors converged and *C. vulgaris* gradually left the system (Chapter 3, Section 3.3.4), due to its poor settleability (Barros et al., 2015). The similar microbiota structure between reactors at the end of the experimentation was also reflected on the genus level (Figure S4.2).

To appreciate the temporal variability of the bacterial communities inside the reactors, the relative abundance of both reactors at phylum level, were grouped before and after T28 (Figure 4.5). It is worth noting that both reactors reached full nitrification after T28 (Figure 4.6). Hereafter, the bacterial community in both reactors, evolved towards a microbiota different from WW. The most abundant phyla that developed after T28, stabilized in both reactors. In particular, *Planctomycetes*, *Cyanobacteria*, and *Nitrospirae* increased in the reactors while *Proteobacteria* and *Bacteroidetes* decreased.

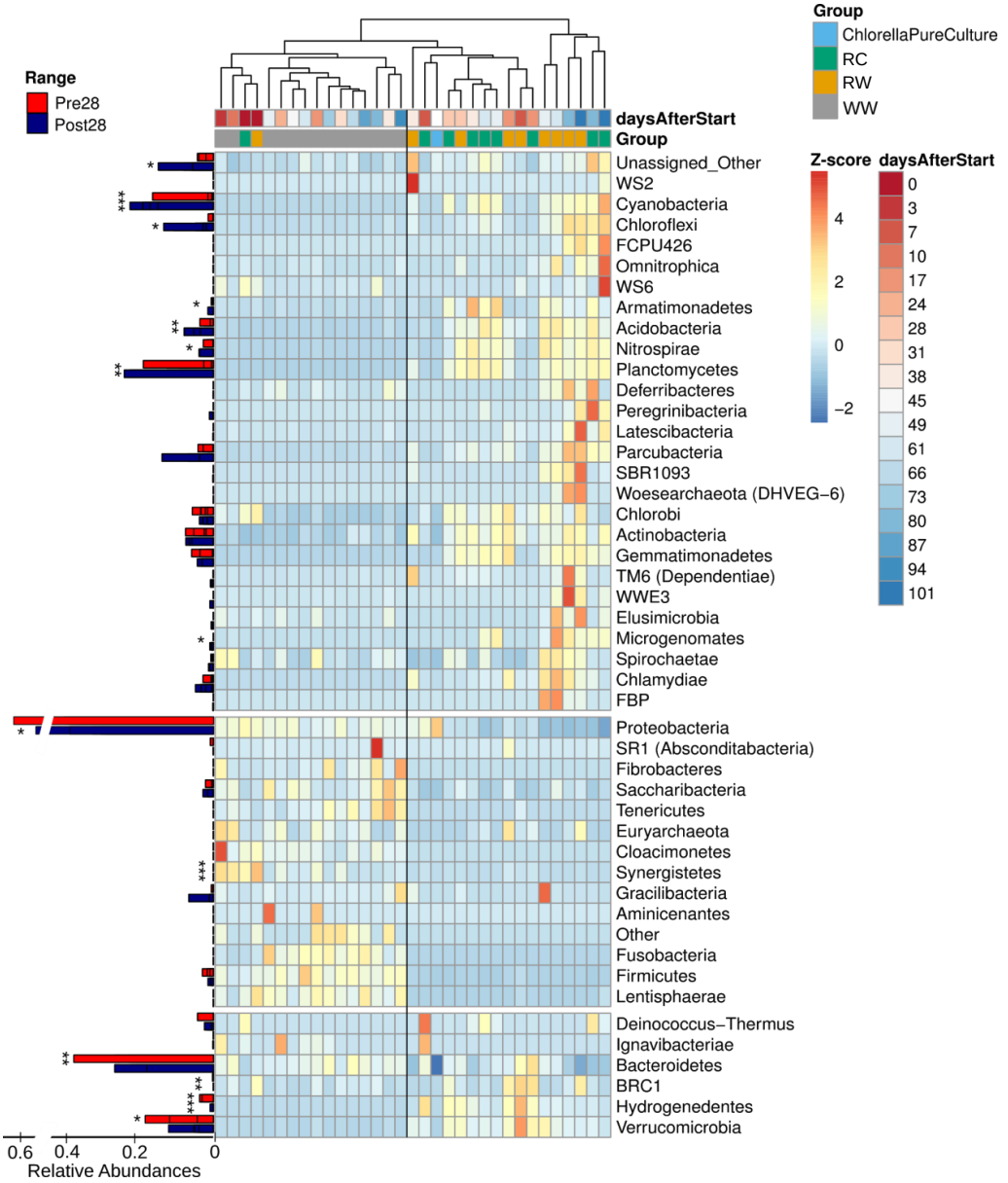

Figure 4.5 *Heat-map of the most abundant phyla according to days of sampling and groups. Change in the color from blue to red refers to the row Z-score. Barchart refers to the relative abundance of each phylum before (pre28) and after (post28) the 28th day of sampling in RC and RW. Welch t-test with Benjamini-Hochberg correction: *** P<0.005; ** P<0.01; * P<0.05.*

4.3.4 Initial inoculation of *C. vulgaris* delays the development of full-nitrification

Bacterial communities that are responsible for nitrification are called "nitrifiers" and include ammonia oxidizing bacteria (AOB) and nitrite oxidizing bacteria (NOB) (Johnston et al., 2019). To complete the oxidation from ammonium to nitrates is essential that AOB and NOB coexist.

The correlation of AOB and NOB dynamics with ammonium oxidation was made by comparing over time the effluent concentrations of N-forms from the reactors with the relative abundances of *Nitrosomonadaceae* and *Nitrospiraceae* bacterial families (Figure 4.6). The family *Nitrosomonadaceae* includes the majority of known AOB (Prosser et al., 2014), while the family *Nitrospiraceae* comprised the genus Nitrospira (i.e. the dominant known NOB in engineered systems (Daims 2014; Wu et al., 2019).
In both reactors, ammonium oxidation consisted at the beginning in a partial nitrification (i.e. residual effluent ammonium and significant nitrite accumulation). Full nitrification was reached after T28 and T24 in RC and RW, respectively, concurrently with the development of the families *Nitrosomonadaceae* and *Nitrospiraceae*.
At T7 (i.e. with no feeding) *Nitrosomonadaceae* abundance increased in RW (1.9%) and hardly in RC (0.2%) (Figure 4.6A). *Nitrosomonadaceae* remained in RW at concentration higher than 0.7% except for day 38. At T40, RW was not able to remove ammonium completely (due to biomass washout at T38) and at the same time, the relative abundance of *Nitrosomonadaceae* was close to zero. In RC, *Nitrosomonadaceae* increased with time until T28 and afterwards remained at concentration higher than 1%.
The development of *Nitrospiraceae* in both reactors followed nitrate production (Figure 4.6B) as a result of nitrite oxidation. In particular, the abundance of *Nitrospiraceae* in RC strong positively correlated with effluent nitrates ($R=0.95$, $p<0.001$; Figure S4.3). The RC showed a delay in the development of full nitrification linked to considerable pH fluctuations during the cycle until T35 (Figure S4.1). In particular, microalgae, through photosynthesis, increase the pH that

may inhibit bacteria (Choi et al., 2010), especially NOB (Liu et al., 2015). In RW, *Nitrospiraceae* presented a faster establishment from the beginning. Similar to what observed for *Nitrosomonadaceae*, at T38 *Nitrospiraceae* was almost absent in RW, which coincided with a worsening in TKN removal efficiency at T40 (Figure 4.2).
In both reactors, once reached the complete ammonium oxidation, only nitrates were present in the effluent and the relative abundance of *Nitrosomonadaceae* and *Nitrospiraceae* stabilized. The presence of *C. vulgaris* in RC delayed indirectly the development of full nitrification. In particular, the pH fluctuation linked with the photosynthetic activity of *C. vulgaris* delayed at the beginning the establishment of *Nitrosomonadaceae* and inhibited the presence of *Nitrospiraceae*. Similarly, Huang et al. (2015) reported that *Nitrosomonadaceae* and *Nitrospiraceae spp.* relative abundances lowered in presence of algae compared to the control reactor seeded only with activated sludge, resulting in decreased nitrification efficiency.

In addition, these results demonstrated the central role of AOB and NOB in N-removal, even if present at low concentrations.

The denitrification process was not favored inside the reactors since light was provided 24 hours (i.e. continuous photosynthetic oxygenation). However, anoxic condition may have occurred in the deeper part of the flocs resulting in a spontaneous partial denitrification. Since a lot of heterotrophic bacteria are facultative anaerobe able to perform denitrification (Wang et al., 2018), no bacterial family was considered in particular.

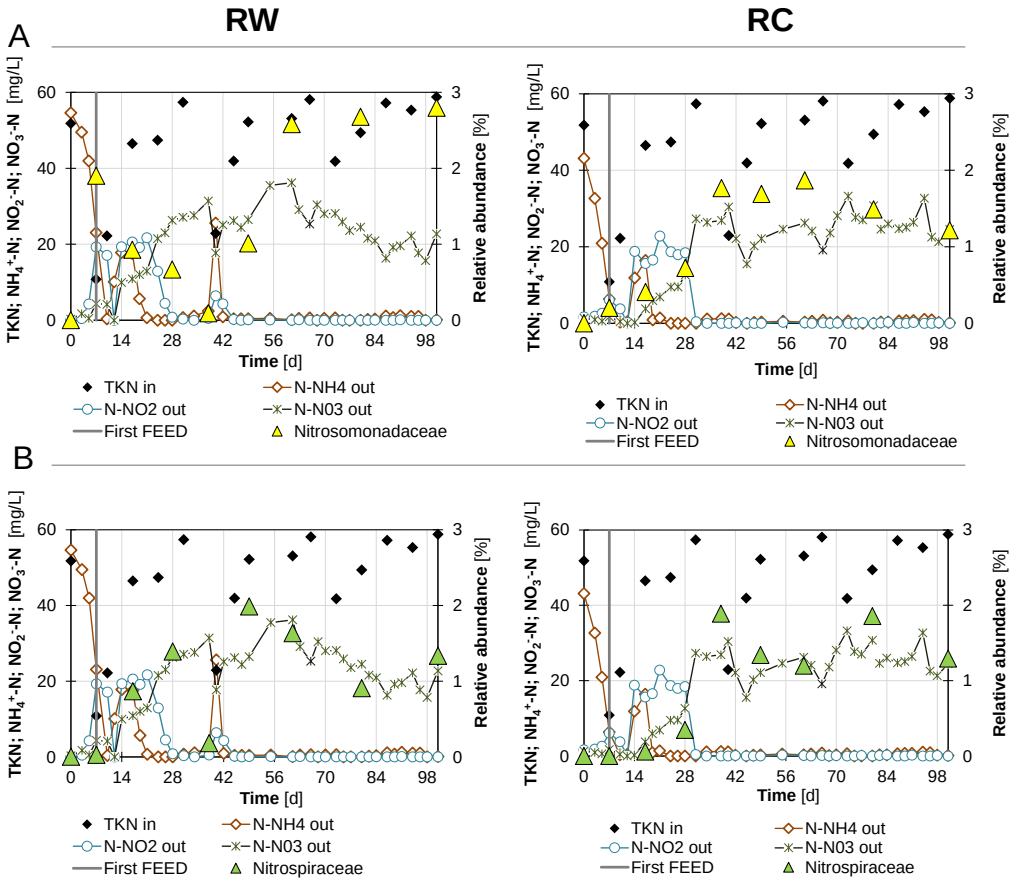

Figure 4.6 *Superimposition over time between effluent N-forms and relative abundance of the families (A) Nitrosomonadaceae and (B) Nitrospiraceae. Influent TKN was added for completeness.*

4.3.5 Shotgun metagenomics identified novel photobioreactors-associated bacterial species

To explore the reactors-associated microbiome at the species level and to possibly discover previously uncharacterized bacteria, shotgun metagenomics was performed on a total of 4 samples from the two reactors at T0 and at T101 (Figure 4.1). Metagenomic profile at the species-level was obtained with MetaPhlAn2 (Truong et al., 2015), from which a total of 575 taxa were identified. Out of the 20-most abundant species, *Arcobacter cryaerophilus* and *Bacteroides graminisolvens* were the most abundant in reactors at T0 while *Pseudanabaena sp.* SR411 and *Nitrospira defluvii* at T101, with some differences between the reactors. Bacterial species representative of the T0 (which also reflects the WW microbiome) were previously found in raw wastewater (sewage). In particular, *Arcobacter cryaerophilus* is an emerging pathogen, associated with human and animal gastroenteritis (Ferreira et al., 2016). Taxonomies found in T101 were instead representative of the reactors acclimatation process. Interestingly, while *Nitrospira defluvii* was previously isolated and characterized from activated sludge (Spieck et al., 2016), to our knowledge, there is no report of its presence in microalgal-bacterial consortia. Similarly, *Pseudanabaena sp. SR411*, a filamentous cyanobacterium possibly capable of nitrogen removal, was isolated only from Susquehanna River (Sullivan et al., 2018). *Pseudanabaena sp.* is a common and harmful species in freshwater *Cyanobacteria* blooms (Gao et al., 2018).

Using a similar assembly approach to that published in Pasolli et al. (2019), we retrieved 29 high-quality (i.e. >95% completeness and <5% contamination, Parks et al., 2015) metagenome-assembled genomes (MAGs) from reactors samples. None of the MAGs matched with anything known at the time of writing this work. In particular, these genomes distributed over 26 SGBs that have never been previously described and thus represent novel taxa. We relied on the taxa of the closest reference genomes for the mechanism of assignment a taxonomic label to the newly defined SGBs. In particular, we were not able to assign taxa at the species level, neither at the genus level which were therefore defined

to as “unknown SGBs” (uSGBs) (Pasolli et al., 2019). The SGB 35246, which is composed of one MAG only, results to be the only exception because of the presence of three Reference Genomes in the same FGB with the same taxonomic label k_Bacteria|p_Nitrospirae|c_Nitrospira|o_Nitrospirales|f_Nitrospiraceae (Table 4.1). 11/26 (0.42%) uSGBs belonged to the RC samples, all but 1 from T101. 15/26 (0.58%) uSGBs belonged to the RW samples, with 3/15 SGBs from the T0 sample. There was at least one genome retrieved per SGB. Interestingly, RC and RW at T101 shared three uSGBs, with an average nucleotide identity (ANI) close to 99% (Table 4.1).

To investigate the acclimatation process towards a more stabilized community, we also retrieved MAGs from the pilotPR sample (Chapters 6, 13) using the same approach described, obtaining 10 high-quality uSGBs (Table 4.1) which were included in the phylogenetic analysis. RC shared one uSGB with the pilotPR with a 99.76% ANI value, while RW shared a uSGB with 98.50% ANI value (Table 4.1). New SGB were found especially at T101 because microalgal-bacterial consortia that treat wastewater are still unexplored (Mishra et al., 2019).

Retrieved genomes	Retreived from	Time point	SGB type	Closer taxonomic level assigned	ANI*
1	RW	T0	uSGB	k__Bacteria|p__Chlorobi	
1	RW	T0	uSGB	k__Bacteria|p__Proteobacteria	
1	RW	T0	uSGB	k__Bacteria|p__Proteobacteria	
1	RW	T101	uSGB	k__Bacteria|p__Cyanobacteria	
1	RW	T101	uSGB	k__Bacteria|p__Bacteroidetes	
1	RW	T101	uSGB	k__Bacteria|p__Candidatus_Kapabacteria	
1	RW	T101	uSGB	k__Bacteria|p__Nitrospirae|c__Nitrospira|o__Nitrospirales|f__Nitrospiraceae	
1	RW	T101	uSGB	k__Bacteria|p__Proteobacteria	
1	RW	T101	uSGB	k__Bacteria|p__Proteobacteria	
1	RW	T101	uSGB	k__Bacteria|p__Proteobacteria	
1	RW	T101	uSGB	k__Bacteria|p__Proteobacteria	
1	RW	T101	uSGB	k__Bacteria|p__Nitrospirae	
1	RW	T101	uSGB	k__Bacteria|p__Bacteroidetes	
1	RC	T0	uSGB	k__Bacteria|p__Proteobacteria	
1	RC	T101	uSGB	k__Bacteria|p__Cyanobacteria	
1	RC	T101	uSGB	k__Bacteria|p__Bacteroidetes	
1	RC	T101	uSGB	k__Bacteria|p__Bacteroidetes	
1	RC	T101	uSGB	k__Bacteria|p__Candidatus_Parcubacteria	
1	RC	T101	uSGB	k__Bacteria|p__Proteobacteria	
1	RC	T101	uSGB	k__Bacteria|p__Proteobacteria	
1	RC	T101	uSGB	k__Bacteria|p__Proteobacteria	
1	PRpilot	na	uSGB	k__Bacteria|p__Cyanobacteria	
1	pilotPR	na	uSGB	k__Bacteria|p__Proteobacteria	
1	pilotPR	na	uSGB	k__Bacteria|p__Proteobacteria	
1	pilotPR	na	uSGB	k__Bacteria|p__Bacteroidetes	
1	pilotPR	na	uSGB	k__Bacteria|p__Bacteria_unclassified	
1	pilotPR	na	uSGB	k__Bacteria|p__Candidatus_Roizmanbacteria	
1	pilotPR	na	uSGB	k__Bacteria|p__Proteobacteria	
1	pilotPR	na	uSGB	k__Bacteria|p__Proteobacteria	
1	pilotPR	na	uSGB	k__Bacteria|p__Nitrospirae	
1	pilotPR	na	uSGB	k__Bacteria|p__Proteobacteria	
2	RW; RC	T101	uSGB	k__Bacteria|p__Bacteroidetes	98.67
2	RW; RC	T101	uSGB	k__Bacteria|p__Chloroflexi	99.9
2	RW;RC	T101	uSGB	k__Bacteria|p__Chlorobi	98.67
2	pilotPR;RW	T101	uSGB	k__Bacteria|p__Cyanobacteria	98.5
2	pilotPR;RC	T101	uSGB	k__Bacteria|p__Chloroflexi	99.76

* average nucleotide identity (ANI) was computed between the two putative genomes retrieved in two different samples and assigned to the same SGB.

Table 4.1 *List of uSGBs retreived from photobioreactors samples and closer taxonomic assignment*

4.4 Conclusion

Collectively, our results show that the initial algal inoculation plays a minor role during the start-up of photobioreactors and it does not affect in the long-term the treatment removal performances and the bacterial community of photobioreactors treating real municipal wastewater.

Even if the bacterial community that established over time in photobioreactors was quite different from the predominant bacteria present in the influent wastewater, the present findings confirm that wastewater microbiota is sufficient to start-up a photobioreactor. In view of the full-scale application, this means avoiding high sterilization cost of wastewater and initial inoculation of microalgae.

In addition, these results suggest that after an acclimation period (about 60 days) in which the bacterial population experiences a progressive change with time, the microbiota converges into a stable structure that adapts to the operational conditions, despite the initial presence of an inoculated microalgae.

Since there are few studies on microbiota evolution in photobioreactors treating real municipal wastewater, future research is needed to confirm these initial findings and to replicate results in a larger scale. Moreover, the use of shotgun metagenomics enabled the discovery of new environmental species associated to photobioreactors, even if from few samples. Increasing the number of samples would be of interest in unravelling the composition of photobioreactors-associated microbiota and its functions, and to explore the uncultured and uncharacterized milieu of photobioreactors-associated microbiota.

Acknowledgements

The authors would like to thank Giovanna Flaim (Edmund Mach Foundation, Italy) who gifted *Chlorella vulgaris*.

Supplementary material

Day [d]	**COD** [mg/L]	**sCOD** [mg/L]	**TKN** [mg/L]	**NO_2^--N** [mg/L]	**NO_3^--N** [mg/L]	**total P** [mg/L]	**PO_4^{3-}-P** [mg/L]
0	324	142	52	0.0	1.0	5.8	3.0
7	127	44	11	0.2	2.2	2.9	0.5
10	168	57	22	0.1	0.7	3.3	0.7
17	300	123	47	0.5	0.9	5.3	1.6
24	376	143	47	0.1	1.3	6.4	3.3
31	314	133	57	0.1	0.9	6.0	3.6
40	136	58	23	0.5	3.6	3.4	1.8
45	233	92	42	0.6	1.5	4.6	2.8
49	282	120	52	0.0	0.3	5.7	3.5
61	408	147	53	0.3	0.8	6.7	3.8
66	368	107	58	0.4	0.3	5.8	3.4
73	220	102	42	0.4	1.0	4.2	2.7
80	394	165	49	0.1	0.9	5.9	3.4
87	267	123	57	0.1	0.9	5.7	5.0
94	306	188	55	0.1	0.8	5.4	4.0

Table S4.1 *WW characteristics*

Day [d]	**sCOD** [mg/L]	**NH_4^+-N** [mg/L]	**NO_2^--N** [mg/L]	**NO_3^--N** [mg/L]	**PO_4^{3-}-P** [mg/L]
0	118	54.6	0.1	0.3	3.2
3	-	49.5	0.4	1.7	3.0
5	47	41.9	4.3	0.5	3.2
7	54	23.1	19.3	4.3	3.0
10	-	0.4	17.1	4.2	1.8
12	35	10.1	0.0	0.0	-
14	58	17.8	19.3	9.9	1.5
17	-	17.6	20.6	10.9	2.0
19	58	5.6	19.1	12.0	1.9
21	61	0.7	21.7	12.9	2.2
24	29	0.0	12.9	21.5	2.8
26	30	0.0	4.5	23.0	2.7
28	27	0.0	0.8	26.3	3.1
31	29	0.7	0.3	27.1	3.0
34	24	1.1	0.0	27.6	3.2
38	-	2.4	0.5	31.4	3.6
40	42	25.6	6.4	17.7	4.2
42	40	0.9	4.3	25.1	3.5
45	19	0.4	0.2	26.2	2.2
47	19	0.4	0.0	24.4	3.0
49	24	0.4	0.1	26.5	2.9
55	34	0.5	0.1	35.5	3.8
61	29	0.1	0.0	36.2	2.0
63	21	0.5	0.1	29.1	4.3
66	23	0.6	0.0	25.3	3.7
68	15	0.0	0.0	30.4	4.0
70	20	0.5	0.0	28.0	3.9
73	22	0.6	0.0	28.1	3.4
75	19	0.0	0.0	25.9	3.3
77	20	0.0	0.0	23.6	2.8
80	26	0.0	0.0	24.5	3.1
82	19	0.2	0.0	21.6	3.2
84	34	0.3	0.0	20.9	3.7
87	26	1.1	0.0	16.3	3.7
89	23	0.7	0.0	19.2	3.6
91	16	1.2	0.1	19.6	3.7
94	28	1.0	0.0	22.2	3.0
96	21	1.0	0.0	17.7	3.0
98	13	0.0	0.0	15.7	4.0
101	23	0.1	0.0	22.7	2.5

Table S4.2 *Effluent characteristics of RW*

Day [d]	**sCOD** [mg/L]	**NH_4^+-N** [mg/L]	**NO_2^--N** [mg/L]	**NO_3^--N** [mg/L]	**PO_4^{3-}-P** [mg/L]
0	467	43.1	1.6	1.3	3.1
3	-	32.7	1.8	0.9	2.7
5	49	20.9	2.6	0.6	1.2
7	49	6.3	6.1	1.7	0.5
10	-	0.3	3.8	0.4	0.1
12	29	0.4	0.1	0.0	-
14	29	11.8	18.8	0.2	0.3
17	-	16.4	15.6	3.7	0.1
19	58	0.9	16.5	5.9	0.3
21	55	1.4	22.8	6.9	0.3
24	55	0.0	18.7	9.5	0.1
26	51	0.0	17.9	9.5	0.9
28	49	0.0	18.4	12.6	0.8
31	31	0.0	0.4	27.3	0.3
34	25	1.1	0.0	26.4	0.8
38	34	1.2	0.0	26.9	0.1
40	27	1.1	0.0	30.4	1.7
42	34	0.2	0.1	22.1	1.4
45	23	0.0	0.0	15.5	1.2
47	24	0.2	0.0	20.2	2.7
49	30	0.3	0.0	22.1	2.6
55	32	0.5	0.3	24.6	0.6
61	57	0.3	0.1	26.2	2.9
63	26	0.5	0.0	24.1	4.8
66	30	0.8	0.1	19.1	4.5
68	21	0.1	0.0	23.6	5.1
70	22	0.3	0.1	28.1	4.8
73	22	0.6	0.0	33.2	3.5
75	23	0.0	0.0	27.7	4.7
77	19	0.0	0.1	27.0	4.2
80	29	0.0	0.0	30.7	4.6
82	26	0.3	0.1	24.6	4.5
84	20	0.3	0.3	26.0	4.3
87	29	0.6	0.0	24.7	4.3
89	19	0.7	0.0	25.1	4.5
91	23	0.7	0.2	26.4	4.5
94	21	1.0	0.0	32.7	3.0
96	18	0.9	0.0	22.5	4.3
98	29	0.2	0.1	21.3	4.4
101	18	0.1	0.0	24.5	2.1

Table S4.3 *Effluent characteristics of RC*

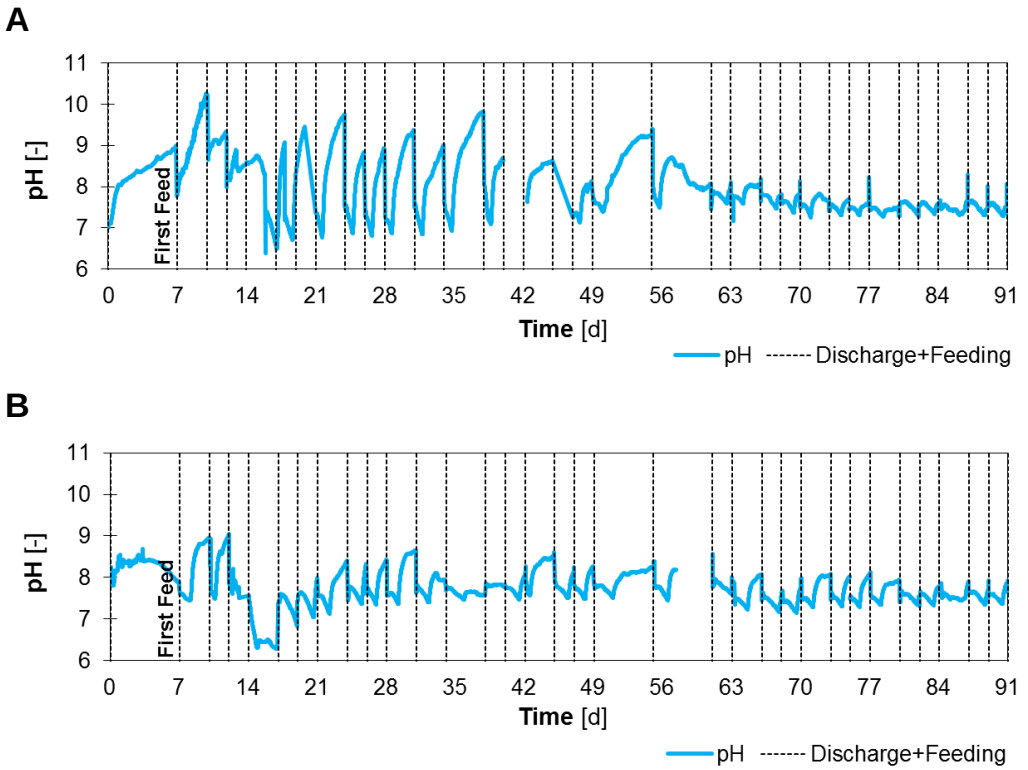

Figure S4.1 *Evolution of pH over time in (A) RC, inoculated with C. vulgaris and (B) RW, without initial microalgal inoculum.*

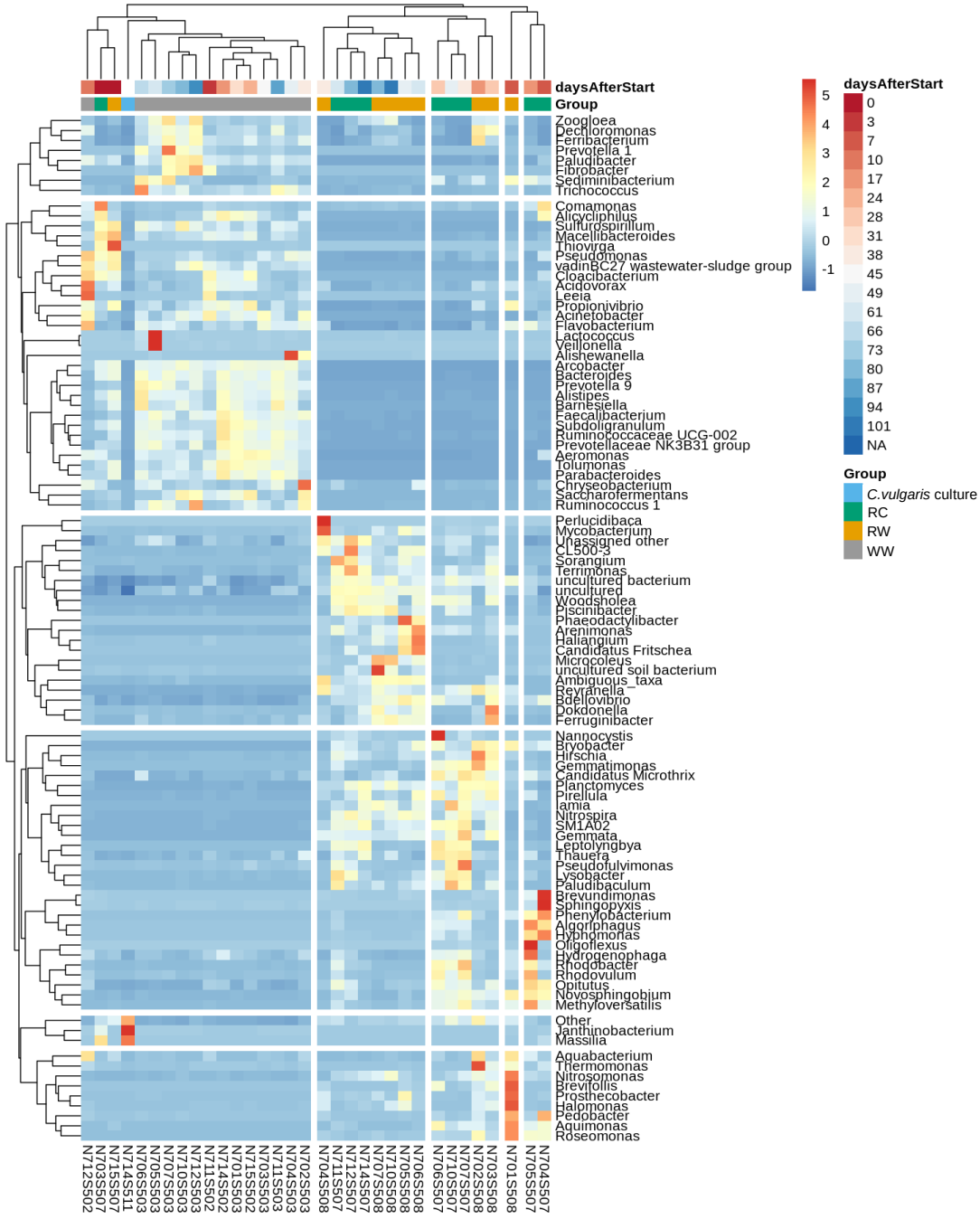

Figure S4.2 *Heatmap of the top-100 most abundant genera according to days of sampling and groups. RW: photobioreactor with wastewater; RC: photobioreactor with wastewater and C. vulgaris inoculum; WW: wastewater after primary sedimentation. Change in the color from blue to red refers to the row Z-score.*

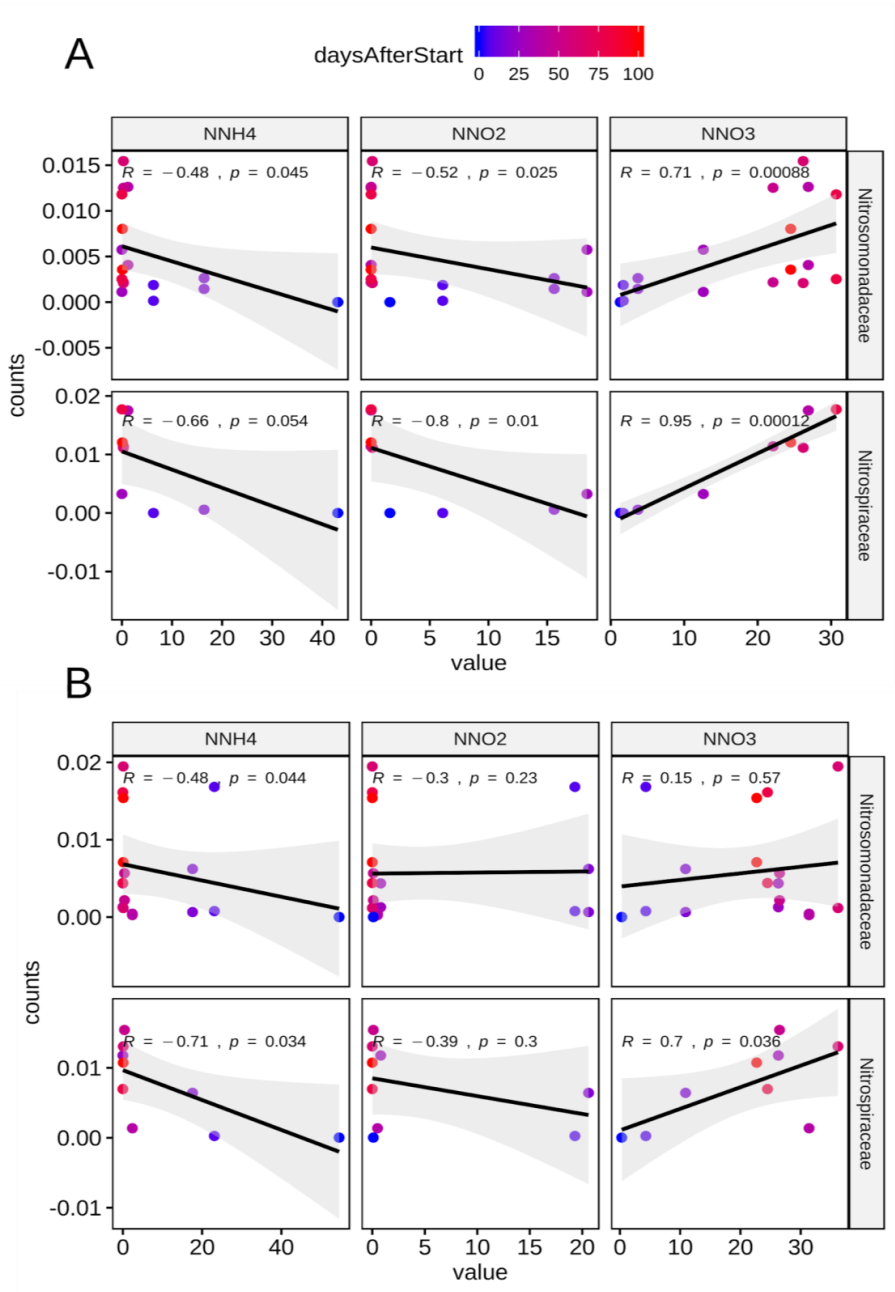

Figure S4.3 *Correlation between bacterial family and effluent nitrogen compounds for (A) RC and (B) RW, according to the Spearman's correlation coefficient (R).*

CHAPTER 5

PHOTOBIOREACTORS START-UP AND INITIAL MICROALGAL INOCULATION: A FLOW CYTOMETRY INVESTIGATION

The influence of the initial microalgal inoculation on the composition of the microbial community developed in the experiment presented in Chapter 3 was investigated through flow cytometry (FCM).
FCM analysis revealed that the microalgae initially inoculated gradually left the system with the effluent. Photosynthetic organisms, entered with the influent wastewater, established in both reactors that over time converged into a similar microalgal-bacterial consortium. Therefore, it was concluded that initial microalgal inoculation is unnecessary to start-up photobioreactors treating real wastewater .

This research was made in collaboration with Agenzia per la Depurazione (ADEP) - Autonomous Province of Trento

This Chapter is based on:
Petrini S., Foladori P., Bruni, L., Andreottola G. *The role of initial microalgal inoculation on the start-up of photobioreactors treating real wastewater, and its outcome in the long term: A flow cytometry investigation.* Bioresource Technology Reports, UNDER REVIEW

Abstract

Microalgal-bacterial consortia represent a sustainable alternative to activated sludge in the treatment of wastewater. However, little is known about the role of initial microalgal inoculation on the start-up of photobioreactors and the development of a microalgal-bacterial consortium that treats real wastewater.

One photobioreactor inoculated with *Chlorella vulgaris* (RC) and another identical photobioreactor without inoculation (RW) were fed with real municipal wastewater and run until steady-state conditions were reached in the treatment. The development and the composition of the microalgal-bacterial consortia were monitored with flow cytometry (FCM). Fluorescent and scattering signals were used to distinguish and quantify microalgae and bacteria both in the mixed liquor and in the effluents.

FCM analysis revealed that microalgae spontaneously developed inside RW. *Chlorella vulgaris* gradually left RC with the effluent because characterized by low settleability. At the end of acclimation, the ratio microalgae/bacteria resulted comparable in the two reactors. Bacterial population in both reactors presented a very slow growth during the first 20 days. Afterwards, they increased concomitantly with the decreasing in effluent concentrations of both microalgae and bacteria.

Despite the initial differences, the composition of both reactors converged into a similar microalgal-bacterial consortium, structured in dense aggregates.

In conclusion, the results show that the initial microalgal inoculation has a negligible role in the development of a stable microalgal-bacterial consortium because 1) the inoculated microalgae gradually left the system, due to the low settleability; 2) microalgal-bacterial consortia can develop spontaneously when treating real wastewater.

5.1 Introduction

In a context of climate change, wastewater treatment plants (WWTP) based on activated sludge process are no longer sustainable due to the large energy consumption, with related greenhouse gas (GHG) emissions, and excess sludge disposal. In recent decades, microalgal-bacterial consortia have been attracting increasing attention as a promising alternative solution thanks to the symbiotic

exchange of oxygen and CO_2 (Muñoz and Guieysse, 2006; Wang Y. et al., 2016; Gonçalve et al., 2017). Photosynthetic oxygenation is a cost-effective and sustainable means to replace mechanical aeration, which may account for 50% of the energy consumption of WWTP (Mamais et al., 2015), resulting in reduced GHG emissions.

Microalgal-bacterial consortia have been tested in the treatment of different types of wastewater, showing good removal efficiency (Cai et al., 2013; Arcila and Buitrón, 2016; Wang Y. et al., 2016; Lee and Lei, 2019). While several studies have focused on the application of single microalgal species inoculated in photobioreactors treating synthetic or sterilized wastewater (Cuellar-Bermudez et al., 2017), various studies have reported the development of spontaneous microalgal-bacterial consortia in photobioreactors treating real wastewater (Arango et al., 2016; Cho et al., 2017; He et al., 2013; Kang et al., 2018; Tsioptsias et al., 2016).
In view of the full-scale application, resident-wastewater microorganisms cannot be avoided (Xu et al., 2009; He et al., 2013; Saunders et al., 2016) without incurring high sterilization costs. Therefore, it is important to understand the role and the outcome of the initial microalgal inoculation when treating real wastewater.

Some studies have investigated the impact of different inoculation ratios and their fate in photobioreactors (Su et al., 2012; Arango et al., 2016; Sun L. et al., 2019). However, none of these have monitored the acclimation period until steady-state conditions were reached. Therefore, still little is known about the evolution of microalgal-bacterial consortia (García et al., 2018) and if the microalgae inoculated persist in the system in the long-term. Comparative studies without initial microalgal inoculation would clarify if inoculation is essential to start-up a photobioreactor or if only wastewater is sufficient for the development of a stable microalgal-bacterial consortium.

The main objective of the research reported in this study was to monitor the evolution and the composition of microalgal-bacterial consortia treating real municipal wastewater with the focus on the role of the initial microalgal

inoculation. To this end, two identical photobioreactors were started-up and fed with real municipal wastewater; one reactor (named RC) was initially inoculated with *Chlorella vulgaris* (*C. vulgaris*) while the other (named RW) was not inoculated. The phase of acclimation was monitored for three months with flow cytometry (FCM), from the first days of feeding and until steady state conditions were reached.

Microalgal-bacterial consortia are complex microcosms and FCM is a useful tool to interpret changes in biomass composition and characteristics (Luo et al., 2018). FCM's main advantages are: (i) an accurate multi-parametric analysis and (ii) short analysis time.
In this research, FCM was used to characterize qualitatively and quantitatively the composition of the microalgal-bacterial consortia that developed in RC and RW. In addition, the effluents of the reactors were also analyzed to evaluate which kind of populations left the system and to what extent. Photosynthetic microorganisms were distinguished by their red autofluorescence (dark red in microalgae, orange/red in cyanobacteria) while bacteria were marked with green fluorescence (using SYBR-Green I). The microalgal-bacterial consortia composition was compared to evaluate whether the initial inoculum of *C. vulgaris* was able to remain in RC or was gradually and spontaneously replaced by photosynthetic microorganisms entered with the influent wastewater.

In view of the full-scale application, this study contributes to unravelling the role of initial microalgal inoculation on the start-up of photobioreactors and the development of a microalgal-bacterial consortium that treats real wastewater.

5.2 Materials and Methods

5.2.1 Experimental set-up

Two identical photobioreactors (named RC and RW) were installed and run in parallel as photo-sequencing batch reactors, according to the configuration previously described in Chapter 3 (Figure 5.1). Briefly, the reactors had a

working volume of 1.5 L. Mixers prevent the biomass from settling. A fluorescent lamp provided a light intensity of 45 μmol m^{-2} s^{-1}, with a photoperiod of 24 h/d. No mechanical aeration was provided. The reactors were operated at room temperature (24±2.0°C).
Except for the first week of acclimation without feeding, both reactors were fed with the same municipal wastewater 3 times per week, with a volumetric exchange ratio of 50% (0.75 L), resulting in a hydraulic retention time of about 4 days. Before discharge, solids were separated by a 1-hour sedimentation, which favored the natural selection of settleable flocs (Hu et al., 2017).
As regards the treatment performance, both reactors ensured high removal efficiency of organic matter, ammonium, and total suspended solids with no statistically significant differences (Chapter 3).

5.2.2 Microalgal strain inoculated in RC

RC was initially inoculated with *C. vulgaris* and wastewater, while RW was started only with wastewater, without an initial microalgal inoculum. *C. vulgaris* was chosen because widely studied in regard to wastewater treatment (He et al., 2013; Ryu et al. 2014; Gonçalves et al., 2016). Pre-inoculum growth was conducted in Algae Broth medium modified by Allen (1952). The culture was settled and used as inoculum in RC.

5.2.3 Influent municipal wastewater

Real municipal wastewater was collected after the primary sedimentation of the full-scale WWTP Trento Nord (Trento, Italy). The average composition of wastewater, indicated in Chapter 3, was in agreement with typical values expected in pre-settled wastewater (Tchobanoglous et al. 2003). No filtration of the wastewater was performed, so that microorganisms naturally present in the influent entered both RC and RW, affecting the population dynamics.

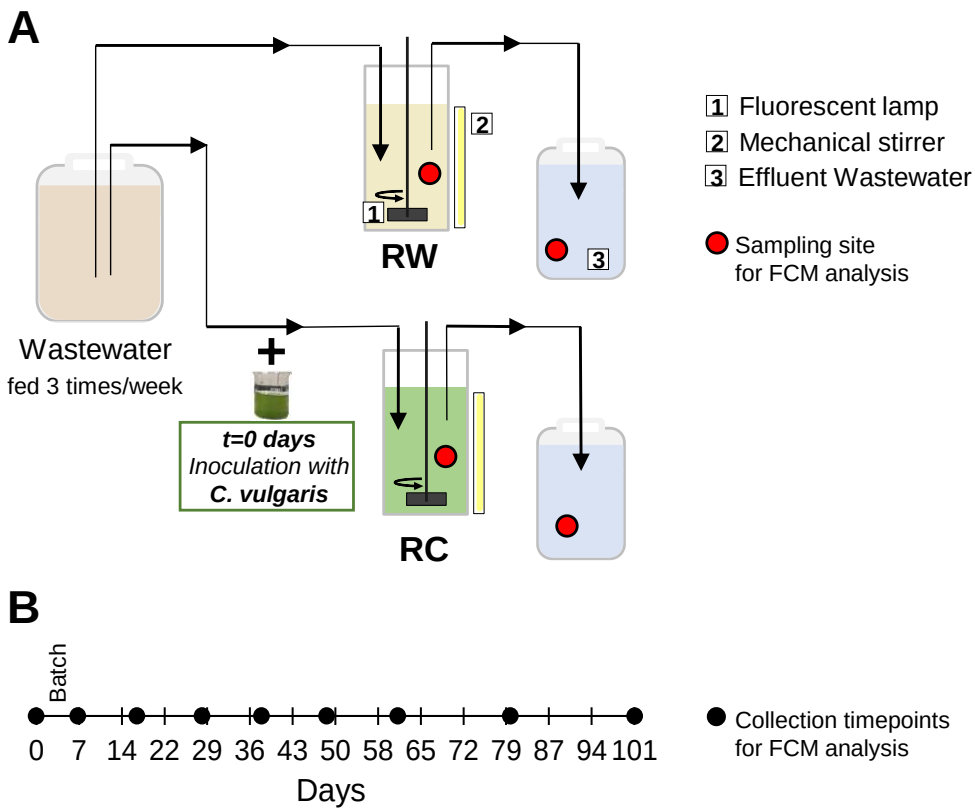

Figure 5.1 *(A) Scheme of the photobioreactors operated as photo-sequencing batch reactors and fed with real wastewater (B) Sample collection timepoints for FCM analysis. Legend: RW: photobioreactor started only with wastewater; RC: Photobioreactor inoculated at t=0 day with C. vulgaris and wastewater; FCM: flow cytometry.*

5.2.4 Sampling

The reactors were monitored for 101 days, in order to observe the entire acclimation period and a subsequent steady-state phase of some weeks.
Two types of samples were collected for FCM analysis from RC and RW (Figure 5.1): (1) the effluent wastewater discharged, after settling, at the end of the cycles; (2) the mixed liquor (biomass) in the reactors. Samples were collected at the beginning of the experiment (0 days), after the first week of acclimation in batch (7 days) and then at regular intervals (every 10 days until day 47 and then

every 21 days) as summarized in Figure 5.1B. Samples were immediately stored at 4°C in the dark until further processing. Starting from day 7, the settleability was measured in both reactors in concomitance with sample collection for FCM analysis.
Samples were collected in concomitance with sample of mixed liquor for high-throughput sequencing (Chapter 4).

5.2.5 Sample preparation prior to FCM analysis

5.2.5.1 Pre-treatment of mixed liquor

The procedure applied here is in accordance to that described in Chapter 12.
Samples of mixed liquor were firstly diluted 1:5 v/v in Phosphate-Buffered-Saline solution (PBS, 3 g K_2HPO_4, 1 g KH_2PO_4 and 8.5 g NaCl per Liter; pH = 7.2) obtaining a volume of 100 mL that underwent ultrasonication to disaggregate the small flocs that progressively formed in the reactors. Then, the sonicated sample was further diluted 1:10 v/v in PBS. Finally, 1-mL was filtered on 20-μm membrane (Celltrics, Sysmex Partec, Germany). The final dilution was 1:50 v/v, which made it possible to obtain an optimal cell concentration for FCM analysis, around 10^9-10^{10} cells/L.
Ultrasonication was performed using a Branson 250 Digital Ultrasonifier (Emerson, USA) operating at 20 kHz, equipped with an immersed tip and a cold bath to avoid increase in temperature of the sample during sonication.
In this investigation, the specific energy applied during sonication (E_s) was 25 kJ L^{-1}. E_s was calculated by multiplying the applied power (expressed in W) and the time of sonication (expressed in seconds) and dividing by the treated volume (in L). Chapter 12 demonstrated that E_s of 90 kJ L^{-1} is optimal to disaggregate dense clusters in microalgal-bacterial consortia with a cell density (bacteria + microalgae) higher than 1.0E+12 cells/L. Foladori et al. (2007; 2010) indicated E_s of 25 kJ L^{-1} as optimal for the pretreatment of raw and settled wastewater with cell density of 1.0-2.0E+11 cells/L. The difference in these E_s levels was due to the fact that small aggregates in wastewater require a lower

energy level for their dispersion without extensive cell destruction, while dense flocs or granules, with size up to 1 mm, are strongly bonded and therefore higher energy level is required. In our case, E_s of 25 kJ L^{-1} was chosen because the cell density during acclimation was expected to vary in the order of magnitude from 1.0E+09 to 1.0E+11 cells/L, not so different from that of raw wastewater tested by Foladori et al. (2007). To be noted is that at the beginning of the experiment mixed liquor of reactors consisted of wastewater (RW) and wastewater plus *C.vulgaris* (RC). The application of E_s of 25 kJ L^{-1} made it possible to disperse the small aggregated cells without destroying them.

5.2.6 Pre-treatment of effluents

Effluent samples were not pre-treated. Dilution was not necessary; only in rare cases, with a particularly turbid effluent (i.e. Effluent from RW at day 38) a dilution 1:50 v/v in PBS was performed. An aliquot of 1 mL was only filtered at 20-μm to prevent clogging of the nozzle in the flow cytometer.

5.2.7 Flow cytometry

FCM analyses were performed with an Apogee-A40 flow cytometer (Apogee Flow Systems, UK) equipped with an Argon laser (excitation wavelength at 488 nm). Green fluorescence (Channel FL1) was collected at λ=515-545 nm. Red fluorescence (Channel FL3) was collected at $\lambda \geq 610$ nm. Data acquisition was set on green and red fluorescence distributions, to eliminate the noise produced by non-fluorescent particles or debris, which passed the 20-μm filtration.
As discussed in Chapter 12, microalgae can be distinguished from bacteria using red and green fluorescence, and two scattering signals (FALS, Forward Angle Light Scattering and LALS, Large Angle Light Scattering). For each sample, two aliquots were processed as follows:

1) An unstained sample was immediately analyzed and served to detect microalgae. Photosynthetic microorganisms emit red autofluorescence produced by their natural pigments therefore can be easily detected with-

out staining the sample. In addition, microalgal cells produce high values of FALS and LALS that can be well recognized in the scattering hystograms (Chapter 12);

2) A sample was stained to detect bacteria. Since bacteria are not fluorescent, they can be detected only after staining with fluorescent dyes. In addition, bacteria are smaller than microalgal cells and thus produce a lower intensity in the FALS and LALS hystograms (Chapter 12). SYBR-Green I (SYBR-I; λ_{ex} = 495 nm, λ_{em} = 525 nm; Thermo Fisher Scientific, USA) was used for cell staining. SYBR-I is a DNA-specific fluorescent dye producing green fluorescence. An amount of 10 μL of dye, after dilution 1:30 v/v of commercial stock in dimethyl sulfoxide (DMSO, Merck, Germany), was added to 1 mL of the cell suspension and incubated at room temperature for 15 min in the dark.

Microalgae were identified in the unstained sample, as red cells in the FL1-FL3 cytogram gated by high FALS and LALS intensity. Conversely, bacteria were identified in the stained sample as green cells in the FL1-FL3 cytogram gated by the low FALS and LALS intensity.
For each analysis, more than 20,000 cells were enumerated. Cell concentration was recorded in events/μL and then expressed in cells/L taking into account the dilution of the analyzed sample. FCM data were analyzed using Apogee Histogram Software (Apogee Flow Systems, UK).

5.2.8 Analytical methods

Chemical Oxygen Demand (COD) and Total Suspended Solids (TSS) were analyzed according to Standard Methods (APHA, 2012). Settleability was measured according to the standard methods for Settleable Solids (APHA, 2012).
DO and temperature were recorded every 15 min using OXI340i meters coupled with the sensor CellOx®325 (All from WTW, Germany).
A SQ-520 quantum sensor (Apogee Instruments, USA) was used to measure light intensity as photosynthetically active radiation (PAR).

5.3 Results and Discussion

5.3.1 Qualitative comparison of biomasses in the reactors

In Figure 5.2, the cytograms FL1-FL3 compare reactors RC and RW with regard to the subpopulations of microalgae (detected in unstained samples, 1st and 3rd columns in Figure 5.2) and bacteria (in stained samples, 2nd and 4th columns in Figure 5.2) at days 0, 7, 38 and 80. Microalgae (both eukaryotic microalgae and prokaryotic cyanobacteria) contain photosynthetic pigments that may have different levels of auto-fluorescences but mainly emitting in the red field (high FL3 intensity). Bacteria are stained with SYBR-I and emit green fluorescence (high FL1 intensity).

At the beginning of acclimation (0-7 days in Figure 5.2), only RC, inoculated with *C. vulgaris*, was characterized by a population of cells emitting red fluorescence. In RW microalgae were negligible and only the bacteria naturally present in wastewater formed a well-defined population.

Despite no microalgal inoculation in RW, just after 7 days of acclimation a small population of microalgae was detected, which became broader at day 38 (Figure 5.2). The population of microalgae that established in RW was different to that in RC. As shown in the cytograms in Figure 5.2 (1st and 3rd columns), at 38 days, the photosynthetic cells (Unstained samples) in RW were in a different position with respect to those in RC, which meant that they were characterized by a remarkably different red intensity. Microscopic observations of RW biomass identified the presence of some *Chlorella* and filamentous microalgae (Chapter 3).

Over time in both reactors the consortia organized into a granular structure and flocs enriched in filamentous photosynthetic microorganisms (especially cyanobacteria), in which *C. vulgaris* was only a minor group. Comparing the cytograms of the last period of acclimation (Figure 5.2, day 80), the populations of microalgae and bacteria that established in RC and RW, were similar. As regards the bacteria population, FL1 intensity of bacteria remained quite similar in both reactors and along the acclimation period (Figure 5.2, 2nd and 4th columns). Over time, only a broader shape was observed (Figure 5.2, day

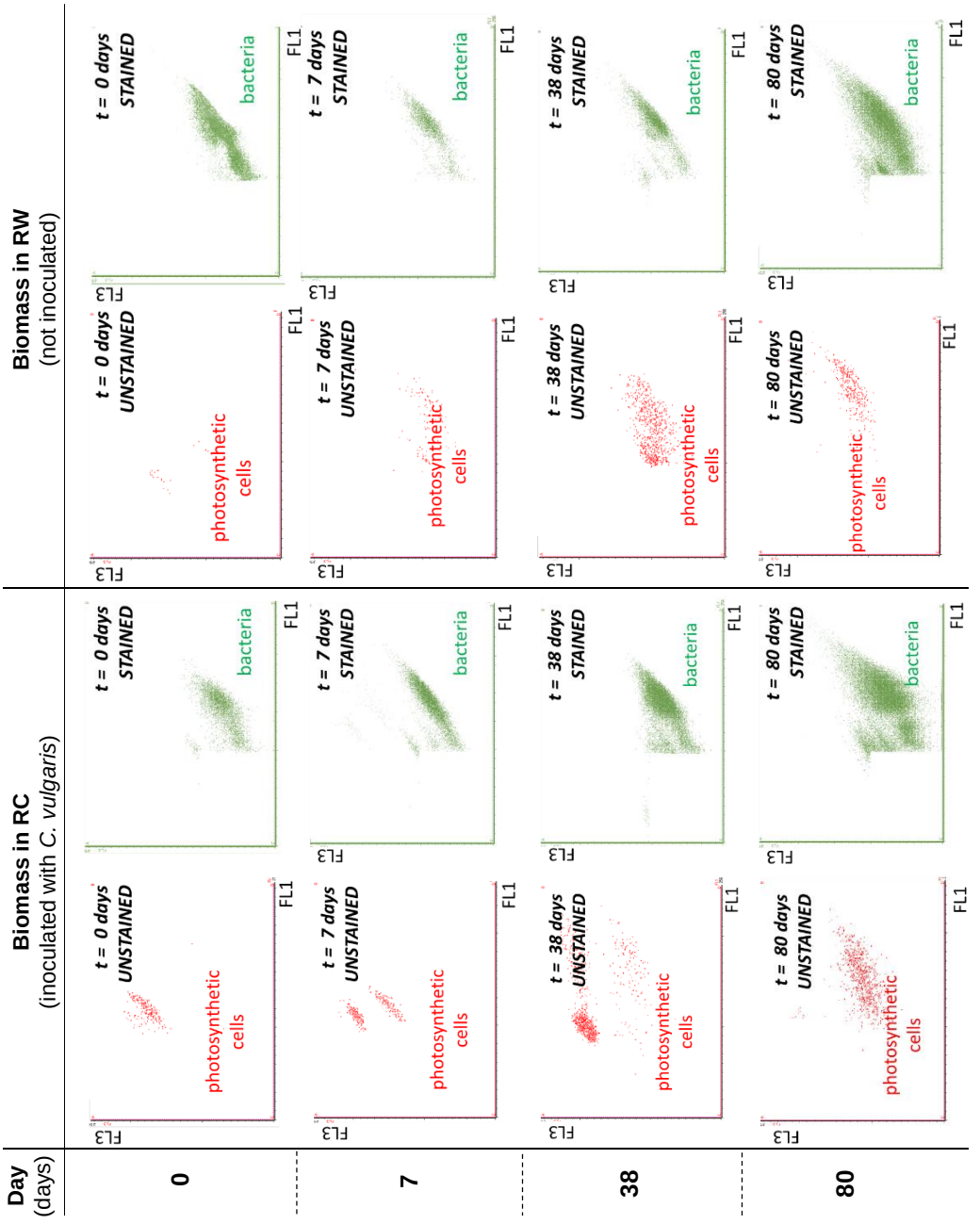

Figure 5.2 *Cytograms of the microalgal-bacterial consortia (biomass) in RC and RW during acclimation. Photosynthetic cells and bacteria are detected in FL1 (green fluorescence) - FL3 (red fluorescence) dot plots.*

80), which may indicate a wider diversity in the community.

5.3.2 Quantitative comparison of biomasses in the reactors

During acclimation the concentration of bacteria in the biomass of both reactors increased progressively over time (Figure 5.3A). Bacteria concentration in RC, inoculated with *C. vulgaris*, was always higher than in RW. During the entire experimentation, the average bacteria concentration was 4.3E+11 cells/L in RC and 2.8E+11 cells/L in RW. This was matched by TSS concentrations, always higher in RC than RW (Chapter 3).

Over time, the dynamic of the bacterial population was similar in both reactors (Figure 5.3A). During the first 20 days, the concentration varied slowly in both RC and RW. Thereafter, the concentration increased rapidly, at a rate of about 1.2E+10 cells L^{-1} d^{-1} (calculated as the slope of experimental data in Figure 5.3A).

At the end of the experimentation, the bacteria concentrations were comparable, resulting 1.1E+12 cells/L in RC and 0.8E+12 cells/L in RW. To be noted is that the growth of heterotrophic bacteria is related to COD removal. Both systems showed no significant differences in the treatment of organic matter, with high COD removal efficiency. Except for the first week of acclimation, the average COD removal was 89±5% in RC and 89±7% in RW (Chapter 3).

The growth of heterotrophic bacteria depended on the removed organic load. Consequently, because the removed loads were similar, also the growth curves were quite parallel (Figure 5.3A). Therefore, it can be concluded that the inoculum of *C. vulgaris* did not significantly affect organic matter removal and the growth curves of bacteria in RC and RW. These observations have been confirmed by García et al. (2018) and by Su et al. (2012), who reported similar COD removal with different inocula of microalgae and activated sludge.

With regard to microalgae (Figure 5.3B), the concentration was higher in RC because of the initial inoculation of *C. vulgaris*. At the beginning, microalgae in RC (2.8E+09 cells/L) were 30 times more numerous than in RW (9.3E+07 cells/L). Then, during acclimation, the wastewater-born microalgae spontaneously grew

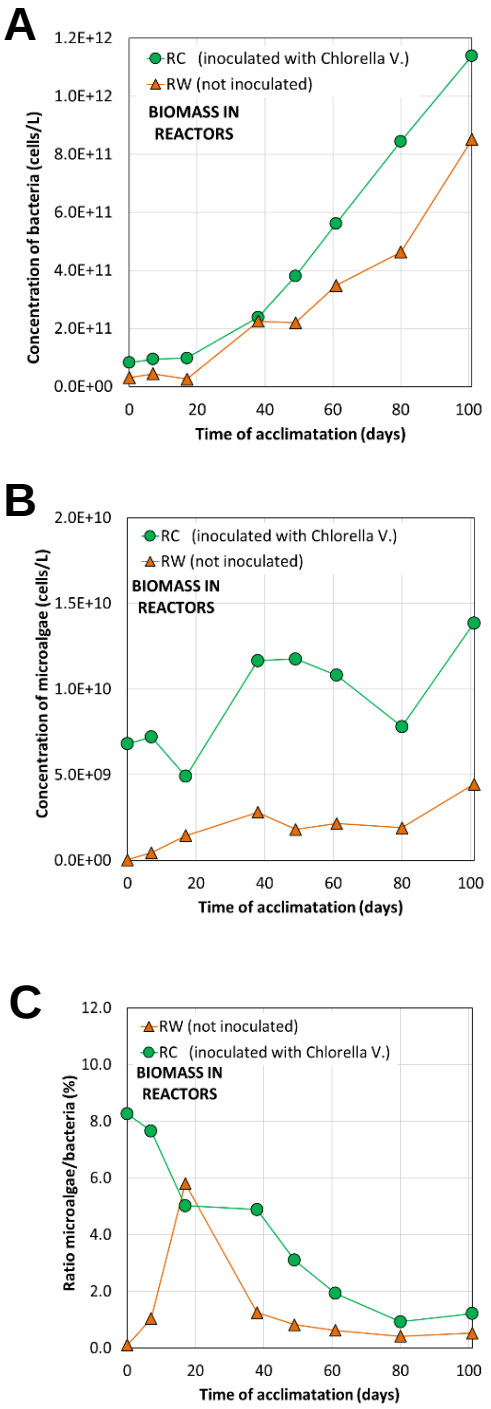

Figure 5.3 *Biomass concentrations in RC and RW during acclimation: (A) bacteria, (B) microalgae, (C) microalgae/bacteria ratio.*

in RW and their number gradually increased. However, microalgae in RW never reached the concentration recorded in RC. At the end of the experimentation, microalgae in RC (1.4E+07 cells/L) were only 1.4-fold those in RW (1.0E+07 cells/L).

To be noted is that the growth of microalgae (Figure 5.3B) was slower than the growth of bacteria (Figure 5.3A). The reason was a self-shading effect. The rapid growth of heterotrophic bacteria and the accumulation of inert material in the flocs resulted in an increase of floc size that limited the light penetration and thus the photosynthetic activity and the microalgal metabolism.

In Figure 5.3C, the ratio of microalgae to bacteria over time is shown. The high percentage of microalgae initially inoculated in RC, progressively diminished (Figure 5.3C). At the end of acclimation, the microalgae/bacteria ratio was comparable in the two reactors.

Therefore, the initial microalgal inoculation in RC was unnecessary. Moreover, microalgae naturally entering with the influent wastewater even if in small amounts, were able to adapt and grow as demonstrated by the increase in microalgal cells in RW (Figure 5.3B). However, native microalgae in RW were not able to reach the concentration of RC.

5.3.3 Qualitative comparison of effluent wastewater from the reactors

Figure 5.4 shows the cytograms FL1-FL3 of the effluent wastewater from RC and RW during the acclimation.

With regard to the effluent microalgae (unstained samples, 1st and 3rd columns in

both reactors, indicating an important shift in the amount and composition. At day 7, two small sub-groups were detected in both RC and RW effluents; while at day 38 a major group dominated in RC effluent. At the end of acclimation (day 80) only a small amount of microalgae left the reactors with the effluents, without evidence of particular subgroups. In fact, the consortia inside the reactors evolved towards a stable structure of dense flocs with good settleability,

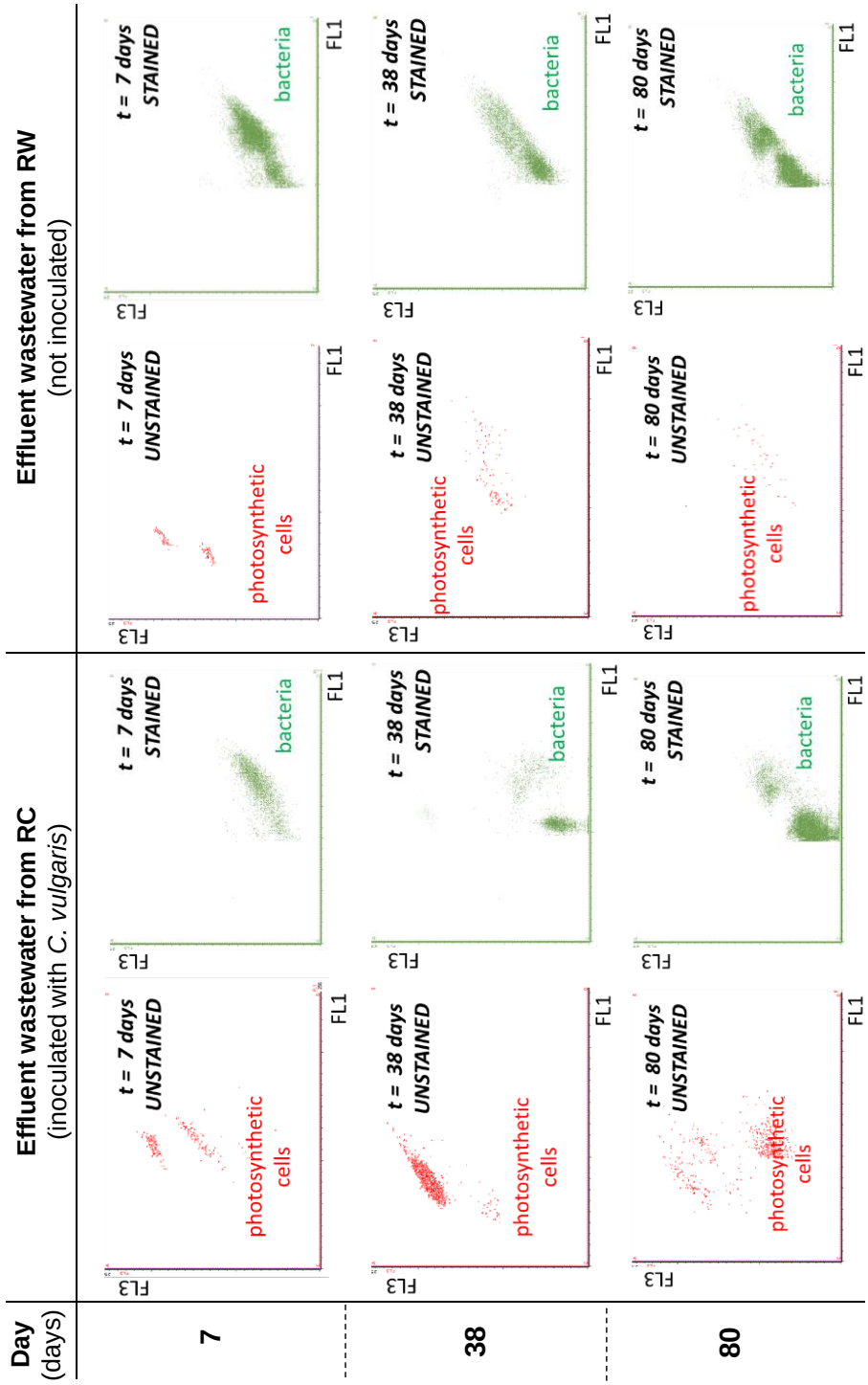

Figure 5.4 *Cytograms of the effluent wastewater from RC and RW during acclimation. Photosynthetic cells and bacteria are detected in FL1 (green fluorescence) - FL3 (red fluorescence) dot plots.*

resulting in a very low concentration of microorganisms in the effluents (Chapter 3).

As regards effluent bacteria, the cytograms (stained samples, 2nd and 4th columns in Figure 5.4) indicate a change in the composition over time in both reactors. Although the bacteria in the effluents of RC and RW had a different evolution during the acclimation, at day 80 the sub-groups of effluent bacteria were similar in RC and RW effluents.

5.3.4 Quantitative comparison of effluent wastewater from the reactors

The concentrations of bacteria and microalgae in the effluent wastewater during the acclimation period are shown in Figure 5.5.

The concentrations of microorganisms in the effluents of RC and RW differed greatly during the first 38 days (Figure 5.5A-B). A large part of microalgae, in particular, left RC (Figure 5.5B).

As shown in Figure 5.5B, effluent microalgae from RW were quantitatively negligible during the entire experimentation (2.2E+08 cells/L on average). Conversely, the initial suspension of *C. vulgaris* in RC was characterized by low settleability that did not allow its permanence in RC. *C. vulgaris* has negatively charged surface and colloidal stability in suspension (Barros et al., 2015) therefore is not able to aggregate in flocs and settle. In fact, in the first 20 days the effluents of RC had a bright green color (Figure 3.5). During the first 20 days, the photosynthetic cells (mainly *C. vulgaris*) leaving RC with the effluent were 2.8-3.7E+09 cells/L, one order of magnitude higher than RW (Figure 5.5B).

Other authors have also reported on small unicellular microalgal species (like *Chlorella* spp.). inoculated in photobioreactors that gradually left the systems because of poor settleability and low flocculation capacity (Arango et al., 2016; Muñoz and Guieysse, 2006; Barros et al., 2015).

Together with *C. vulgaris*, also a significant number of bacteria left RC during the first 20 days (effluent bacteria were 2.3-3.6E+10 cells/L; Figure 5.5A). Contrarily, the concentration of bacteria in the effluent of RW was one order of

magnitude lower (3.7-9.4E+09 cells/L).

The high presence of bacteria in the effluent of RC could be associated with the high pH values (up to 10 in the first 20 days, Chapter 3) in RC caused by an intense photosynthetic activity of *C. vulgaris* that may have generated a selective pressure on bacteria (Krustok et al., 2015).

High values of pH may cause difficulties in adaptation of heterotrophic bacteria and even inhibit bacterial growth (Muñoz and Guieysse, 2006; Choi et al., 2010). Choi et al. (2010) reported a delay in the growth of nitrifiers and thus in the development of nitrification in reactors inoculated with microalgae. A similar behavior was observed during this experimentation and has been discussed in detail in Chapter 3 and 4.

In RC, the selective pressure caused by high pH values (high photosynthetic activity), may have hindered the floc formation and favored the outflow of free bacterial cells. Conversely, in RW, without an initial algal inoculum, microalgae needed more time to grow (Figure 5.3B) and pH never exceed 9. Therefore, bacteria grew without specific limitations from the outset.

At day 38, a worsening in settleability (turbid supernatant, Chapter 3) occurred in RW, resulting in a biomass washout from the reactor. As shown in Figure 5.5, microalgae and bacteria in the effluent reached a peak at day 38, and the concentrations increased up to 4.9E+10 cells/L for bacteria and 1.2E+09 cells/L for microalgae. Interestingly, this corresponded to a worsening in the removal efficiency of TKN at day 40 (Chapter 4).

Compared to the biomass concentrations in the reactors (Section 5.3.2), each discharge of the effluent resulted in a washout of 10% of bacteria and 19% of microalgae. This strong selective pressure favored the permanence in the reactors of the microorganisms embedded in settleable flocs, while floating cells, free in the bulk liquid, left the systems with the effluents. Therefore, with time the growth of flocculent microorganisms structured in dense aggregates was enhanced.

At day 48, the concentrations of microalgae and bacteria leaving the systems decreased drastically in both RC and RW (Figure 5.5A-B). This corresponded to a concomitant enrichment of bacteria in both reactors (see Figure 5.3A).

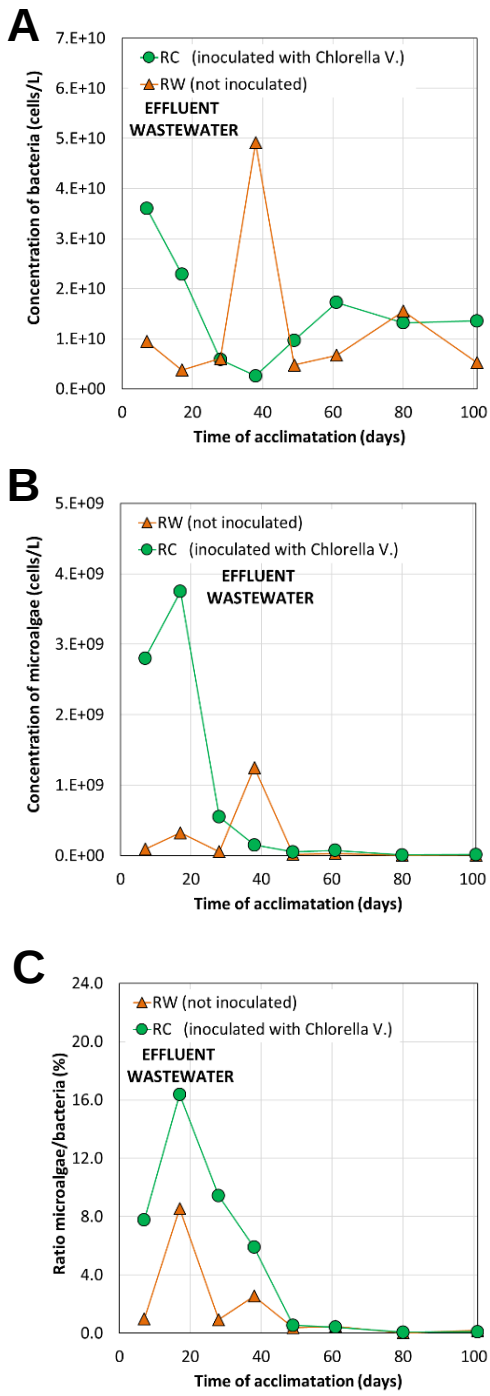

Figure 5.5 *Biomass concentrations in the effluent wastewater from RC and RW during acclimation: (A) bacteria , (B) microalgae, (C) microalgae/bacteria ratio.*

At the end of acclimation, the effluent from RC matched the effluent concentrations of bacteria and microalgae from RW. As shown in Figure 5.5C, the ratio of microalgae to bacteria in the effluent became similar from day 48 onward.

5.4 Conclusion

The evolution and the composition of two microalgal-bacterial consortia developed in photobioreactors treating real municipal wastewater and started with (RC) or without (RW) initial microalgal inoculation (*C. vulgaris*) were investigated with flow cytometry.

At the beginning of the acclimation microalgae were present only in RC because inoculated with *C. vulgaris*. FCM analysis revealed that microalgae spontaneously developed inside RW just after 7 days of acclimation. Microalgae in RC resulted always higher than RW, however they decreased passing from an initial concentration 30 times higher than RW to 1.4 times at the end of the experimentation.
Bacterial population in both reactors presented a very slow growth during the first 20 days. Afterwards, they increased at a rate of about 1.2E+10 cells L^{-1} d^{-1}. Concomitantly, the concentrations of microalgae and bacteria leaving the systems decreased drastically. During the first 20 days, the effluent of RC was characterized by high concentration of microalgae, mainly *C. vulgaris*, due to their low settleability. With time, the settling phase favored in both systems the exit of floating cells, free in the bulk liquid, while flocculent microorganisms organized in flocs enriched in filamentous photosynthetic microorganism.
At the end of the acclimation, the microalgal-bacterial consortia established in both reactors presented similar characteristic and were characterized by low solids concentrations in the effluents.

Overall, this study show that microalgae can spontaneously develop and established in photobioreactors, entering the system with the real wastewater. The inoculated microalgae (*C. vulgaris*) left the system because characterized by low settleability. At the same time their influence on bacterial grow was

limited. In fact, both systems presented a similar bacterial population at the end of the experimentation. Therefore, it can be concluded that initial microalgal inoculation to start-up photobioreactors treating real wastewater is unnecessary.

Acknowledgements

The authors would like to thank Giovanna Flaim (Edmund Mach Foundation, Italy) who gifted *Chlorella Vulgaris*.

CHAPTER 6

LONG-TERM PHOTOBIOREACTOR TREATING REAL MUNICIPAL WASTEWATER

This Chapter provides a comprehensive picture of the performances of a stable wastewater-borne microalgal-bacterial consortium acclimatized for 2 years in a lab-scale photo-sequencing batch reactor. This reactor, called Pilot, represents the core of the research activity and it worked for the entire experimentation. The feasibility to treat real municipal wastewater through photosynthetic aeration, was demonstrated. The removal mechanisms involved were analyzed. Biomass macrostructure and good settling properties were shown. The central role of light was stated together with the necessity of redefine process parameters consolidated for activated sludge (such as kinetics and optimal biomass concentration).
Some topics deepened in the next Chapters are briefly introduced:
- Improvement of total N removal and opportunities for energy saving (Chapter 7);
- Online parameters for real-time control of the process (Chapter 8);
- Effect of HRT and sunlight on the treatment performance (Chapter 9);
- Optimal TSS content to ensure high ammonium removal rate (Chapter 10);
- Measurement of the removal kinetics (Chapter 11).

This Chapter is based on:
Petrini S., Foladori P., Andreottola G., 2018. *Laboratory-scale investigation on the role of microalgae towards a sustainable treatment of real municipal wastewater.* Water Science and Technology 78, 1726-1732. https://doi.org/10.2166/wst.2018.453

Abstract

Engineered microalgal-bacterial consortia are an attractive solution towards a low-cost and sustainable wastewater treatment that does not rely on artificial mechanical aeration. In the research conducted for this study, a bench-scale photo-sequencing-batch reactor (PSBR) was operated without external aeration. A spontaneous consortium of microalgae and bacteria was developed in the PSBR at a concentration of 0.8-1.7 g TSS/L. The PSBR ensured removal efficiency of 85±8% for COD and 98±2% for Total Kjeldahl Nitrogen (TKN). Nitrogen balance revealed that the main mechanisms for TKN removal was autototrophic nitrification, while N assimilation and denitrification accounted for 4% and 56%, respectively. The development of dense microalgal-bacterial bioflocs resulted in good settleability with average effluent concentration of 14±17 mg TSS/L. The ammonium removal rate was 2.9 mg N L^{-1} h^{-1}, which corresponded to 2.4 mg N g TSS^{-1} h^{-1}. Although this specific ammonium removal rate is similar to activated sludge, the volumetric rate is lower due to the limited TSS concentration (3 times less than activated sludge). Therefore, the PSBR footprint appears less competitive than activated sludge. However, ammonium was completely removed without artificial aeration, resulting in a very cost-effective process. Only 50% of phosphorus was removed, suggesting that further research on P uptake is needed.

6.1 Introduction

The conventional wastewater treatment plants (WWTPs), based on the activated sludge configuration, ensure high efficiency in pollutant removal. However, WWTPs are today facing some serious issues: (1) large energy consumption, mainly associated with mechanical aeration of bioreactors; (2) increasing amounts of excess sludge, which cause expenditures for treatment and disposal, and environmental impacts; (3) Greenhouse Gases (GHG) emissions like CO_2, CH_4 and N_2O, which contribute to the growing problem of global warming.

In regard to energy consumption, WWTPs have been estimated to use about 1% of the national electricity consumption (Cao, 2011; Shen et al., 2015; Zhang et al., 2016). A large amount of the energy is used in WWTPs to meet stringent

targets on effluent water quality. At the same time, since energy mainly originates from fossil sources, WWTPs contribute to climate change. In this context, actions aimed at maintaining good quality effluents but reducing WWTP energy consumption are imperative.

As regards excess sludge production, restrictions in disposal routes may occur in many countries, leading to a progressive increase in costs. Sludge treatment and disposal may generate expenditures from 250€ to more than 1000€ per tonne of dry mass (mean 470±280€/t in European countries; Foladori et al., 2010a).

These aspects entail a paradigm shift in the configurations of conventional WWTPs towards solutions that are more environmentally and economically sustainable. A promising emerging alternative to treat wastewater is to couple bacteria with microalgae (Judd et al., 2015). In fact, in the presence of light, through photosynthesis, microalgae produce oxygen to support bacterial activity (oxidation of organic matter and ammonium), contribute to CO_2 mitigation by photosynthetic fixation, and permit nutrients recycling by assimilation of N and P. In return, bacteria produce carbon dioxide, which is essential for photosynthesis. The exploitation of microalgal-bacterial symbiosis, together with sunlight, may lead to a low- or no-energy treatment process that does not rely on artificial mechanical aeration (Quijano et al., 2017), resulting in a process more sustainable than WWTPs based on activated sludge (Molinuevo-Salces et al., 2010).

Among the best-known systems based on microalgal-bacterial consortia, high rate algal ponds (HRAPs) are the most widespread. HRAPs are open shallow ponds with long Hydraulic Retention Times (HRTs, 3-10 d) and low depth (0.1-0.3 m) (Posadas et al., 2015). Although they are characterized by low-energy consumption compared to conventional WWTPs (Godos et al., 2009), they require a large use of land (Gonzalez-Fernandez and Muñoz, 2017). This high footprint is the major drawback in countries where land is scarce and expensive. Moreover, HRAPs can only be controlled to a limited extent, so that efficient N removal may be difficult to achieve in sensitive areas.

Closed photobioreactors (PBRs) make it possible to overcome these limitations

because: (1) they can be built vertically to minimize land requirements, and (2) the process conditions can be easily controlled to guarantee high pollutant removals and efficient nitrification (Karya et al., 2013; Muñoz and Guieysse, 2006). In recent years, engineered PBRs have gained increasing attention in the treatment of municipal wastewater (Su et al., 2011) since they could become a cost-effective and sustainable solution in the future.

At the moment, there are only few studies on wastewater-borne microalgal-bacterial consortia developed in PBRs (Kang et al., 2018). Therefore, little is known about the removal process and the operational aspects of these systems. Indeed, a more detailed knowledge is required about: (i) kinetics of biomass, (ii) efficiency of separation between biomass and treated wastewater, (iii) energy savings, (iv) sludge production.

The aim of this study is to provide a comprehensive picture of the performances of a stable wastewater-borne microalgal-bacterial consortium acclimatized for two years in a bench-scale sequencing PBR (PSBR) treating real municipal wastewater. Since no external aeration was provided, oxygen was supplied only by microalgal photosynthesis. Instead of exploiting sunlight, artificial light was supplied in order to guarantee a constant light intensity and a stable photoperiod. In this way, the influence of daylight variations was avoided and the interpretation of data was easier.

The focus was on the following key factors that affect the entire performance of the PBRs and the sustainability of the process: (1) removal efficiencies of Chemical Oxygen Demand (COD), Total Kjeldahl Nitrogen (TKN) and total phosphorus with the aim of meeting the EU discharge limits; (2) biomass macrostructure and settling properties; (3) kinetics of ammonium removal; (4) online parameters, such as dissolved oxygen (DO) and pH, for real-time control of the process; (5) opportunities for energy saving.

6.2 Materials and Methods

6.2.1 Influent wastewater

Influent pre-settled wastewater was collected from a full-scale municipal WWTP (Trento Nord plant, Italy). No filtration of the wastewater was performed; in this way, the microorganisms naturally present in the influent wastewater acclimatized, resulting in a microalgal-bacterial consortium.

6.2.2 Photo-sequencing batch reactor

A bench-scale cylindrical photobioreactor (Colaver, Italy) with a working volume of 2 L was used (Figure 6.1). The system was operated as a sequencing batch reactor (PSBR) equipped with peristaltic pumps(Kronos Seko, Italy), a magnetic mixer (AGE, Velp, Italy) and a lamp (8 led x 0.5 W; Orion, Italy) controlled by timers (TR 612 top2, Theben, Germany) .
The mixer was set at 200 rpm to ensure mixing and prevent the biomass from settling. Sunlight entered the laboratory but the reactor was never directly exposed. In fact, light was supplied by a cool-white lamp. The light intensity provided, measured as photosynthetically active radiation (SQ-520 quantum sensor, Apogee Instruments, USA), was 25±5 μmol m^{-2} s^{-1}. The photoperiod was set at 16 h of light and 8 h of dark.
The PSBR cycle (48 h) comprised 4 four phases: (1) Feed, 0.08 h; (2) React, 47.5 h; (3) Settlement, 0.5 h; (4) Draw, 0.08 h. The React phase consisted of two photoperiods of 16 h light/8 h dark, resulting in a sequence of periods with high and low DO values. Wastewater was fed at rate of 0.7 L/cycle resulting in a HRT of 5.6 d. No external aeration was provided, so that oxygen was supplied only by photosynthesis. Temperature of mixed liquor was 22.2°C on average during the 7-month experimentation.

6.2.3 Microalgal-bacterial consortium

Microscopic observations were performed using a Nikon Labophot EFD-3 Microscope equipped with epifluorescence apparatus (Nikon, Japan). Observations under blue and green light excitation were used to distinguish: (1) photosynthetic microorganisms, emitting red autofluorescence due to their pigments; (2) heterotrophic bacteria emitting green fluorescence after staining with SYBR-Green I (Invitrogen, USA). The biomass naturally developed in the PSBR consisted of a consortium of eukaryotic microalgae, prokaryotic cyanobacteria and bacteria, acclimatized for a two-year period (2016-2017). Total suspended solids (TSS) were maintained in the PSBR at a concentration ranging from 0.8 g TSS/L to 1.7 g TSS/L (average TSS of 1.2 g TSS/L during the 7-month experimentation).

6.2.4 Analytical methods

Analyses of total COD, TSS, TKN, NH_4^+-N, NO_2^--N, NO_3^--N, total P and PO_4^{3-}-P were performed on influent and effluent wastewater according to Standard Methods (APHA, 2012). Soluble COD (sCOD) was measured after filtration on 0.45-μm-membrane. The analysis of TSS was also used to determine the

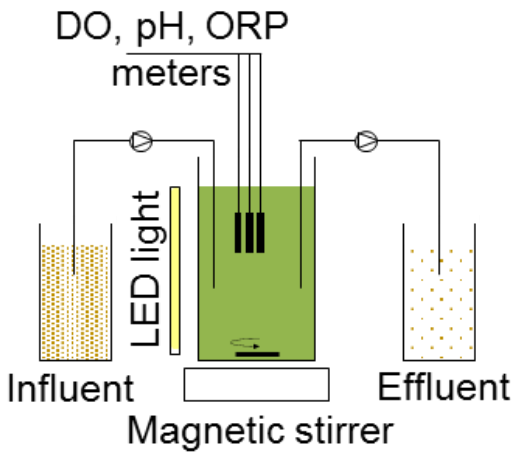

Figure 6.1 *Scheme of the PSBR.*

biomass concentration in the PSBR. DO, pH and temperature were measured continuously with online probes (Multi3410 and pH3310 meters, WTW, Germany). Track studies were performed in the PSBR to measure the profiles of N forms during a typical cycle. Samples were collected every hour, then filtered and analyzed for N-forms.

6.3 Results and Discussion

6.3.1 High removal efficiency of COD and TKN

The microalgal-bacterial consortium in the PSBR resulted in a very effective symbiotic collaboration. Oxygen supplied by microalgal photosynthesis met the biological demand for the oxidation of the influent compounds. Therefore a very high removal efficiency of COD and TKN was achieved, 85±8% and 98±2%, respectively. The mutualistic relationship between bacteria and microalgae sustained the organic matter removal and nitrification without mechanical aeration being necessary. At the same time, the CO_2 resulting from organic matter decomposition by bacterial activity, was available for microalgal photosynthesis. In this way, wastewater biodegradation was achieved without an external supply of both O_2 and CO_2, while decreasing CO_2 emission from wastewater to atmosphere. The profiles of influent COD and effluent sCOD concentrations, during the 7-month experimentation, are shown in Figure 6.2A. The influent COD of 262±97 mg/L on average was reduced to 33±8 mg COD/L in the effluent, largely meeting the EU discharge limit (125 mg COD/L, according to EU Directive 91/271/EEC).

TKN concentration diminished from 54±18 mg TKN/L on average in the pre-settled wastewater to 1.0±0.8 mg TKN/L and 0.6±1.0 mg NH_4^+-N/L in the effluent (Figure 6.2B). Despite the strong fluctuation of the influent TKN concentration, which surpassed 100 mg TKN/L, a complete and stable nitrification occurred in the PSBR during all the 7 months of experimentation. Nitrites were negligible (0.1±0.4 mg NO_2^--N/L) in the effluent, while nitrates were 13.7±8.7 mg NO_3^--N/L on average. Based on nitrogen balance in the PSBR, the mech-

anisms of TKN removal were: (1) biomass assimilation, which accounted for approximately 4% of removed TKN, (2) autotrophic nitrification, which converted all the remaining TKN into nitrate. Then heterotrophic denitrification during phases at zero-DO accounted for 56%. A fourth potential mechanism of N removal could be ammonia volatilization, but it was excluded because pH in the PSBR was 7.6±0.3 on average, and thus not high enough to support the stripping. The high concentration of ammonium in municipal wastewater is an ideal substrate for microalgae and cyanobacteria (Krustok e al., 2016), but the major mechanism for TKN removal in the PSBR was autotrophic nitrification. The percentage of TKN removed through biomass assimilation was very low (4%) because the microalgal processes designed for wastewater treatment (like this PSBR) are associated with low excess sludge production in comparison with processes aimed at maximizing the algal biomass productivity and harvesting.

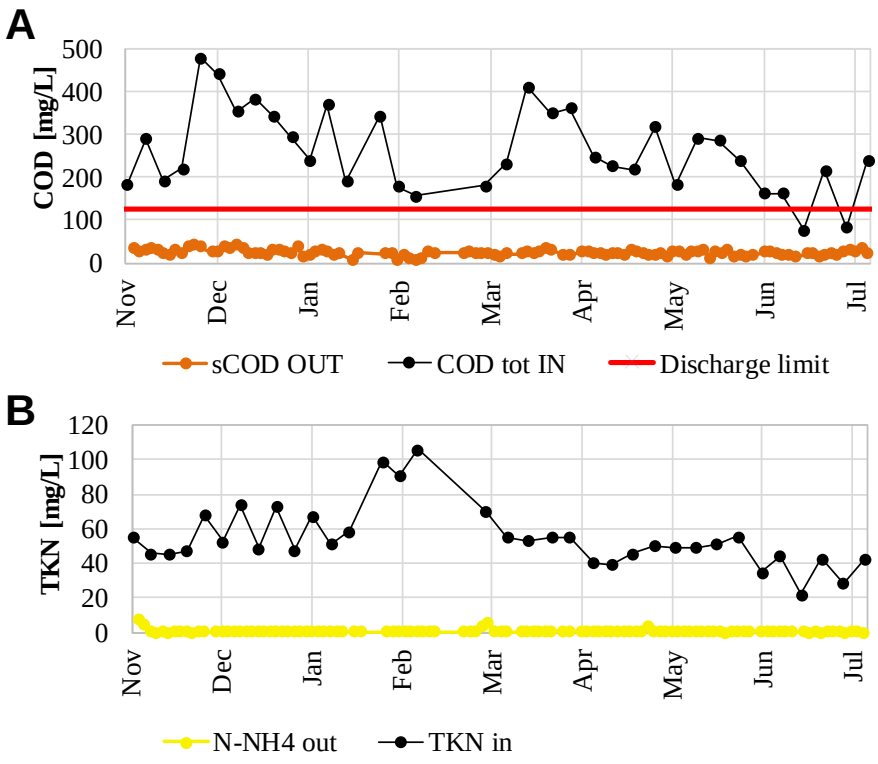

Figure 6.2 *Influent and effluent concentrations of: (A) COD and sCOD compared to EU discharge limits; (B) TKN and NH_4^+-N.*

6.3.2 Dense flocs of microalgae and bacteria ensured good settleability

A microalgal consortium treating unsterilized real wastewater would inevitably contain a mixed community of microalgae, bacteria and cyanobacteria (Arango et al., 2016; Kang et al., 2018). Microscopic observations of the microbial community spontaneously developed in the PSBR showed the presence of *Chlorella spp.*, *Diatoms spp.* and filamentous cyanobacteria embedded in dense flocs together with a large amount of heterotrophic bacteria (Figure 6.3). Green and red fluorescence (Figure 6.3B) indicate the composition of the flocs: (i) green cells represent heterotrophic bacteria, stained with SYBR-Green I, (ii) red cells correspond to photosynthetic microorganisms because of red autofluorescence linked to photosynthetic pigments.

The structure of the microalgal-bacterial consortium results in an ideal self-sustaining system where oxygen was produced by photosynthetic microorganisms and immediately used by the adjacent heterotrophic bacteria. Moreover, the presence of dense microalgal-bacterial bioflocs ensured good settleability properties with an average effluent TSS concentration of 14±17 mg TSS/L.

Various studies have reported wastewater treatment with microalgal-bacterial consortia better than with single bacterial or algal systems, with the further advantage of lower biomass harvesting cost compared to algal systems alone (Muñoz et al., 2005; Su et al., 2011; Liu L. et al., 2017).

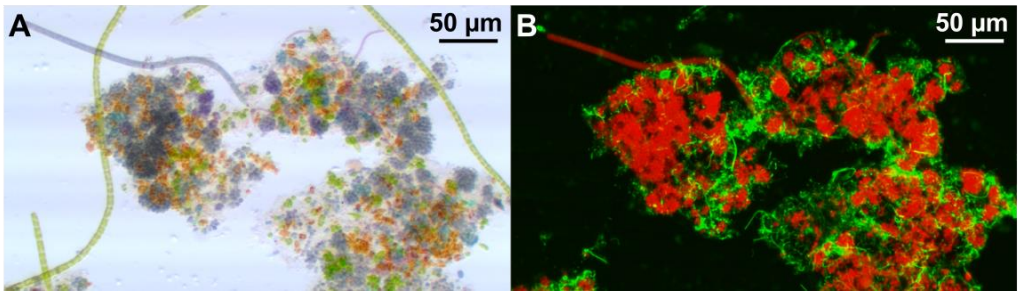

Figure 6.3 *Structure of the microbial community: (A) flocs under visible light; (B) flocs composed by photosynthetic microorganisms (red fluorescence) and heterotrophic bacteria (green fluorescence).*

6.3.3 Profiles of N forms during the typical PSBR cycle and online parameters (DO, pH)

Track studies were performed to monitor the profiles of NH_4^+-N, NO_2^--N, NO_3^--N during a typical cycle after the addition of influent wastewater (Figure 6.4). In the light phase, ammonium was removed rapidly. In the track study in Figure 6.4A, ammonium decreased from the initial concentration of 13.8 mg NH_4^+-N/L to zero in approximately 6 hours. At the same time, the concentration of NO_3^--N increased by 9.0 mg NO_3^--N/L (Figure 6.4A). Therefore, a partial simultaneous nitrification-denitrification was observed in the PSBR because of local anoxic conditions that occur within the dense microalgal-bacterial aggregates or during phases with DO near zero (Figure 6.4B).

The ammonium removal rate was calculated by considering the slope of the straight line that interpolates the experimental NH_4^+-N concentrations over time. In the track study shown in Figure 6.4, the volumetric rate resulted 2.9 mg N L^{-1} h^{-1}, which corresponded to a specific rate of 2.4 mg N g TSS^{-1} h^{-1} at TSS concentration of 1.2 g TSS/L.

Ammonium removal occurred during the light phase and without external aeration. Oxygen was produced continuously in the system due to photosynthetic activity. However, in the presence of a high oxygen demand for ammonium oxidation, DO concentration in the bulk liquid was close to zero for several hours (Figure 6.4B). The real-time measurements of DO and pH made it possible to identify the complete removal of ammonium (Chapter 8). In particular, two simultaneous characteristic points were detected : (1) the “Ammonia Valley” which is a relative minimum in the pH profile; (2) the “DO breakpoint” which corresponds to a sudden increase in the DO profile not caused by a higher irradiation.

Comparing the ammonium removal rate of the PSBR with conventional activated sludge-based processes, the following aspects can be observed:

- the specific ammonium removal rate (in terms of mg N g TSS^{-1} h^{-1}) was similar to the typical nitrification rate assumed for activated sludge. Although algal process may present slow biokinetics (Judd et al., 2015), here

the ammonium removal was supported by autototrophic nitrification;
- the TSS concentration in the microalgal-bacterial consortium was 1.2 g TSS/L on average, approximately three times less than activated sludge;
- the volumetric ammonium removal rate (in terms of mg N L^{-1} h^{-1}) was significantly lower than activated sludge, so that the PSBR appears less competitive in terms of foot-print;
- the major advantage of the PSBR process is that ammonium was completely removed without external energy supply, resulting in a very cost-effective process.

6.3.4 Improvement of total N removal can be coupled with energy saving

Effluent nitrates from the PSBR remained relatively high, reaching an average concentration of 13.7±8.7 mg N/L in the experimentation. These values did not permit to reach the effluent total nitrogen (TN) of EU regulation for sensitive areas, which imposes a maximum annual average of 10 or 15 mg N/L depending on the Population Equivalent. Therefore, nitrate removal needed to be improved through optimization of denitrification, especially during dark periods when photosynthesis does not occur and anoxic conditions can take place. As discussed in details in Chapter 7 the applied strategies were: (1) feeding of influent wastewater during the dark periods, in order to couple the availability of COD and anoxic conditions; (2) reduction of mixing during the dark periods. In this way, TN concentration in the effluent was lowered to 6.3±4.4 mg N/L, which enabled compliance with the European Directive (Chapter 7). Alternatively, another interesting approach could be the implementation of a shortcut N-removal (Wang et al., 2015). In this case the temporary accumulation of nitrites, which occurs in the final part of ammonium removal (as shown in Figure 6.4B), could be exploited to shortcut the conventional nitrification/denitrification process, obtaining benefits in terms of energy and carbon supply.

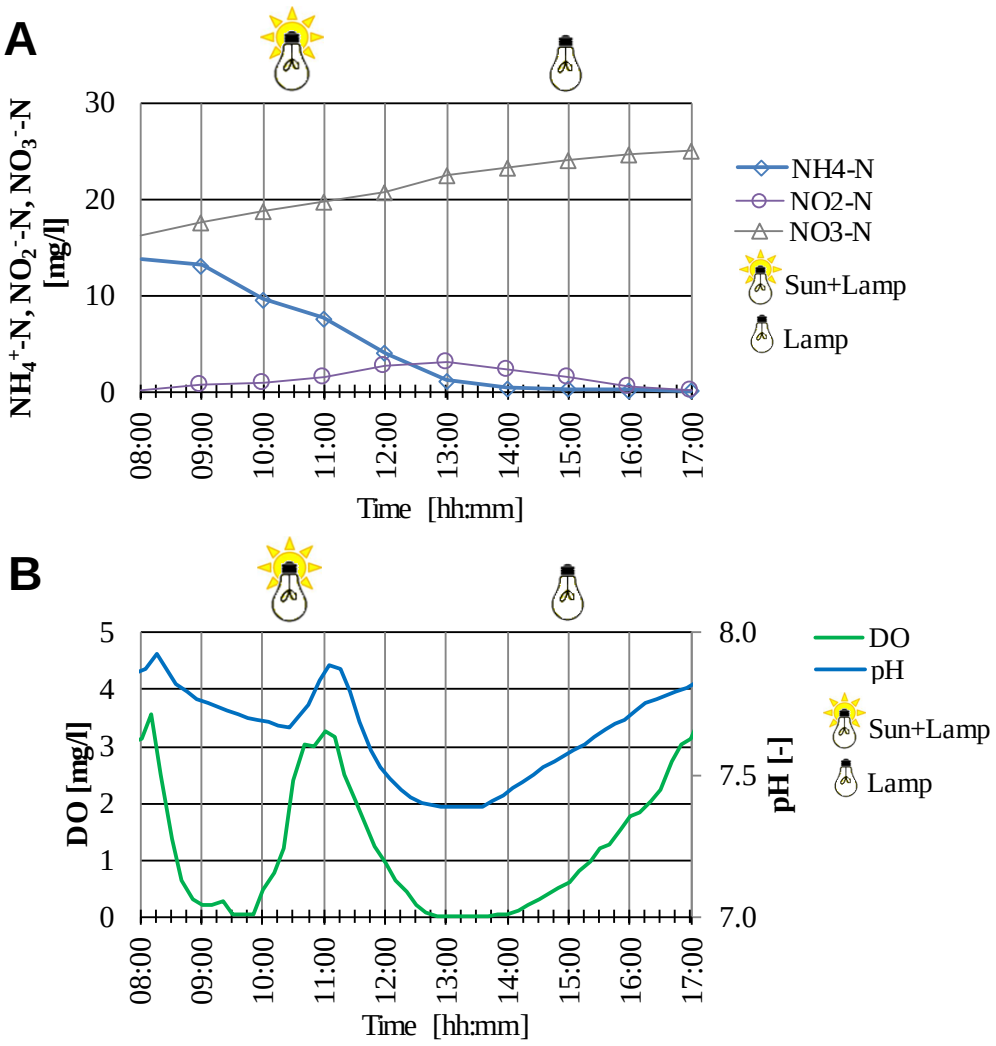

Figure 6.4 *Track study during a typical cycle: (A) profiles of NH_4^+-N, NO_2^--N and NO_3^--N ; (B) profiles of online parameters DO and pH.*

6.3.5 Limited removal efficiency of phosphorus due to low sludge production

As regards phosphorus, only an average removal of 50±19% was achieved in the PSBR during the 7-months of experimentation. The influent concentration passed from an average of 4.7±1.8 mg P/L to an average of 2.3±0.9 mg P/L in the effluent (Figure 6.5). To guarantee effluent TP under EU discharge limits

for sensitive areas (maximum annual average of 1 or 2 mg N/L depending on the Population Equivalent), the removal should be improved. This is an open issue that requires further research. The algal systems are expected to incorporate a significant amount of P for their synthesis (Powell et al., 2008), but in this PSBR the synthesis of biomass was limited. Considering the excess sludge production in the PSBR of 0.03 g TSS/d, the direct consequence is a limited P uptake from wastewater. Other findings in the literature highlight that photobioreactors aimed at purifying wastewaters according to low discharge limits usually present lower applied loads and longer retention times, and thus excess sludge production is low (Judd et al., 2015).

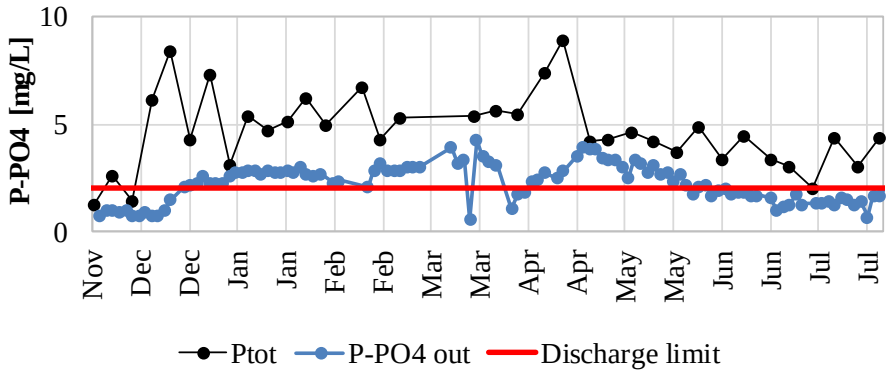

Figure 6.5 *Total P concentration in the influent wastewater and PO_4^{3-}-P in the effluent.*

6.3.6 Towards a cost-effective and sustainable wastewater treatment based on wastewater-born microalgal-bacterial consortium

This study has shown that the photosynthetic activity, able to produce a sufficient amount of oxygen to support COD and TKN removal, is the key variable of the process. Thus, light is a new factor to take into account, while DO concentration is not so meaningful when it is near zero for a long period of the cycle. Photosynthetic aeration is a very promising alternative in place of the mechanical aeration used in activated sludge. Furthermore, the challenge of

applying a PSBR system is to exploit daylight, since it is a renewable energy and the cheapest and most sustainable option (Chapter 9). However, there is still much to understand. Process parameters, consolidated for activated sludge, need to be redefined in the microalgal-bacterial consortia. In particular, further research is required to assess kinetic parameters (Chapter 11) and the optimal TSS content in PSBRs in order to avoid self-shading but increase the volumetric kinetics (Chapter 10).

6.4 Conclusion

The microalgal-bacterial consortium proved to be effective for real municipal wastewater treatment.
In particular:

- Photosynthetic oxygenation produced by a constant irradiation for 16 h/d (with intensity lower than natural solar irradiation), is sufficient to sustain complete nitrification and oxidation of organic compounds;
- The nitrification rate of the microalgal-bacterial consortium is comparable to that of mechanically aerated conventional processes (activated sludge);
- The system ensures high removal efficiency of COD and modest P removal;
- The biomass is characterized by good settleability.

Acknowledgements

©IWA Publishing [2018]. The definitive peer-reviewed and edited version of this article is published in Water Science and Technology 78(8):1726-1732(2018) https://doi.org/10.2166/wst.2018.453 and is available at www.iwapublishing.com.

Supplementary material

Here is reported a brief comment on the wastewater treatment performances of the Pilot, recorded from November 2016 to November 2018.
These results were presented at the 16th IWA Leading Edge Conference on Water and Wastewater Technologies, (Edinburgh, UK, 10-14 June 2019), in the poster *Nutrient removal and microbial community analysis of a stable microalgal-bacterial consortium treating real municipal wastewater*. Petrini S., Foladori P., Armanini F., Beghini F., Segata N., Andreottola G.

Microalgal-bacterial consortia have gained increasing attention in wastewater treatment. However, to date little is known about the performances of microalgal-bacterial consortia naturally developed in real municipal wastewater (Kang et al., 2018). In particular, long-term systems operating with such type of wastewater have been rarely characterized.

The treatment performances of the Pilot were monitored for 2 years (from November 2016 to November 2018, Table S6.1).

For the entire period the Pilot was operated as a photo-sequencing batch reactor (PSBR) with a photoperiod of 16 h of light/8 h of dark, and fed with the municipal wastewater collected after the primary sedimentation of the WWTP Trento Nord (Trento, Italy). The cycle length was kept at 48 hours and the influent rate at 0.7 L/cycle (HRT 5.6 d). Along the experimentation, the operational regime was slightly modified (Chapter 7), however the changes did not affect significantly the overall treatment performance.
Pure strains of microalgae were never inoculated instead biomass developed spontaneously.

Parameter	**Concentration (mg/L)**		**Removal efficiency (%)**
	Influent	**Effluent**	
COD	250±96	68±9	67±16
sCOD	122±48	24±9	78±13
Total N (TN)	56±18	15.1±7.2	72±13
TKN	52±17	3.6±0.7	93±3
NH_4^+-N	48±16	0.5±0.7	99±2
NO_2^--N	0.2±0.4	0.1±0.3	-
NO_3^--N	1.2±0.8	11.4±7.2	-
Total P (TP)	5.0±1.8	3.2±0.8	32±19
PO_4^{3-}-P	2.9±1.1	2.3±0.8	21±19
TSS	103±60	39±48	61±23

Table S6.1 *Characterization of the influent and effluent wastewater and removal efficiency of the Pilot from November 2016 to November 2018 (avg.±st.dev.).*

The system was able to treat real municipal wastewater without artificial aeration. The photosynthetic oxygen production proved to be sufficient to guarantee organic matter and ammonium oxidation over the entire experimentation with removal efficiency of 67±16% for COD, 93±3% for TKN and 99±2% for NH_4^+-N (Table S6.1).

As show in Figure S6.1A, despite the fluctuations of the influent COD, the system guaranteed an effluent COD under the EU discharge limit (EU Directive 91/271/EEC) with an average effluent concentration of 68±9 mg COD/L.

Ammonium was mainly removed by nitrification with a subsequent nitrate accumulation in the system (Figure S6.1B) that resulted in an average effluent concentration of 11.4±7.2 mg NO_3^--N/L. Biomass assimilation accounted only for 4% of removed TKN, while ammonia volatilization and stripping was excluded because pH never reached values over 9.

About phosphorous, the system removed about 32±19% of Total P (TP). As shown in Figure S6.1C phosphorous removal was not characterized by a constant trend as COD and NH_4^+-N, resulting in an effluent PO_4^{3-}-P of 2.3±0.8 mg P/L, very variable over time. The low P removal was linked to a limited P uptake, while precipitation due to pH variation could be excluded. Further investigations are needed to understand mechanisms and to optimize P removal.

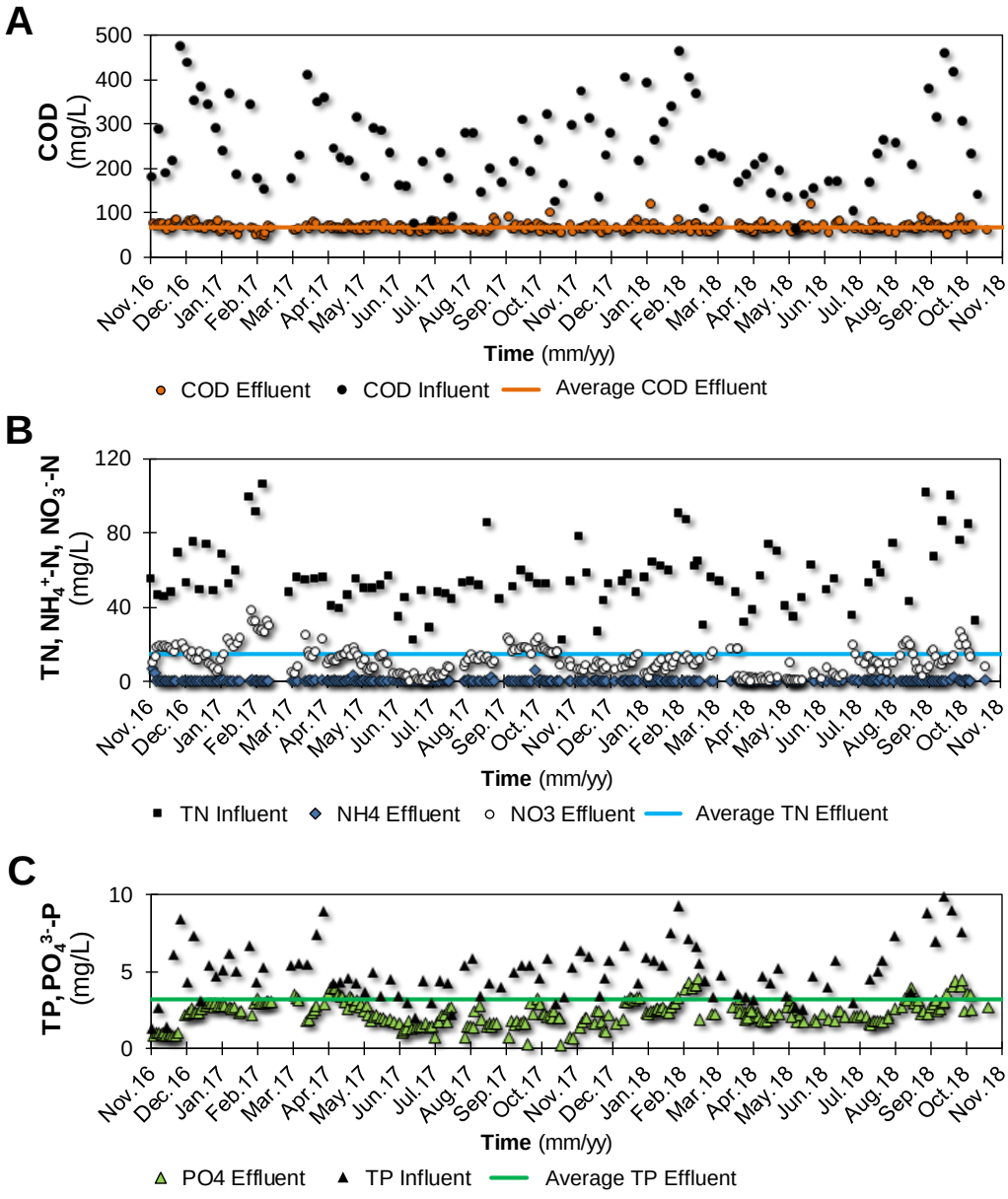

Figure S6.1 *Time course of influent and effluent concentration of (A) COD, (B) Nitrogen forms and (C) Phosphorous forms, from the Pilot between November 2016 and November 2018.*

CHAPTER 7

ENHANCED NITROGEN REMOVAL AND ENERGY SAVING

The operational regime of the lab-scale photo-sequencing batch reactor (Pilot) introduced in Chapter 6 was modified to optimize nitrogen removal, in particular to enhance denitrification. The operational conditions were modified one at a time and also with a view to energy saving, in order to improve the global sustainability of the process.
At the end, denitrification was ensured through feeding during the dark period and the intermittent use of mixer. In this way EU discharge limit in sensitive areas were met for nitrogen with an important energy-saving.

This Chapter is based on:
Foladori P., Petrini S., Nessenzia M., Andreottola G., 2018. *Enhanced nitrogen removal and energy saving in a microalgal-bacterial consortium treating real municipal wastewater.* Water Science and Technology 78, 174-182. https://doi.org/10.2166/wst.2018.094

Abstract

The optimization of total nitrogen removal from municipal wastewater was investigated in a laboratory-scale photo-sequencing batch reactor (PSBR) operated with a mixed microalgal-bacterial consortium spontaneously acclimatized to real wastewater. No external aeration was provided in the PSBR to reduce energy consumption: oxygen was only supplied by the microalgal photosynthesis. The enhancement of total nitrogen removal was achieved through: (1) feeding of wastewater in the dark phase to provide readily biodegradable COD when oxygen was not produced, promoting denitrification; (2) intermittent use of the mixer to favor simultaneous nitrification-denitrification inside the dense flocs and to achieve 41% energy saving with respect to continuous mixing. Efficient COD removal (86±2%) was observed, obtaining average effluent concentrations of 37 mg/L and 22 mg/L of total COD and soluble COD, respectively. TKN removal was 97±3%, with an average effluent concentration of 0.5±0.7 mg NH_4^+-N/L. Assimilation of nitrogen by heterotrophic bacteria accounted only for 4% of TKN removal, whilst the major part of TKN was nitrified. In particular, nitrification rate was 1.9 mg N L^{-1} h^{-1} (specific rate 2.4 mg N g TSS^{-1} h^{-1}), measured at dissolved oxygen near zero, when the oxygen demand was higher than the oxygen produced by photosynthesis. Total nitrogen of 6.3±4.4 mg N/L was measured in the effluent after PSBR optimization.

7.1 Introduction

The treatment of real wastewater with microalgal-bacterial consortia has gained increasing attention in the last few years because the synergistic effects of microalgae and heterotrophic bacteria can be exploited for carbon and nitrogen removal through nitrification-denitrification, ensuring a significant energy saving (Su et al. 2012; Zhang et al. 2012; He et al. 2013; Quijano et al. 2017; Abinandan and Shanthakumar, 2015; Wang L. et al. 2016; Arcila and Buitrón, 2017).

However, when ammonium removal occurs with nitrifiers in activated sludge, a huge amount of electrical energy is required to supply air in aerobic bioreactors. This energy consumption, represents up to half of the energy expenditure of a

wastewater treatment plant (WWTP) based on activated sludge. In particular, considering the annual energy consumption for air supply in aerated tanks in the range 4.7-28 kWh PE^{-1} y^{-1} (Foladori et al. 2015), a medium size WWTP (20,000 Population Equivalent, PE) may consume 94-560 MW/y which corresponds to an annual cost of 11,000-64,000 €/y (average EU electricity price for industrial consumers of 0.114 €/kWh; Eurostat, 2017).

These figures emphasize the need to explore new alternatives aimed at reducing energy consumption and associated costs of wastewater treatment in WWTPs. In this context, the development of heterogeneous microalgal-bacterial consortia offers the possibility of moving towards quasi-zero-energy consumption; in particular, the oxygen produced by photosynthetic microorganisms may support the oxidation of organic matter and ammonium by heterotrophic and nitrifying bacteria (Van den Hende et al. 2014). Suspended-biomass reactors operating as photo-sequencing batch reactors (PSBR) represent a common configuration for the laboratory-scale implementation of microalgal-bacterial consortia (Arcila and Buitrón 2016; Wang Y. et al. 2016) because of the easy setup with small pumps and timers.

With regard to nitrogen removal in microalga-bacteria consortia, the main mechanisms are biomass assimilation, nitrification-denitrification and, when high pH values are reached, ammonia volatilization (Wang Y. et al., 2016; Delgadillo-Mirquez at al., 2016). González-Fernández et al. (2011) observed that microalgal assimilation of nitrogen is frequently overestimated. Su et al. (2011), treating municipal wastewater with a mixed population of microalgae and bacteria, observed that denitrification was considered to be a possible removal mechanism, while ammonia volatilization was excluded due to the pH being lower than 8.5.

In spite of the advantage of oxygen production by photosynthetic microorganisms, dissolved oxygen (DO) released in the bulk liquid may become excessive and may inhibit the transformation of nitrates into nitrogen gas through heterotrophic denitrification, which requires strictly anoxic conditions. Thus, it may be difficult to meet the legal requirements for total nitrogen in the effluent if the operational strategies in the microalgal system are not optimized. Wang

et al. (2015) achieved 90% of nitrogen removal by alternating light and dark periods and without artificial aeration, but to promote denitrification during the dark period, an organic carbon source was added.
The present experimental study focuses on the optimization of total nitrogen removal in a laboratory-scale PSBR fed with real wastewater and operated with a mixed consortium of microalgae, cyanobacteria and bacteria. The phases in the PSBR were feeding, react, settling and draw, but no idle phase was included in the cycles. The length of the phases and the photoperiod (light/dark) were combined so as to affect the duration of the aerobic and anoxic periods and promote nitrification and denitrification, without the need for an additional external carbon source. This paper contributes to the optimization of a PSBR, in terms of enhancement of nitrogen removal, reduction of the time of treatment, and energy saving where possible, thus improving the global sustainability of the system.

7.2 Materials and Methods

7.2.1 Influent wastewater

Influent municipal pre-settled wastewater was collected after the primary settler of the Trento Nord WWTP (100,000 PE) and fed in a lab-scale photobioreactor. No filtration of the influent wastewater was performed before the feeding in the reactor. This allows the microorganisms naturally present in the influent wastewater to enter in the reactor, thus affecting significantly the composition of the microalgal-bacterial consortium developed in the system. Table 7.1 shows the concentrations of the main parameters in the influent pre-settled wastewater: COD, soluble COD (sCOD), Total Kjeldahl Nitrogen (TKN), NH_4^+-N, NO_2^--N, NO_3^--N, Total Nitrogen (TN), Total Phosphorus (TP), PO_4^{3-}-P and Total Suspended Solids (TSS). The average concentrations are in agreement with typical values expected in pre-settled wastewater (Tchobanoglous et al. 2003).

Parameter	Concentration [mg/L]
COD	257±91
sCOD	120±42
TKN	55±20
NH_4^+-N	50±14
NO_2^--N	0.1±0.1
NO_3^--N	1.2±0.9
TN	54±22
TP	4.8±1.5
PO_4^{3-}-P	2.8±0.9
TSS	184±122

Table 7.1 *Characterization of influent pre-settled wastewater (avg±st.dev.; No.samples = 30).*

7.2.2 Photo-sequencing batch reactor

The PSBR setup consists of a cylindrical bench-scale reactor made of Pyrex glass with diameter of 0.13 m, height of 0.29 m and a working volume of 2 L (Colaver, Italy) not sealed from atmosphere (Figure 7.1A). The system was equipped with:

- peristaltic pumps (Kronos Seko, Italy) for pumping the influent and discharge the effluent; 0.7 L of influent wastewater was fed per cycle;
- cool-white lamp, 8 led x 0.5 W, 0.18 m high and 0.065 m width (Orion, Italy), arranged on one side of the PSBR;
- magnetic mixer set at 200 rpm (AGE, Velp, Italy) used to maintain the biomass in suspension during the reacting phase, but avoiding excessive turbulence and reoxygenation from air;
- timers (TR 612 top2, Theben, Germany) to control on/off of pumps, lamp and mixer.

A light intensity of 30 μmol m^{-2} s^{-1} (expressed as photosynthetically active radiation, PAR) was measured inside the reactor near the top of the liquid surface, in the most exposed point. Light intensity was originated by solar light penetration into the laboratory and the lamp, but the reactor was never exposed to the direct

sunlight. This light intensity is in the same order of magnitude of other studies in the literature (for example 63 μmol m^{-2} s^{-1} in Karya et al., 2013; 90 μmol m^{-2} s^{-1}, in Mennaa et al., 2015) but lower than the PAR in outdoor plants which surpasses 200 μmol m^{-2} s^{-1} (light irradiances that saturate photosynthesis). It is worth noting that no external aeration was provided in the PSBR (in order to reduce energy consumption and move towards an energy-zero system); the oxygen available in the reactor was only supplied by the microalgae photosynthesis. The temperature of the mixed liquor during the experimentation was 22.8°C on average.
An acclimatized microalgal-bacterial consortium spontaneously developed for more than one year in the PSBR was employed in this study, which was carried out from January to July 2017. Microscopic observations of the biomass showed the presence of *Chlorella*, diatoms, many filamentous cyanobacteria and heterotrophic bacteria embedded in flocs.

7.2.3 Operational strategy in the PSBR

The typical PSBR cycle was based on the following phases: (1) feeding, with duration of 5 min; (2) react, 47.5 hours; (3) settling, 30 min; (4) draw, 5 min. The photoperiod was 16 hours of light + 8 hours of dark and the sequence of the light and dark periods is summarized in Figure 7.1B. A constant photoperiod using artificial light allowed us to control the photoperiod and understand the process clearly. The sequence of light and dark causes the alternation of high and low oxygen in the bulk liquid and thus the alternation of aerobic and anoxic conditions, which can be advantageously exploited for optimizing nitrogen removal from wastewater.

In order to enhance total nitrogen removal and save energy in the PSBR, four different operational regimes were applied during the experimentation (Figure 7.1B):

- LOW: feeding at the beginning of the light phase (at 8:00) and continuous mixing during the react phase. This basic operational regime was used as

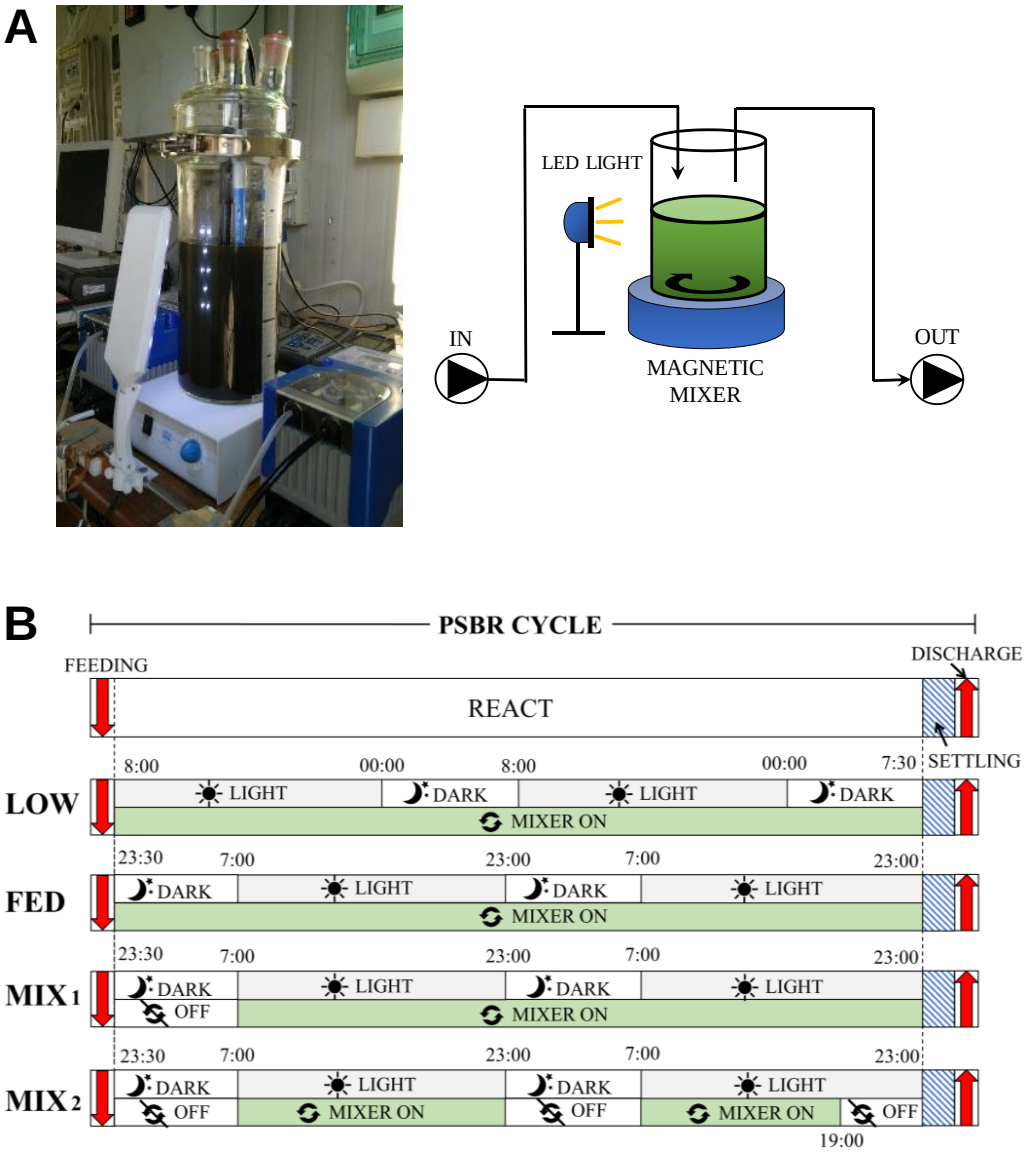

Figure 7.1 *(A) Lab-scale PSBR; (B) Operating cycles during the 4 regimes (LOW, FED, MIX_1, MIX_2)*

the control/starting point, but it did not meet the EU discharge limits in sensitive areas for total nitrogen (15 mg N/L for 10,000 < PE < 100,000; 10 mg N/L for PE > 100,000), requiring progressive optimizations;

- FED: feeding at the beginning of the dark phase (at 23:30) and continuous mixing in the react phase; the aim was to create an anoxic phase at the

beginning of the cycle (to exploit readily biodegradable COD, RBCOD, and the anoxic conditions of the influent wastewater) in order to promote denitrification and thus to enhance total nitrogen removal;

- MIX_1: feeding at the beginning of the dark phase (at 23.30) and mixer off until the beginning of the light phase (at 07.00); the aim was to create an anoxic phase at the beginning of the cycle and to reduce the energy consumption by stopping the mixing for 7.5 hours in the cycle (16% of energy saving);
- MIX_2: feeding at the beginning of the dark phase (at 23.30) and mixer off during all the dark phases and before the end of the react phase (at 19.00); the aim was to create longer anoxic conditions to enhance denitrification and to reduce the energy consumption by stopping the mixing for 19.5 hours in the cycle (41% of energy saving).

Due to the good settleability of the biomass in all the operational regimes, the duration of the settling phase (30 min) was appropriate and remained unchanged.

7.2.4 Analytical methods

The chemical parameters COD, sCOD, TKN, NH_4^+-N, NO_2^--N, NO_3^--N, TP, PO_4^{3-}-P and TSS were analyzed in the influent and effluent wastewater according to the Standard Methods (APHA 2012). Influent TN was estimated as the sum of TKN and NO_x-N. The parameter sCOD was measured after filtration of the sample on 0.45-μm membrane. Fractionation of COD in the influent wastewater aimed at distinguishing soluble and particulate biodegradable COD was performed by respirometry (Vanrolleghem et al. 1999; Ziglio et al. 2001). TSS in the mixed liquor (APHA 2012) was measured to determine the concentration of the microalgal-bacterial consortium in the PSBR. Dissolved oxygen (DO) and temperature were measured with Multi3410 meter and FDO®925 sensor (WTW, Germany). Oxidation-reduction potential (ORP) and pH were measured continuously (every 10 min) with pH3310 meter coupled with the electrodes Sentix®ORP and Sentix®41, respectively (all from WTW, Germany).

PAR was measured with quantum sensor SQ-520 (Apogee Instruments, USA). Microscopic observations were performed using a Nikon Optiphot EFD-3 Microscope (Nikon, Japan) for the morphological characterization of the microalgal-bacterial consortium.

7.2.5 Track studies

Track studies were performed in the PSBR to measure the dynamics of the N-forms during the typical cycle. Samples were collected every hour, then filtered and finally analyzed for NH_4^+-N, NO_2^--N and NO_3^--N. The volumetric removal of NH_4^+-N (or the production of NO_3^--N) expressed as mg N L^{-1} h^{-1} was estimated using the slope of the straight line that interpolates the experimental concentrations over time during the track study. The correspondent specific rate expressed as mg N g TSS^{-1} h^{-1} was obtained by dividing the volumetric rate by the TSS concentration in the mixed liquor. The removal rate was also expressed per unit of surface for appreciating the foot-print of the system, taking into account the height of mixed liquor in the reactor.

7.2.6 Statistical analysis

A Student's t test, producing a p value, was applied to evaluate the significant difference in results. Significance was assumed at $p<0.05$

7.3 Results and Discussion

7.3.1 PSBR ensures robust and efficient COD removal (>85%) in all the operational regimes

The profiles of COD and sCOD concentrations in the influent and effluent wastewater during the 6-months experimentation are shown in Figure 7.2. Although large variations of COD concentration in real wastewater were common (257±91 mg/L), the average concentrations in the effluent were 37±7 mg COD/L (range min-max equal to 21-54 mg COD/L), without statistically significant variations among the operational regimes. These results largely met the EU limit for discharge (125 mg COD/L, according to EU Directive 91/271/EEC). The effluent total COD was measured analytically or calculated summing the soluble COD (22 mg sCOD/L on average) and the particulate COD estimated from effluent TSS concentration, VSS/TSS ratio of mixed liquor (0.80 on average) and the conversion factor 1.42 g COD/gVSS.
High removal efficiency of COD was achieved in all the PSBR operational regimes (86±2% on average), indicating that the variations of influent loads and the stopping of mixing did not affect significantly the organic matter removal. The PSBR appeared a very robust process to treat real municipal wastewater. For a comparison, COD removal > 70% was found by Arango et al. (2016) in the treatment of municipal wastewater with an average influent sCOD of 410 mg/L in a PSBR inoculated with microalgae and activated sludge. COD removal efficiency > 80% was found in a PSBR for the treatment of synthetic wastewater with 420 mg COD/L (Gutzeit et al. 2005). The removal of COD from municipal wastewater by microalgal-baterial consortia has been reported to be a very effective process (Gutzeit et al. 2005; Su et al. 2012).
The fractionation of influent COD permits to understand the composition of the effluent COD (Henze et al. 2008):

- particulate inert COD (X_I = 46±16 mg/L; 18% of COD) and particulate biodegradable COD (X_S = 100±36 mg/L; 39%) can be flocculated on suspended solids;

- soluble biodegradable COD (S_S = 95±34 mg/L; 37%) is rapidly biodegraded;
- soluble inert COD (S_I = 16±5 mg/L; 6% of COD) cannot be removed and thus it leaves the system in the effluent.

This COD fractionation suggests that the effluent soluble COD (22±6 mg/L) was mainly composed by the soluble inert fraction of the influent wastewater (SI) which passed unchanged through the PSBR, while the rest may be soluble microbial products (SMPs) originated from substrate metabolism and biomass decay (Azami et al. 2012).
The particulate COD in the effluent was associated to some suspended solids floating and leaving the system during the discharge. The effluent TSS concentration was around 13 mg TSS/L during the whole experimentation, indicating a very good sedimentation of the biological flocs developed in the PSBR.
With regards to the removal of nutrients in the whole experimentation, average P concentration decreased from 4.8±1.5 mg/L in the influent to 2.5±0.8 mg/L in the effluent (average removal efficiency of 47±19%), while N removal is discussed in depth in the following sections.

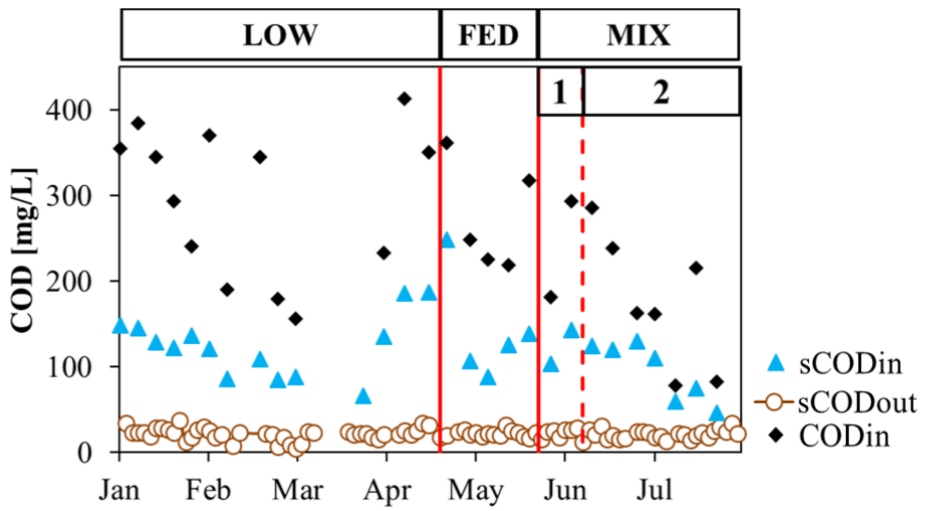

Figure 7.2 *Profiles of COD and sCOD in the influent and effluent wastewater.*

7.3.2 TKN removal >95% occurs in the PSBR at near-zero DO

The influent TKN (55±20 mg N/L) was almost entirely removed in the PSBR, leading to effluent concentrations of 1.5±2.1 mg N/L, 0.5±0.7 mg NH_4^+-N/L and 0.1±0.4 mg NO_2^--N/L.

There are three ways in which TKN and ammonium can be transformed by the microalgal-bacterial consortium: ammonia volatilization, assimilation by biomass and nitrification. In particular, volatilization was negligible in this PSBR because pH in the reactor was 7.6±0.3 on average during the whole experimentation, while ammonia volatilization requires relatively high pH values. Nitrogen is also assimilated and incorporated into biomass through cell synthesis during the growth of heterotrophs and, to a less extent, autotrophs (Tchobanoglous et al., 2003). The real amount of N removed by net microbial biomass growth was estimated taking into account sludge production, which was 0.03 g TSS/d. Considering the specific content of N in biomass (0.10 g N/g VSS), an amount of 2.4 mg N/L was used daily for the net growth. This accounts for about 4% of the TKN transformed in the system. This highlight that sludge production and nutrient uptake in PSBRs applied for the high efficient treatment of real municipal wastewater may be significantly lower than that expected in PSBRs specifically designed to maximize algae growth.

The N mass balance reveals that the major role in TKN removal in the PSBR was played by the autotrophic nitrification. Analogously, Karya et al. (2013) observed that nitrification accounted for more than 80% of ammonium removal during the treatment of synthetic artificial wastewater in an open photo-bioreactor inoculated with nitrifying activated sludge and a pure culture of *Scenedesmus spp.*.

The very low concentration of NH_4^+-N in the effluent wastewater (< 1.0 mg/L in 89 samples, with the exception of only 3 cases) demonstrates that nitrification was complete during the 6-months experimentation and not negatively affected by the different operational regimes implemented in the PSBR. As shown in Figure 7.3, the average TKN removal efficiency was 97±3% and very stable during the whole period, even when the influent TKN concentration reached

very high values around 100 mg N/L (Figure 7.3).

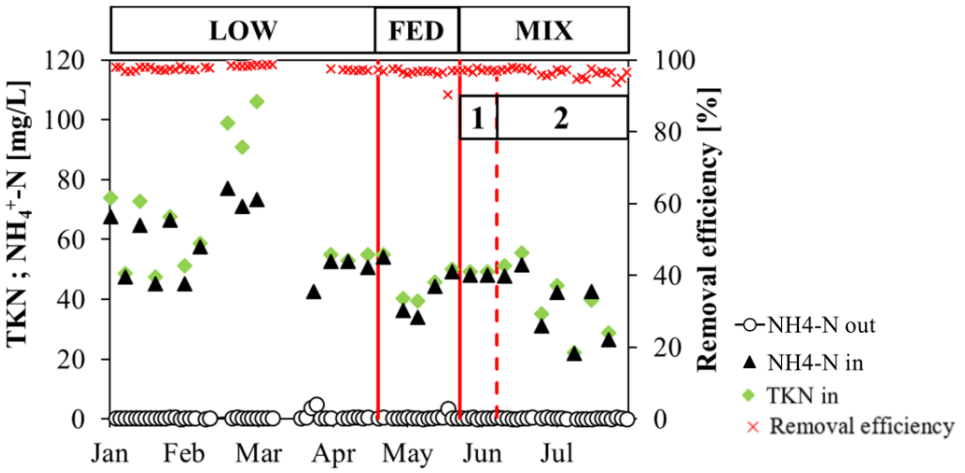

Figure 7.3 *Profiles of TKN and NH_4^+-N in the influent and effluent wastewater and removal efficiency of TKN.*

On the basis of these considerations, the nitrification kinetic in the PSBR reactor was investigated in depth. Track studies were carried out in the reactor after the addition of influent wastewater with a known amount of ammonium and the time profiles of NH_4^+-N, NO_2^--N, NO_3^--N were measured. The results obtained in a typical track study carried out during the light phase of the LOW operational regime (used as control) are shown in Figure 7.4. The decrease of ammonium occurred rapidly and the initial concentration of 14 mg NH_4^+-N /L was completely removed in less than 7 hours, corresponding to a nitrification rate of 1.9 mg N L^{-1} h^{-1}. Considering that the biomass in the PSBR was 0.8 g TSS/L, a specific nitrification rate of 2.4 mg N g TSS^{-1} h^{-1} was calculated. Similar results for nitrification kinetics were found during the other operational regimes (FED, MIX_1, MIX_2) which did not affect significantly the ammonium removal.

Considering the hourly nitrification rate, a daily rate of 30 mg N L^{-1} d^{-1} can be calculated for a daily photoperiod of 16/24 h, which corresponds to a surface removal rate of 5.4 g NH_4^+-N m^{-2} d^{-1} (considering the reactor's diameter of 0.13

m, top surface area of 0.0133 m^2 and volume of 0.0024 m^3). This specific value gives an approximate estimate of the footprint. For a comparison, 10.2 g NH_4^+-N m^{-2} d^{-1} was found in a flat PSBR with irradiance an order of magnitude higher than this experimentation (Rada-Ariza et al., 2017).

The specific value of 2.4 mg N g TSS^{-1} h^{-1} found for the microalgal-bacterial consortium is similar to the specific nitrification rate reported in the literature for activated sludge systems (Tchobanoglous et al., 2003). However, the important difference is that the microalgal-bacterial consortium works with a limited TSS concentration (around 1 g TSS/L) to allow light to penetrate in the biomass, while activated sludge works at 4 g TSS/L. This results in a significant difference in the volumetric nitrification rate of microalgal consortia and activated sludge. However, a further investigation is needed at real-scale to evaluate the volumetric nitrification rate of microalgal-bacterial consortia under more realistic conditions.

From Figure 7.4 it is immediate to observe that the decrease of ammonium occurred even during a long period (> 5 h) with DO concentrations near zero. Since no external aeration was provided in the PSBR, the photosynthetic activity was the only responsible for the oxygen production during the light phase. In the presence of NH4+, the oxygen demand required for nitrification surpassed the amount produced by photosynthesis, resulting in a near zero DO concentration. Then, when ammonium was completely depleted, DO concentration increased gradually, reaching values above 5 mg O_2/L.

Concerning the profile of NO_3^--N, the initial concentration of 14 mg N/L increased to 19.5 mg N/L at the end of the track study, indicating that only 40% of the ammonium removed was found as nitrates. The explanation of this low increase in nitrates is that simultaneous nitrification-denitrification occurred in this PSBR. The availability of soluble COD, which passed from 121 mg/L in the influent wastewater to 17 mg/L at the end of the track study, may support denitrification. Analogous observations were found by Tiron et al. (2015) in activated algae granules treating low-strength wastewater in a PSBR. In the present reactor, dense clusters of microalgae, bacteria and abiotic solids were also observed, and this may contribute to originate conditions for a partial

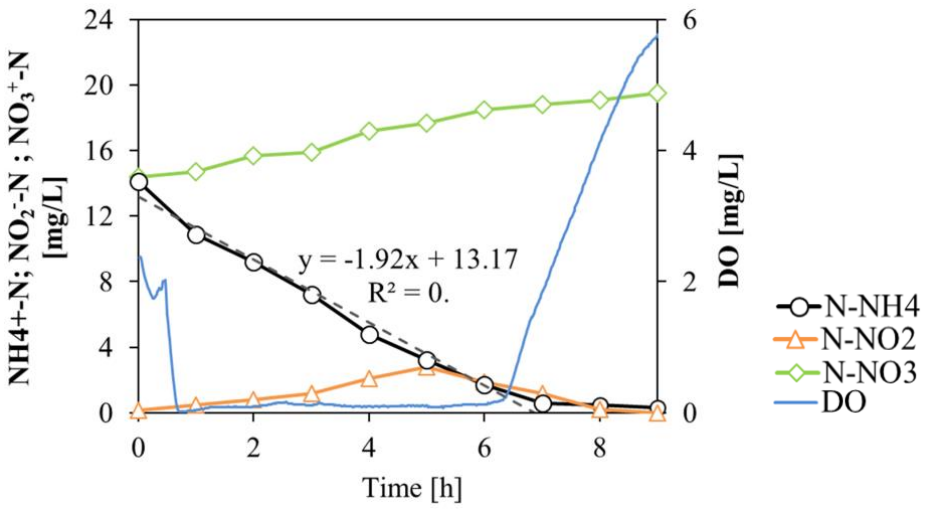

Figure 7.4 *Track study of NH_4^+-N, NO_2^--N and NO_3^--N in the PSBR together with DO profile, to evaluate nitrification kinetic during the light phase.*

denitrification.

Although the near-zero DO phase may suggest the absence of oxygen, it must not be confused with a completely anoxic phase, because photosynthesis occurred and oxygen was continuously produced in the system, but oxygen was not enough to satisfy the requirement of the biomass. The advantage to realize nitrification of municipal wastewater by exploiting the oxygen produced in a microalgal-bacterial consortium, without the need of artificial aeration, may offer very powerful opportunities in the evolution of WWTPs. However, further research is needed to prove the feasibility of the process under real condition in order to evaluate the influence of the main parameters variations (e.g. light supply, mass transfer and temperature).

7.3.3 Total nitrogen < 10 mgN/L in the effluent through the enhancement of denitrification in the PSBR

The LOW operational regime, used as the control, produced a concentration of TN in the effluent wastewater in the range 6.8-40.0 mg N/L, which was over the limits of 10-15 mg N/L (as an annual average) for discharge in sensitive

areas imposed by EU Directive 91/271/EEC (Figure 7.5). The high TN concentration in the effluent, largely composed by nitrates, was the result of: (1) slight assimilation of N by biomass and (2) only partial denitrification.
To enhance TN removal, efforts aimed at increasing the assimilation of N by pure microalgae do not seem to be so effective, because assimilation permits moderate N removal rates, often requires a longer reaction time and thus larger volumes for the treatment of wastewater.
The great advantage of using microalgal-bacterial consortia instead of pure microalgal strains is that bacterial nitrification can be exploited to speed up ammonium removal. Then a higher TN removal can be achieved by ensuring a denitrification step (Rada-Ariza et al. 2017).
In our case, the microalgal-bacterial consortium removed 30 mg N L^{-1} d^{-1} for a daily photoperiod of 16/24 hours, which was noticeably higher than those found by Álvarez-Díaz et al. (2017) (N removal of 6.6 mg N L^{-1} d^{-1}) treating secondary effluents under 14/24 hours of light with Chlorella sorokiniana. A similar N removal (6.63 mg N L^{-1} d^{-1}) was reported by Cabanelas et al. (2013) in the case of Chlorella vulgaris treating urban wastewater under 14/24 hours of light.
Concerning denitrification, there could still be room for improvement, when suitable conditions were applied in the PSBR. In the LOW operational regime the ORP profile (data not shown) assumed negative values only for 2-4 hours per cycle after the feeding phase, not long enough to create the conditions for full denitrification in the system. Therefore, the enhancement of TN removal was investigated through the optimization of the denitrification process, but without worsening the effluent quality in terms of COD and NH_4^+-N. This was achieved with the following modifications:

1. The time of feeding (FED operational regime): wastewater was fed during the dark period instead of the light period, in order to provide readily biodegradable COD, required for denitrification, during the dark period when oxygen is consumed but not produced;
2. The intermittent use of the mixer (MIX operational regime): switched on

during the light phases, when the biomass requires complete exposure to the light for photosynthesis, and switched off during the night, to avoid turbulence, favor denitrification inside flocs and energy saving; in this phase the biomass settled but the process was not negatively affected.

As shown in Figure 7.5, the application of the FED and MIX operational regimes resulted in a gradually decreasing profile of TN. The average TN concentration in the effluent was 21 ± 8.8 mg N/L in the LOW operational regime (not optimized), 16.2 ± 3.8 mg N/L in the FED regime, and 10.6 ± 2.9 mg N/L in the MIX_1 regime, reaching the lowest average value of 6.3 ± 4.4 mg N/L in the MIX_2 regime, which met the EU regulation limits. The enhancement of total N removal due to the progressive optimization of the PSBR was evident only when the MIX regimes were applied. In fact, no statistically significant difference was observed between the LOW and FED regimes, while effluent TN decreased significantly in the the MIX_1 and MIX_2 regimes ($p < 0.05$).
The decrease of TN occurred along with the extension of the period with negative ORP in the cycle. ORP values in the range -50 to -200 mV, which are favorable for denitrification, were measured for periods of 7-8 hours during the night in the MIX_2 regime. In this case, the mixer was switched off in the light phase (at 19:00, for 4 hours before settling and discharge), in order to move toward anoxic conditions before feeding, thus favoring denitrification at the beginning of the subsequent cycle.

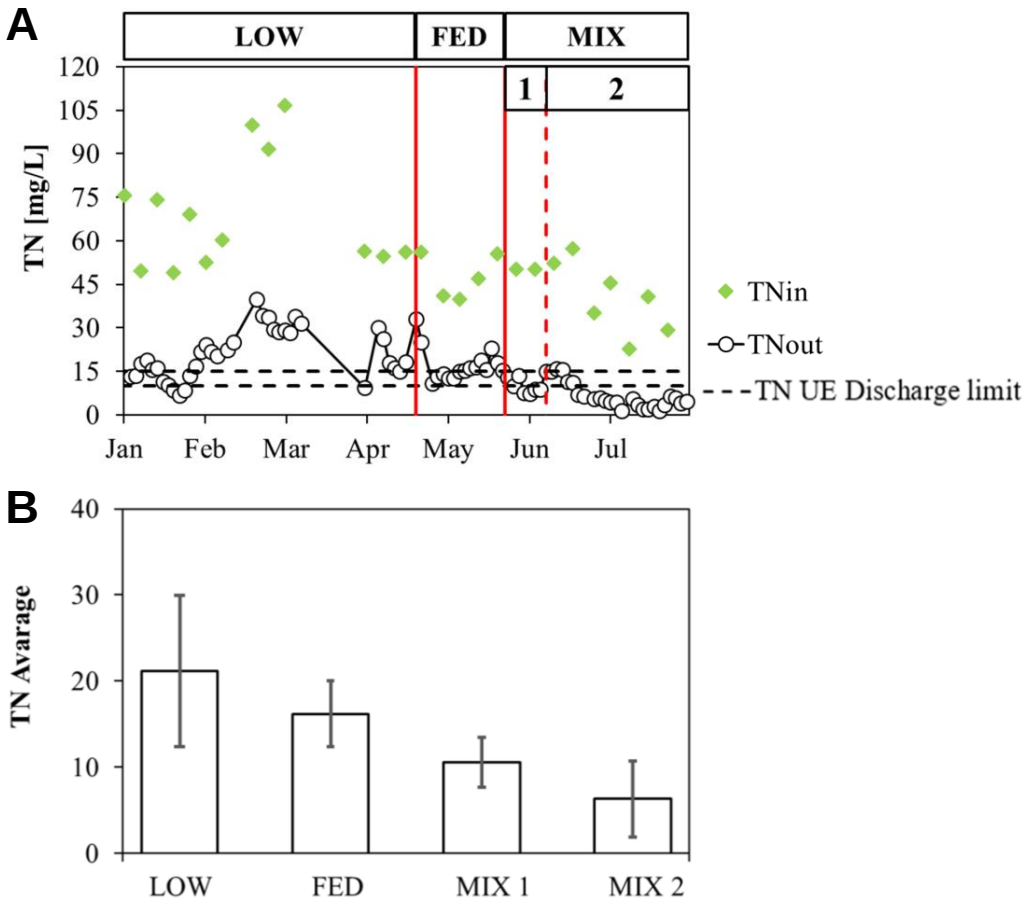

Figure 7.5 *(A) Profiles of Total Nitrogen in the influent and effluent wastewater compared with the discharge limit (EU Directive 91/271/EEC); (B) average effluent concentration and st.dev. for each operational regime.*

7.4 Conclusion

The total nitrogen removal in a PSBR fed with real wastewater and operated with a mixed microalgal-bacterial consortium was investigated and optimized to achieve effluent TN concentrations in accordance with EU requirements for discharge in sensitive areas.
COD and TKN removal in the whole experiment were 86±2% and 97±3%, producing an average effluent concentration of 37 mg COD/L and 0.5±0.7 mg NH_4^+-N/L. In spite of long periods with DO near zero during the PSBR cycle, due to an oxygen demand higher than photosynthesis production, the nitrification rate was 1.9 mg N L^{-1} h^{-1}, corresponding to a specific rate of 2.4 mg N g TSS^{-1} h^{-1}. PSBR optimization was aimed at enhancing denitrification through the feeding during the dark and the intermittent use of the mixer; in this way, the total nitrogen in the effluent during the MIX_2 regime reached 6.3±4.4 mg N/L. In conclusion, the PSBR allowed the nitrification of municipal wastewater under laboratory conditions without the need for artificial aeration and with an important energy saving, while simultaneous denitrification was exploited to enhance total nitrogen removal. However, considering the ability of microalgae or associated bacteria to synthesize N_2O, further research is needed to couple the nitrogen balance with a greenhouse gas mass balance.

Acknowledgements

The authors thanks Giovanna Flaim (Fondazione Edmund Mach, Italy) for the cooperation in the investigation of microalgae in the photobioreactor.

CHAPTER 8

MONITORING THE EVOLUTION OF THE REMOVAL PROCESS THROUGH REAL-TIME PARAMETERS

The Pilot (Chapter 6) was monitored with online sensors of DO (dissolve oxygen), pH and ORP (oxidation-reduction potential) to detect characteristic points along these profiles that reveal the evolution of the wastewater treatment.
The complete ammonium oxidation corresponded to two simultaneous characteristic points, while absolute peaks marked the conclusion of the oxidation process.
It emerged that the treatment was completed long before the end of the cycle. Therefore, the system could be optimized by reducing the HRT (Chapter 9).

This Chapter is based on:
Foladori P., Petrini S., Andreottola G., 2018. *Evolution of real municipal wastewater treatment in photobioreactors and microalgae-bacteria consortia using real-time parameters.* Chemical Engineering Journal 345, 507-516. https://doi.org/10.1016/j.cej.2018.03.178

Abstract

In the treatment of real municipal wastewater with photo-sequencing batch reactors (PSBR), operating strategies able to achieve high levels of pollutant removal, but reduce the hydraulic retention time (HRT), are imperative for making microalgal-bacterial consortia more competitive than conventional activated sludge systems. In regard to real-time monitoring, on-line probes like Dissolved Oxygen (DO), pH and oxidation-reduction potential (ORP) are cheap and reliable, but their exploitation has been largely overlooked in PSBRs. This paper proposes the use of DO, pH and ORP profiles to reveal the evolution of wastewater treatment in a PSBR treating real municipal wastewater with a mixed consortium of microalgae and bacteria. The PSBR ensured removal efficiency of 87±5% for COD and 98±2% for TKN without external aeration; indeed, photosynthesis was the only driver of the oxygen production. Considering the combined effects of photosynthetic oxygenation and microbial oxygen consumption, some practical information was gathered to understand the complex profiles of the on-line parameters. During dark and light phases, Zero-DO values, DO and pH raises, and their relative peaks were discussed to evaluate correctly the conclusion of the wastewater treatment and therefore to adjust the duration of the PSBR cycle. In particular: (1) two simultaneous "characteristic points", "Ammonia valley" (pH profile) and "DO breakpoint" (DO profile), detected univocally the complete ammonium removal; (2) the absolute peaks of DO, pH and ORP at maximum irradiance revealed that wastewater treatment was complete and the cycle could be concluded. In this way, these characteristic points were exploited for the optimization of the PSBR cycle, which was concluded after 15-26 h, reducing the HRT by more than 45%.

8.1 Introduction

Microalgal-based wastewater treatments have been studied since the early 1950s (Ludwig et al.,1951). However, in recent years, they have received increasing attention due to the sustainability of engineered photobioreactors that are moving towards small footprint and energy saving. The growing problem of global warming, the increasing energy consumption in the water sector, and the high costs of excess sludge disposal entail a paradigm shift in the configura-

tions of conventional wastewater treatment plants (WWTPs) to become more environmentally and economically sustainable. In this regard, a particularly attractive alternative may be the use of microalgae-bacteria consortia as an engineered system, where symbiotic relations between microalgae and bacteria may be advantageously exploited for wastewater treatment (Muñoz and Guieysse, 2006; Su et al., 2011; Arcila and Buitrón, 2016; Wang Y. et al., 2016; Gonçalve et al., 2017).

Most of the recent literature focuses on the use of pure microalgae strains to treat synthetic wastewater (or filtered wastewater) excluding bacteria inocula and microorganisms naturally present in real wastewater. Therefore, the reproducibility of real operational conditions of WWTPs is limited because the development of complex and heterogeneous consortia of microalgae, cyanobacteria and aerobic/anaerobic microorganisms, is hindered. Although microalgae and natural algal blooms have been tested in combination with enriched bacterial strains (Karya et al., 2013; Mujtaba et al., 2017) or activated sludge (Wang L. et al., 2016; Alcántara et al., 2015; Mujtaba and Lee, 2017), the scientific literature on the treatment of real wastewater with microalgal-bacterial consortia is still extremely scant.

Suspended-biomass reactors operating at lab scale as photo-sequencing batch reactors (PSBR) are among the configurations most used for the implementation of microalgal consortia (Van Den Hende et al., 2014). PSBRs offer the advantages of batch feed and sequencing phases that are operations easy to implement and control.

Knowledge about pollutant removal in PSBRs with microalgal-bacterial consortia is still in its infancy. However, preliminary results appear promising. García et al. (2017) observed in a photobioreactor with hydraulic retention time (HRT) of 2 days, an organic matter removal of 89±2%, similar to that typically achieved in conventional activated sludge systems and in conventional high rate algal ponds treating domestic wastewater.

Regarding total nitrogen and ammonium removal, microalgal-based systems may be inefficient (e.g. slow nitrogen assimilation, low efficiency of NH_4^+ nitrification) requiring very long HRTs in the range of 2-5 days (Judd et al., 2015;

Sutherland et al., 2014). In contrast, HRTs up to 1 day are enough to obtain nitrogen removal efficiencies of 60-80% in conventional nitrification-denitrification activated sludge systems. Therefore, the design of operating strategies able to achieve high levels of nitrogen removal with reasonable HRTs is essential to make microalgal-bacterial consortia more competitive than activated sludge systems, especially for PSBRs.

PSBRs monitoring is usually based on chemical analyses. Although chemical analyses are essential for evaluating effluent quality and pollutants removed loads, they are expensive, time-consuming and cannot be exploited in real-time because they are available with a certain delay. For real-time monitoring, on-line analyzers of direct chemical parameters (such as ammonium, nitrate+nitrite, phosphate, etc.) could be applied, but they require a certain level of maintenance (in some cases, frequent calibrations) and they are not always accessible at reasonable costs. Conversely, probes that measure indirect parameters such as Dissolved Oxygen (DO), pH and oxidation-reduction potential (ORP), are cheap, robust, reliable and user-friendly (Peng et al., 2006; Olsson et al., 2005).

The importance of real-time monitoring based on DO, pH and ORP profiles has already been demonstrated in activated sludge systems such as sequencing batch reactors (SBRs) and alternating oxic-anoxic activated sludge (Peng et al., 2006; Paul et al., 1998; Tanwar et al., 2008). In these studies, variations along profiles have made it possible to detect"characteristic points" useful for understanding the ongoing biological processes (Martín et al., 2012). More precisely, a characteristic point is a key indicator of the activated sludge process, denoted by a sharp change along a parameter profile. Usually, this variation coincides with the depletion of a compound or the transition from one process to another. For example, the end of nitrification in activated sludge SBRs can be identified by a point of minimum in the pH profile called "Ammonia Valley" and a flex in the DO curve called "DO breakpoint" that occurs simultaneously (Andreottola et al., 2001; Kim and Hao, 2001). Similarly, the end of the denitrification process corresponds to the "nitrate knee", a flex in the ORP profile (Andreottola et al., 2001; Kim and Hao, 2001). The presence of a characteristic point may suggest

that the treatment process is complete and therefore that the treatment phase can be concluded (Paul et al., 1998; Tanwar et al., 2008, Zanetti et al., 2012) while the absence suggests that the cycle needs to be prolonged to guarantee the required removal performance. The variation of online indicator such as pH, ORP and DO were demonstrated closely related with the nutrient removal performance, and this permits to establish the real time control of bioprocesses (Zhao et al., 2016).

In regard to photobioreactors, nutrient removal is dependent on a number of parameters, including DO concentration and pH. Although DO and pH monitoring occurs with a certain frequency in PSBRs (Su et al., 2011; Karya et al., 2013; Tiron et al., 2015; Wang et al., 2015) the data have not yet been used as means to control or manipulate the process. Indeed, these key parameters appear to have been largely overlooked in PSBRs (Judd et al., 2015).

Considering the necessity of reducing HRTs of PSBRs, and thus footprint and energy consumption, the possibility to adopt on-line DO/pH/ORP sensors to control and optimize the process, appears very interesting.

This paper explores real time monitoring of DO, pH and ORP in a PSBR treating real municipal wastewater with a mixed consortium of microalgae and bacteria. The objective is to find some characteristic points that may help understand how the treatment process evolves over time.

Microalgae-based processes are affected by natural light. Since photosynthesis produces oxygen and induces pH variations, the evolution of DO, pH and ORP profiles may differ significantly from that observed in activated sludge processes, for which a wide literature exists. In this case, the profiles induced by photosynthetic microorganisms overlap with the profiles produced by bacterial processes. This results in complex 24-h profiles more difficult to understand.

To our knowledge, this is the first time that DO, pH and ORP profiles have been investigated in depth in a PSBR treating real wastewater with a mixed microalgal-bacterial consortium. This paper provides some suggestions on how to understand these profiles in detail.

8.2 Materials and Methods

8.2.1 Influent wastewater

Influent pre-settled wastewater was collected from the Trento Nord municipal WWTP (Italy), which treats a population equivalent (PE) around 100,000 PE. Before the feeding in the PSBR, no filtration of the wastewater was performed. In this way, solids and microorganisms naturally present in the pre-settled wastewater were fed into the reactor.

8.2.2 Photo-sequencing batch reactor

The PSBR consists of a cylindrical bench-scale reactor made of Pyrex glass (0.29 m high and 0.13 m wide) with a working volume of 2 L, not sealed from atmosphere (Figure 8.1A). The system was operated with pumps, a lamp and a mixer controlled by timers. Peristaltic pumps (Kronos Seko, Italy) were used to pump the influent and discharge the effluent. The volume of influent wastewater fed into the PSBR every cycle was 0.7 L.
Sunlight entered the laboratory but the reactor was never directly exposed. Consequently, light was also supplied by a cool-white lamp (8 led × 0.5 W; Orion, Italy) arranged on one side of the reactor. Since daylight may vary in intensity and time, the artificial light was used to ensure a photoperiod of 16 h. In this way, a better understanding of on-line profiles was possible because a certain amount of irradiance was guaranteed throughout the light period. During the reaction phase, the biomass was mixed by a magnetic stirrer set at about 200 rpm to avoid excessive turbulence and reoxygenation from air. To be noted is that absolutely no external aeration was provided. Temperature of mixed liquor was 22.2°C on average. Biomass that occasionally stuck to the reactor walls, was detached in order to allow light penetration into the reactor.
A consortium of microalgae and bacteria was acclimatized for more than one year in the PSBR. Microscopic observations showed the presence of *Chlorella*, diatoms and filamentous cyanobacteria embedded in dense flocs together with a large amount of heterotrophic bacteria (Figure 8.1B). This experimentation

was carried out on the acclimatized biomass, from November 2016 to March 2017. Total suspended solids (TSS) in the PSBR were maintained at a concentration of approximately 1.3 g TSS/L. This biomass concentration was identified as optimal for fully exploiting volumetric kinetics and light diffusion (data not shown).

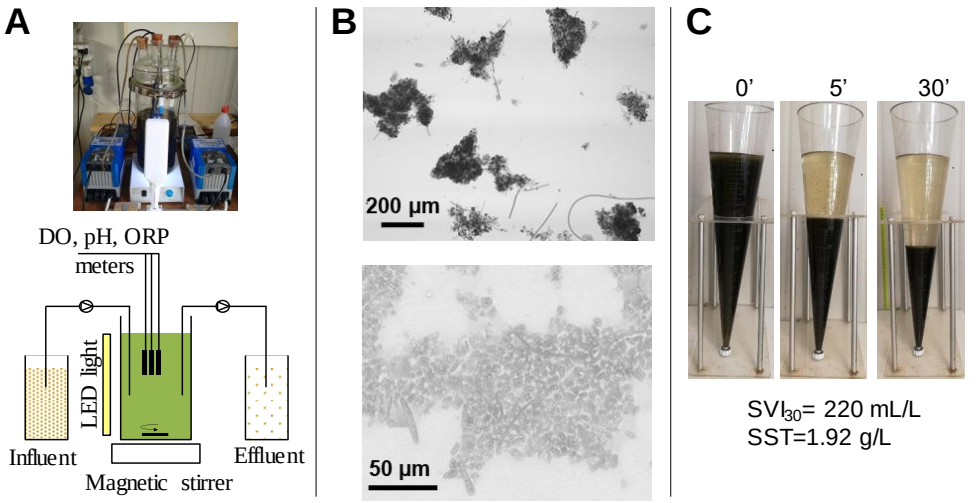

Figure 8.1 *(A) The photo-sequencing batch reactor. (B) Microscopic observations of microalgae-bacteria clusters. (C) Very good settleability of the biomass in the Imhoff cone.*

8.2.3 Typical cycle in the PSBR

The PSBR cycle consisted of four phases with a total duration of 48 h: (1) Feed, with a duration of 0.08 h; (2) React, 47.5 h; (3) Settlement, 0.5 h; (4) Draw, 0.08 h. The React phase comprised two photoperiods of 16 h light/8 h dark. The sequence of light periods (LP1, LP2) and dark periods (DP1, DP2) is shown in Figure 8.2. The cycle started at 8.00 a.m. with the Feed phase. Then, the first light phase (LP1) began immediately after the feeding. The sequence of light and dark resulted in an alternation of periods with high and low DO. As shown in Figure 8.2, light periods (LPs) affected microalgal photosynthesis, stimulating oxygen production and thus favouring aerobic conditions. Instead, during dark periods (DPs), oxygen was consumed by both bacteria and microalgal respiration, and

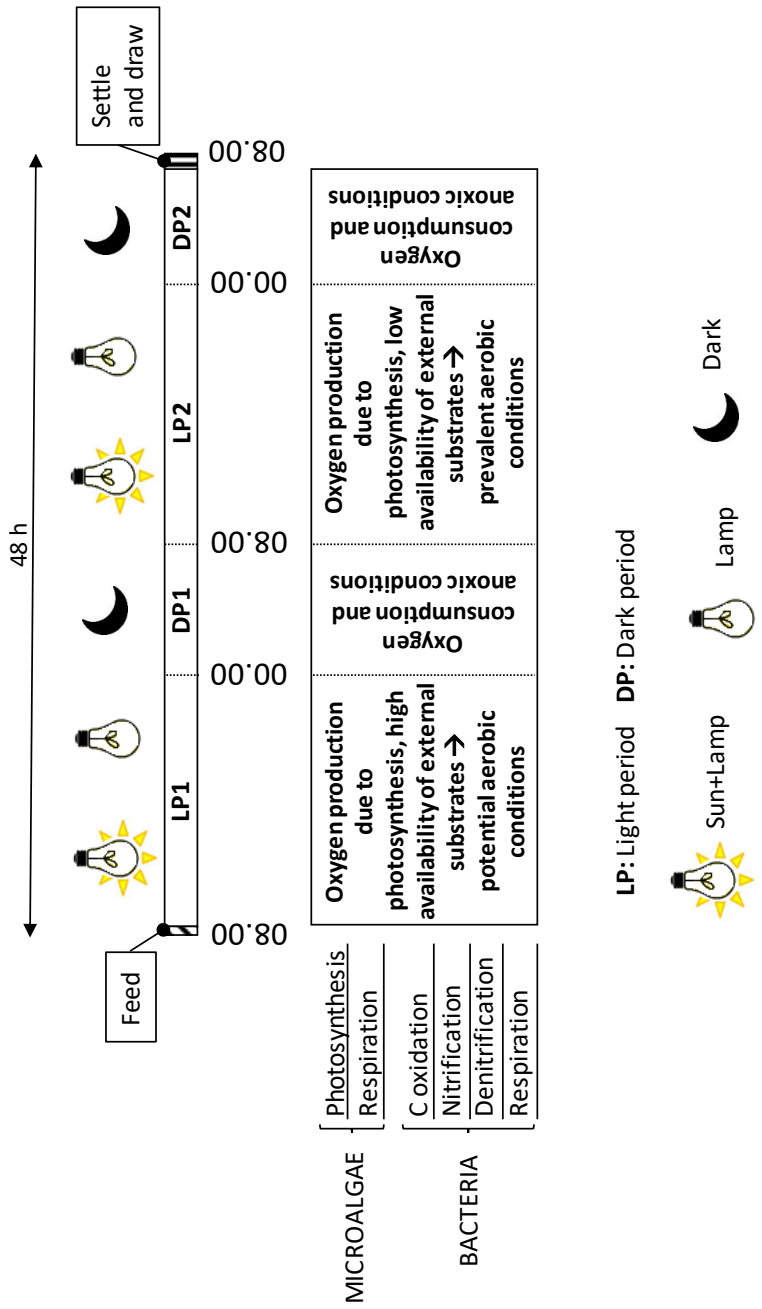

Figure 8.2 *Sequence of the light and dark periods, and overview of the ongoing-biological process in the PSBR typical cycle.*

therefore anoxic conditions occurred.
Due to the good settleability of the biomass (Figure 8.1C), only a period of 0.5 h was assigned to the Settlement phase.

8.2.4 Analytical methods

The following chemical parameters were analyzed in influent and effluent wastewater according to Standard Methods (APHA, 2012): total COD, soluble COD (sCOD), TSS, TKN, NH_4^+-N, NO_2^--N, NO_3^--N, and PO_4^{3-}-P. The parameter sCOD was measured after filtration of the sample on 0.45-μm membrane. TSS were measured in the mixed liquor, according to APHA (APHA, 2012), to determine the biomass concentration in the PSBR.
DO, pH, ORP and temperature were continuously recorded (every 10 min). DO and temperature were measured with an OXI340i meter coupled with the sensor CellOx®325 and with a Multi3410 meter equipped with the sensor FDO®925 (all from WTW, Germany). The parameters pH and ORP were measured with pH3310 meters coupled with the electrodes Sentix®41 and Sentix®ORP, respectively (all from WTW, Germany).
Light intensity (irradiance, IRR) was measured as photosynthetically active radiation (PAR) using a SQ-520 quantum sensor (Apogee Instruments, USA) placed inside the reactor, near the top of the liquid surface. Artificial light provided an average light intensity of 25±5 μmol m^{-2} s^{-1}.
Microscopic observations were performed using a Nikon Labophot EFD-3 Microscope (Nikon, Japan) to characterize the morphology of the microalgal-bacterial consortium.

8.2.5 Track studies

Track studies were performed in the PSBR to measure the dynamics of the N-forms during a typical cycle. Samples were collected every hour, then filtered and analysed for NH_4^+, NO_2^- and NO_3^-. The volumetric removal/production rate of nitrogen compounds (mg N L^{-1} h^{-1}) was estimated considering the slope of the straight line that interpolates the experimental concentrations over time.

The specific removal/production rate of nitrogen compounds (mg N g TSS^{-1} h^{-1}) was obtained by dividing the volumetric rate by the TSS concentration in the mixed liquor.

8.3 Results and Discussion

8.3.1 PSBR ensures removal efficiency of COD>85% and TKN>95% without external aeration

The main characteristics of influent and effluent wastewater together with the removal efficiency are shown in Table 8.1. The average concentrations of COD, sCOD, TSS, N and P forms in the influent wastewater match typical values expected in pre-settled wastewater (Tchobanoglous et al., 2003).

Although real wastewater presented large fluctuations of influent concentrations (Figure 8.3), high and stable removal efficiency were observed in the PSBR for COD (87±5%, Figure 8.3A), producing average effluent concentrations of 34±9 mg COD/L and 25±9 mg sCOD/L (Table 8.1). These results are comparable to those observed in the microalgal treatment of secondary domestic wastewater in outdoors pilot raceways which showed COD removal efficiency in the range 80-90% (Posadas et al., 2015) permitting to respect the discharge limits according to Directive 98/15/CEE.

The effluent TSS concentration was very low (7.4±6.2 mg TSS/L on average), due to the good settleability of the biomass developed in the PSBR which formed dense aggregates of microalgae, bacteria and inerts which entered the system with the real wastewater. This behavior differed significantly from that reported by other studies, where the uses of pure *Chlorella* or other pure strains have often been associated with difficult sedimentation and separation problems (Muñoz and Guieysse, 2006; Christenson and Sims,2011; Park et al., 2011). By contrast, the development of mixed microalgal and bacteria consortia can ensure a significant improvement in settleability (Arcila and Buitrón, 2016; Van Den Hende et al., 2014); hence, they are currently gaining increasing attention in wastewater treatment.

Parameter	**No. samples**	**Concentration** [mg/L]		**Removal efficiency**
	Influent-Effluent	Influent	Effluent	[%]
COD	16-45	292±101	34±9	87±5
sCOD	16-45	119±21	25±9	79±3
TKN	16-45	64±20	1.2±1.2	98±2
NH_4^+-N	16-45	55±13	0.6±1.2	99±3
NO_2^--N	16-45	0.1±0.1	0.1±0.1	-
NO_3^--N	16-45	1.1±0.3	19.0±7.4	-
Total N	16-45	66±20	20±7	68±10
PO_4^{3-}-P	16-45	2.7±0.8	2.2±0.8	16±17
TSS	16-13	143±72	7.4±6.3	93±4

Table 8.1 *Characterization of influent and effluent wastewater and removal efficiency in the PSBR (avg±st.dev.).*

With regard to nitrogen forms, average TKN removal efficiency was 98±2% (Figure 8.3B). As a result of a stable nitrification in the system, effluent ammonium was 0.6±1.2 mg NH_4^+-N/L, effluent nitrites were negligible, while nitrates were 19.0±7.4 mg NO_3^--N/L. These results are in agreement with the observation of Zhang et al. (2018) in algal-bacterial granules in a photobioreactor treating synthetic domestic wastewater. In this study the ammonia removal efficiencies was 97-99%, with negligible values of nitrites and accumulation of nitrates (Zhang et al., 2018).

In the microalgal treatment of secondary wastewater, the influence of pH 7-9 on nitrification was negligible and ammonium was rapidly oxidized by nitrification, which prevented NH_4^+-N stripping (Posadas et al., 2015).

The mass balance of total nitrogen indicated that 68±10% was removed by synthesis and spontaneous denitrification. Anoxic conditions favorable for denitrification occurred in various instances: (i) during the dark phases of the PSBR cycle, when DO drop to zero because not supplied by photosynthesis; (ii) during the light phases, when oxygen demand surpassed photosynthetic oxygenation, within the dense clusters of microalgae, bacteria and abiotic solids. For a comparison, Zhang et al. (2018) observed TN removal efficiency from

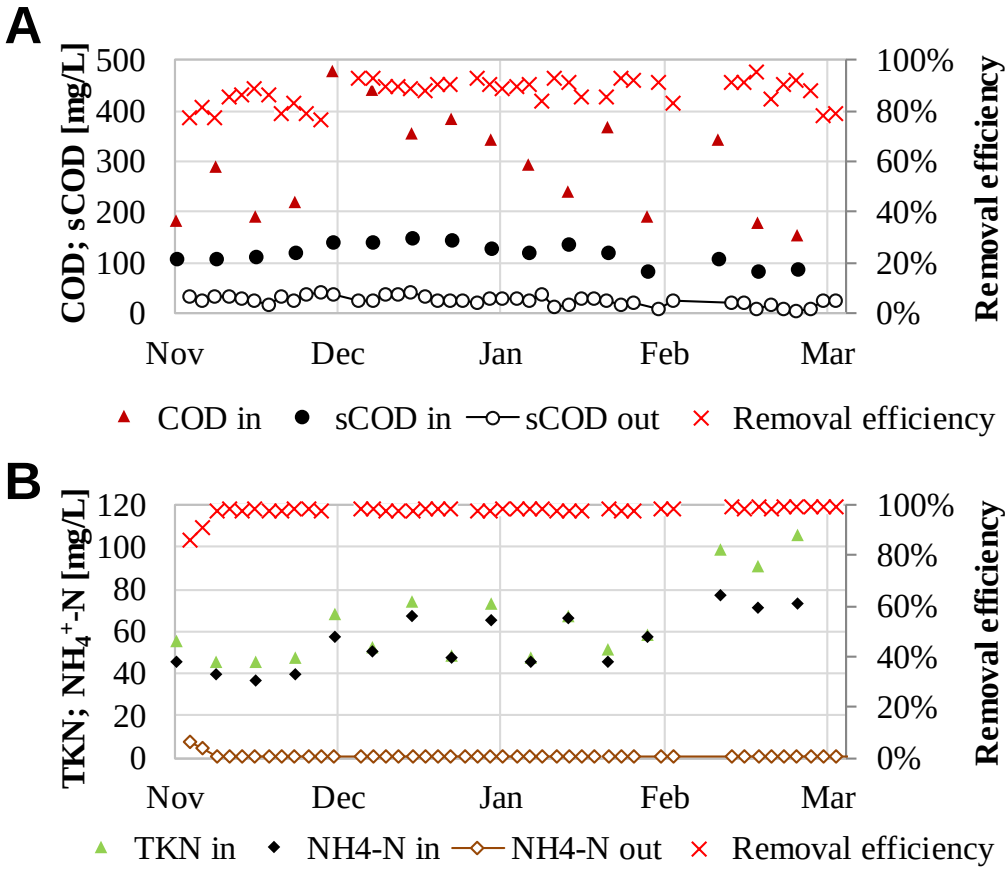

Figure 8.3 *(A) COD and sCOD in the influent and effluent wastewater and removal efficiency of COD; (B) TKN and NH_4^+-N in the influent and effluent wastewater and removal efficiency of TKN*

59.8% to 70.5% after the formation of mature granules in a photobioreactor. The detailed monitoring of a typical cycle (48 h) is shown in Figure 8.4 where the variations of NH_4^+-N, NO_3^--N and sCOD are indicated over time. The profiles DO and pH were clearly correlated with both light and nutrient removal performance. DO dropped to zero immediately after feeding and remained very low during LP1 and DP1 periods, while pH eventually reached a valley due to the nitrification process. The concentration in the influent wastewater was 234 mg COD/L and 78 mg sCOD/L and it decreased during the LP1 period due to the aerobic oxidation, leading to a minimum sCOD of 21 mg/L.

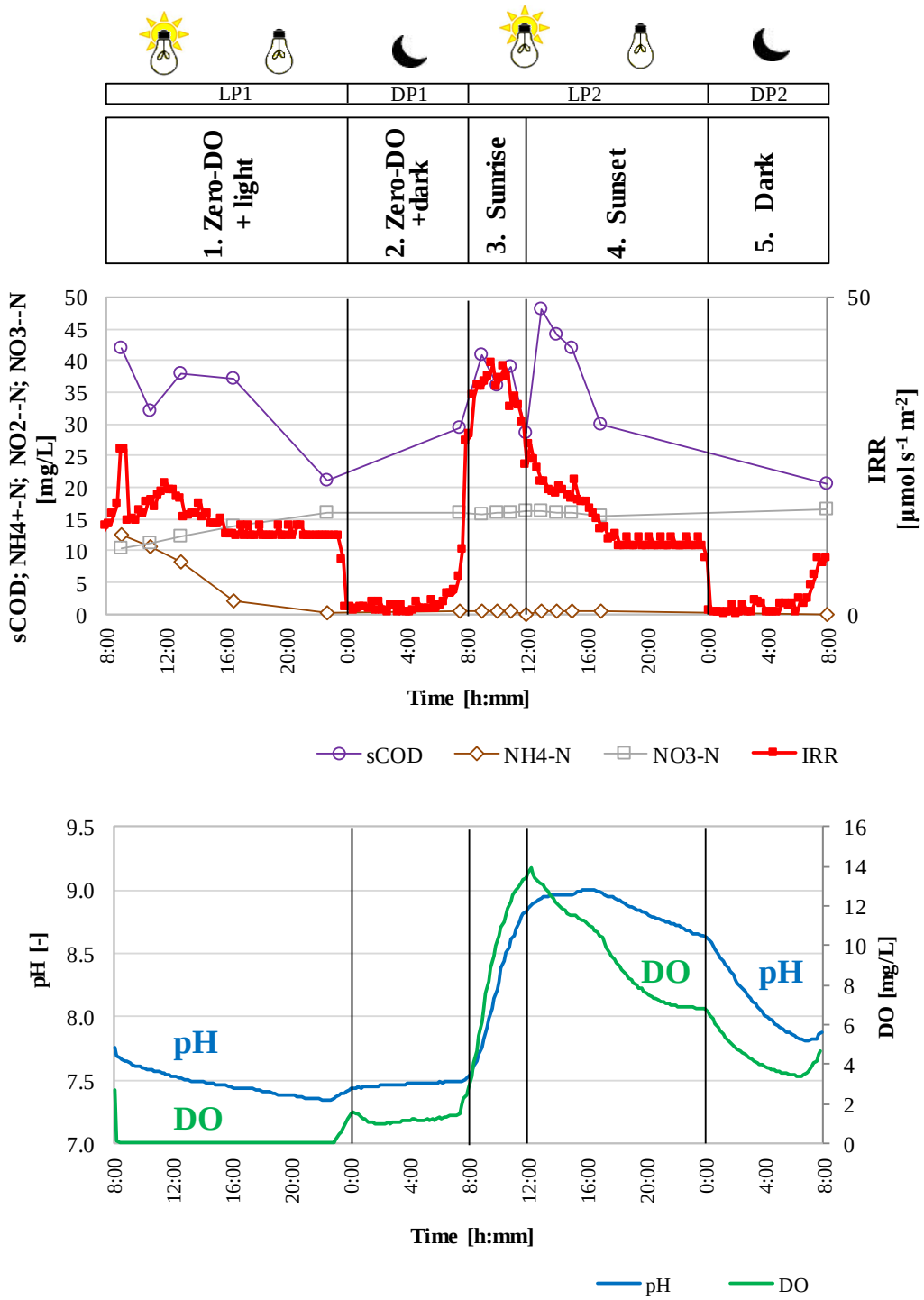

Figure 8.4 *Profiles of COD, NH_4^+-N, NO_2^--N and NO_3^--N during light and dark phases in an entire 48-hour typical cycle. (B) Profiles of online parameters pH and DO.*

At the beginning of the subsequent LP2 period, pH and DO increased rapidly and sharply as a result of the absence of ammonium and the presence of light which favoured photosynthesis. Surprising, the profile of sCOD correlates with irradiance. A significant release of sCOD was observed in coincidence with the peaks of DO and pH. This behavior is not clear and further investigation is required. The sCOD increase may be the results of the release of Soluble Algal Products but the mechanisms of their formation and their effects are still not clear. At the end of the cycle, the sCOD stabilized, resulting in an effluent COD concentration of 21 mg/L.
Since no external aeration was provided, photosynthetic activity was the only driving force to produce the oxygen necessary for COD oxidation and TKN nitrification. Hence, the consortium of cyanobacteria, microalgae and heterotrophic/nitrifying bacteria resulted in a symbiotic system able to ensure a self-sustained treatment process with high removal efficiency of COD and TKN. Similar observations were highlighted by García et al. (2017) treating domestic wastewater in a novel anoxic-aerobic photobioreactor.

8.3.2 The light source affects the shape of the DO profile: sunlight *vs.* artificial light

DO and Irradiance were monitored throughout some typical PSBR cycles. To study the effect of the light source on photosynthetic activity, and thus on DO profile, the feeding phase was skipped. In this way, the influence of oxygen consumed by bacteria to oxidize readily biodegradable substrates was excluded. Without feeding, only endogenous respiration of the biomass occurred. Therefore, the changes of DO in the reactor were mainly associated with light variations, and thus photosynthetic oxygenation, because biomass respiration consumed approximately a small amount of oxygen over time.
The effect of sunlight and artificial light on photosynthetic activity was examined in detail. Three different cases were considered. Figure 8.5 shows the effect of sunlight (Figure 8.5A), artificial light (Figure 8.5B) and both (Figure 8.5C) on DO profile.

In the case of sunlight (Figure 8.5A), the daily variations of irradiance shape a steep and narrow curve with a peak around midday. This produces a perfectly overlapped DO profile with a coinciding peak. Also, Posadas et al. (2015), treating primary domestic wastewater in outdoor raceways, showed that DO variations were well correlated with the sunlight, regardless of the raceway configuration and operational conditions. Instead, because artificial light (Figure 8.5B) produces a constant irradiance, it generates a step-function profile that reflects the adopted photoperiod (lamp on from 08.00 to midnight). As in the case of sunlight, the DO profile follows that of irradiance. Figure 8.5B shows that DO initially increases and then remains approximately constant until the end of the light period. On reaching the saturation level, DO changes smoothly because of temperature (data not shown). As soon as the lamp is turned off, without photosynthetic oxygenation, DO decreases as a result of endogenous respiration. The profile of irradiance produced by sunlight was completely different

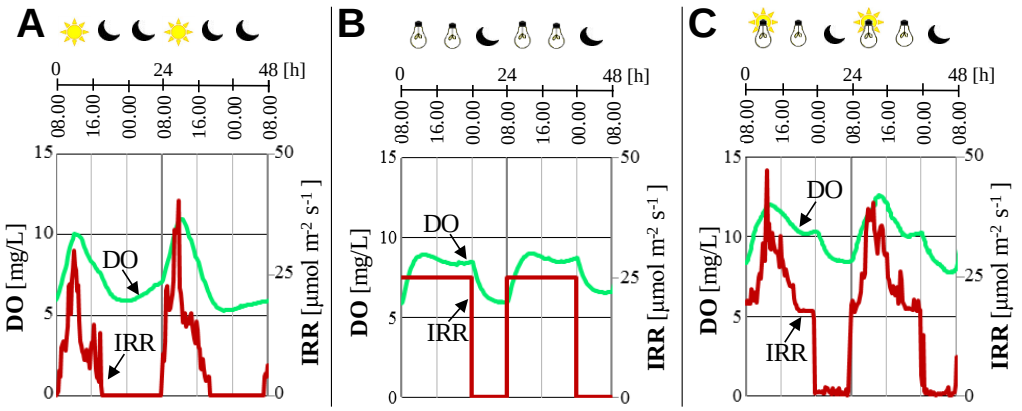

Figure 8.5 *Irradiance and DO profiles during the PSBR cycle (without feeding) with different light sources: (A) sunlight; (B) artificial light; (C) sunlight+artificial light.*

from that produced by artificial light. Consequently, DO profiles with different shapes were generated by different rates of photosynthesis in the PSBR.
In the third case, the combination of sunlight and artificial light (Figure 8.5C) produces an irradiance profile comparable to the superposition of each individual case. As a consequence, the DO profile is the combination of the single

effects previously observed: (i) maximum DO values at midday when solar irradiance is maximum; (ii) relatively high DO values during the whole light-phase supported by artificial light; (iii) gradual DO decrease during the dark when the light is off. As shown in Figure 8.5C, DO values are higher than those obtained with a single light source, in some cases reaching oversaturation level.
These simple observations yielded better understanding of the complex DO profiles generated in the PSBR throughout the experimentation, feeding influent real wastewater in the presence of sunlight and artificial light. A detailed description of the observed DO profiles is provided in Section 8.3.3.

8.3.3 The profiles of DO, pH and ORP reveal the evolution of wastewater treatment

The profiles of irradiance, DO, pH and ORP during three typical cycles in the PSBR, fed with real wastewater, are shown in Figure 8.6. All the profiles were clearly affected by the alternation of light and dark periods during the cycle and, in particular, by sunlight during the first part of the light periods. As shown in Figure 8.6A, maximum irradiance took place around midday.
During a typical cycle very strong variations of parameters occurred:

i. DO varied greatly from zero to oversaturation (Figure 8.6B). As in the case presented in Figure 8.5C, the DO profile followed that of irradiance. However, feeding wastewater resulted in a long period at DO zero over the first part of the cycle. Hence, much larger DO variations were observed;
ii. pH ranged from 7.5 to 9.0 (Figure 8.6C);
iii. ORP changed from negative values immediately after feeding (around −200 mV), to positive values at the end of the light periods (around +200 mV). This change indicates the transition from an initial reducing environment (negative ORP values) to an oxidizing environment (positive values) (Figure 8.6D). It is well known that the ORP measurement is not a true thermodynamic parameter and that the absolute ORP value does not furnish any process significance, it being a mere indicator of the oxidative-reductive state of the system.

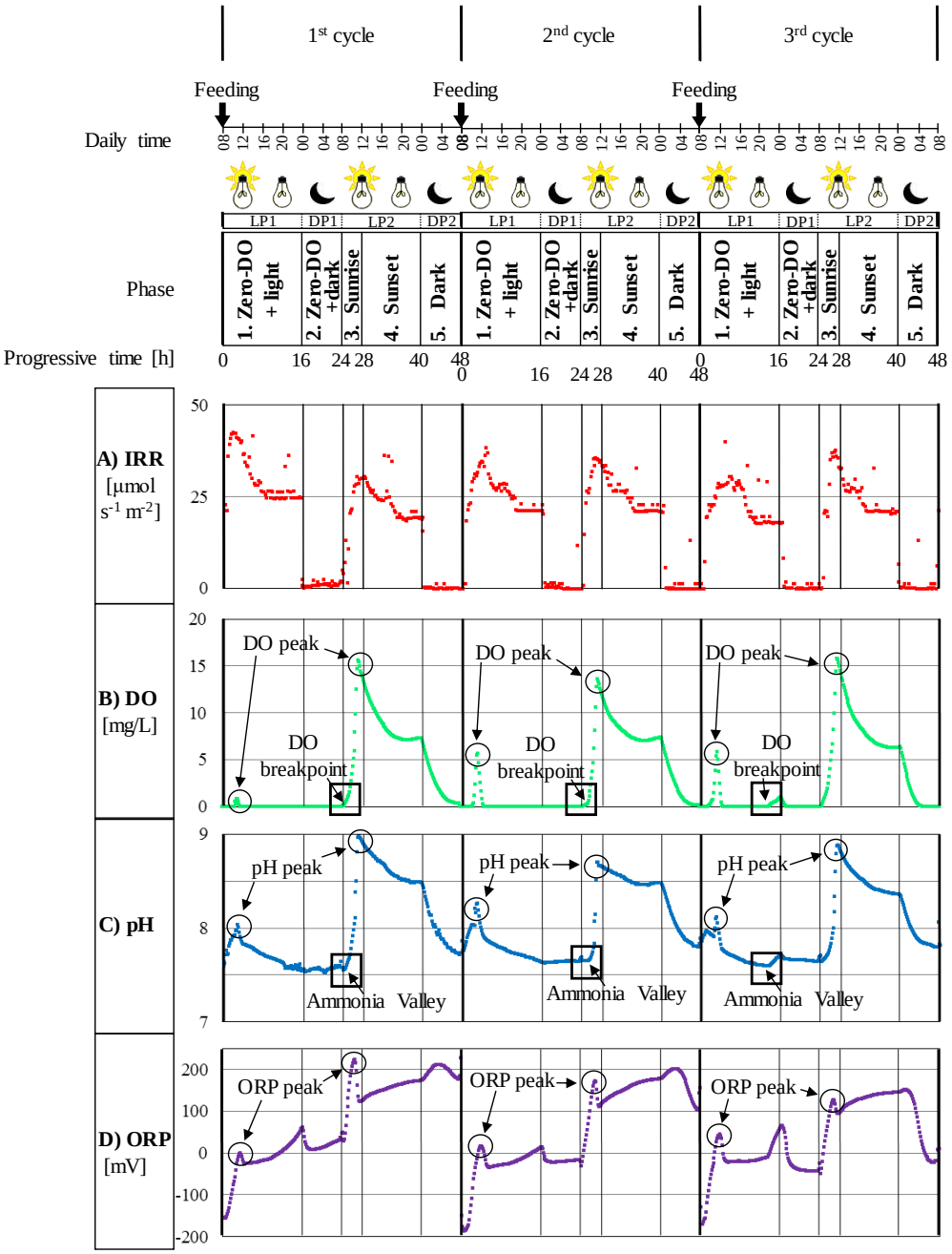

Figure 8.6 *Sequence of three typical cycles in the PSBR and profiles of irradiance, DO, pH, ORP. The profiles reveal a sequence of typical phases affected by the alternation of light and dark periods, and related to the treatment process.*

On simultaneous consideration of the profiles of irradiance, DO, pH and ORP (Figure 8.6A-D, respectively), it is possible to identify a sequence of significant phases for each cycle:

1. "Zero-DO+light" phase (progressive time = 0-16 h): this usually coincides with the first light period (LP1) and is characterized by DO values close to zero (Figure 8.6B). Immediately after the feeding phase, the system requires a huge amount of oxygen to oxidize the biodegradable substrates and ammonium of the influent wastewater. Since this phase is identified during the LP1, light is available (Figure 8.6A) and thus photosynthesis occurs. Although oxygen is continuously provided in the system, it is not enough to satisfy the requirement of the biomass. Therefore, DO is zero (Figure 8.6B) because oxygen is immediately consumed by bacteria to oxidize biodegradable COD and NH_4^+. Other studies confirmed that nitrifiers were active in removing ammonium even if the oxygen concentration was close to 0 mg/L (Yang et al., 2018).
   In some cycles, a very short DO peak may appear in this phase, in particular around midday when solar irradiation is maximum. As explained in section 3.2, photosynthesis is affected by available light, and hence a peak of the irradiance could result in a higher oxygen production that may momentarily surpass the biological demand. As a consequence of enhanced photosynthetic activity, also a pH peak may be noted (Figure 8.6C). Photosynthesis induces pH increase because of HCO_3^- uptake (see Section 8.3.3.2). Figure 8.6C shows that after the maximum irradiance, pH decreased until the end of this phase. Therefore, there was another process that counterbalanced the photosynthesis effect on pH. Since wastewater contains ammonia, the pH decrease was induced by nitrifying bacteria (see Section 8.3.3.1).
   This phase presents conditions with apparently no oxygen, but it must not be confused with an anoxic phase where oxygen is not available. In fact, even if DO is zero, the presence of oxygen can be recognized because the ORP profile increases towards positive values (Figure 8.6D), indicat-

ing oxidative conditions. Stimulated by solar irradiance, photosynthesis ensures a reasonable production of oxygen. In this phase, it is pointless to provide external oxygen, while it is more advantageous completely to exploit the free-of-charge oxygen provided by photosynthetic organisms (microalgae and cyanobacteria). Despite oxidative condition at the end of this phase, zero-DO values suggest that the oxidation process is not completed, and hence some biodegradable COD and NH_4^+ may still be in the reactor. If nitrification is not completed, nitrite, along with nitrate, may be found.

2. "Zero-DO+dark" phase (progressive time = 16-24 h): this is defined by the beginning of the first dark period (DP1) and zero-DO concentration. In the dark, no oxygen production occurs, and respiration (i.e. oxygen consumption) results in a zero-DO concentration. Figure 8.6D shows that as soon as the light is turned off, the ORP profile presents an immediate decrease and then remains approximately stable during the whole dark period. In this phase, local anoxic condition may occur. Therefore, if biodegradable COD is available, denitrification of nitrate produced during the "Zero DO+light-phase" may take place. However, since the pH profile does not show a significant trend (Figure 8.6C), denitrification is a minor process.
3. "Sunrise" phase (progressive time = 24-28 h): this is denoted by a significant increase in the DO concentration that usually occurs during the second light period (LP2) when solar irradiance increases. The DO reaches a peak, in correspondence to the maximum irradiance that occurs around midday. As observed in Section 8.3.2, the DO peak may reach oversaturation level. In this phase, the oxygen production surpasses the oxygen demand of the biomass. Because biodegradable substrates were depleted in the previous phases, only a small residual NH_4^+ concentration may remain and oxygen is mainly consumed by respiration. Indeed, the DO profile shown in Figure 8.6B is similar to that of Figure 8.5C (observed when only respiration occurred). Since photosynthetic oxygenation prevails over oxygen consumption, DO increases sharply (Figure 8.6B). Also

ORP increases significantly towards positive values (Figure 8.6D), indicating oxidative conditions. In this phase, along with DO, pH increases remarkably due to photosynthesis. This effect was not counterbalanced by the acidification produced by bacterial nitrification due to the scarcity or absence of NH_4^+ that was consumed in the previous phases.
High DO values together with high ORP values (oxidative condition) suggest that the oxidation process is completed. Therefore, biodegradable COD and NH_4^+ have been consumed. Since the nitrification is completed, only nitrate should be found.

4. "Sunset" phase (progressive time = 28-40 h): this is characterized by the decrease of DO together with the decrease of solar irradiance.
   As a consequence of the progressive reduction of solar irradiance during the second light period (LP2), photosynthetic activity slows down. Therefore, since endogenous respiration is almost constant while oxygen production diminishes, this results in a decreasing DO profile (Figure 8.6B). Depending on the balance between produced and consumed oxygen, DO profile may decrease with a more or less steep slope. However, if the production of oxygen equals the oxygen consumed by the biomass, DO profile may remain constant. As shown in Figure 8.6D, high ORP values demonstrates that DO is enough to maintain oxidative conditions. The reduction of photosynthetic activity lead to a less uptake of HCO_3^- (see Section 8.3.3.2) and therefore pH profile decreases progressively (Figure 8.6C).
5. "Dark" phase (time = 40-48 h): this coincides with the second dark period (DP2). Due to the absence of photosynthesis in the dark, DO is progressively consumed and, depending on the respiration rate, may reach zero. Since in this phase only respiration occurs, the slope of DO profile can be exploited to calculate the Oxygen Uptake Rate (OUR) of the biomass (Figure 8.7). Considering the three cycles of Figure 8.6, an average volumetric OUR of 1.8±0.3 mg O_2 L^{-1} h^{-1} was obtained taking into account the linear part of the curves (Figure 8.7). The volumetric OUR obtained corresponds to a specific value of 1.6±0.3 mg O_2 TSS^{-1} h^{-1} (TSS = 1.18±0.1 g TSS/L).

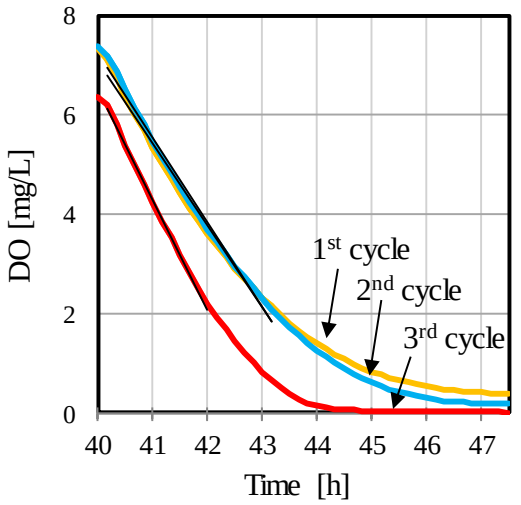

Figure 8.7 *Endogenous Oxygen Uptake Rate of the biomass obtained from the profile of DO concentration during the "Dark" phase.*

The OUR calculated certainly corresponds to the endogenous respiration of the biomass, because in this final phase of the cycle biodegradable substrates and ammonium can be considered completely oxidized. As shown in Figure 8.6D, ORP decreases as a consequence of oxygen consumption but does not reach low negative values. ORP reaches the minimum values (<-100 mV) during the subsequent feeding of anaerobic fresh wastewater that induces a change from aerobic conditions to a fermentation stage. Although local anoxic condition may occur inside the flocs, denitrification of the remaining nitrate can be excluded because biodegradable COD is not available.

From the profiles of DO, pH and ORP it was possible to identify some relevant characteristic points (discussed in the following sections). These characteristic points may be exploited in the on-line control and optimization of the process.

8.3.3.1 "DO breakpoint" and "ammonia Valley" reveal the end-point of ammonium

No external aeration was provided in the PSBR, and oxygen was produced only during the light periods of the cycle. As observed in Section 8.3.3, bacterial oxidation, in particular nitrification, causes a consumption of DO that may drop to zero (Zero DO+light phase). In regard to nitrification, the utilization of alkalinity leads to a progressive decrease of pH according to the following reaction, Eq.8.1 (Tchobanoglous et al., 2003).

$$0.098CO_2 + NH_4^+ + 1.863O_2 \rightarrow 0.0196C_5H_7NO_2 + 0.98NO_3^- + 0.0941H_2O + 1.98H^+ \quad (8.1)$$

As shown in Figure 8.6C, pH decreases during the "Zero-DO+light phase" indicating that the acid-based effect by nitrification dominated in the reactor. Once nitrification is complete and ammonium is totally oxidized, DO is no longer consumed for this purpose, and its concentration raises very rapidly and sharply due to the continuous oxygen production by photosynthesis (Sunrise phase, Figure 8.6B), which depends on the available light. Consequently, also pH increases sharply (Figure 8.6C).

The endpoint of ammonium originates a characteristic point in the DO profile called "DO breakpoint", indicated in the three cycles of Figure 8.6B. The "DO breakpoint" occurs in concomitance with a characteristic point in the pH profile as shown in Figure 8.6C: when ammonium is completely depleted, pH starts to rise and a local minimum called "Ammonia valley" occurs in the pH profile. The increase in pH could be due to stripping of CO_2 from the system, but She et al. (2016) suggested that it might be related to the buffer capacity of the medium after ammonium oxidation is finished.

Since TKN load is widely fluctuating in the influent real wastewater, the completion of nitrification may have different durations, so that Ammonia valley may appear in the "Zero-DO+light" phase (see 3rd cycle in Figure 8.6C) or in the subsequent "Sunrise" phase (see 1st and 2nd cycles in Figure 8.6C).

The perfect correspondence between the endpoint of ammonium and the two characteristic points (DO breakpoint and Ammonia valley) was demonstrated

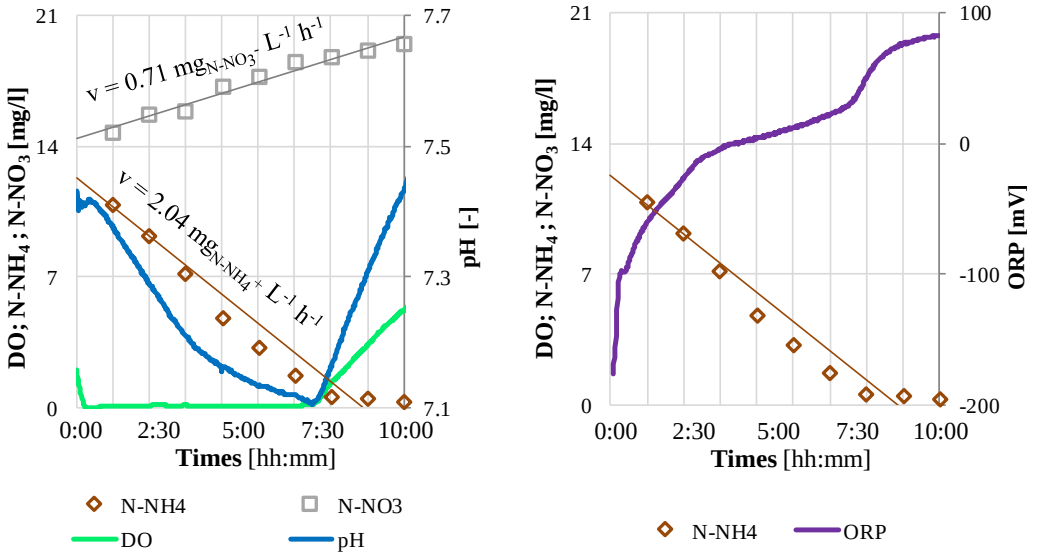

Figure 8.8 *Track study in the PSBR to demonstrate the coincidence of two characteristic points (DO breakpoint+Ammonia valley) and the endpoint of ammonium.*

in the track study of Figure 8.8.

Figure 8.8A shows that as soon as ammonia oxidation is completed, DO and pH rise sharply. Also the ORP profile showed a change in slope (Figure 8.8B), but this behavior was not always appreciable in all the cycles. Thus, ORP is not recommended for an on-line control of the process. Conversely, the two characteristic points "DO breakpoint" and "Ammonia valley" can be recognized very well and can thus be usefully exploited to identify the conclusion of the cycle when ammonium removal is required. The breakpoint in the DO curve, also named "DO breakpoint", coupled with the "Ammonia valley" was effectively used by She et al. (2016) to indicate the end point of nitritation and to adjust the duration of the aerobic phase in accordance with the variation of influent NH_4^+-N concentration, avoiding from high DO and excess aeration.

In the track study of Figure 8.8, the ammonium removal rate was 2.04 mg NH_4^+-N L^{-1} h^{-1} (corresponding to 2.57±0.32 mg NH_4^+-N g TSS^{-1} h^{-1}; TSS concentration in the PSBR was 0.79±0.1 g TSS/L). To be noted is that this remarkable nitrification rate was obtained without external aeration (thus without elec-

tric energy) and with a DO profile close to zero. Moreover, the specific rate of 2.57±0.32 mg NH_4^+-N g TSS^{-1} h^{-1} was similar to typical ranges expected for activated sludge.
At the same time, nitrates were produced at a rate of 0.71 mg NO_3^--N L^{-1} h^{-1} (corresponding to 0.90±0.12 mg NO_3^--N g TSS^{-1} h^{-1}, approximately half of the nitrification rate), indicating that denitrification occurred due to the low DO in the bulk liquid.

8.3.3.2 Limited removal efficiency of phosphorus due to low sludge production

As shown in Section 8.3.2, the maximum irradiance is associated with the maximum of photosynthetic activity. According to the following reaction (Eq.8.2, Wiley, 1993), HCO_3^- uptake dominates the acid-base effect of photosynthesis. Therefore, during the light periods a pH increase is induced in the system so that HCO_3^- uptake may result in a peak of pH at maximum irradiance.

$$106HCO_3^- + 16NH_4^+ + HPO_4^{2-} + 92H^+ \rightarrow C_{106}H_{263}O_{110}N_{16}P + 106O_2 \quad (8.2)$$

In regard to photosynthetic oxygenation, at maximum irradiance, oxygen consumption affects the extent of the DO peak. The relative maximum in the ORP profile appears in correspondence to the peak of irradiance due to aerobic conditions stimulated by a higher rate of photosynthesis.
The coincidence between the maximum irradiance and the absolute peaks of DO, pH and ORP can be appreciated in the “Sunrise” phase of Figure 8.6.
During the “Zero-DO+light” phase, there is a large amount of biodegradable substrate to be oxidized. Therefore, due to high oxygen consumption the peaks of DO is very small and in some cases it may be difficult to recognize (Figure 8.6B). In this phase, nitrification counterbalances the acid-base effect of photosynthesis, affecting the extent of pH peak (Figure 8.6C). Moreover, a less marked ORP peak (Figure 8.6D) is the result of the feed of anaerobic fresh wastewater which induces anoxic conditions and thus negative ORP values at the beginning of the cycle.
In the subsequent “Sunrise” phase, when the irradiance is maximum, the peaks

of DO, pH and ORP become more sharply defined and reach higher values, because the biodegradable substrates are completely removed.
To sum up, the achievement of well-defined absolute peaks of DO, pH and ORP is the signal that the wastewater treatment is completed and consequently that the cycle can be concluded. Considering the cycles in Figure 8.6, control over the process on the basis of these characteristic points permits conclusion of the treatment after 15-26 h instead of 48 h, reducing the HRT by more than 45%.

8.4 Conclusion

This paper has demonstrated that is possible to exploit continuous measurement of the on-line parameters DO, pH and ORP to evaluate correctly the conclusion of the wastewater treatment and thus shorten the HRT of a PSBR. Although photosynthetic oxygenation strongly affects DO, pH and ORP, characteristic points revealing the state of the ongoing biological process were detected along these complex profiles:

- "Ammonia valley" (pH profile) and "DO breakpoint" (DO profile) as key indicators of the complete ammonium removal;

- Absolute peaks of DO, pH and ORP in conjunction with maximum irradiance, as detectors of COD and TKN complete removal, indicating that the PSBR cycle could be ended.

Absolute peaks of DO, pH and ORP in conjunction with maximum irradiance, as detectors of COD and TKN complete removal, indicating that the PSBR cycle could be ended. In this way, the PSBR cycle was shortened by more than 45%, resulting in a significant reduction of foot-print and costs of the treatment.

Acknowledgements

The authors thanks Giovanna Flaim (Fondazione Edmund Mach, Italy) for her assistance in the investigation of microalgae in the photobioreactor and Andrea Pacini for his help during the experimental work.

CHAPTER 9

UNDERSTANDING THE EFFECT OF HRT AND OUTDOOR CONDITIONS ON THE TREATMENT PERFORMANCE

Data collected over two years from the Pilot (Chapter 6), have proved the capability of the system to treat wastewater. Real-time monitoring (Chapter 8) demonstrated that the system can be optimized, in particular that HRT (Hydraulic Retention Time) could be reduced. In this Chapter, the wastewater treatment performance at different HRTs and the influence of outdoor conditions (sunlight and temperature fluctuations) were explored for future optimization.

This Chapter is based on:
Petrini S., Foladori P., Andreottola G. *Understanding the effect of HRT on microalgal-bacterial consortia treating real municipal wastewater in lab-scale photoreactors under indoor and outdoor conditions.* In preparation

Abstract

Microalgal-bacterial based wastewater treatment represents an attractive alternative solution to activated sludge. Photosynthetic oxygenation supported by sunlight may lead to a low-energy wastewater treatment that does not rely on artificial aeration. However, to make microalgal-bacterial consortia competitive against activated sludge, the system should be operated at reduced hydraulic retention time (HRT).
In this studies, two identical photobioreactors, fed with real municipal wastewater, were run in parallel under different HRTs (2.9, 1.4 and 1d). One reactor (RI) was operated inside and the other was installed outside (RO) to compare the effect of different light sources (artificial light and sunlight, respectively) on the treatment process.
RO and RI exhibited COD removal efficiency up to 75% at HRT of 1 d (applied load up to 330 mg L^{-1} d^{-1}). While, both reactors reached their limit in ammonium removal at HRT of 1.4 d with a COD applied load higher than 150 mg L^{-1} d^{-1} that corresponded to a TKN applied load of about 50 mg L^{-1} d^{-1}.
To reduce the HRT and at the same time ensure nitrogen removal, photosynthetic oxidation should provide enough oxygen to sustain bacterial activity of both heterotrophs and nitrifiers. RO and RI showed similar performances however photosynthetic oxygenation in RO was supported only by sunlight (i.e. a cost-effective light source).

9.1 Introduction

The activated sludge process is highly energy consuming mainly because of the energy inputs associated to oxygen supply (Sun Y. et al., 2019). In fact, mechanical aeration may account for 50% of the energy consumption of a wastewater treatment plant (WWTP) (Mamais et al., 2015).
In the last decades, the combination of microalgae with bacteria has been regarded as a promising sustainable alternative to activated sludge as photosynthetic oxygenation may sustain the treatment process (Posadas et al., 2013; Van den Hende et al., 2014 ; Anbalagan et al., 2016; Quijano et al., 2017).
Microalgal-bacterial consortia have proved to be effective in the treatment of different type of wastewater (Cai et al., 2013; Arcila and Buitrón, 2016; Wang Y. et al., 2016) ensuring at the same time good settleability (Su et al., 2011; Ramanan et al., 2016). However, this technology is in its early stage of development and

there are still some challenges to overcome in view of the full-scale application (Molinuevo-Salces et al., 2019; de Jesús Martínez-Roldán and Ibarra-Berumen, 2019).
Usually photobioreactors (PBRs) are operated at hydraulic retention time (HRT) between 2 and 6 days, much higher with respect to activated sludge (Muñoz and Guieysse, 2006). A high HRT results in a high land-requirement (i.e. high footprint) imposing a disadvantage for microalgal-based processes compared to conventional treatment (Anbalagan et al., 2016).
Microalgae represent a cost-effective means of producing O_2 (Kang et al., 2018). However, for a favorable energy and economic balance of microalgal-based processes, exploitation of sunlight is the most suitable solution.
Closed PBRs represent a promising implementation of microalgal-bacterial consortia to compete against activated sludge (Posadas et al. 2017). Compared to open PBRs, closed PBRs can be built vertically, have a higher light harvesting and the process conditions are easily controlled (de Jesús Martínez-Roldán and Ibarra-Berumen, 2019).

To date, wastewater-born microalgal-bacterial consortium treating real municipal wastewater in closed photobioreactor have been rarely studied (Krustok et al., 2015; Kang et al., 2018). Photo-sequencing bacth reactors represent a common configuration for implementation at a lab-scale (Arcila and Buitrón, 2016; Wang L. et al., 2016).

The aim of this study was to evaluate the influence of the HRT and of the light source (artificial light and sunlight) on the treatment performance (organic matter and nitrogen removal) of a wastewater-born microalgal-bacterial consortium treating real municipal wastewater. This experimentation represents an optimization of a long running pilot-scale photobioreactor that proved to be effective in the treatment of real municipal wastewater working at HRT 5.6 d (Chapter 6). Real time monitoring of dissolved oxygen (DO), pH and oxidation-reduction potential (ORP) showed that the HRT of the long running pilot-scale photobioreactor could be shortened by more than 45 % (Chapter 8).

Two photobioreactors, fed with the same real municipal wastewater, were

run in parallel. One reactor (RI), was installed indoors and photosynthetic oxygenation was supported by an artificial lamp. The other reactor, named RO, was operated outdoor with sunlight as the solely light source. The reactors were operated under three different HRTs (2.9, 1.4 and 1 d) to evaluate their removal treatment performances (COD and nitrogen removal). To note, the HRT affect the applied load of organic matter and nutrient removal. In particular, at low HRTs correspond high applied loads to remove.

In view of full-scale application, this study provides valuable information on the limit of the treatment performances of PBRs fed with real municipal wastewater (variable influent concentrations) and on the feasibility to working under outdoor conditions (sunlight), which vary in time.

9.2 Materials and Methods

9.2.1 Experimental setup

Two identical reactors, named RI and RO, were installed (Figure 9.1A). RI was operated indoors while RO outdoors. The reactors were transparent Pyrex glass cylinders (diameter 12 cm, height 20 cm; Colaver, Italy), with a working volume of 2 L. RI, placed inside the laboratory, was illuminated with a LED lamp (8 led × 0.5 W; Orion, Italy) arranged on one side of the reactor and was never exposed to sunlight. The LED lamp supplied a photosynthetically active radiation (PAR) intensity of 45 μmol m^{-2} s^{-1} at the inner wall, in the most exposed part. RO, placed outside the laboratory (Coordinates in decimal degrees: 46.082 N, 11.110 E), was illuminated only by sunlight therefore the light intensity and the hours of light varied with time. To prevent RO overheating, the system was placed outdoor in a such way as to avoid prolonged exposition to direct sunlight.

For each reactor, peristaltic pumps (Kronos Seko, Italy) fed the influent and discharged the effluent. Magnetic mixers (AGE, Velp, Italy) set at 200 rpm, ensured mixing and prevented the biomass from settling. Timers (TR 612 top2, Theben, Germany) switched on and off devices (pumps, mixers and the artificial lamp

of RI).
The reactors were not sealed off from atmosphere and no external (mechanical) aeration was provided. No pH adjustment was performed. Average water temperature was 25±3 and 27±5 °C in RI and RO, respectively. RO temperature fluctuated more due to the outdoor daily variations while the temperature inside the lab was controlled. The average temperature of RO is higher because the experimentation was performed mainly during the summertime (from June to the beginning of October).
Biofilm formation was observed on the walls of both reactors and thus once a week, the walls were cleaned.

9.2.2 Influent wastewater

Both reactors were fed with the same real municipal wastewater. Wastewater was collected after the primary sedimentation of Trento Nord WWTP (Trento, Italy). Table 9.1 shows the average composition of the influent wastewater considering the entire experimental period. Before feeding the wastewater into the reactors, no filtration was performed therefore microorganisms naturally present in the influent wastewater entered the systems.

Parameter	**Influent Wastewater** [mg/L]
COD	192±78
sCOD	84±33
TN	50.3±20.8
TKN	48±20
NH_4^+-N	34.6±12.7
NO_2^--N	0.2±0.3
NO_3^--N	2.5±1.1
TP	5.6±1.3
TSS	85±65
Sample n.	14

Table 9.1 *Characterization of the influent wastewater considering the entire experimental period (avg±st.dev.).*

9.2.3 Microalgal-bacterial consortium

The reactors were inoculated with a consortium spontaneously developed in a photo-sequencing batch reactor fed with the same real municipal wastewater and working from more than two years (Chapter 6). The consortium was composed of eukaryotic microalgae, cyanobacteria, heterotrophic bacteria and nitrifiers.

9.2.4 Operational regime

The reactors were operated as photo-sequencing batch reactors. Each cycle consisted of consecutive phases: (i) Feeding, (ii) Reaction, (iii) Settling, and (4) Drawing. The operational regime was modified to study the treatment performances of the reactors working at different HRTs (2.9, 1.4 and 1 day) without acclimation in between. The operating period was 55, 47 and 14 d at HRT of 2.9, 1.4 and 1 d, respectively.

As reported in Table 9.2, the daily flow rate (Q) was increased by performing more cycles in a day. The operating cycles implemented to tests the different HRTs are schematized in Figure 9.1B. For both reactors, Feeding and Drawing had a duration of 5 min each. Settling was set at 30 min and then it was lowered to 20 min at HRT 1 d to give more space to the Reaction phase. The cycles were designed on RO to exploit sunlight for the most part of the Reaction phases. Therefore, the cycles started at different times for each HRT applied.

A photoperiod of 16 hours of light and 8 hours of dark was ensured to RI throughout the entire experimentation (Table 9.2). The artificial lamp was turned on at 07:00 a.m. and turn off at 23:00 p.m. Since RO was exposed to sunlight, the photoperiod varied according to seasonal variation. In particular, it reduced from a maximum of 15 h of light and 9 h of dark (in June - HRT=2.9 d) to a minimum of 10.5 h of light and 13.5 h of dark (in October - HRT=1 d) (Table 9.2).

The settling phase enabled to uncoupled HRT from SRT (Sludge Retention Time). In both reactors, biomass was never extracted and exited the system with the effluent or was destroyed for chemical analysis.

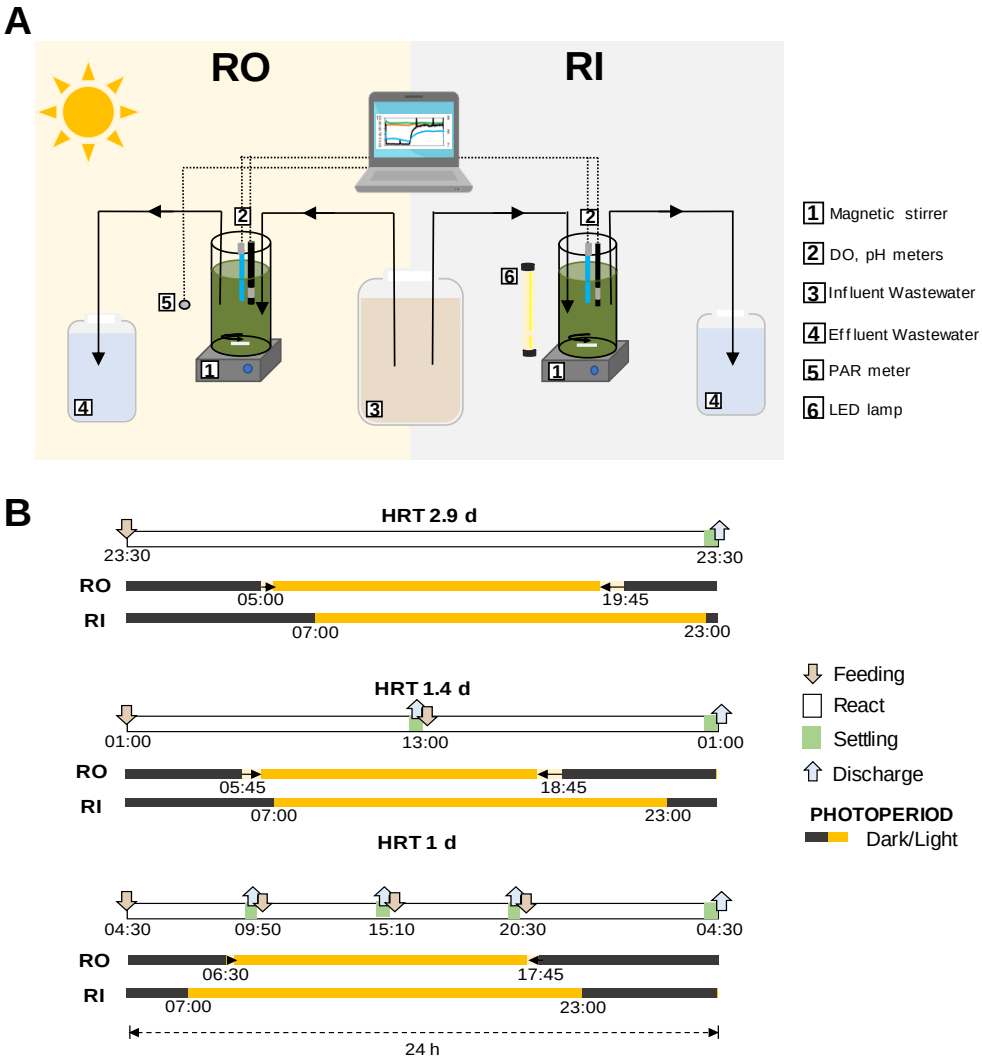

Figure 9.1 *(A) Scheme of the experimental apparatus. (B) Operating cycles at different HRTs.RO: photobioreactor operated outdoors; RI: photobioreactor operated indoors.*

	Q [L/d]	**Cycles/d**	**Cycle length** [h]	**Photoperiod** [h]			
				RI		**RO**	
				Light	Dark	Daylight	Night
HRT 2.9	0.7	1	24	16	8	15 ⟶13	09 ⟶ 11
HRT 1.4	1.4	2	12(x2)	16	8	13 ⟶11	11⟶ 13
HRT 1	2	4	5.3(x3) 8(x1)	16	8	11⟶10.5	13⟶ 13.5

Table 9.2 *Operational parameters of RI and RO for each HRT applied.*

9.2.5 Analytical methods

Total Chemical Oxygen Demand (COD), soluble COD (sCOD), Total Suspended Solid (TSS), Total Kjeldahl Nitrogen (TKN), NH_4^+-N, NO_2^--N, NO_3^--N and total P (TP) were analyzed according to Standard Methods (APHA, 2012). sCOD was measured after filtration of the sample on 0.45 μm membrane. Total N (TN) was defined as the sum of TKN, NO_2^--N and NO_3^--N.
DO and temperature were measured with Multi 3310 meters coupled with the sensors FDO®925; pH was measured with pH3310 meters coupled with the electrodes Sentix®41 (all from WTW, Germany). Temperature, DO and pH were recorded in both reactors for at least three consecutive HRTs for each HRT applied. Light intensity was measured as photosynthetically active radiation (PAR). A SQ-520 quantum sensor (Apogee Instruments, USA) placed outdoors next to RO was used to record sunlight intensity.

9.2.6 Calculations

To evaluate the treatment performance of RI and RO, the removal efficiency (η), the applied load (AL) and the removed load (RL) were calculated for COD, TKN and TN according to Eq. 9.1, 9.2 and 9.3, respectively. X_{IN} is the influent concentration (i.e. COD_{IN}, TKN_{IN} and TN_{IN}); X_{OUT} represents the effluent concentration ($sCOD_{OUT}$, NH_4^+-N_{OUT} and TN_{OUT}, respectively); Q is the flow rate and varied with the HRT (Table 9.2); V is the working volume and was kept constant to 2 L in both reactors throughout the experimentation.

$$\eta = \frac{X_{IN} - X_{OUT}}{X_{IN}} \tag{9.1}$$

$$AL = \frac{X_{IN} \cdot Q}{V} \tag{9.2}$$

$$RL = \frac{(X_{IN} - X_{OUT}) \cdot Q}{V} \tag{9.3}$$

9.2.7 Statistical analysis

To investigate if the treatment performances of RI and RO could be considered significantly different, the statistical significance was evaluated using the Student's paired *t*-test with significance at P<0.05 or P<0.01. Unpaired *t*-test was used to assess the difference between the influent concentrations for each HRT applied (P<0.05). Statistical calculations were done using Microsoft® Excel (Microsoft Corporation, USA).

9.3 Results

Average effluent TSS concentrations were 16±14 and 14±13 mg/L throughout the entire experimentation, in RI and RO respectively. These low effluent TSS proved that both systems had settleable biomass and that the solids that left the reactors did not affect very much the effluent concentrations.

9.3.1 COD removal

The average COD influent concentrations were 163±95, 210±71 and 244±80 mg/L (not significantly different, P>0.05) and corresponded to an average applied load of 53±30, 139±49 and 292±65 mg L^{-1} d^{-1} at HRT of 2.9, 1.4 and 1 d, respectively.
The average sCOD effluent concentrations were 30±18, 33±13 and 34±6 mg/L for RI and 35±10, 28±6 and 40±11 mg/L for RO, at HRT of 2.9, 1.4 and 1 d respectively. The respective average COD removal efficiencies were 71±26%, 81±9% and 88±3% for RI and 66±23%, 85±6% and 86±3% for RO. The COD removal efficiency increased passing from HRT of 2.9 d to 1.4 d. For each HRT, effluent COD concentrations and removal efficiency of RI and RO were not significantly different (Figure 9.1A, 1B). In spite of different HRTs, RI and RO effectively removed the influent COD with global average removal efficiencies of 80±17% and 79±16%, respectively. Even at high applied COD load (292±65 mg L^{-1} d^{-1} at HRT of 1 d) both systems guaranteed low effluent COD concentrations (34±6 mg/L RI and 40±11 mg/L RO). COD removed load increased at

low HRTs (and thus at high applied loads) in both reactors without significant differences (P>0.05) (Figure 9.1C). The COD removed loads were 53±30, 139±49 and 292±65 mg L^{-1} d^{-1} in RI and 53±30, 152±57 and 292±65 mg L^{-1} d^{-1} in RO, at HRT of 2.9, 1.4 and 1 d, respectively.

As shown in Figure 9.2D, the temperature did not affect the COD removal in both reactors. In fact, high removal loads were guarantee also at temperature lower than 25°C. In Figure 9.2D, it can be observed the linear correlation between the applied load and the removed load for both RI and RO. The removed load decreased slightly at applied load higher than 200 mg L^{-1} d^{-1} (i.e. the data are more distant to the bisector that represents 100% removal efficiency).

However, both reactors did not reach their limits about COD removal. Removal efficiency higher than 75% were guaranteed also at the highest applied loads (Figure 9.1E). Therefore, there is the possibility to increase further the COD applied load and thus to lower the HRT. However, the performances of the reactors in the removal of the nutrients should be also considered.

Overall, RI and RO presented a comparable behavior in the removal of COD, both reactors were able to withstand the applied load with no significant differences.

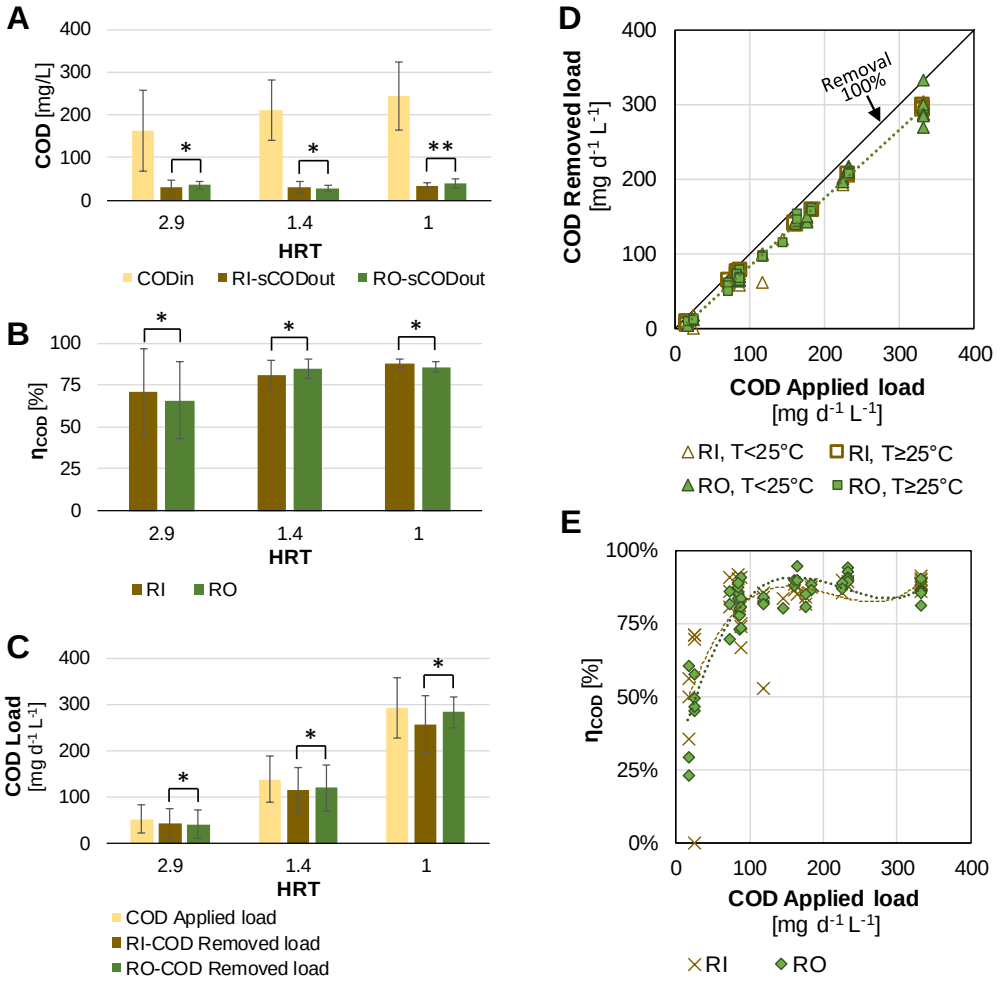

Figure 9.2 *For each HRT tested, in RI and RO: (A) Average COD influent concentration and average effluent sCOD concentration; (B) Average COD removal efficiency and (C) Average COD applied and removed load. Paired t-test: * P<0.05; ** P<0.01; (D) COD removed load vs applied load according to the temperature. The bisector represents 100% removal efficiency; (E) COD removal efficiency vs COD applied load.*

9.3.2 TKN removal

The average influent TKN concentrations (not significantly different, P>0.05) accounted for 49±25, 53±24 and 53±18 mg/L at HRT of 2.9, 1.4 and 1 d. The respective TKN applied loads resulted of 16±8, 33±15 and 64±15 mg L^{-1} d^{-1}.
The average effluent concentrations of NH_4^+-N resulted 0.3±0.1, 9.9±10.5 and 42.1±14.9 mg/L in RI and 0.3±0.1, 8.1±11.2 and 40.9±15.8 mg/L in RO at HRT of 2.9, 1.4 and 1 d, respectively, and were not significantly different (P>0.05 at HRT of 2.9 and 1 and P>0.01 at HRT of 1.4 d, Figure 9.3A).
Considering each HRT, also the TKN removal efficiency of RI and RO were not significantly different (Figure 9.3B), with average TKN removal efficiency of 99±0%, 83±15% and 37±12% for RI and 99±0%, 88±16% and 39±15% for RO at HRT of 2.9, 1.4 and 1 d respectively. The treatment removal of TKN worsened in both reactor at lower HRTs and thus at higher applied loads. Consequently, effluent NH_4^+-N increased and TKN removal efficiency decreased. Both reactors showed the worst performances at HRT of 1 d.
The TKN removed loads were not significantly different in RI and RO for each HRT, and they slightly increased passing from HRT of 2.9 d to 1.4 d (Figure 9.3C). The TKN removed loads were 16±8, 26±11 and 22±4 mg L^{-1} d^{-1} in RI and 16±8, 30±13 and 23±5 mg L^{-1} d^{-1} in RO, at HRT of 2.9, 1.4 and 1 d.
Even if TKN removal performances were not significantly different (Figure 9.3A-C, P at least higher than 0.01), RO showed a higher TKN treatment removal (considering the average values), especially at HRT of 1.4 d.
The high effluent ammonium concentrations at HRT of 1 d (Figure 9.3A), highlighted that both reactors reached their limit in TKN removal. In Figure 9.3D, three zones can be distinguished: (i) TKN removed load increased linearly with TKN applied load up to 30 mg L^{-1} d^{-1}, with the highest removal efficiency (data on the bisector); (ii) removed load unstable but tended to increase for TKN load up to 60 mg L^{-1} d^{-1}; (iii) decreasing TKN removal load at higher applied load. The interpolation of the data in Figure 9.3D shows that RO ensured higher removed load than RI for the same applied load. Experimental data refer to a wide range of temperature (21-28°C for RI and 18-35°C for RO) however no

significant correlation between removed load and temperature was observed (Figure 9.3D).

Figure 9.3E highlights the worsening of TKN removal efficiency at increasing TKN applied load. For TKN applied load lower than 30 mg L^{-1} d^{-1}, RO ensured removal efficiency closed to 100% (except for one value, 66%) while RI removal efficiency ranged between 69% and 100% (Figure 9.3E). This resulted in effluent NH_4^+-N concentration lower than 2 mg/L in RO (except 13 mg/L that corresponds to 66% of removal efficiency) and up to 10 mg/L in RI (Figure 9.3F). For applied load higher than 30 mg L^{-1} d^{-1} the removal efficiency resulted highly variable for both reactors and so effluent NH_4^+-N concentrations (Figure 9.3E, 3F).

With TKN applied load up to 30 mg L^{-1} d^{-1}, both reactors presented high and stable TKN removal. At low HRTs (and thus at high applied load), TKN removal worsened, especially at HRT of 1 d. The increasing effluent TKN whit lower HRTs, showed that the reactors reached their treatment capacity limit for ammonium. While, COD removal was always guaranteed. The relationship between COD applied load and ammonium removal is examined in Section 9.4.

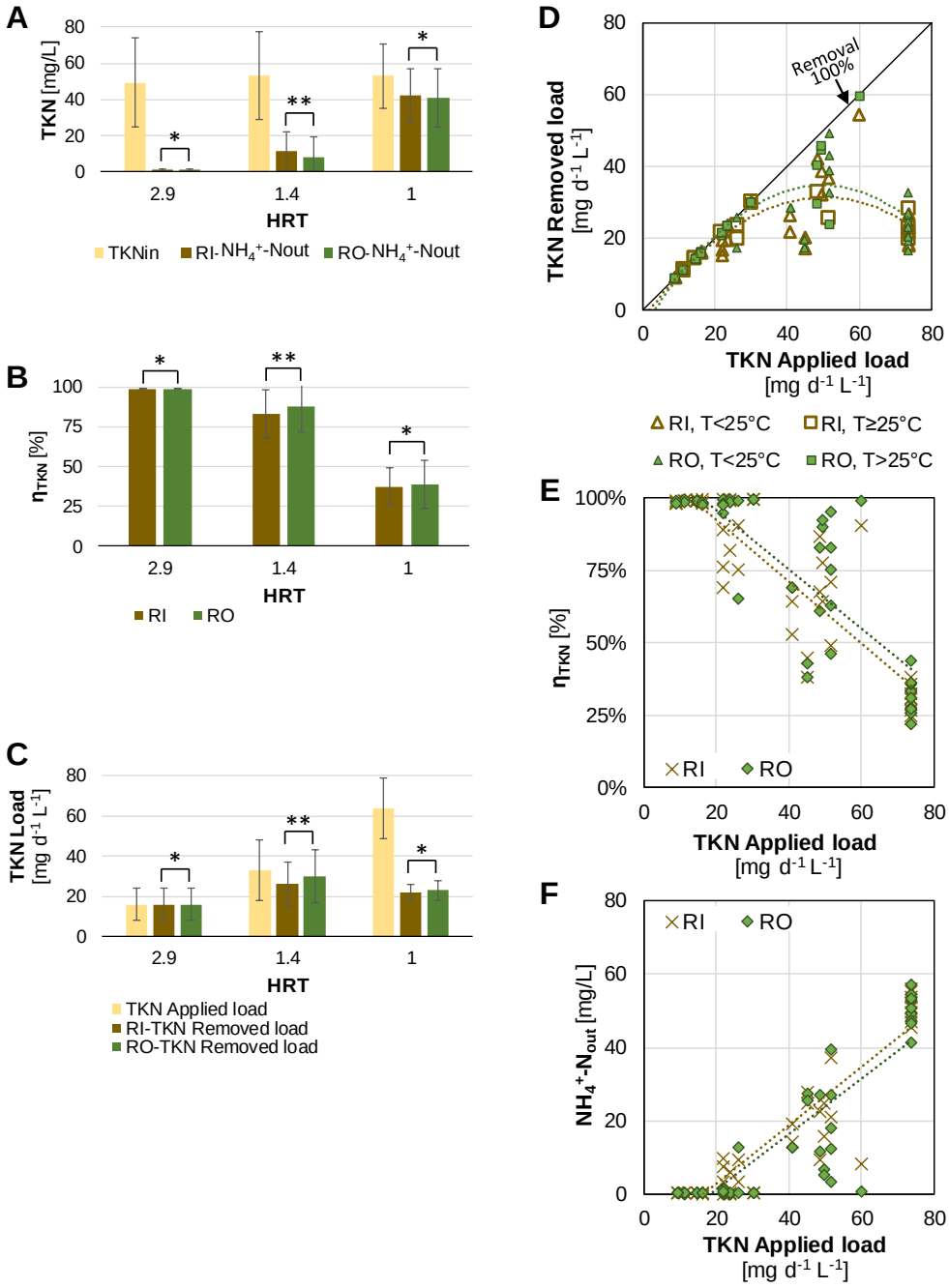

Figure 9.3 *For each HRT tested, in RI and RO: (A) Average TKN influent concentration and average effluent NH_4^+-N concentration; (B) Average TKN removal efficiency and (C) Average TKN applied and removed load. Paired t-test: * P<0.05; ** P<0.01; (D) TKN removed load vs applied load according to the temperature. The bisector represents 100% removal*

9.3.3 TN removal

The influent TKN concentration and effluent NH_4^+-N, NO_2^--N and NO_3^--N in RI and RO are shown in Figure 9.4.
For HRT of 2.9 d, effluent ammonium and nitrites were negligible in both RI and RO while effluent nitrates were higher in RI, on average 19.1±7.1 mg N/ L in RI and 9.5±7.0 mg N/L in RO. Since nitrogen entered the systems mainly in the form of TKN (Average influent TKN 48±20 mg/L, Table 9.1) the presence of effluent nitrates suggested that part of the influent TKN was oxidized through nitrification. At HRT of 1.4 d effluent ammonium increased to 9.9±10.5 and 8.1±11.2 mg N/L in RI and RO respectively (Figure 9.3A). At the same time, nitrates decreased gradually in RI resulting in an average effluent concentration of 10.3±5.4 mg N/L, and on average in RO (11.6±5.8 mg N/L). Nitrites partially accumulated in RI (average effluent concentration 1.2±0.9 mg N/L) while were negligible in RO. As soon as the operational regime was modified to HRT of 1 d, effluent ammonium increased in both systems up to 56.0 and 57.2 mg N/L in RI and RO, respectively. Then effluent ammonium gradually decreased resulting in average effluent concentrations of 42.1±14.9 and 40.9±15.8 mg N/L in RI and RO. Effluent nitrites were negligible in both reactors while nitrates were very low, (3.0±1.8 and 2.7±1.7 mg N/L on average in RI and RO, respectively).
In both reactors, effluent ammonium increased at lower HRTs and concomitantly effluent nitrates decreased suggesting that nitrification was hindered by high applied loads (especially COD applied load, see Section 9.4). Thus, TN removal was affected by the extent of the nitrification process.

The influent TN concentrations at HRT of 2.9, 1.4 and 1 d were not significantly different (P>0.05) and resulted 53±25, 55±25 and 54±20 mg/L, respectively. The correspondent TN applied loads were 17±8, 37±16 and 66±16 mg L^{-1} d^{-1}. Effluent TN of RI and RO were significantly different only at HRT of 2.9 d (P<0.01) (Figure 9.5A), on average 20±7 and 11±8 mg/L, respectively. TN removal efficiency (on average 54±17% in RI and 75±16% in RO) (Figure 9.5B) and TN removed load (Figure 9.5C) were also significantly different (P<0.01).
Effluent TN increased in both RI and RO to average concentration of 23±10 mg

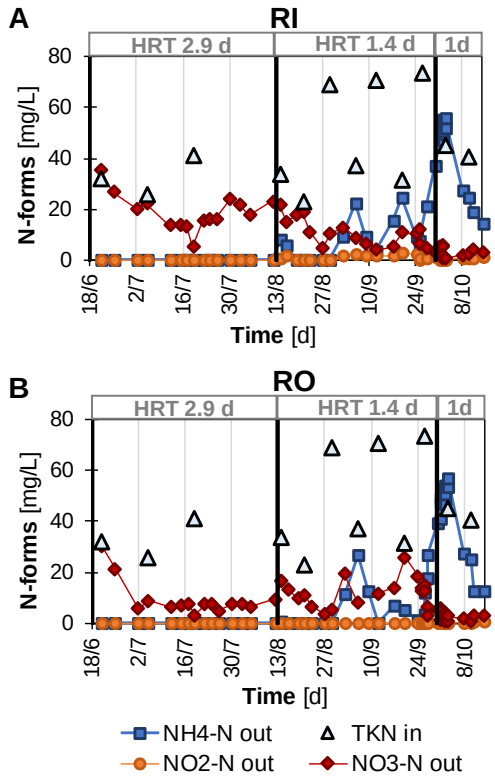

Figure 9.4 *Influent TKN and effluents NH_4^+-N, NO_2^--N and NO_3^--N in (A) RI and (B) RO. Vertical black lines indicate a switch to a different HRT regime.*

N/L and 21±11 mg N/L at HRT of 1.4 d, and to 47±15 mg N/L and 45±16 mg N/L at HRT of 1 d, respectively (Figure 9.5A). TN removal efficiency was not significantly different in RI and RO at HRT of 1.4 and 1 d (P>0.01, Figure 9.5B), and decreased passing from HRT of 1.4 d (52±13% in RI and 61±11% in RO) to HRT of 1 d (31±8% and 34±12%, respectively) (Figure 9.3C). The TN removed loads were 19±11 and 19±3 mg L^{-1} d^{-1} in RI and, 23±11 and 21±4 mg L^{-1} d^{-1} in RO at HRT of 1.4 and 1 d, respectively. While the removal efficiency decreased in both reactors passing form HRT of 1.4 d to 1 d (Figure 9.5 B), the TN removed load remained almost constant (Figure 9.5C).

Figure 9.5D shows that TN removed load depending on the TN applied load, followed a pattern similar to the one observed for the TKN (Figure 9.3D), reach-

ing a maximum TN removed load (around 20 mg L^{-1} d^{-1}) for TN applied load higher than 30 mg L^{-1} d^{-1}. Unlike for TKN, both reactors never reached 100% TN removal (i.e. no data on the bisector of Figure 9.5D). Finally, for both reactors there was not a clear correlation between temperature and TN removed load.

About the influence of the TN applied load on the effluent TN, an increasing trend can be observed in Figure 9.5E. However, unlike for TKN (Figure 9.3F), at low TN applied loads, low effluent TN was not guaranteed. Effluent TKN and nitrates accounted for the effluent TN. Therefore, while at low applied load nitrification ensured complete ammonium oxidation in both reactors (resulting in negligible effluent ammonium, Figure 9.3F), nitrate removal (i.e. denitrification and microalgae uptake) was not guaranteed by the operational conditions (Figure 9.4). Thus, effluent TN was affected by the presence of nitrates in both RI and RO.

At the highest applied load, TN effluent was mainly composed of effluent ammonium (Figure 9.3F, 5E).

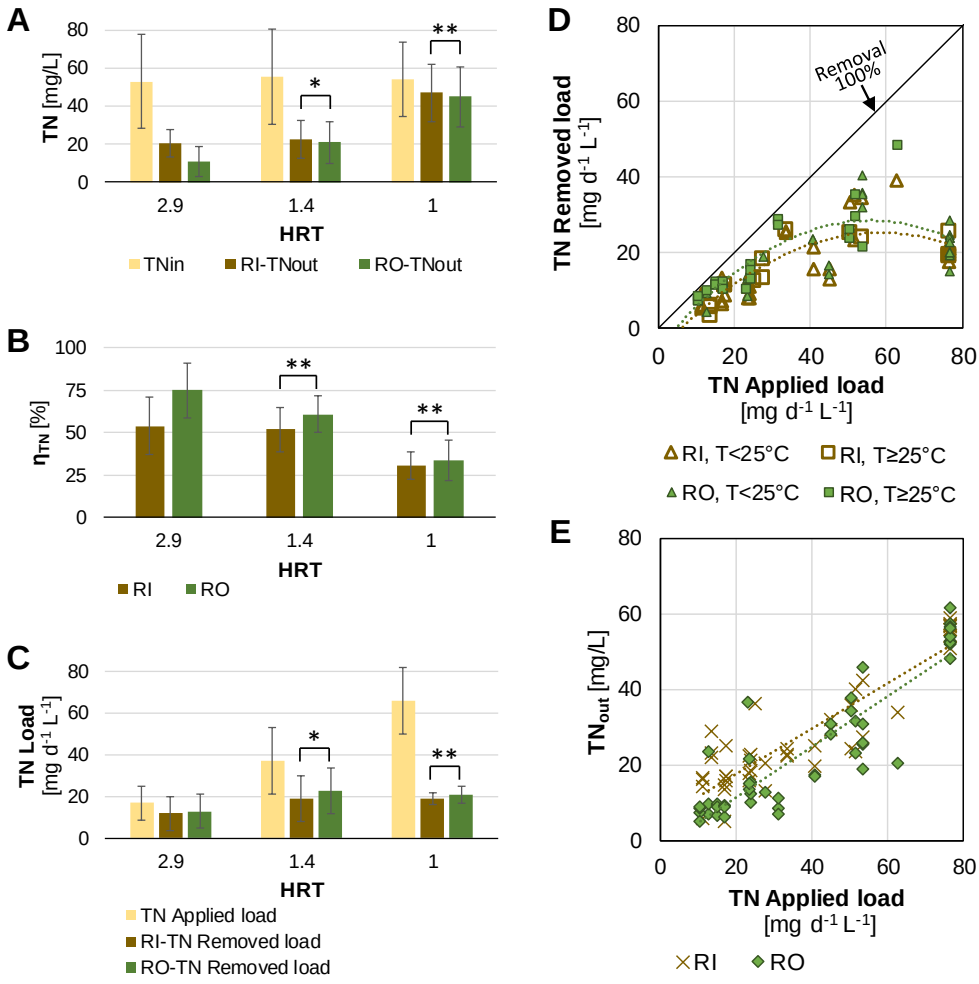

Figure 9.5 *For each HRT tested, in RI and RO: (A) Average influent and effluent concentrations of TN; (B) Average TN removal efficiency and (C) Average TN applied and removed load. Paired t-test: * P<0.05; ** P<0.01; (D) TN removed load vs TN applied load according to the temperature. The bisector represents 100% removal efficiency; (E) Effluent TN vs TN applied load.*

9.4 Discussion

The influent concentrations varied with time because real municipal wastewater was used. However, for each HRT tested the characteristics of the influent wastewater were not significantly different (P>0.05). Therefore, it was assumed that the influent wastewater characteristics did not affect the reactors performances. On the other hand, the applied load, which increased for low HRTs, was the main operational parameters that influenced the treatment removal. The other parameters that may have affected the treatment process are the light condition (intensity and duration) and the temperature. The hours of light and the light intensity were kept constant in RI, while RO was subject to environmental conditions (Table 9.2).

RI and RO proved to be effective in COD removal with performances not significantly different. Both systems guaranteed COD removal efficiency up to 75% at HRT of 1 d. These results suggested that the reactors did not reach the limit of COD treatment capacity, therefore the COD applied load could be further increased.

Stable and high COD removal efficiency (higher than 70%) was reported by Anbalagan et al. (2016) treating real municipal wastewater in lab-scale PBRs operated at HRTs of 6, 4 and 2 d. Tang et al., (2016) reported COD removal efficiency of around 90% in lab-scale PBRs operated at HRT of 15 h. Although Tang et al. (2016) supported the treatment with limited artificial aeration (Aeration rate < 1 L/min), the potential of microalgal-bacterial consortium in COD removal was shown.

At high COD applied load the oxygen demand of heterotrophic bacteria increases and as a consequence nitrifiers may result limited. As shown in Figure 9.6A, the average DO during a cycle decreased at high COD applied load in both reactors, therefore the bacterial activity (especially nitrification) could have resulted oxygen limited. RO presented higher residual DO, probably thanks to more favorable light conditions (data not shown).

The photosynthetic activity was affected by the light therefore the amount of the oxygen produced did not varied significantly throughout the experimentation,

in particular in RI since light conditions were kept constant. On the contrary at low HRTs, the applied load increased and so the oxygen demand for bacterial activity.

Effluent nitrates at HRT of 2 and 1.4 d suggested the occurrence of nitrification that was confirmed by the identification of the characteristic points of "Ammonia valley" and "DO breakpoint" along the pH and DO profile, respectively (data not shown) (Chapter 8). At HRT of 1.4 and 1 d, effluent ammonium increased in both reactors because of high COD applied loads (Figure 9.6C) that resulted in a decrease of TKN removal efficiency (Figure 9.6D). High COD applied load increased the oxygen consumption of heterotrophic bacteria reducing the availability of oxygen. Therefore, nitrifiers were disadvantaged thus nitrification reduced.

Also, Ye et al. (2018b) reported a worsening in nitrification associated to low level of DO. The authors operated a lab-scale PBR at HRT of 16 h, in which oxygen was supplied by both photosynthetic oxygenation and limited artificial aeration (Aeration rate ≤0.4 L/min). At reduced aeration intensity (from 0.2 to 0.1 L/min), the ammonium removal efficiency dropped from about 99% to less than 78% because microalgae could not provide enough oxygen to nitrifiers (Ye et al., 2018b).

The presence of nitrites in the effluents in both reactors (Figure 9.6B) indicated that NOB (Nitrite Oxidizing Bacteria) were more limited than AOB (Ammonium Oxidizing Bacteria) at high applied load (i.e. limited oxygen availability). At TKN applied load higher than 20 mg L^{-1} d^{-1}, effluent nitrites increased in both reactors. To note, nitrite concentrations in the effluent of RI resulted always higher than RO (Figure 9.6B).

At HRT of 1.4 and 1 d, as a result of absent nitrification, ammonium was not oxidized to nitrates. Therefore, effluent nitrate concentrations lowered at increasing effluent ammonium.

Nitrogen can be removed for nitrification/denitrification, ammonia volatilization (at pH>9) and biomass uptake (Delgadillo-Mirquez et al., 2016; Wang Y. et al., 2016b). Heterotrophic bacteria require slow amount of nutrients for their

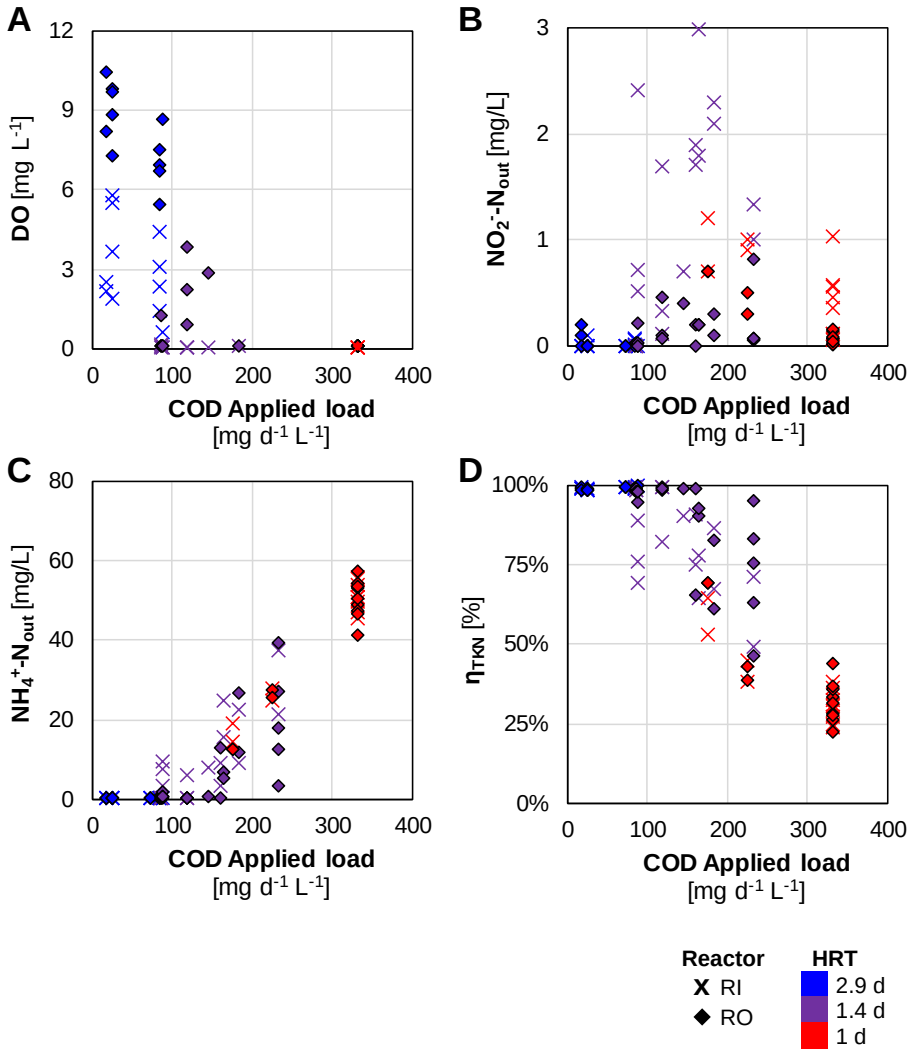

Figure 9.6 *(A) Average DO concentration during a cycle vs COD applied load. (B) Effluent NO_2^--N vs COD applied load. (C) Effluent NH_4^+-N vs COD applied load. (D) TKN removal efficiency vs COD applied load.*

growth. However, at high applied COD load the amount of nitrogen for bacterial synthesis could not be negligible. The fraction (f) of the nitrogen consumed for bacterial synthesis considering the COD removed was assumed equal to 0.045 g N/g $COD_{removed}$. f was estimated according to Eq. 9.4, considering typical values of activated sludge models for heterotrophic bacteria (Henze et al., 2008): (i) theoretical yield coefficient (Y_h) of 0.45 g $VSS_{produced}$/g $COD_{removed}$ and (ii)

biomass nitrogen content (f_N) of 0.1 g N/g VSS (VSS: Volatile Suspend Solids).

$$f = Y_h \cdot f_N \tag{9.4}$$

The nitrogen removed for bacterial synthesis was estimated multiplying the COD removed for the coefficient *f*. As shown in Figure 9.7, at high COD removed load (that corresponded to high COD applied load) the main nitrogen removal mechanisms was bacterial uptake. Therefore, at low HRTs (high applied load) the nitrogen removed for bacterial synthesis increased while the part removed by nitrification (ammonium oxidation) decreased.
RO showed a higher TKN treatment removal (considering the average values) than RI, especially at HRT of 1.4 d, thanks to more favorable conditions of light (sunlight) (Ye et al., 2018b) and temperature.
To further optimize the reactors, the operational conditions should be modified to enhance photosynthetic oxigenation in order to provide enough oxygen to sustain both heterotrophs' and nitrifiers' activities. Biomass concentration should be optimized to concentrate the microbial biomass while ensuring nitrification (Chapter 10). Light conditions represent a key aspect (Lee et al., 2015 ; Ye et al., 2018b) and, following the principle of sustainability, the exploitation of sunlight is the most suitable option.

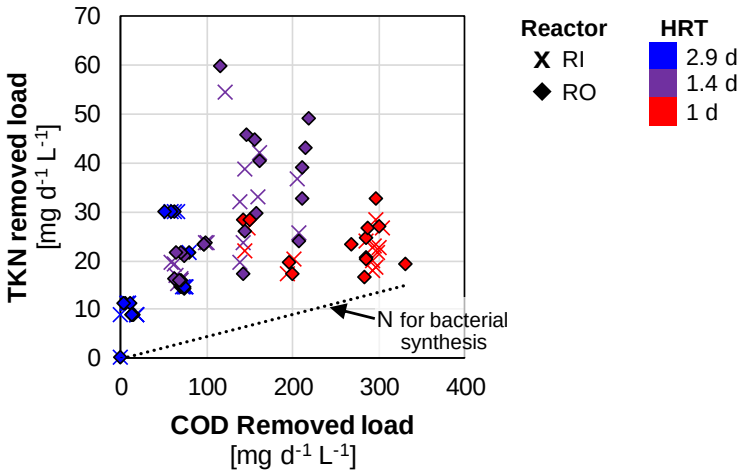

Figure 9.7 *TKN removed load vs COD removed load. The dotted black line represents the estimated N uptake for bacterial synthesis.*

9.5 Conclusion

RO and RI showed a similar performance in the removal of COD and nitrogen but with the great difference that photosynthetic oxygenation in RO was supported only by sunlight (no energy requirements to supply light).
Both reactors guaranteed COD removal efficiency of 75% at applied load up to 330 mg L^{-1} d^{-1} (HRT of 1 d). At HRT of 1.4 d, TKN removal of both RI and RO resulted unstable, worsening at TKN applied load higher than 60 mg L^{-1} d^{-1} (HRT of 1 d).
At low HRTs, the high COD load applied resulted in an increase of oxygen consumption by heterotrophic bacteria. Consequently, the availability of oxygen reduced and thus ammonium removal by nitrification because nitrifiers were limited.
The reactors reached their limit in ammonium removal at HRT of 1.4 d with a COD applied load higher than 150 mg L^{-1} d^{-1} that corresponded to a TKN applied load of about 50 mg L^{-1} d^{-1}. At HRT of 1.4 d, the average effluent ammonium concentration was 9.9±10.5 and 8.1±11.2 mg N/L in RI and RO, respectively.
To reduce the HRT and at the same time ensure nitrogen removal, the operational conditions should be modified to enhance photosynthetic oxidation in order to provide enough oxygen to sustain both heterotrophs and nitrifiers activity. Biomass concentration should be optimized according to light condition to increase sunlight exploitation by microalgae and guarantee at the same time high removal load.

Acknowledgements

The authors would like to thank Alessandro Ferraro for his help during the experimental work.

CHAPTER 10

THE INFLUENCE OF BIOMASS CONCENTRATION ON THE NITRIFICATION RATE

In this Chapter, the influence of the biomass concentration (measured as Total Suspended Solids, TSS) on the bacterial nitrification rate was explored in two different photo-sequencing batch reactors.
All the analyzed microalgal-bacterial consortia showed a solid-limited kinetic at low TSS concentrations and a light-limited kinetic at higher concentrations. A simplified mathematical model was proposed to describe this relationship.
In addition, a standardized procedure to define the optimal TSS concentration that guarantees the maximum ammonium removal rate, was proposed.

This Chapter is based on:
Foladori P., Petrini S., Andreottola G., 2020. *How suspended solids concentration affects nitrification rate in microalgal-bacterial photobioreactors without external aeration.* Heliyon 6, e03088. https://doi.org/10.1016/j.heliyon.2019.e03088

Abstract

The use of microalgae for the treatment of municipal wastewater makes possible to supply oxygen and save energy, but must be coupled with bacterial nitrification to obtain nitrogen removal efficiency above 90%. This paper explores how the concentration of Total Suspended Solids (TSS, from 0.2 to 3.9 g TSS/L) affects the nitrification kinetic in three microalgal-bacterial consortia treating real municipal wastewater. Two different behaviors were observed: (1) solid-limited kinetic at low TSS concentrations, (2) light-limited kinetic at higher concentrations. For each consortium, an optimal TSS concentration that produced the maximum volumetric ammonium removal rate (around 1.8-2.0 mg N L^{-1} h^{-1}), was found. The relationship between ammonium removal rate and TSS concentration was then modelled considering bacteria growth, microalgae growth and limitation by dissolved oxygen and light intensity. Assessment of the optimal TSS concentrations makes possible to concentrate the microbial biomass in a photobioreactor while ensuring high kinetics and a low footprint.

10.1 Introduction

Ammonium oxidation is mandatory in sensitive areas due to eutrophication risks and its toxicity for aquatic life (Kennish and Jonge, 2011). In municipal wastewater treatment plants (WWTPs) ammonium undergoes full nitrification, a process with a considerable effect on the design, footprint and costs (Jaramillo et al., 2018). In particular, very high electrical energy is required to supply a large amount of external oxygen for nitrification (Åmand et al., 2013; Luo et al., 2019).

Within this context, in recent years, microalgal-bacterial consortia have gained increasing attention as they are able to produce an ideal self-sustaining system that treat wastewater with high ammonium removal efficiency (Subashchandrabose et al., 2011; Liu J. et al., 2017; Wang et al., 2018). Although both microalgae and cyanobacteria (hereafter referred to as microalgae) are able to utilize various forms of nitrogen, with ammonium being preferred (Krustok e al., 2016; Wang Y. et al., 2016), this direct uptake of nitrogen is not enough to obtain a removal efficiency above 90-95% in municipal wastewater with competitive

HRT (Hydraulic Retention Time) with respect to activated sludge (Judd et al., 2015). Combination with bacterial nitrification is thus a likely solution (Leong et al., 2018; Vargas et al., 2016; González-Fernández et al., 2011; Rada-Ariza et al., 2017; Ye et al., 2018a).

Photosynthetic oxygenation makes it possible to sustain organic matter removal and nitrification without the need for external energy, except natural light. At the same time, CO_2 resulting from organic matter decomposition is fixed by microalgae. In this way, wastewater treatment can be achieved saving energy and mitigating CO_2 (Vu and Loh, 2016; Gonçalves et al., 2017).

While open system as high rate algae ponds (HRAPs) can only be controlled to a limited extent, closed photo-bioreactors (PBRs) are more suitable for optimization and efficient nitrification (Karya et al., 2013; Wang et al., 2018). However, in PBRs, important design parameters such as kinetics have been largely overlooked (Decostere et al., 2016) and the removal process appears slower and less robust than activated sludge (Judd et al., 2015). This may arise mainly from some limitations, such as the lower biomass concentration in PBRs compared to activated sludge and the lower volumetric ammonium removal rates.

In aerated suspended solids processes, as activated sludge, an increase in the concentration of solids is expected to produce higher volumetric removal rates (Henze et al., 2008) and thus a smaller volume and footprint for the plant, if a sufficient amount of external oxygen is provided. However, in microalgal-bacteria based systems an excessive increase in solids concentration may reduce the light penetration, causing self-shading, reducing in-situ photosynthetic oxygenation and limiting the overall microbial oxidation kinetic (Anbalagan et al., 2017). Knowledge of the optimal solids concentration in a given microalgal-bacterial system is therefore of extreme importance (Sun L. et al., 2019).

A very broad range of solids concentrations, from 0.1 to 8 g TSS/L (TSS, Total Suspended Solids) has been reported with open or closed systems (Judd et al., 2015). In general, the literature recommends not maintaining biomass concentrations at excessively high levels in order to avoid self-shading phenomena (Bilad et al, 2014; Udaiyappan et al., 2017; Luo et al., 2017). However, until now, little has been known about the influence of solids concentration on the perfor-

mances and kinetics of PBRs and no rational approach and systematic study exist to estimate the optimal value.
This paper explores how solids concentrations (in terms of TSS) affect the kinetics of bacterial nitrification in microalgal-bacterial consortia treating real municipal wastewater, without external aeration. In particular, consortia derived from two different PSBRs (Photo-Sequencing-Batch-Reactors) and composed of bacteria, microalgae and inert compounds were considered.
For each consortium, the ammonium removal rate was experimentally determined through AUR (Ammonium Utilisation Rate) tests at different TSS concentrations. Then the optimal solids concentration was estimated by modelling the ammonium removal rate as a function of TSS. Dissolved oxygen and light intensity were taken into account as limiting factors for bacteria and microalgae, respectively. Since there is not a consolidated mathematical expression to describe light limitation (Béchet et al., 2013), the Monod, Steele and Platt-Jassby models were all regarded. It was speculated that the optimal TSS concentration, for a given system, may depend on floc structure and dimension as well as mixing regime and operational factors (such as light distribution and geometry). The assessment of the optimal TSS concentrations enables the microbial biomass in a PBR to be concentrated rationally, keeping the volumetric ammonium removal rate as high as possible.
This paper provides new insights into the design of PBRs in order to ensure high ammonium removal without external aeration, and to lower footprint.

10.2 Materials and Methods

10.2.1 Photo-sequencing batch reactors

Two PSBRs, named PSBR1 and PSBR2, were implemented as described in Chapter 6 and managed with continuous feeding of wastewater (performances were partially reported in Chapter 6). The working volume was set at 1.5 L and 2 L for PSBR1 and PSBR2, respectively. Every 48 h, a volume of 0.75 L and 0.7 L was fed into PSBR1 and PSBR2, respectively, resulting in a Hydraulic Retention

Time (HRT) of 4 d and 5.8 d; in agreement with other experiences in literature that indicate a range between 2 and 6 d (Muñoz and Guieysse, 2006). It is worth noting that these systems were not optimized with respect to the HRT and there was scope for a significant footprint reduction.
The two PSBRs differed in the length of photoperiod as indicated in Figure 10.1: (1) PSBR1 was continuously illuminated and produced "Consortium 1A" and "Consortium 1B"; (2) PSBR2 alternated light phases and dark phases to simulate real conditions and produced "Consortium 2".
PSBRs were illuminated with artificial lights arranged on one side of the reactors. Light was supplied to PSBR1 by a fluorescent lamp (F30W/33, General Electric, UK) and to PSBR2 by a led lamp (8 led×0.5 W; Orion, Italy), which provided a constant photosynthetically active radiation (PAR) of 45 μmol m^{-2} s^{-1} and 30 μmol m^{-2} s^{-1}, respectively
Light intensities were measured with a quantum sensor SQ-520 (Apogee Instruments, USA) near the top of the liquid surface inside the reactors. A constant PAR was applied for two reasons: (1) to exclude the daily and seasonal influence of sunlight fluctuations on the microbial activity and the consequent difficulties in the interpretation of parameters (Lee et al., 2015); (2) to avoid the risk of photoinhibition of the nitrifying bacteria and mitigation of this risk by TSS (Vergara et al., 2016). In this way, only the TSS concentration was considered as affecting light penetration and shading.
External addition of supplementary CO_2 was not required in the PSBRs. The CO_2 produced by bacteria was enough to maintain the pH in the optimal range.

10.2.2 Influent real wastewater

The PSBRs were fed with pre-settled wastewater collected from the Trento Nord municipal WWTP (Italy) which receives the sewerage of about 100,000 population equivalent. No filtration of wastewater was performed before feeding. The average composition of the influent pre-settled wastewater is shown in Table 10.3.

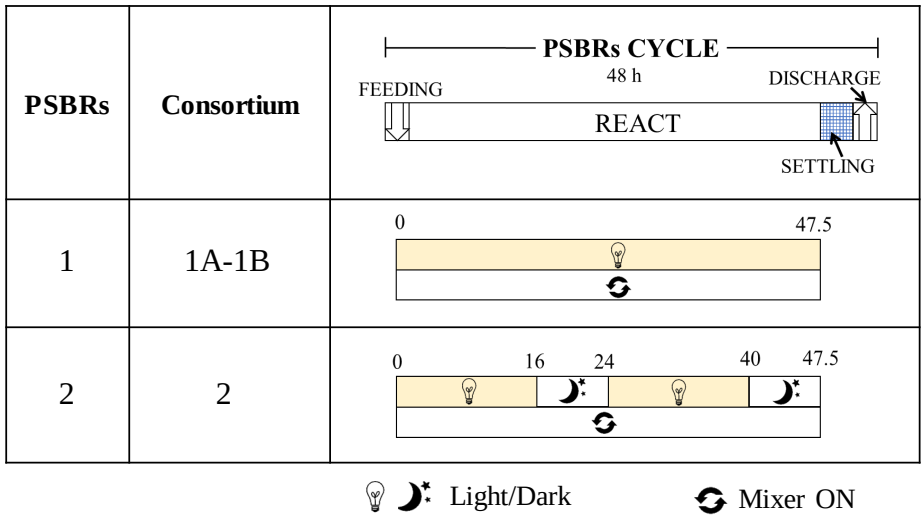

Figure 10.1 *PSBRs cycle and respective consortia. Focus on the applied light and dark conditions.*

10.2.3 Microalgal-bacterial consortia

The feeding with real wastewater originated spontaneous microalgal-bacterial consortia composed of heterotrophic and ammonium oxidizing bacteria, eukaryotic microalgae and cyanobacteria. The microorganisms embedded in flocs were characterized by high robustness in response to load fluctuations and good settleability. The development, through natural selection, of such a complex community was favored by real wastewater according to Krustok et al. (2015).

10.2.4 Analytical methods

Total COD (tCOD; Chemical Oxygen Demand), TSS, TKN (Total Kjeldhal Nitrogen), NH_4^+-N, NO_2^--N, NO_3^--N, Total N and Total P were analyzed according to Standard Methods (APHA, 2012). Soluble COD (sCOD) was measured after filtration of the sample on 0.45-μm-membrane. The parameter TSS in the mixed liquor was measured using the gravimetric method after filtration of the mixed liquor on membranes with a pore size of 0.45 μm and drying at 105°C. TSS was assumed as a reference for the biomass concentration inside the PSBRs.

Although total solids (both suspended or dissolved) may contribute to hindering the passage of light through the solution. TSS analysis was used here instead of total solids as it is the common measurement to quantify solids in WWTPs. To facilitate comparison with conventional activated sludge processes, the most widespread systems worldwide, TSS were therefore considered to be more appropriate here. Microscopic observations were performed using a Nikon Optiphot EFD-3 Microscope (Nikon, Japan) to morphologically characterize the microalgal-bacterial consortia. Online probes (all from WTW, Germany) were applied to measure Dissolved Oxygen (DO), temperature and pH continuously in the PSBRs.

10.2.5 AUR tests

Ammonium utilization rate (AUR) was measured for each microalgal-bacterial consortium at various TSS concentrations. The AUR tests were performed in the PSBRs in batch mode. Prior to start of the AUR test, a sample was analyzed to check ammonium concentration in the PSBR. Then, a known amount of ammonium was added in the PSBR to achieve an initial concentration of approximately 15 mg NH_4^+-N/L. In cases with a pH lower than 7 at the beginning of the test, a buffer solution was added to raise pH to around 8 in order to prevent nitrification inhibition due to low pH. The duration of the test was 4-6 hours. Samples were collected every hour and analyzed for NH_4^+-N, NO_2^--N and NO_3^--N after filtration on 0.45-μm membranes. The volumetric AUR was calculated considering the slope of the straight line that interpolates the experimental NH_4^+-N concentrations over time and was expressed as mg N L^{-1} h^{-1}. The specific AUR was calculated dividing the volumetric AUR by the TSS concentration and was expressed as mg N g TSS-1 h-1. AUR tests were performed with the aim of evaluating TSS influence on the nitrification rate. Therefore, each consortium was tested at five different TSS concentrations. Low TSS concentrations were obtained by extracting part of the mixed liquor and diluting the remaining part with effluent wastewater (to not alter the saline composition). High TSS concentrations were obtained reducing the working

volume (not exceeding -15%) by extracting the supernatant. To avoid qualitative and quantitative biomass variations, tests were performed within a week with 18 h between consecutive tests.

10.2.6 Modelling the ammonium removal rate

A simple model was implemented to explain the relationship between ammonium removal rate and TSS concentration. In the model, two main processes were considered:

1. aerobic growth of nitrifying biomass, responsible for ammonium oxidation and oxygen consumption;
2. photoautrophic growth of microalgae, responsible for the production of oxygen used in nitrification.

10.2.6.1 Nitrifying bacteria growth

Under constant environmental parameters (temperature and pH) and a non-limiting substrate (NH_4^+ in this case), the specific growth rate of nitrifying bacteria (μ_N; Eq. 10.1) depends only on their maximum specific growth rate ($\mu_{N,max}$) and a limiting factor that is a function of the oxygen concentration (S_O) in the mixed liquor.

$$\mu_N = \mu_{N,max} \cdot f(S_O) \tag{10.1}$$

10.2.6.2 Photoautotrophic algal growth

Analogously, in the case of non-limiting factors for microalgae except light, the specific growth rate of microalgae (μ_{ALG}; Eq. 10.2) depends on their maximum specific growth rate ($\mu_{ALG,max}$) and a function of the light intensity (I).

$$\mu_{ALG} = \mu_{ALG,max} \cdot f(I) \tag{10.2}$$

10.2.6.3 Conceptual model

Using the Activated Sludge Models (ASMs) framework (Henze et al., 2000), a simplified Gujer matrix (Table 10.1) was written to describe synthetically the

processes involved in the production and consumption of the component S_O. In this matrix, α_1 and α_2 are stoichiometric coefficients, while X_N and X_{ALG} are the concentrations of nitrifying biomass and microalgae biomass, respectively.

N°	**→Component** **↓Process**	S_O	**↓Process rate**
1	Aerobic growth of nitrifying bacteria	$-\alpha_1$	$\mu_{N,max} \cdot f(S_O) \cdot X_N$
2	Photoautrophic growth of microalgae	$+\alpha_2$	$\alpha_2 \cdot \mu_{ALG,max} \cdot f(I) \cdot X_{ALG}$

Table 10.1 *Simplified Gujer matrix considering the two processes affecting the component S_O.*

From the Gujer matrix, the derivative of S_O with respect to time was described in Eq. 10.3.

$$\frac{dS_O}{dt} = -\alpha_1 \cdot \mu_{N,max} \cdot f(S_O) \cdot X_N + \alpha_2 \cdot \mu_{ALG,max} \cdot f(I) \cdot X_{ALG} \tag{10.3}$$

During the AUR tests, the oxygen produced by microalgae was completely consumed by the nitrifying bacteria, resulting in a constant (zero) S_O. The derivative dS_O/dt was therefore zero. The Eq. 10.3 can be rearranged to express $f(S_O)$ as described in Eq. 10.4.

$$f(S_O) = \frac{\alpha_2 \cdot \mu_{ALG,max} \cdot f(I) \cdot X_{ALG}}{\alpha_1 \cdot \mu_{N,max} \cdot X_N} \tag{10.4}$$

The ratio $X_N/X_{ALG}$is a property of a given consortium and does not change during a relatively short AUR test. It can thus be considered as a constant. The terms α_1, α_2, $\mu_{N,max}$ and $\mu_{ALG,max}$ are also constant. All these terms were therefore grouped in a single constant value, k, defined in Eq. 10.5.

$$k = \frac{\alpha_2 \cdot \mu_{ALG,max} \cdot X_{ALG}}{\alpha_1 \cdot \mu_{N,max} \cdot X_N} \tag{10.5}$$

In this way, oxygen limitation ($f(S_O)$) was expressed as a simplified function of light limitation ($f(I)$) in Eq. 10.6.

$$f(S_O) = k \cdot f(I) \tag{10.6}$$

The specific rate of substrate utilization (in this case ammonium) is related to the specific growth rate of bacteria taking into account the yield coefficient of nitrifiers ($Y_{X/N}$) as described in Eq. 10.7.

$$\text{Specific ammonium removal rate} = \frac{\mu_N}{Y_{X/N}} = \frac{\mu_{N,max} \cdot f(S_O)}{Y_{X/N}} \tag{10.7}$$

Finally, replacing $f(S_O)$ (Eq. 10.6) and grouping the constants in the symbol k'', the specific ammonium removal rate results a function of X only (see Eq. 10.2.6.3).

$$\text{Specific ammonium removal rate} = k'' \cdot f(I) =$$

$$= \begin{cases} k'' \dfrac{I}{K_I + I} = k'' \dfrac{I_0 \cdot e^{-k' \cdot X}}{K_I + I_0 \cdot e^{-k' \cdot X}} & \text{(Monod)} \\ k'' \cdot \dfrac{I}{I_S} exp\left(1 - \dfrac{I}{I_S}\right) = k'' \cdot \dfrac{I_0 \cdot e^{-k' \cdot X}}{I_S} exp\left(1 - \dfrac{I_0 \cdot e^{-k' \cdot X}}{I_S}\right) & \text{(Steele)} \\ k'' \cdot Tanh\left(\dfrac{\alpha(I - I_C)}{\mu_{ALG,max}}\right) = k'' \cdot Tanh\left(\dfrac{\alpha(I_0 \cdot e^{-k' \cdot X} - I_C)}{\mu_{ALG,max}}\right) & \text{(Platt-Jassby)} \end{cases} \tag{10.8}$$

The volumetric ammonium removal rate (Eq. 10.9) was obtained by multiplying the specific rate (Eq. 10.2.6.3) by the concentration of solids per unit of volume (X).

$$\text{Volumetric ammonium removal rate} = k'' \cdot f(I) \cdot X \tag{10.9}$$

10.2.6.4 Functions for light limitation

Various functions have been proposed in literature to describe the limitation of light intensity on microalgal growth (Béchet et al., 2013; Wagner et al., 2016). Here three proposals were considered according to Table 10.2.

In the functions of Table 10.2, the light intensity, I, was expressed according to Lambert-Beer's law (Eq. 10.10) that considers the attenuation of incident

Function name	f(I)	Parameters	Reference
Monod	$\frac{I}{K_I + I}$	K_I	Béchet et al. (2013)
Steele	$\frac{I}{I_s} exp\left(1 - \frac{I}{I_s}\right)$	I_S	Wagner et al. (2016)
Platt-Jassby	$Tanh\left(\frac{\alpha(I - I_C)}{\mu_{ALG,max}}\right)$	I_C,$\mu_{ALG,max}$	Wagner et al. (2016)

Table 10.2 *Functions considered for describing the light limitation, according to Wagner et al. (2016)*

light intensity (I_0) due to the solid concentration in the reactor (X), while k' is the extinction coefficient.

$$I = I_0 \cdot e^{-k' \cdot X} \tag{10.10}$$

10.2.7 Statistical analysis

Statistical calculations were done with Microsoft®Excel. To find the best fitting for the experimental results, regression analysis was performed using the least-square method in Microsoft®Excel. This method finds the optimal parameter values by minimizing the sum of the squared residuals (experimental data minus model predictions).

10.3 Results and Discussion

10.3.1 Performances of the PSBRs in the removal of TSS, COD and N forms

The PBR configured as a sequencing batch reactor, that includes separated phases for settling and discharge, favored the selection of microalgae-bacteria bioflocs with good settleability in agreement with other studies in the literature (inter alia Arcila and, Buitrón, 2016). Mean removal of TSS (Table 10.3) was 76±18% in PSBR1 (effluent concentrations of 59±58 mg TSS/L) and 94±8% in PSBR2 (effluent concentrations of 14±18 mg TSS/L), indicating a slightly

better performance of PSBR2 in the settling of solids. The microalgal-bacterial consortia developed in the PSBRs were composed of flocs and dense aggregates with a settling velocity comparable to that of efficient granular sludge (data not shown). This aspect is extremely important to sustain cost-efficient microalgae separation by gravity sedimentation, according to other observations in literature (Tiron et al., 2015).

The removal efficiency of COD (η_{COD}) in the PSBRs (Table 10.3) was calculated according Eq. 10.11, taking into account the soluble COD (sCOD) in the effluent in order to exclude the influence of non-settleable solids that depends on the structure of the consortia.

$$\eta_{COD} = \frac{tCOD - sCOD}{tCOD} \cdot 100 \tag{10.11}$$

η_{COD} was 89±4% and 91±4% in PSBR1 and PSBR2 respectively, with no significant differences among the systems. These values were similar to the efficiency of conventional activated sludge municipal wastewater treatment. It is worth noting that this performance was obtained here without artificial aeration. COD was mainly oxidized by heterotrophic bacteria using DO and nitrates as electron acceptors, although a moderate contribution by microalgae under mixotrophic growth cannot be excluded (Alcantara et al., 2015). The DO for bacteria was produced by photosynthesis, while nitrates were produced from nitrification.

Ammonium removal was 96±7% and 99±2% in PSBR1 and PSBR2, respectively (Table 10.3), without significant differences between the two systems. This high performance was similar to that of activated sludge, but in the PSBRs the bacterial nitrification was supported by the photosynthetic oxygenation capacity of the microalgal-bacterial consortia. TKN removal was affected by the nitrogen content in the effluent TSS that depends on settling capacity and was thus higher in PSBR2 (Table 10.3). A significant denitrification was observed especially in PSBR2 under dark conditions, when DO in the PSBR dropped to zero.

Theoretically, total N removal may be attributed to a number of simultaneous processes (Liu J. et al., 2017): (i) bacterial nitrification followed by denitrification and loss of N_2 in the atmosphere; (ii) biomass uptake of nitrogen, (iii) ammonia

stripping and loss in the atmosphere. Here the average Total N removal, 50±14% and 69±10% in PSBR1 and PSBR2 respectively (Table 10.3), was mainly due to nitrification and partial denitrification. Conversely, N assimilation into biomass was relevant marginally, as a consequence of the small amount of excess sludge produced (data not shown). Ammonia stripping also played a minor role, because pH increased slightly over 9.0 after complete oxidation of the ammonium (Chapter 8). Therefore, the low N assimilation and stripping resulted in a considerable availability of NH_4^+ in the mixed liquor, stimulating the development of nitrifying bacteria. Similar observations have been reported by Karya et al. (2013) in a wastewater-treating PBR, where up to 81-85% of ammonium was nitrified by bacteria rather than being taken up by microalgae. Bacterial nitrification in the system is beneficial as it enables two additional benefits to be obtained: (i) avoidance of NH_3 volatilization, which was replaced by the more sustainable emission of denitrified N_2, (ii) reduction of the inhibitory effects of NH_3 concentration on microalgae growth (Vergara et al., 2016).

		PSBR1		**PSBR2**	
Parameter	**Influent conc.**	**Effluent conc.**	**R.E.**	**Effluent conc.**	**R.E.**
	(mg/L)	(mg/L)	(%)	(mg/L)	(%)
tCOD	301±96	99±6	66±15	41±9	85±6
η_{COD}	-	-	89±4	-	91±4
TKN	63±19	7±4	88±8	2±1	97±2
NH_4^+-N	54.4 ± 12.3	1.9±4.1	96±7	0.6±1.1	99±2
NO_2^--N	0.1±0.1	0.3±0.7	-	0.1±0.1	-
NO_3^--N	1.1±0.3	24.4±8.2	-	18.0±7.7	-
Total N	63±18	31±9	50±14	20±8	69±10
Total P	5.3±1.7	3.7±1.9	36±28	2.6±0.8	40±20
TSS	249±80	59±58	76±18	14±18	94±8

Table 10.3 *Concentrations of influent and effluent wastewater and removal efficiency (R.E.) in the two PSBRs (mean ± standard deviation).*

10.3.2 Measurement of the ammonium removal rates

Figure 10.2 shows a typical AUR test carried out at a solid concentration of 1.0 g TSS/L. Ammonium concentration and pH decrease while nitrates increase due to bacterial nitrification (Dutta and Sarkar, 2015). During the test, nitrite concentrations may increase up to a few milligrams per liter, but they were depleted after the complete removal of ammonium (data not shown). To calculate the ammonium removal rate, the NH_4^+-N data were interpolated linearly. The NH_4^+-N decrease was considered instead of the NO_3^--N increase, as nitrate concentration may be underestimated due to the occurrence of simultaneous denitrification in the inner anoxic zone of the flocs.
In the AUR test in Figure 10.2, the volumetric ammonium removal rate was 1.6 mg NH_4^+-N L^{-1} h^{-1}. For a comparison, the transformation rate of NH_4^+-N into NO_3^--N was evaluated by Tiron et al. (2015) who found values in the range of 0.14-1.5 mg NH_4^+-N L^{-1} h^{-1}. This wide range depended on the level of DO, which varied in that research from zero just after feeding to very high non-limiting values.
With regard to the DO profile during the test in Figure 10.2, in the presence of NH4+ a long phase with DO constantly near zero was observed (called "zero-DO phase" according to Chapter 8). This indicates that the oxygen provided through photosynthesis was used completely for the bacterial nitrification. Despite this zero-DO phase, the process was still proceeding and no significant variations in ammonium removal rate were observed during the test.

10.3.3 Influence of TSS on the ammonium removal rate

A series of AUR tests were performed to measure the ammonium removal rate at different TSS concentrations, from 0.2 to 3.9 g TSS/L considering all the microalgal-bacterial consortia (but under the same PAR and mixing), according to the synthesis in Figure 10.3. The range of TSS concentrations tested here was wider than others in literature. García et al. (2017) applied biomass concentrations from 1.2±0.3 g TSS/L to 2.8±0.3 g TSS/L. Other studies investigated nutrient removal at concentrations up to 1.37 g TSS/L (Judd et al., 2015). Especially

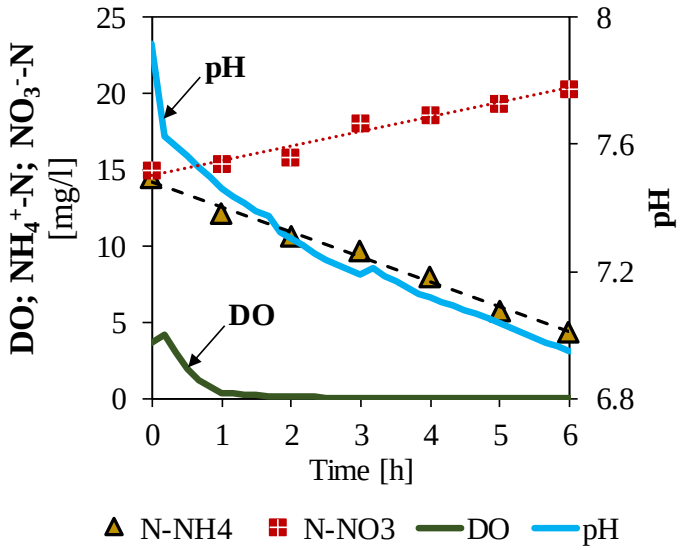

Figure 10.2 *Profiles of NH_4^+-N, NO_3^--N, DO and pH during a typical AUR test (example of a test carried out at 1.0 g TSS/L). The slope of the linear fitting of NH_4^+-N data represents the ammonium removal rate.*

when pure algal strains were considered, solid concentrations were relatively low; for example, the maximum concentration was 1.2 g/L for *Chlorella sp.* (Li et al., 2011). In this way, the present research contributes by adding results at relatively high TSS concentrations.

The results obtained here are shown in Figure 10.3, where the volumetric ammonium removal rate (expressed as mg N L^{-1} h^{-1}) and the specific ammonium removal rate (expressed as mg N g TSS^{-1} h^{-1}) are plotted as a function of the TSS concentration.

10.3.3.1 The maximum volumetric ammonium removal rate identifies the optimal TSS concentration

For all the consortia, a rise in the volumetric ammonium removal rate occurred when the TSS concentration increased (Figure 10.3). An optimal condition then appeared, when the nitrification rate reached the maximum value. A further increase in TSS concentration did not provide an advantage in terms of nitrification rate, despite a larger availability of biomass. In fact, for

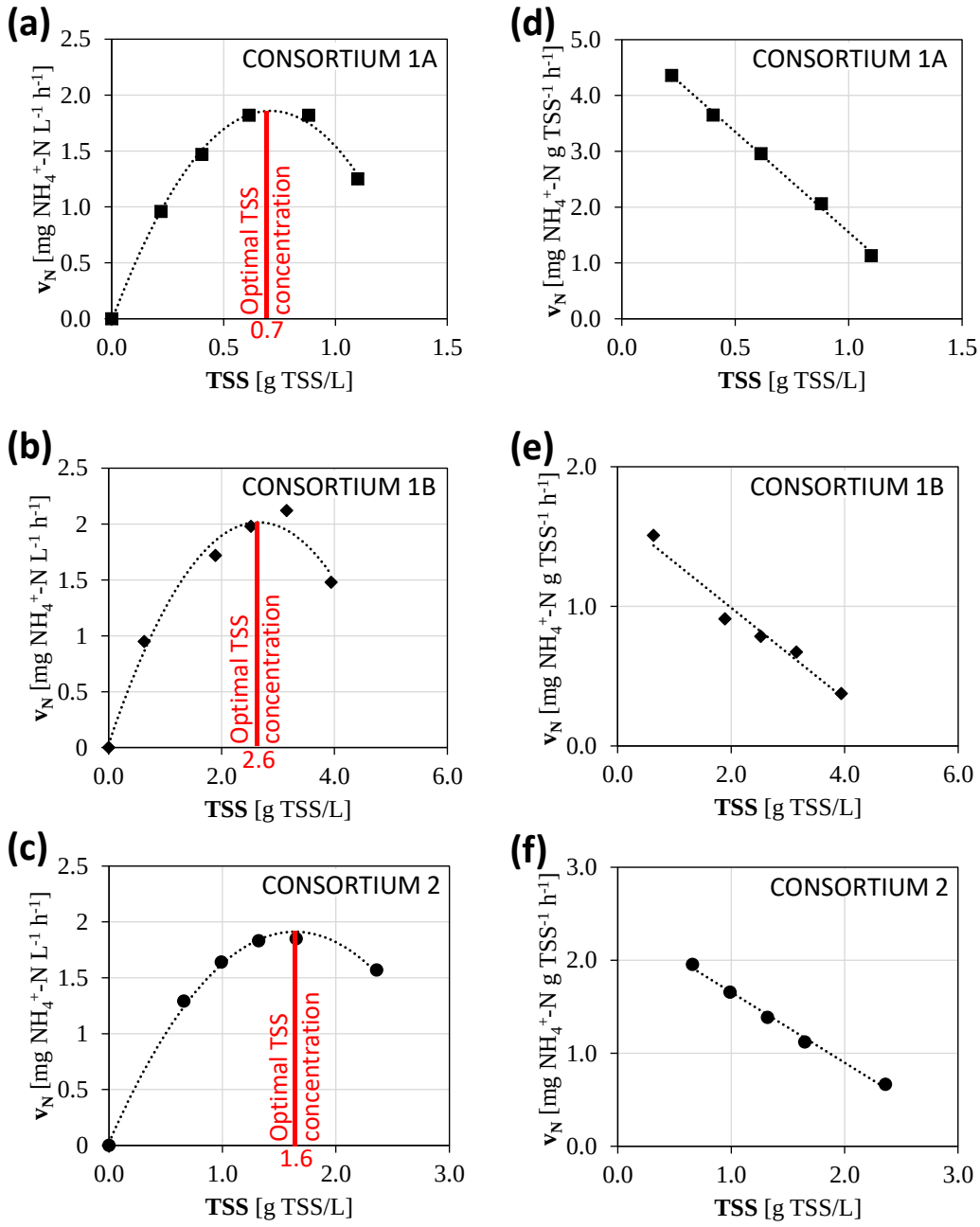

Figure 10.3 *Volumetric and specific ammonium removal rate as a function of the TSS concentration for three microalgal-bacterial consortia. (a),(b),(c) Volumetric rate for consortia 1A, 1B and 2, respectively. The optimal TSS concentration that produces the maximum removal rate is indicated for each consortium.(d), (e), (f) Specific rate for consortia 1A, 1B and 2, respectively.*

higher solid concentrations, a decrease in the volumetric ammonium removal rate was observed.
In more detail, two parts can be distinguished:

1. a first rising part: a higher concentration of solids produces a higher volumetric ammonium removal rate. In this part, the process occurs with enough light and DO, and the nitrification rate is only limited by the amount of biomass (solid-limited kinetic);
2. a second decreasing part: a mutual shading of biomass occurs. Light penetration is reduced and nitrification rate is limited by the lower oxygen production rate caused by the increased shadow effect (Udaiyappan et al., 2017) (light-limited kinetic).

Between these parts, the maximum ammonium removal rate identifies the optimal TSS concentration for a system. Different values were observed for each consortium: the optimum was 0.7, 2.6 and 1.6 g TSS/L for consortia 1A, 1B and 2, respectively (Figure 10.3). This difference was associated with the different structure of the flocs, compared in Figure 10.4, that directly affects the self-shading. In the case of consortia 1A and 2 (Figure 10.4) the biomass was organized in a larger amount of medium-sized flocs (average floc size of 0.4 mm and 0.2 mm, respectively, Table 10.4) that formed a higher turbid suspension where self-shading was predominant. Conversely, the structure of consortium 1B (Figure 10.4) was based on sparse very large granules with an average floc size 0.6 mm (Table 10.4) (and up to 1.5 mm) which allowed light to pass more efficiently through the suspension.

10.3.3.2 The volumetric ammonium removal rate is similar among consortia

The maximum volumetric ammonium removal rates (found in correspondence with the optimal TSS concentration) for each microalgal-bacterial consortium are compared in Table 10.4. The rates were comprised in a small range of 1.8-2.0 mg NH_4^+-N L^{-1} h^{-1}. These values were remarkably higher than other results in literature. The NH_4^+-N transformation rate was up to 1.6 mg NH_4^+-N

L^{-1} h^{-1}, as referred by Tiron et al. (2015). Ammonium reduction of 0.81-7.66 mg NH_4^+-N L^{-1} d^{-1} (corresponding to hourly values of up to 0.32 mg NH_4^+-N L^{-1} h^{-1}) was reported by Riaño et al. (2012).

The fact that the consortia investigated were characterized by similar maximum ammonium removal rates (Table 10.4) can be explained by similar TKN loads applied in the PSBRs, that supported a similar growth of nitrifying biomass in the three consortia (nitrification was demonstrated to be the only important process in nitrogen oxidation, see Section 10.3.1). In other words, the amount of nitrifying bacteria (X_N, expressed as g VSS/d; VSS = Volatile Suspended Solids) depended on the composition of the influent wastewater and the removed load (ΔTKN, expressed in g TKN/d), according to the relationship in Eq. 10.12 (Tchobanoglous et al., 2003), where Y_N is the specific yield for nitrifiers (expressed as g $VSS_{produced}$/g $TKN_{removed}$).

$$X_N = Y_N \cdot \Delta TKN \tag{10.12}$$

Conversely, the amount of microalgal biomass produced in the consortia also depended on the availability of external factors such as light or CO_2.

At a given TKN influent load, a consortium developed with a higher TSS concentration does not contain a larger nitrifying biomass, but rather a larger microalgal biomass.

Microscopic observations of the consortia revealed bacteria, microalgae and cyanobacteria embedded with inert solids forming dark green or brown dense flocs and granules (Figure 10.4). In particular: (1) the consortia 1A and 2 were characterized by the smallest flocs (average floc size of 0.4 mm and 0.2 mm, respectively, Table 10.4) with a limited presence of filamentous microorganisms; (2) consortium 1B was formed by larger granules with an average floc size of 0.6 mm (Table 10.4) and it was the consortium with the largest presence of filamentous cyanobacteria. Notwithstanding that consortium 1B, characterized by the highest TSS concentration (i.e. 2.6 g TSS/L), was the richest in photosynthetic cyanobacteria, the nitrification rate was approximately the same (Table 10.4).

In synthesis, while the amount of nitrifying bacteria in a given consortium is

strictly associated with the TKN load in the influent, the microalgal biomass may exploit external resources and may increase freely in the system. Therefore, despite a higher TSS concentration in a consortium, the maximum volumetric nitrification rate is primarily the result of the applied TKN load.

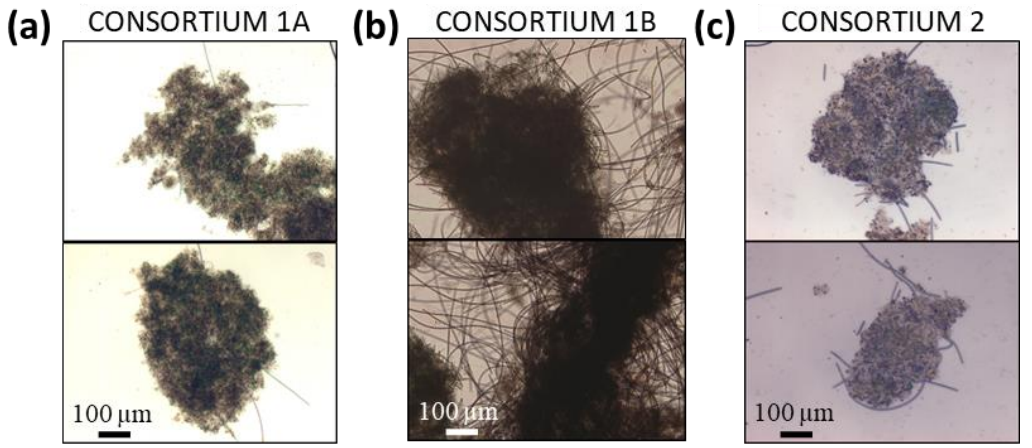

Figure 10.4 *Comparison of the flocs structure for the three microalgal-bacterial consortia. (a) consortium 1A, (b) consortium 1B and (c) consortium 2.*

Consortium	1A	1B	2
Average floc size (μm)	400	600	200
TSS (g TSS/L)	0.7	2.6	1.6
Maximum volumetric ammonium removal rate (mg NH_4^+-N L^{-1} h^{-1})	1.86	2.01	1.91

Table 10.4 *Comparison of the floc size, the TSS concentration and the maximum volumetric ammonium removal rate for the three microalgal-bacterial consortia.*

10.3.3.3 The specific ammonium removal rate decreases with TSS concentration

The specific ammonium removal rate as a function of TSS was interpolated with a linear fitting for each consortium (Figure 10.3). In all three cases, the

very high regression coefficient ($R^2 > 97\%$) indicated the high strength of the linear correlation.

The comparison between the three consortia is shown in Figure 10.5, where a clear decreasing behavior can be observed. The higher specific rate of 4.4 mg NH_4^+-N g TSS^{-1} h^{-1} was found at the lowest concentration of 0.2 g TSS/L, while it decreased progressively to 0.4 mg NH_4^+-N g TSS^{-1} h^{-1} (reduction by 91%) at the highest concentration of 3.9 g TSS/L. A distinct change in slope was observed at a TSS concentration of around 0.6 g TSS/L. At concentrations <0.6 g TSS/L (Figure 10.5), the higher specific removal rates were due to two different but coexisting effects:

1. High oxygen production: the scarce biomass permitted an easier passage of light in the reactor and thus the production of oxygen was greater. A higher DO concentration originated an enhanced diffusion of oxygen and thus a larger part of the flocs became aerobic. As a consequence, more biomass was reached by oxygen and the specific ammonium removal rate resulted higher;
2. Low oxygen consumption: DO consumption was lower because less bac-

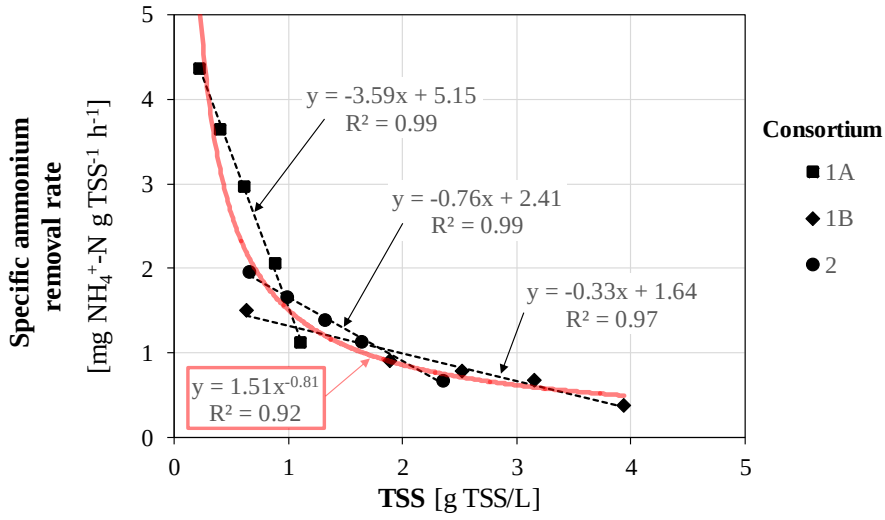

Figure 10.5 *Specific ammonium removal rate as a function of TSS for the three microalgal-bacterial consortia.*

teria consumed less oxygen. As a consequence a greater availability of oxygen remained for the biomass and the specific rate of nitrifiers resulted higher.

At concentrations > 0.6 g TSS/L (Figure 10.5), most of the light was absorbed by a thin layer of biomass that produces oxygen only in the external part of the flocs, while lack of light and oxygen occurred in the deeper layers. Other authors have indicated that light shading may occur in PBRs when operating at a biomass concentration higher than 1 g/L (Luo et al., 2017).
Despite the fact that the specific removal rate was higher at low TSS concentrations, it led to an even smaller volumetric rate (expressed as mg N L^{-1} h^{-1}) due to the low availability of biomass in the PSBR.
In PBRs aimed at obtaining complete wastewater treatment, it is preferable to obtain the highest volumetric ammonium removal rate rather than the highest specific rate, in order to reduce the footprint of the plant. With higher TSS, photosynthesis may be less efficient, but it may be enough to produce a sufficient amount of oxygen to support full nitrification.

10.3.4 Experimental results fit to the simplified model

The experimental results of the specific and volumetric ammonium removal rate were then fitted according to the conceptual model described in Section 10.2.6.3 and including three different equations to describe light limitation (Table 10.2). The results are summarized in Figure 10.6.
For all the functions, the model enabled a good fitting of the experimental data to be obtained for both volumetric and specific rates. Monod's equation was slightly worse and this was not surprising as it was based on the simplest form. However, all the fitted curves very clearly confirmed the occurrence of two well defined parts, already observed in Section 10.3.3.1: (1) the rising part, where low TSS and a solid-limited kinetic occurs; (2) the decreasing part where high TSS and a light-limited kinetic occurs and the ammonium removal rate tends progressively to zero. The model used here for the fitting of the experimental results was able to describe the relationship between the ammonium removal

rate and the TSS concentration in a PBR. This finding may help in the management of the complex microalgal-bacterial consortia involved in PBR and to identify the optimal conditions for design.

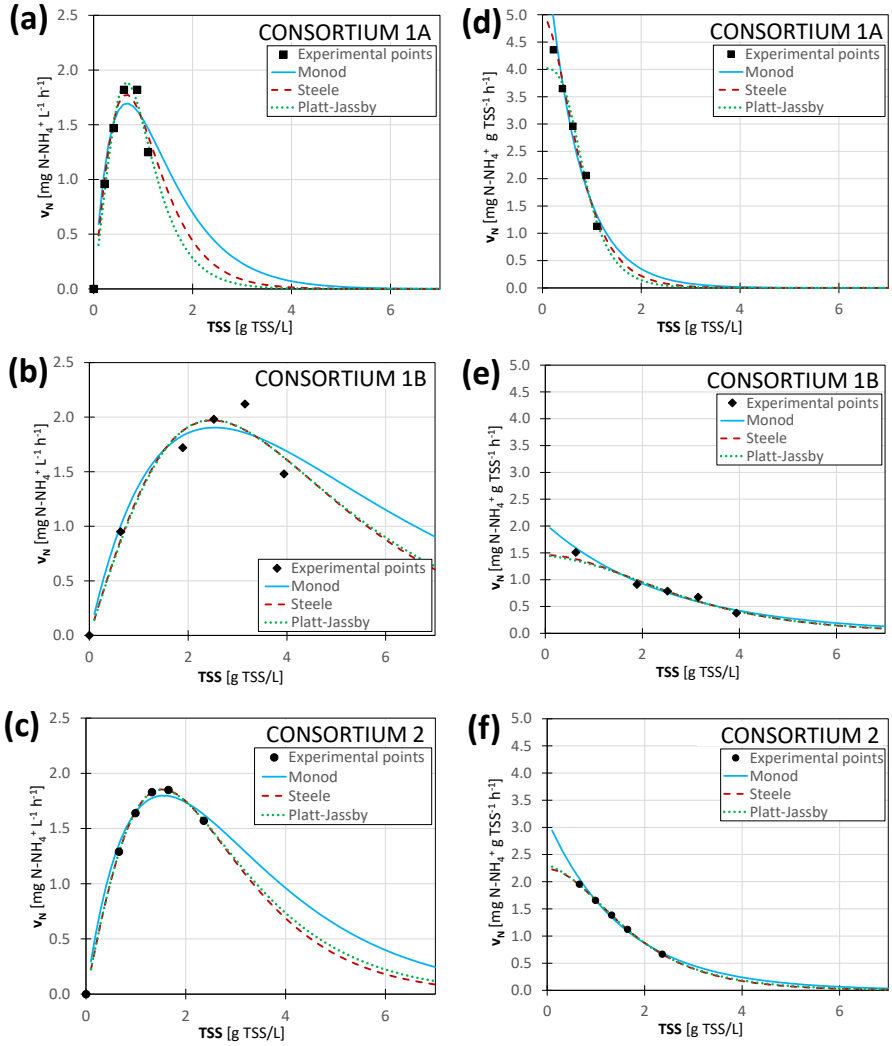

Figure 10.6 *Results of the fitting of volumetric and specific ammonium removal rate as a function of the TSS concentration for the three microalgal-bacterial consortia.(a),(b),(c) Volumetric rate for consortia 1A, 1B and 2, respectively. (d), (e), (f) Specific rate for consortia 1A, 1B and 2, respectively.*

10.4 Conclusion

This paper proposes a standardized procedure for measuring both volumetric and specific ammonium removal rate in batch tests under a given value of irradiance and for a given TSS concentration. Performing 4-5 batch tests at different TSS concentrations with a duration of 4-5 hours each, it was possible to identify easily the optimal interval of TSS associated with the maximum ammonium removal rate of the system. When TSS concentration differs from this optimum value, the nitrification kinetic decreases due to: (1) a solid-limited kinetic when TSS is below the optimum, originated by an insufficient amount of biomass in the system, (2) a light-limited kinetic when TSS is above the optimum, due to a less efficient exploitation of light and production of oxygen. The optimal TSS concentration able to produce the maximum volumetric ammonium removal rate (around 1.8-2.0 mg N L^{-1} h^{-1}) was found for three microalgal-bacterial consortia. A good fitting with a mathematical model (based on bacteria and microalgae growth and limitation by DO and light intensity according to Monod, Steele and Platt-Jassby equations) confirmed the experimental relationship between ammonium removal rate and TSS concentration. Assessment of optimal solids concentration can thus help in the design of PBRs when enhanced nitrification is required to meet stringent nitrogen limits for the discharge of wastewater.

Acknowledgements

The authors would like to thank Andrea Pacini and Mirco Nessenzia for their help during the experimental work.

CHAPTER 11

RESPIROMETRY TO ASSESS PHOTOTROPHIC, HETEROTROPHIC AND NITRIFYING ACTIVITY

A respirometer used to test activated sludge was modified and a procedure was developed to test microalgal-bacterial consortia under light and dark conditions.
The microalgal-bacterial consortium developed in the Pilot (Chapter 6), was tested to determine the microorganisms' activities in endogenous condition, in the presence of readily biodegradable organic matter and in the presence of ammonium.
The respirometric approach proposed here adds experimental kinetic results needed in the PBR design and modelling.

This Chapter is based on:
Petrini S., Foladori P., Donati, L., Andreottola G. *Comprehensive respirometric approach to assess photosynthetic, heterotrophic and nitrifying activity in microalgal-bacterial consortia treating real municipal wastewater.* Biochemical Engineering Journal, UNDER REVIEW.

Abstract

The design of photobioreactors (PBR) to treat municipal wastewater is still in the early stages of development. Kinetics of activated sludge cannot be used for PBRs because consortia differ in composition, growth and decay rates. In this paper, respirometry was extended to a microalgal-bacterial consortium developed for 2 years in a PBR treating municipal wastewater. Kinetic and stoichiometric parameters (20°C) were estimated for endogenous respiration, biodegradable COD oxidation and nitrification. A comprehensive respirometric approach was adopted. It was based on the Oxygen Production Rate (OPR) of photosynthetic microorganisms and the Oxygen Uptake Rate (OUR) of the overall biomass, and it included data processing and corrections. The gross OPR (gOPR) was 9.8±0.2 mg O_2 g TSS^{-1} h^{-1}; using microalgae quantified by flow cytometry, the per-cell gOPR was 11 fmol O_2 $cell^{-1}$ h^{-1}. This oxygen was utilized for COD oxidation with rate of 18.0 and 19.3 mg COD g TSS^{-1} h^{-1} under light and dark, respectively. Biomass yield (Y_{COD}) was 0.66 on average, similar to the typical values of activated sludge. The nitrification rate in the dark was 0.92 mg NH_4^+-N g TSS^{-1} h^{-1}. The stoichiometric oxygen-over-ammonium coefficient ($f_{O_2/NH}$) was 4.4 g O_2/g N under dark conditions (similar to activated sludge), but lower under light ones (2.8 g O_2/g N). The respirometric approach proposed here added experimental kinetic results needed in the PBR design.

11.1 Introduction

Photobioreactors (PBRs) based on microalgal-bacterial consortia, which couple nitrifying, heterotrophic and photosynthetic microorganisms, are an alternative and very promising technology with which to improve the sustainability of wastewater treatment. Their main advantage is that microalgal photosynthesis releases dissolved oxygen that can be exploited by bacteria, reducing or eliminating the need for mechanical aeration and thus energy costs in wastewater treatment plants (WWTPs). In addition, organic matter and nitrogen removal is performed not only by bacteria, but also by microalgae that use these sources for their mixotrophic metabolism.

Conventional wastewater treatments, based on activated sludge, are character-

ized by huge energy consumption, high management costs and problematic disposal of large amounts of excess sludge. Conversely, PBRs may treat real wastewater with lower energy requirements and reduced carbon dioxide emissions thanks to photosynthesis, in simplified plant configuration, and enhance the recovery of energy from the excess biomass produced (Alcantara et al., 2015; Sforza et al., 2018). Therefore, microalgal-bacterial based treatment has attracted increasing attention as a future candidate to replace activated sludge in WWTPs.

The good removal performances of PBRs have been already demonstrated at lab- and pilot-scale, but the design procedures remain still largely undefined (Brindley et al., 2010). Therefore, more experimental data are needed to increase the knowledge of the treatment removal dynamics in these systems. Parameters used to design activated sludge processes may be not suitable for PBRs because the microalgal-bacterial consortia differ greatly in microbial composition, growth and decay rates. The measurement of the overall activity and kinetics of biomass is the starting point for the design and modeling of PBRs (Decostere et al., 2014).

A common approach in PBRs is to measure separately the kinetics of each microorganism group (heterotrophs, nitrifiers, microalgae), as each group would be present in the consortium as a stand-alone species. However, kinetics may differ significantly when microorganisms grow separately in pure culture or coexist, due to the interactions that occur in the microalgal-bacterial consortium. Respirometry is a fast, cheap and intuitive approach based on the profiles of dissolved oxygen (DO) and it has been extensively used for activated sludge to measure growth kinetics, sludge decay rate and stoichiometric coefficients (Spanjers et al., 1998). Depending on the protocols and the methods used in the experiments, respirometric tests may offer information-rich profiles and precise estimated parameters when extended to photosynthetic systems (Tang et al., 2014; Rossi et al., 2020). The data acquisition is analytically simple because the continuous measurement of DO can be fully automated, thus avoiding sampling errors and bias (Tang et al., 2014). In particular, from the slope of the DO profiles, the following activity rates can be calculated: (1) Oxygen Produc-

tion Rate (OPR) of photosynthetic microorganisms in the light and (2) Oxygen Uptake Rate (OUR) of the overall consortium in the dark. If OPR is considered positive, OUR is seen as negative. The OPR-OUR difference is known as "net oxygen production" or "net photosynthesis" (Ippoliti et al., 2016).

Various experimental protocols have been proposed in the literature to measure DO dynamics (Table 11.1), but the results may be not always comparable (Brindley et al., 2010). Decostere et al. (2013) proposed a combined respirometric-titrimetric unit to calibrate a basic kinetic model for microalgae. Tang et al. (2014) suggested the need for rapid, simple and reliable methods to determine the photosynthetic activity of phototrophs. Rossi et al. (2018) developed a respirometric protocol to determine OPR and OUR in a microalgal-bacterial consortium: alternation of light/dark phases and dosing of specific substrates were used to activate microalgal and bacterial metabolisms. In this way, Rossi et al. (2018) evaluated microalgal and nitrifying activity and demonstrated the feasibility of including respirometric tests in monitoring procedures of PBRs. Sforza et al. (2018) used respirometry to investigate the reduction of the net oxygen production by microalgae due to their mixotrophic metabolism. In Sforza et al. (2019) kinetics of *Chlorella protothecoides* were measured under autotrophic, heterotrophic and mixotrophic conditions. Vargas et al. (2016) measured the activity of a consortium of microalgae and nitrifying bacteria developed from the aerobic sludge of wastewater treatment plants.

The comparison in Table 11.1 highlights that many respirometric tests were carried out on single species of pure microalgal cultures and often in absence of bacteria. Therefore, these measurements give results that cannot be transferred directly in the design of PBRs that are fed with real municipal wastewater rich in natural bacteria (Rossi et al., 2018). Moreover, since most cultures were fed with synthetic wastewater (Table 11.1) it was not possible to ascertain the complex interactions that may occur in a complex medium such as real wastewater (Pastore et al., 2018). To our knowledge, no respirometric measurements have been performed previously on mixed microalgal-bacterial consortia spontaneously acclimatized with real wastewater for long periods (years).

The present paper gives insight into the net photosynthesis and the oxygen requirements for biomass maintenance and substrate removal of a microalgal-bacterial consortium spontaneously developed for more than two years in a PBR treating real municipal wastewater. This steady-state PBR was very efficient in the treatment of wastewater and for a long time furnished a constant quality biomass for respirometric tests. The consortium was composed by photosynthetic microorganisms, heterotrophic bacteria and nitrifying bacteria capable of performing removal efficiency of pollutants higher than 90% without artificial aeration but exploiting photosynthesis Chapter 6.

The proposed approach for respirometric tests was developed in agreement with the literature (Decostere et al., 2014, Rossi et al., 2018, Sforza et al., 2018). Compared to other respirometric studies that last a fixed time (from minutes to hours), this study proposes a standard, accurate and simply procedure to determine the photosynthetic and bacterial activities during the complete removal of external substrates until the endogenous (basal) respiration is reached.

The tests were performed on a microalgal-bacterial consortium, not on single species, so as to monitor the global activity, considering the interactions that may occur among microorganisms. Photosynthetic and respiration activities of the consortium were determined with emphasis on the kinetic and stoichiometric parameters involved in the oxidation of readily biodegradable COD (Chemical Oxygen Demand) and ammonium, which are the most important pollutants to be removed from wastewater, in order to meet the discharge regulations. This method may serve as a standard procedure for the evaluation of parameters useful in the design of PBRs.

Type of approach	**Reference microorganisms**	**Substrate for feeding**	**Reference**
Respirometry	Nitrifiers, *C. emersonii*, uncultured cyanobacterium	Synthetic WW	Choi et al. (2010)
Fiber-optic oxygen sensors	*C. sorokiniana*	Specific medium	Kliphuis et al. (2011)
Respirometry-titrimetry	*C. vulgaris*	Synthetic WW	Decostere et al. (2013, 2014)
Respirometry	*C. vulgaris*, Microcystis aeruginosa (cyanobacteria)	Specific medium	Tang et al. (2014)
DO, light- dark of 5', max 30'	*Isochrysis galbana*	Culture medium	Ippoliti et al. (2016)
Respirometry	Mixed culture of microalgae (mainly Chlorophyceae)	Effluent of an anaerobic urban WWT	Ruiz-Martinez et al. (2016)
Respirometry	Nitrifying bacteria and microalgae	WW	Vargas et al. (2016)
Profiles of DO	*Dinophyceae, Cryptophyceae, Coscinodiscophyceae*	Specific medium	Mantikci et al. (2017)
Respirometry	*C. vulgaris*	Synthetic WW	Najm et al. (2017)
Respirometry	*C. protothecoides* + activated sludge	Synthetic WW	Pastore et al. (2018)
Respirometry	Microalgal- bacterial consortium	Effluent from biogas plant	Rossi et al. (2018)
Respirometry	*C. protothecoides* + activated sludge	Real and synthetic WW	Sforza et al. (2018)
Respirometry	*C. protothecoides*	Artificial medium	Sforza et al. (2019)
Respirometry	Spontaneously microalgal-bacterial consortium	Real municipal WW	This study

Table 11.1 *Respirometric approaches applied to microalgal-bacterial consortia. DO: Dissolved Oxygen. WW: Wastewater. C.: Chlorella.*

11.2 Materials and Methods

11.2.1 Microalgal-bacterial consortium

The tested microalgal-bacterial consortium was collected from a sequencing-batch PBR, with a volume of 2 L, working for more than 2 years and fed constantly with real municipal wastewater. Pure strains of microalgae were never inoculated in the PBR, with the aim of exploring spontaneous evolution of the consortium representative of full-scale applications. For the same reason, supplementary CO_2, air or oxygen were not supplied in the system and pH was measured but not controlled.

Light was provided by a LED lamp (8 led×0.5 W; Orion, Italy). The light intensity, measured with a SQ-520 quantum sensor (Apogee Instruments, USA), was in the range 30±5 μmol m^{-2} s^{-1} as photosynthetically active radiation (PAR). The flow rate of the influent wastewater was 0.35 L/d.

The characteristics of the influent municipal wastewater are reported in Table 11.2. Wastewater was collected after the primary sedimentation of the Trento Nord WWTP (Trento, Italy).

The removal efficiency of the PBR under steady state conditions are indicated in Table 11.2 and are averages calculated over a period of 2.2 year (807 days). The effluent quality (Table 11.2) met the requirements for the discharge in surface waters (EU Directive 91/271/EEC). All the physical-chemical analyses indicated in Table 11.2 were conducted according to Standard Methods (APHA, 2012).

Due to the low applied load in the PBR (approximately a third of that applied in conventional activated sludge), no exponential growth was observed, with a low production of excess biomass (data not shown). TSS concentration in the PBR was around 0.9-1 g TSS/L with VSS/TSS ratio of 0.88 (VSS, Volatile Suspended Solids).

Aliquots of mixed liquor were periodically extracted from the PBR and put in the respirometer to test the microalgal-bacterial consortium. At the end of the

respirometric tests the mixed liquor was put back into the PBR to avoid the loss of biomass from the system.

11.2.2 The respirometer

The respirometer consisted of a cylindrical glass vessel (12 cm diameter × 19 cm height) with a maximum working volume of 1.4 L. The system was heat-jacketed to work at controlled temperature (20°C) and mixed with a magnetic stirrer (Figure 11.1A). The configuration was very similar to the one commonly used for activated sludge and exhaustively described in the literature (Ziglio et al., 2001; Spanjers and Vanrolleghem, 2016). The respirometer follows the "liquid phase - static gas -static liquid (LSS) principle" (Spanjers and Vanrolleghem, 2016), which is the simplest respirometric principle due to the absence of flowing liquid and gas; this is a great advantage in view of routine measurements of kinetics. Moreover, the LSS principle can be implemented to measure the respiration rate semi-continuously both in the lab and in the field (Spanjers and Vanrolleghem, 2016).
For the respirometric tests under light conditions, a LED strip light (length of about 4 m, 60 LEDs per meter with a maximum power of 10.8 W per meter; V-TAC Europe Ltd, Bulgaria) was arranged in a circular configuration (Figure 11.1B). The light intensity was set with an electronic dimmer and the tests

Parameter	**Influent real wastewater** [mg/L]	**Effluent** [mg/L]	**Removal efficiency** [%]
COD	258±163	68±9	66±17
TSS	119±102	40±46	65±30
NH_4^+-N	47.4±16.1	0.5±0.7	99±2
TN	55±21	16±8	69±17
TP	5.3±2.3	3.3±0.9	31±23

Table 11.2 *Long term characterization (2.2 years) of influent and effluent wastewater and removal efficiency of the PBR (avg ± st.dev.). COD: Chemical Oxygen Demand; TSS: Total Suspended Solids; TN: Total Nitrogen; TP: Total Phosphorous.*

were performed at 90±5 μmol m^{-2} s^{-1}. Under light and dark conditions, the respirometer was covered with an aluminum foil (Figure 11.1B) to avoid the influence of external light.
Dissolved Oxygen (DO) was recorded every 5 seconds using a Multi3510 meter equipped with the sensor FDO®925 (WTW, Germany). The data acquisition system controlled the DO by turning the LED lights on and off on the basis of defined set-points in the DO profile. In this way it was possible to alternate light and dark phases when light was turned on and off, respectively. The automated control was specifically developed by the authors (OXILISA, University of Trento).

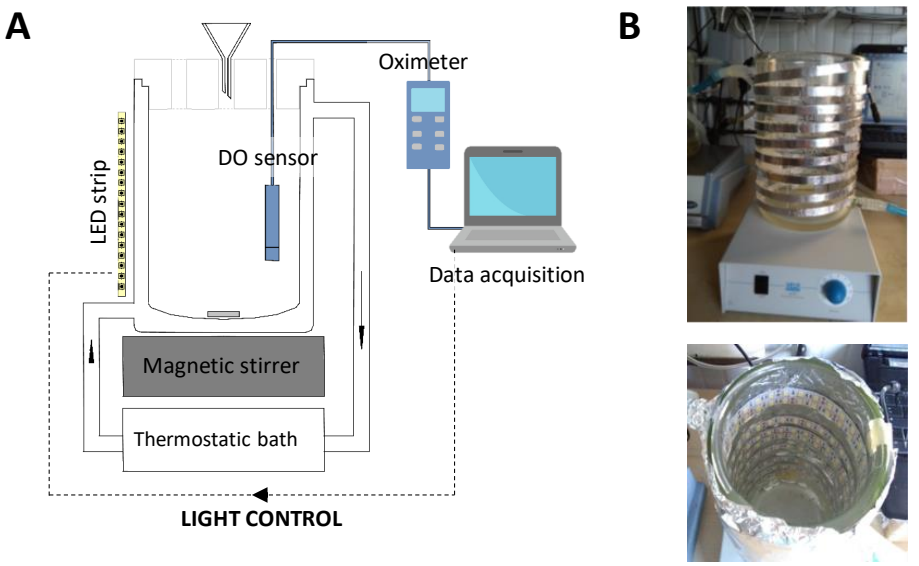

Figure 11.1 *(A) Respirometric apparatus; (B) Respirometer equipped with led and covered with aluminum foil for respirometric tests with alternated light/dark conditions.*

11.2.3 Procedure of the respirometric tests

For the respirometric tests, the mixed liquor was taken from the PBR and put in the respirometer. The biomass concentration in the mixed liquor was quantified as TSS following the Standard Methods (APHA, 2012). In some cases, the mixed liquor was diluted with the treated effluent in order to obtain a final

volume of 1.4 L with a biomass concentration around 0.9-1 g TSS/L, which was considered optimal for investigating microalgal-bacterial consortia. In fact, at higher TSS concentrations, the oxygen uptake rate would be too high and DO concentration may decrease rapidly to zero in a few minutes.

The procedure applied in the respirometric tests was, in principle, similar to that proposed recently by Sforza et al. (2019), based on a sequence of cycles of light and dark, but with some modifications: (1) the length of the test was not fixed but prolonged to reach a complete removal of the external substrate (in the order of several hours); (2) the duration of light and dark phases was not fixed but varied on the basis of two DO set-points, to maintain DO within the same range during the test (for example in the range 7.5-8.5 mg O_2/L as in Figure 11.2A) and far from limiting conditions for the biomass.

A typical DO profile is shown in Figure 11.2A, and evident in the detail on the left is the high accuracy of DO measurements and high reproducibility in the slope calculation. During the tests, DO concentration dropped rapidly and linearly as soon as the microorganisms were in the dark due to the oxygen consumption for microorganism respiration. In order to allow repeated measurement of the respiration rate, when DO reached the lower set-point, light was switched on so that photosynthetic oxygenation induced a sharp increase in DO concentration up to an upper set-point. Then light was switched off and, in this way, DO started to decrease again. The alternation of dark and light phases resulted in a DO profile with a "sawtooth pattern" (as in the example in Figure 11.2A) where DO consumption and production rate (namely OUR and OPR) can be evaluated simultaneously.

The DO range (between upper and lower set-points) should be chosen wisely because it affects the accuracy of the respirogram: (i) when respiration is slow, a longer time is required to reach the lower DO set-point and too few slopes may be calculated; (ii) when respiration is fast, only a few data of DO concentration can be acquired and the calculation of slope may be less precise (Spanjers and Vanrolleghem, 2016).

With regard to possible effects on the biological activity induced by rapid shifting from dark to light and vice versa, the literature confirms that the photosyn-

thetic capacity of microalgae is not worsened after relatively short dark periods (Myers and Cramer, 1948; Geider et al., 1998). Ruiz-Martinez et al. (2016) observed a rapid increase in DO when light was switched on in a microalgae culture after a very long period in the dark (48 h).

11.2.4 Respirometric data processing

From the acquired DO profile (as the example in Figure 11.2A) the following parameters were calculated:

- the respiration rate expressed as OUR, calculated from the slopes (with linear regression) of the DO concentration when DO declines during dark phases (Figure 11.2B). OUR is a negative value and expressed in mg O_2 L^{-1} h^{-1};
- the net photosynthesis rate expressed as OPR, which is the sum of all processes that either produce or consume oxygen (Kliphuis et al., 2011) and it is observed as DO increases. It is calculated from the slopes (with linear regression) of the DO concentration when DO rises during light phases (Figure 11.2B). OPR is a positive value and expressed in mg O_2 L^{-1} h^{-1};
- the gross photosynthesis rate (gOPR) was calculated at each time point as in Eq. 11.1 (Figure 11.2B).

$$gOPR(t) = OPR(t) - \underbrace{OUR(t)}_{negative} \tag{11.1}$$

The term gOPR denotes the total rate of photosynthesis given by the sum of net photosynthesis (OPR, obtained from positive DO slopes) and dark respiration (OUR, obtained from negative DO slopes). In other words, gOPR is calculated by adding the net produced oxygen rate to the consumed oxygen rate (Kliphuis et al., 2011).

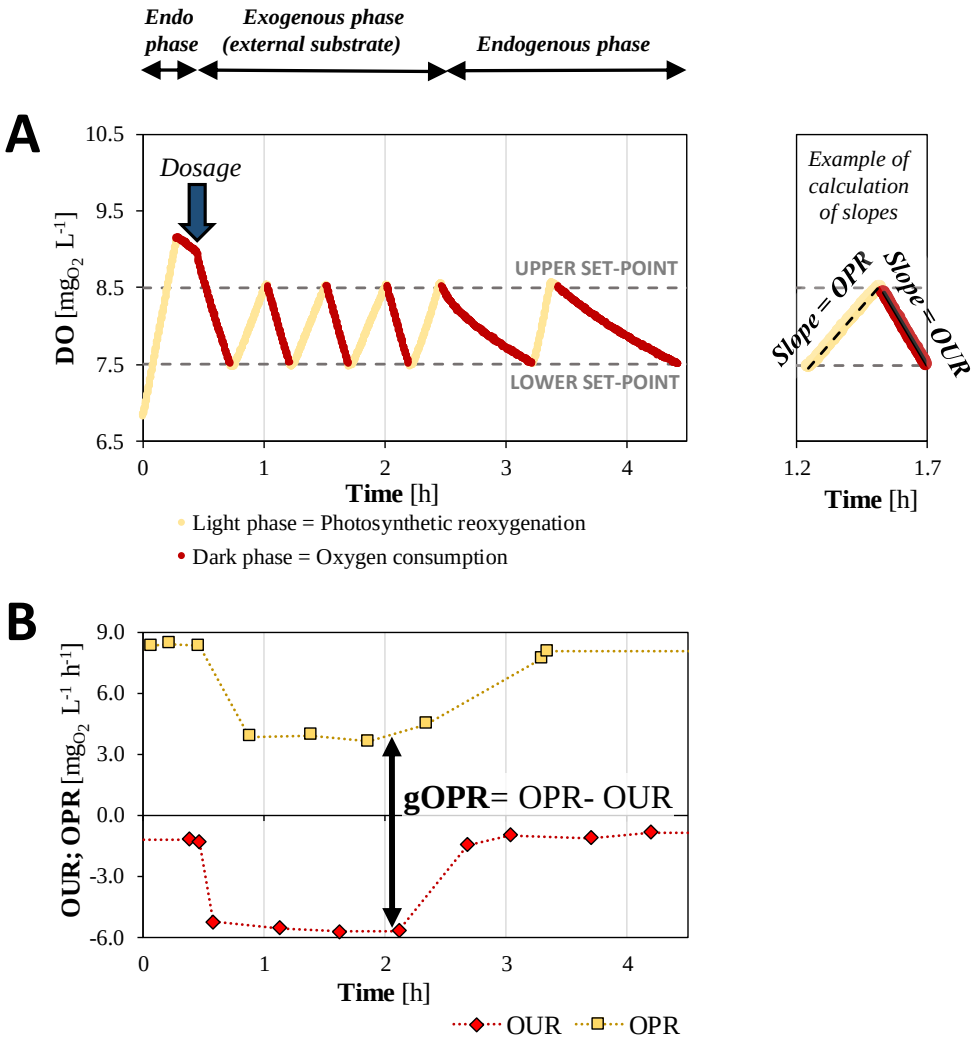

Figure 11.2 *Typical respirometric test that includes exogenous respiration (after the dosage of an external substrate) and endogenous respiration: (A) DO profile; (B) OUR in the dark and OPR in the light; the calculation of gOPR is indicated.*

11.2.5 OPR and OUR respirograms during endogenous and exogenous phases

OUR and OPR were measured as a function of time (t) for a duration of the test of several hours (Figure 11.2B). The profiles of OUR and OPR over time form respirograms. Endogenous phase (without external substrates) and exogenous phase (with external substrates) were investigated. As external substrates, the following aliquots of stock solutions were injected in the respirometer: (1) acetate (CH_3COO^-) at concentration of 5-10 g COD/L to simulate readily biodegradable COD; (2) ammonium chloride NH_4Cl at concentration of 1 g NH_4^+-N/L.
In the respirograms three phases can be distinguished:

1) the endogenous phase (in absence of external substrate), which corresponds to the basal activity of the consortium and gives the minimum OUR and maximum OPR (OUR_{endo}, OPR_{endo});
2) the exogenous phase. After the addition of an external substrate, the biological removal causes a rapid DO consumption. As a consequence, OUR increases depending on the biodegradation rate and at the same time OPR decreases due to the enhanced oxygen demand (Figure 11.2B);
3) the endogenous phase, when the external substrate is completely depleted; the consortium and thus the respirogram, returns to the minimum OUR values and the maximum OPR values (Figure 11.2B).

The oxygen uptake rate for substrate oxidation during the exogenous phase (OUR_{exo} in dark or light) can be calculated as the difference between OUR or OPR profiles and OUR_{endo} or OPR_{endo}, respectively, according to Eq. 11.2 and 11.3.

$$\text{(dark)} \qquad OUR_{exo,dark}(t) = OUR_{endo}(t) - OUR(t) \tag{11.2}$$

$$\text{(light)} \qquad OUR_{exo,light}(t) = OPR_{endo}(t) - OPR(t) \tag{11.3}$$

Specific values (SOPR and SOUR) per unit of TSS can be calculated by dividing OUR and OPR by the TSS concentration in the mixed liquor measured at the

beginning of each test.
For each substrate, the respirometric tests were repeated at least in triplicate.

11.2.6 Correction of the respirograms

11.2.6.1 De-oxygenation

When DO concentration exceeds saturation, a certain amount of oxygen may leave the liquid phase, stripping into the atmosphere. Therefore, in the case of supersaturation, OUR or OPR must be corrected by taking the oxygen transfer rate into account. In the respirometric tests reported in this study, the correction was not made because the DO concentration was maintained at values always below the saturation level.

11.2.6.2 Re-oxygenation

When OUR or OPR are too low, spontaneous re-oxygenation, which is the oxygen transfer from the atmosphere to the liquid phase, cannot be neglected and it can be favored by mixing. Re-oxygenation was estimated in the respirometer with an abiotic test carried out with sterilized biomass that ensured biological OPR and OUR equal to 0, but included the influence of solids density. In this way rising DO was solely due to the re-oxygenation (Figure 11.3A). The mass balance of oxygen was described as reported in Eq. 11.4, where C_s and C are the DO concentrations at saturation (experimental temperature = 20°C) and in the bulk liquid, respectively. The coefficient $k_L a$ is the overall volumetric gas-liquid mass transfer coefficient, and it was estimated following the log-deficit procedure as described in ASCE (ASCE, 1993; Figure 11.3B).

$$\frac{dC}{dt} = k_L a \cdot (C_s - C) \tag{11.4}$$

A value of 0.0059 min^{-1} was found in our research. Values in the same order of magnitude (0.0033 min^{-1}) were reported by Sforza et al. (2019), even if with different respirometers.

During the respirometric test, the variation of DO concentration in the microalgal-bacterial consortium was described with the Eq. 11.5 and 11.6 for dark and light conditions, respectively.

$$\text{(dark)} \qquad \frac{dC}{dt} = \underbrace{k_L a \cdot (C_s - C)}_{positive} + \underbrace{OUR}_{negative} \tag{11.5}$$

$$\text{(light)} \qquad \frac{dC}{dt} = \underbrace{k_L a \cdot (C_s - C)}_{positive} + \underbrace{OPR}_{positive} \tag{11.6}$$

From Eq. 11.5 and 11.6, it is clear that re-oxygenation causes underestimation of real OUR and overestimation of real OPR. The estimation of $k_L a$ made it possible to extrapolate the real biological DO consumption or production, which are OUR or OPR.

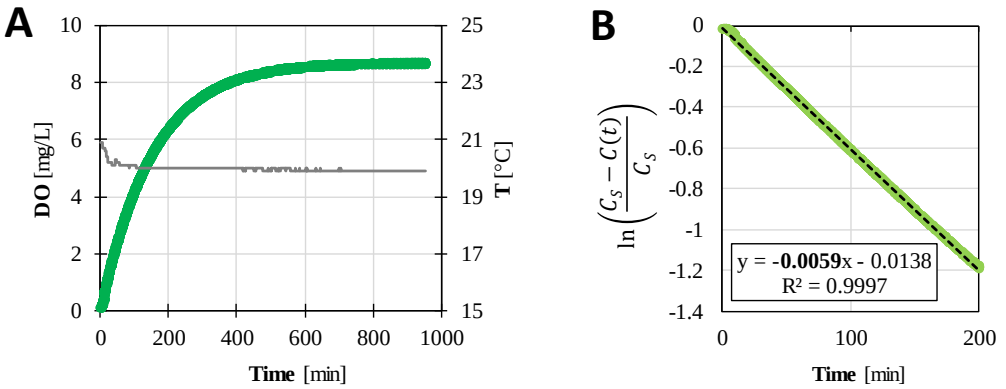

Figure 11.3 *(A) Re-oxygenation in the respirometer due to mixing, evaluated with sterilized biomass. (B) Estimation of $k_L a$ through linear regression*

11.2.6.3 Artificial oxygenation may be required

When the photosynthetic DO production rate is too slow to compensate the DO consumption by the biomass (that is OPR<<OUR), the time required for increasing DO concentration up to the upper set-point (see Figure 11.2A) may be too long. In this case, additional artificial aeration can help to supply the required oxygen. In our research, the microalgal-bacterial consortium did not

require artificial aeration since OPR resulted in the same order of magnitude of OUR.

11.2.7 Flow cytometry

The quantification of microalgae in the mixed consortium was performed by flow cytometry (FCM; model Apogee-A40 supplied by Apogee Flow System, UK)as described in Chapter 12. Briefly, this analysis allowed the rapid and automated detection of microbial cells at rate of several thousands of cells per minute, by acquiring two light scattering signals and three fluorescence signals. Microalgae were detected by exploiting the emitted red autofluorescence due to their natural pigments.
The FCM analysis was based on the following steps:

1) 20 mL of sample was placed in a beaker and diluted 1:5 v/v in Phosphate-Buffered-Saline (PBS, 3 g K_2HPO_4, 1 g KH_2PO_4 and 8.5 g NaCl L^{-1}; pH = 7.2);
2) disaggregation of the suspension to ensure the dispersion of cells using sonication at specific energy of 80 kJ/L;
3) further dilution 1:10 v/v with PBS;
4) filtration on 20-μm-membrane to eliminate coarse particles that could clog the nozzle of the flow cytometer;
5) analysis with FCM and absolute counts of photosynthetic organisms (red fluorescent). Finally, the concentration of cells was expressed per volume (cells/L) or per unit of TSS (cells/g TSS).

11.3 Results and Discussion

The mixed microalgal-bacterial consortium was a very complex community composed of microalgae, cyanobacteria, heterotrophic bacteria and nitrifying bacteria. Still not completely clear is the role of mixotrophic metabolism of photosynthetic microorganisms involved in wastewater treatment and their interactions with the bacteria. How mixotrophy depends on environmental

conditions is still largely unknown, as well as the relative kinetics (Sforza et al., 2019). When photosynthetic microorganisms exploit mixotrophy, a lower amount of oxygen may remain for heterotrophic bacteria and nitrifiers (Sforza et al., 2018). For these reasons, in our research, microalgae, cyanobacteria, heterotrophic bacteria and nitrifying bacteria were not studied as separate groups, and therefore the kinetics were measured for the whole biomass.
The microalgal-bacterial consortium was tested in the dark and in the light applying different metabolic conditions: (1) endogenous phase that occurs in absence of external substrates; (2) removal of readily biodegradable COD represented by acetate; (3) oxidation of ammonium (NH_4^+). The endogenous phase corresponds to the maintenance respiration that is the minimum of energy required for survival (Mantikci et al., 2017), while the exogenous phase regards the utilization of substrates for biosynthesis and thus for growth. In the next sections the results on OUR and OPR are described for all these metabolic conditions.

11.3.1 Endogenous condition (absence of external substrates)

During endogenous dark conditions, photosynthetic microorganisms catabolize internal metabolites accumulated from photosynthesis and heterotrophic bacteria utilize dissolved organic matter derived from the cellular lysis or originated previously from photosynthesis (Mantikci et al., 2017). In the absence of external substrates, it was assumed that the intracellular storage was depleted and the net growth of biomass did not occur. Respiration at zero growth has been termed “maintenance respiration” by Langdon (1998) for phototrophs, heterotrophs and nitrifiers.
Under endogenous conditions with light, only photosynthetic microorganisms grow because through photosynthesis they can use CO_2 as a carbon source, increasing DO at the same time.

Respirograms in the light - In the endogenous phase, OPR is maximum because oxygen is produced in surplus since it is consumed only for maintenance

respiration. An average OPR of 8.3±0.3 mg O_2 L^{-1} h^{-1} was measured at 90±5 μmol m^{-2} s^{-1} (Figure 11.4A), corresponding to a SOPR of 9.5±0.6 mg O_2 g TSS^{-1} h^{-1} (0.23 g O_2 g TSS^{-1} d^{-1} on a daily basis). This value depends on the light intensity used in this study, which was not optimized. It is worth noting that OPR expresses the photosynthetic rate and may rise remarkably at higher illumination (Béchet et al., 2013). SOPR indicated by Najm et al. (2017) in an algal membrane photobioreactor (pure *Chlorella vulgaris*) was 17.3 mg O_2 g $MLSS^{-1}$ h^{-1} under a light intensity of 135 μmol m^{-2} s^{-1}, which was higher than that used in our research. Thus, OPR of mixed microalgal-bacterial consortia depends on the intensity of light. To compare the results of different researches, the irradiance (or better the photosynthetic active radiation) applied in the measurement of OPR should be specified.
Decostere et al. (2014) highlighted that also the biomass concentration affects the maximum OPR. For *Chlorella vulgaris*, the maximum OPR was 1.9 and 4.8 mg O_2 L^{-1} h^{-1} in the case of low (0.1 g DW/L) and high (0.5 g DW/L) biomass concentration, respectively. The corresponding SOPR was thus 0.48 and 0.26 g O_2 g DW^{-1} d^{-1} for low and high biomass concentrations, respectively (Decostere et al., 2014). The reason why the specific photosynthetic activity was lower at higher biomass concentrations was the self-shading effect that occurs when the density increases. The SOPR of 0.23 g O_2 g TSS^{-1} d^{-1} found in the present study at TSS concentration of 0.9±0.1 g TSS/L was very similar to 0.26 g O_2 g DW^{-1} d^{-1} found by Decostere et al. (2014) at 0.5 g DW/L.

Respirograms in the dark - Endogenous OUR was in the range of 0.5±0.1 mg O_2 L^{-1} h^{-1} (Figure 11.4B). These values were in the same order of magnitude as those found by Ruiz-Martinez et al. (2016) for mixed culture of microalgae grown with urban effluent wastewater.
In agreement with the literature (Ruiz-Martines et al., 2016), the endogenous profile decreased over time (t) according to an exponential decay equation (Eq. 11.7).

$$OUR(t) = OUR_0 \cdot e^{-b \cdot t} \tag{11.7}$$

In Eq. 11.7 OUR_0 is the OUR at the beginning of the test, while the decay rate (b)

can be calculated from the slope of the line that interpolates the experimental points of OUR, plotted on a semi-logarithmic graph.

The decay rate for the tested microalgal-bacterial consortium was 0.018±0.003 d^{-1}, particularly small compared to the values measured in conventional activated sludge. In fact, in activated sludge b is 0.24 d^{-1} for heterotrophic bacteria and 0.04 d^{-1} for nitrifying bacteria (Henze et al., 2008). Instead, in microalgal consortia, very variable values of decay rate have been reported in the literature. Decostere et al. (2013) found a decay rate of 0.0096 d^{-1} (0.0004 h^{-1}) for *Chlorella vulgaris* cultivated in a growth medium (BG-11) while Ruiz-Martinez et al. (2016) measured values in the range of 0.12-0.43 d^{-1} (0.005-0.018 h^{-1}) for a microalgae culture mainly composed (>99%) of *Chlorococcales*, grown in a semi-continuous reactor fed with the effluent of a submerged anaerobic membrane bioreactor.

Tang et al. (2014) reported phototrophic decay coefficients of about 0.08 d^{-1} for *Microcystis aeruginosa* (cyanobacterium) and *Chlorella vulgaris* (microalgae) in axenic cultures. The wide differences in the decay rates reported for phototrophs (range of 0.003-0.1 d^{-1} cited by Decostere et al., 2013) may be due to different cultivation conditions (such as growth medium and retention time), short or prolonged respiration tests, metabolic conditions or intracellular storage that may have affected the maintenance respiration. Mantikci et al. (2017) demonstrated that the dark respiration rate of phytoplankton was a function of the intracellular carbon accumulated during previous photosynthetic activity, and thus of the light dose. These authors observed that, in the case of long periods in darkness, from several hours to days, the dark respiration rate of phytoplankton became constant, reaching the maintenance respiration rate. Low values of respiration permit the cell to stay viable for a longer time, and this is an adaptation that serves to survive prolonged dark periods.

The particularly slow decay rate measured in microalgae suggests that their biomass decreases slowly even in the absence of feeding, and this aspect may be positively exploited in PBRs to maintain an efficient biomass even in the case of sporadic feeding.

Comparison between light and dark conditions - Considering OPR of photosynthetic microorganisms under light conditions and OUR of the entire biomass in the dark, the gross photosynthesis rate (gOPR) in endogenous condition was calculated according to Eq. 11.1. The gOPR was 8.8±0.2 mg O_2 L^{-1} h^{-1} and corresponded to a specific value of 9.8±0.2 mg O_2 g TSS^{-1} h^{-1}. The gOPR was very similar to the net OPR because OUR contributed only 6% of gOPR. The gOPR value was associated with a microalgal concentration (measured by FCM) of 2.5×10^{10} cells/L and 2.7×10^{10} cells/g TSS. On the basis of this cell density, a per-cell gOPR of 350 fg O_2 $cell^{-1}$ h^{-1} was calculated. Tang et al. (2014) measured an oxygen production of 3.2 mg O_2/L after 20 min of light (at 50±5 μmol m^{-1} s^{-1}), that corresponded to 9.6 mg O_2 L^{-1} h^{-1}, in the presence of microalgae with a cell density of about 6-7$\times10^9$ cells/L. The per-cell OPR calculated by Tang et al. (2014) was 42±1 and 49±2 fmol O_2 $cell^{-1}$ h^{-1} for microalgae (*Chlorella vulgaris*) and cyanobacteria (*Microcystis aeruginosa*), respectively.
Considering the typical chlorophyll content of microalgal cells, the ideal OPR should be 25-400 fmolO_2 $cell^{-1}$ h^{-1} (Lee and Palsson, 1994). In our case, OPR was 11 fmol O_2 $cell^{-1}$ h^{-1}; this low value may have been due to limited light irradiance and self-shading of the biomass (composed of microalgae and bacteria).

11.3.2 Kinetics with readily biodegradable COD

The respirograms obtained in one of the three respirometric tests with the addition of readily biodegradable COD (acetate) are shown in Figure 11.5, in which the profiles of OPR (in the light, Figure 11.5A) and OUR (in the dark, Figure 11.5B) are compared.

Respirograms in the light - At the beginning of the test, under endogenous conditions, the OPR was maximum. In the respirometric test of Figure 11.5A, the OPR_{endo} had values of 7.4±0.2 mg O_2 L^{-1} h^{-1}. These high values were associated with high photosynthetic capacity (Mantikci et al., 2017). After COD dosage, the OPR decreased due to the increased oxygen demand for the substrate removal that consumed most of the oxygen produced by photosynthesis. The OPR decreased to 1.0±0.4 mg O_2 L^{-1} h^{-1} with a reduction of about 86%. When COD

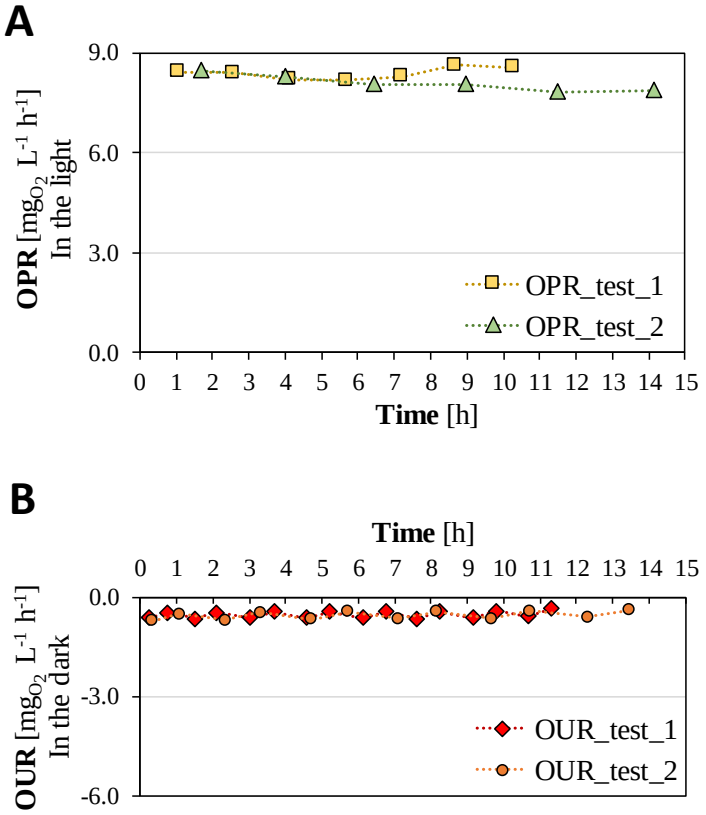

Figure 11.4 *Respirometric tests in endogenous conditions: (A) OPR in the light; (B) OUR in the dark.*

was completely depleted, the system did not require such an amount of oxygen, and OPR increased, returning to the higher endogenous OPR values. Figure 11.5A shows: (1) the endogenous OPR interpolation, where values of OPR_{endo} are at the maximum level due to the scant oxygen demand and (2) the reduction of OPR due to COD oxidation, called $OUR_{exo,COD,light}$, which was calculated according to Eq. 11.3. In the test shown in Figure 11.5, $OUR_{exo,COD,light}$ was 6.5±0.4 mg O_2 L^{-1} h^{-1}.

Respirograms in the dark - In the test shown in Figure 11.5 the endogenous OUR (OUR_{endo}) was initially of about 0.6±0.1 mg O_2 L^{-1} h^{-1} (negative values in Figure 11.5B). In this phase, the external substrates and thus growth were

absent; hence, oxygen was used for maintenance respiration. Then the COD dosage caused an increase of OUR for the oxidation of the substrate. OUR reached a plateau of about 8.3±0.5 mg O_2 L^{-1} h^{-1} on average. When COD was completely depleted, exogenous respiration stopped and OUR returned gradually to the endogenous level. Figure 11.5B shows: (1) the endogenous OUR interpolation, associated with the maintenance respiration of photosynthetic microorganisms and bacteria, also called "dark respiration" where values of OUR_{endo} are at the minimum level, and (2) the exogenous OUR due to COD oxidation, called $OUR_{exo,COD,dark}$, which was calculated according to Eq. 11.2. In the test of Figure 11.5, $OUR_{exo,COD,dark}$ was 7.8±0.5 mg O_2 L^{-1} h^{-1}.

Comparison between light and dark conditions - $OUR_{exo,COD,light}$ and $OUR_{exo,COD,dark}$ are compared in Figure 11.5C. Although OUR is mainly attributed to heterotrophic bacteria, which are largely responsible for COD oxidation in the light and in the dark, heterotrophs are not the only responsible for oxygen consumption. The slightly higher $OUR_{exo,COD,dark}$ (7.8±0.5 mg O_2 L^{-1} h^{-1}) with respect to $OUR_{exo,COD,light}$ (6.5±0.4 mg O_2 L^{-1} h^{-1}) may be associated with two aspects: (1) mixotrophic metabolism of microalgae and/or (2) mitochondrial respiration of eukaryotic microalgae. Although microalgae have mainly an autotrophic metabolism, under dark they can assimilate carbonaceous substrates thanks to a mixotrophic metabolism (Liu et al., 2018; Sforza et al., 2018). This effect may increase the OUR during the dark period, as a consequence of the additional microalgal oxygen consumption. Mitochondrial respiration is a mechanism that enables cells to utilize oxygen to produce energy for a limited period in the dark (Kliphuis et al., 2011). Photorespiration is another mechanism that may affect OUR (Xie et al., 2016; Checchin et al., 2018), but it occurs only above oxygen saturation (around 9 mg O_2/L at the temperature and pressure of our tests).

With regard to specific values (per unit of TSS), in the test shown in Figure 11.5, $SOUR_{exo,COD,dark}$ was 8.6±0.5 mg O_2 g TSS^{-1} h^{-1} and $SOUR_{exo,COD,light}$ was 7.2±0.4 mg O_2 g TSS^{-1} h^{-1}.

The gross photosynthesis rate (gOPR), which is the net photosynthesis rate

plus the dark respiration rate according to Eq. 11.1, is shown in Figure 11.5D. The profile increased slightly after the COD dosage. This may have been due to the limited availability of CO_2 during the endogenous phase while the COD oxidation may have contributed to supplying CO_2 that increased the rate of photosynthesis (in other words, the OPR). However, this speculation needs further experimentation to confirm and explain the variations of gOPR.

Kinetic and stoichiometric parameters - The kinetic parameters under light and dark, and the stoichiometric constant Y_{COD} were measured in triplicate with COD dosages of 40 or 80 mg COD/L. The results are summarized in Table 11.3.

The biomass yield (Y_{COD}) is an adimensional stoichiometric parameter that accounts for the fraction of COD that is synthesized in biomass. Conversely, 1-Y_{COD} accounts for the fraction converted into CO_2. Y_{COD} can be estimated using the expression of Eq. 11.8 (Henze et al., 2008), where ΔCOD is the removed COD (equal to the added readily biodegradable substrate, 40 or 80 mg COD/L), and the mass of oxygen consumed for COD oxidation (ΔO_2) is the integral of the entire exogenous respirogram, including both dark and light phases.

$$Y_{COD} = 1 - \frac{\Delta O_2}{\Delta COD} \tag{11.8}$$

The parameter Y_{COD} was estimated in triplicate (Table 11.3) and proved to be 0.66±0.04 on average. This confirms that the mixed microalgal-bacterial consortium had a stoichiometric parameter perfectly in agreement with the typical value of 0.67 for conventional activated sludge (Henze et al., 2008). Instead, the biomass/carbon yield of microalgae, which is the ratio of organic carbon that is actually fixed in the biomass, was measured by Sforza et al. (2018) using acetate as organic carbon source and a value of 0.78 g C/g C (adimensional) was found for *Chlorella*.

The specific COD oxidation rate (υ_{COD}, expressed as mg COD g TSS^{-1} h^{-1}) was calculated from the exogenous SOUR in the light and in the dark, following Eq. 11.9 and 11.10, respectively.

$$\upsilon_{COD,light} = \frac{SOUR_{exo,COD,light}}{1 - Y_{COD}} \tag{11.9}$$

$$v_{COD,dark} = \frac{SOUR_{exo,COD,dark}}{1 - Y_{COD}} \tag{11.10}$$

The kinetic parameter v_{COD} at 20°C was 19.3±4.8 mg COD g TSS^{-1} h^{-1} on average in the dark, slightly higher than 18.0±4.0 mg COD g TSS^{-1} h^{-1} in the light (Table 11.3).

In the design of PBRs, $v_{COD,light}$ can be assumed for daily hours (for example 12 h/d); instead, COD removal in the dark is only possible when the DO concentration in the bulk liquid is available. Therefore $v_{COD,dark}$ can be assumed only for a couple of hours at the beginning of the night. In the dark, in the absence of photosynthesis, DO undergoes a rapid consumption and when it drops to zero, the oxidation of COD cannot be further supported.

Parameters	**Units**	**Test**			**Avg ± st.dev.**
		1	**2**	**3**	
TSS	[g TSS/L]	1.06	0.88	0.9	**0.89±0.01**
Y_{COD}	[-]	0.7	0.63	0.66	**0.66±0.04**
Kinetics in the light					
$OUR_{exo,COD,light}$	[mg O_2 L^{-1} h^{-1}]	6.2	4.4	6.5	**5.7±1.1**
$SOUR_{exo,COD,light}$	[mg O_2 g TSS^{-1} h^{-1}]	5.8	5	7.2	**6.0±1.1**
$v_{COD,light}$	[mg COD g TSS^{-1} h^{-1}]	19.3	13.5	21.2	**18.0±4.0**
Kinetics in the dark					
$OUR_{exo,COD,dark}$	[mg O_2 L^{-1} h^{-1}]	5.9	5.2	7.8	**6.3±1.3**
$SOUR_{exo,COD,dark}$	[mg O_2 g TSS^{-1} h^{-1}]	5.6	5.9	8.6	**6.7±1.6**
$v_{COD,dark}$	[mg COD g TSS^{-1} h^{-1}]	18.6	15.9	25.3	**19.3±4.8**

Table 11.3 *Kinetic parameters at 20° C in the light and in the dark and the biomass yield (Y_{COD}) of the microalgal-bacterial consortium tested with readily biodegradable COD.*

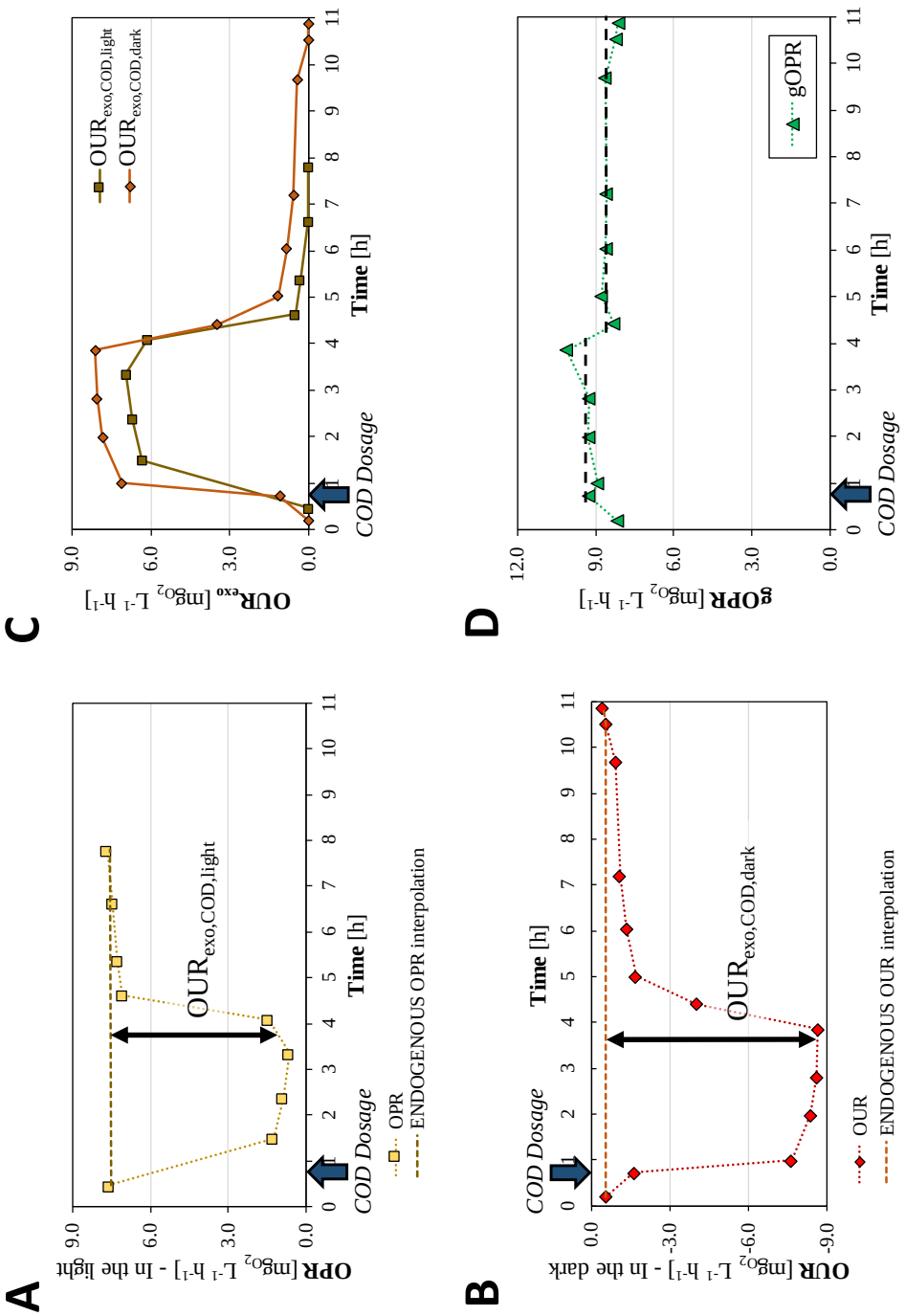

Figure 11.5 *Respirometric test with readily biodegradable COD: (A) OPR in the light; (B) OUR in the dark; (C) comparison between $OUR_{exo,COD,light}$ and $OUR_{exo,COD,dark}$ during the exogenous phase; (D) profile of the gross photosynthesis rate (gOPR).*

11.3.3 Kinetics with ammonium nitrogen (NH_4^+)

The respirometric tests were carried out in the presence of ammonium, but without external carbon substrates and thus with no net heterotrophic growth. Therefore, the uptake of ammonium by heterotrophic bacteria for their synthesis was negligible.
Nitrifiers oxidize ammonium to nitrate but require a supply of oxygen. In microalgal-bacterial consortia for wastewater treatment, the required oxygen may be supplied by photosynthesis (Vargas et al., 2016) thanks to the symbiotic coexistence of photosynthetic microorganisms and bacteria. Moreover, photosynthetic microorganisms can use ammonium for their growth. In particular, ammonium is preferred to nitrate as a nitrogen source for the growth of microalgae and cyanobacteria (Tang et al., 2014).
The respirograms obtained in one of the three respirometric tests after spiking with NH_4^+ are shown in Figure 11.6, where the profiles of OPR (in the light, Figure 11.6A) and OUR (in the dark, Figure 11.6B) are compared.

Respirograms in the light - In the respirometric test of Figure 11.6A, the addition of ammonium caused an immediate reduction of OPR from the maximum value of 9.0±0.4 mg O_2 L^{-1} h^{-1} to a plateau of 6.4±0.1 mg O_2 L^{-1} h^{-1}. When OPR returned to the maximum endogenous OPR, it meant that ammonium removal was completed. Figure 11.6A shows: (1) the endogenous OPR interpolation and (2) the reduction of OPR for ammonium oxidation ($OUR_{exo,NH,light}$), calculated according to Eq. 11.3, which was 2.6±0.1 mg O_2 L^{-1} h^{-1}.

Respirograms in the dark - In Figure 11.6B, the initial endogenous OUR was 0.6±0.1 mg O_2 L^{-1} h^{-1}. After spiking with ammonium, the oxygen demand increased and OUR reached a plateau of 3.9±0.2 mg O_2 L^{-1} h^{-1}. When ammonium was depleted, the profile returned to endogenous OUR values. Figure 11.6B shows: (1) the endogenous OUR interpolation and (2) the exogenous OUR for ammonium oxidation, called $OUR_{exo,NH,dark}$, which was 3.3±0.1 mg O_2 L^{-1} h^{-1} (according to Eq. 11.2).

Comparison between light and dark conditions - Figure 11.6C shows the

comparison between $OUR_{exo,NH,light}$ and $OUR_{exo,NH,dark}$. In the respirograms the values of the plateau differed significantly in the dark or light: $OUR_{exo,NH,light}$ was 2.6±0.1 mg O_2 L^{-1} h^{-1}, significantly lower than 3.3±0.1 mg O_2 L^{-1} h^{-1} in the dark ($OUR_{exo,NH,dark}$), indicating 21% of reduction.
Vergara et al. (2016) investigated with respirometry the influence of light on ammonium oxidation in PBRs, and no significant effects were observed for irradiances below 250 μmol m^{-2} s^{-1}. Due to the moderate irradiance used in the present study (90±5 μmol m^{-2} s^{-1}), the occurrence of photoinhibition of nitrifiers was excluded. Choi et al. (2010) reported that phototrophic microbial growth inhibited the maximum nitrification rate. In particular, in the presence of microalgae (*Chlorella emersonii*) and an uncultured cyanobacterium, the maximum specific OUR measured after the addition of ammonium was reduced by 77% (Choi et al., 2010). Although the nitrifying bacterial community remained constant, the presence of the phototrophic species caused a reduction of nitrifying activity by a factor of 4 (Choi et al., 2010). Choi et al. (2010) concluded that the cause of nitrification inhibition by microalgae and cyanobacteria could be competition for carbon dioxide and NH_4^+ used by both nitrifiers and microalgae. Further research is needed to investigate the interaction between microalgae and nitrification.
With regard to specific values (per unit of TSS), in the test of Figure 11.6, $SOUR_{exo,NH,light}$ was 2.8±0.1 mg O_2 g TSS^{-1} h^{-1} and $SOUR_{exo,NH,dark}$ was 3.6±0.1 mg O_2 TSS^{-1} h^{-1}. These values were approximately half of that found by Rossi et al. (2018) who measured 5.4-7.5 mg O_2 g TSS^{-1} h^{-1}. However, Rossi et al. (2018) used the wastewater coming from an anaerobic process characterized by high ammonium concentration and recalcitrant organics that may have favored the enrichment of nitrifiers in the biomass.

Kinetic and stoichiometric parameters - From the exogenous OUR under light and dark conditions, the kinetic of ammonium oxidation and the stoichiometric coefficient $f_{O_2/NH}$ were calculated in triplicate with dosages of 3 or 6 mg NH_4^+-N/L. The results are shown in Table 11.4.
The oxygen-over-ammonium coefficient ($f_{O_2/NH}$) is given by Eq. 11.11, which

derives from the stoichiometric redox reaction of ammonium oxidation, where ΔNH_4 is the amount of ammonium added and removed in the test and the amount of oxygen utilized (ΔO_2) is the integral under the entire exogenous OUR profile.

$$f_{O_2/NH} = \frac{\Delta O_2}{\Delta NH_4} \tag{11.11}$$

The average $f_{O_2/NH}$ was 2.8±0.3 g O_2/g N in the light and 4.4±0.5 g O_2/g N in the dark.

In the dark, when the photosynthetic activity was absent, $f_{O_2/NH}$ was similar to the values (4.16 or 4.6 g O_2/g N) typically assumed for bacterial nitrification in activated sludge (Tchobanoglous et al., 2003; Henze et al., 2008; Vargas et al., 2016). Vargas et al. (2016) indicated a theoretical yield of 0.281 g NH_4^+/g O_2 for nitrifying bacteria (corresponding to 4.6 g O_2/g NH_4^+-N) in mixed cultures of microalgae and nitrifiers. Instead, the low $f_{O_2/NH}$ found in the light (2.8±0.3 g O_2/g N) may have been due to the growth of photosynthetic microorganisms that subtracted ammonium, resulting in a smaller amount of oxygen required for nitrification.

The specific nitrification rate (υ_{NH}, expressed as mg NH_4^+-N g TSS^{-1} h^{-1}) was calculated in the dark from the exogenous SOUR following Eq. 11.12.

$$\upsilon_{NH} = \frac{SOUR_{exo,NH,dark}}{f_{O_2/NH}} \tag{11.12}$$

The nitrification rate υ_{NH} at 20°C was 0.92±0.14 mg NH_4^+-N g TSS^{-1} h^{-1} on average. This value was very similar to the ammonium removal rate measured in the light (0.91±0.07, Table 11.4) that includes simultaneously both nitrification and phototrophic synthesis.

Taking the ratio VSS/TSS of 0.88 for the microalgal-bacterial consortium into account, an average υ_{NH} of 1.04 mg NH_4^+-N g VSS^{-1} h^{-1} was calculated. Vargas et al. (2016) measured the ammonium removal rate of microalgae and nitrifying bacteria and found values of 0.83 and 2.1 mg NH_4^+ g VSS^{-1} h^{-1}, respectively.

Parameters	**Units**	**Test**			**Avg ± st.dev.**
		1	**2**	**3**	
TSS	[g TSS/L]	0.89	0.8	0.93	**0.87±0.07**
Kinetics in the light					
$OUR_{exo,NH,light}$	[mg O_2 L^{-1} h^{-1}]	2.1	2.2	2.6	**2.3±0.3**
$SOUR_{exo,NH,light}$	[mg O_2 g TSS^{-1} h^{-1}]	2.4	2.7	2.8	**2.6±0.2**
$f_{O_2/NH}$	[mg O_2/ mg NH_4^+-N]	2.5	2.9	3.1	**2.8±0.3**
v_{NH}*	[mg NH_4^+-N g TSS^{-1} h^{-1}]	0.96	0.93	0.83	**0.91±0.07**
Kinetics in the dark					
$OUR_{exo,NH,dark}$	[mg O_2 L^{-1} h^{-1}]	3.8	3.2	3.3	**3.5±0.3**
$SOUR_{exo,NH,dark}$	[mg O_2 g TSS^{-1} h^{-1}]	4.3	4	3.7	**4.0±0.3**
$f_{O_2/NH}$	[mg O_2/ mg NH_4^+-N]	4	5	4.2	**4.4±0.5**
v_{NH}	[mg NH_4^+-N g TSS^{-1} h^{-1}]	1.07	0.8	0.88	**0.92±0.14**

* In the light, v_{NH} is the ammonium removal rate and includes simultaneously nitrification and phototrophic synthesis.

Table 11.4 *Kinetic parameters at 20°C and the coefficient $f_{O_2/NH}$ in the light and in the dark of the microalgal-bacterial consortium tested with NH_4^+-N.*

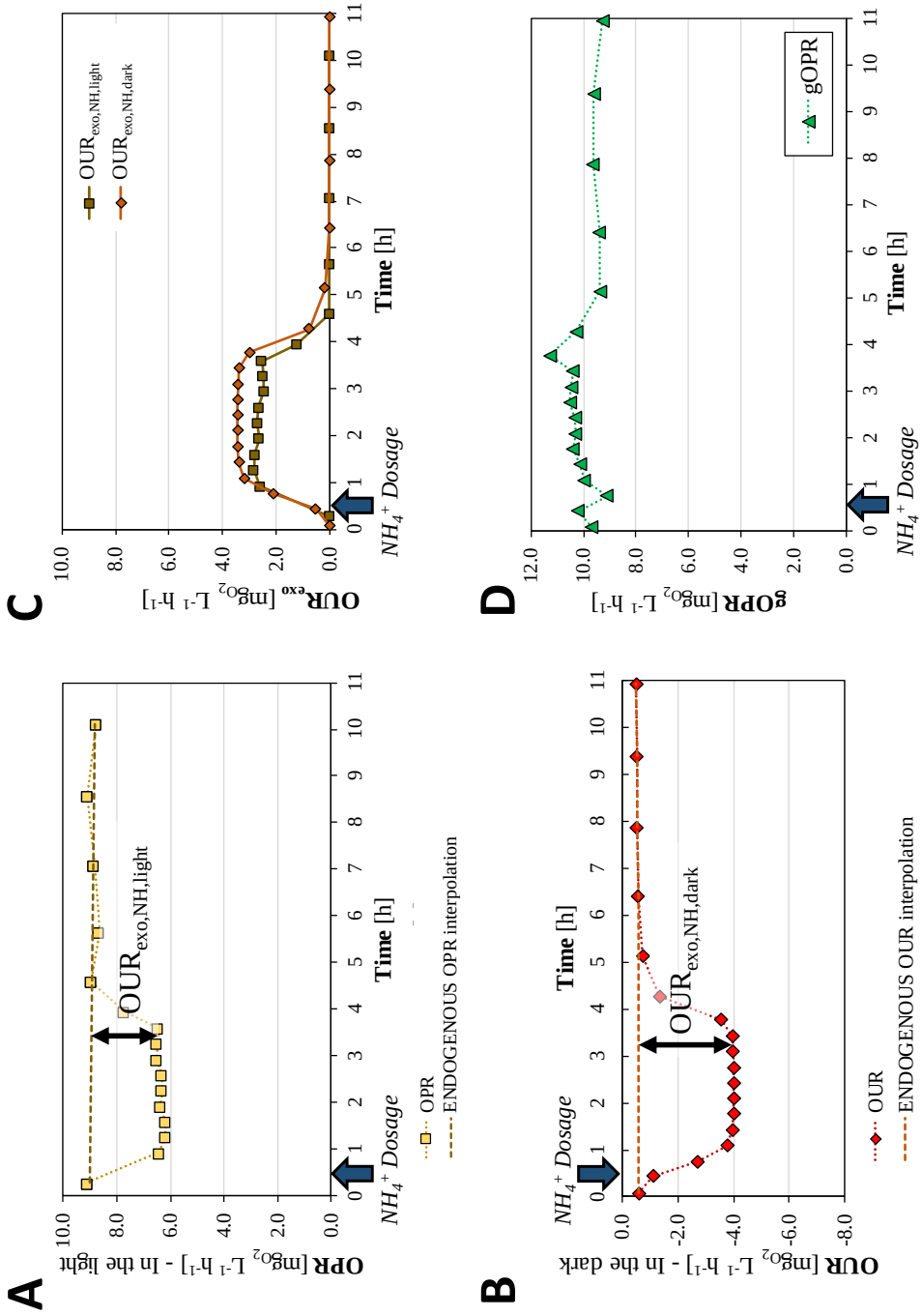

Figure 11.6 *Respirometric test with NH_4^+: (A) OPR in the light; (B) OUR in the dark; (C) comparison between $OUR_{exo,NH,light}$ and $OUR_{exo,NH,dark}$ during the exogenous phase; (D) profile of the gross photosynthesis rate (gOPR).*

11.4 Conclusion

This study has proposed a comprehensive respirometric protocol to characterize the kinetic parameters of microalgal-bacterial consortia treating wastewater.

A consortium, developed in a stable PBR for 2 years, was investigated in endogenous and exogenous conditions, in the presence of readily biodegradable COD and ammonium, separately, under light and dark conditions.

The gross photosynthesis rate (gOPR) was 9.8±0.2 mg O_2 g TSS^{-1} h^{-1}, which corresponded to 11 fmol O_2 $cell^{-1}$ h^{-1} for each microalgal cell. The entire consortium had a very low specific endogenous respiration, which was 0.6±0.1 mg O_2 g TSS^{-1} h^{-1}. At 20°C, in the light and in the dark, the specific COD oxidation rate was 18.0 and 19.3 mg COD g TSS^{-1} h^{-1}, respectively. In the presence of ammonium, the nitrification rate measured in the dark was 0.92±0.14 mg NH_4^+-N g TSS^{-1} h^{-1}.

Respirometry highlighted that gOPR was just barely enough to cover the sum of the SOUR for endogenous respiration, COD oxidation and ammonium oxidation (0.6, 6.7 and 2.6 mg O_2 g TSS^{-1} h^{-1}, respectively). This suggests that in the microalgal-bacterial consortia the availability of oxygen may be limited when treating real municipal wastewater since it contains various compounds to oxidize.

In conclusion, the respirometric approach proposed in this paper may make an additional contribution to the investigation of microalgal-bacterial consortia treating wastewater, adding new information useful in the design of PBRs.

Acknowledgements

The authors would like to thank Laura Bruni (Agenzia per la Depurazione, Provincia Autonoma di Trento, Trento, Italy) for the collaboration in flow cytometric analysis.

CHAPTER 12

ANALYSIS AND QUANTIFICATION OF MICROALGAL-BACTERIAL CONSORTIA USING FLOW CYTOMETRY

In this Chapter the composition of the microalgal-bacterial consortium in the Pilot (Chapter 6) was analyzed with flow cytometry (FCM).

The feasibility of FCM to analyze qualitatively and quantitatively microalgal-bacterial consortia was proved. A multi-step procedure of sample preparation was developed to ensure the accuracy of the FCM analysis. Fluorescent and scattering signals were discussed and interpreted to distinguish and quantify microalgae and bacteria.
The FCM approach proposed represents a valuable tool to enhance the knowledge about the composition and the quantification of microalgal-bacterial consortia, and could be included in monitoring procedures of photobioreactors.

This research was made in collaboration with Agenzia per la Depurazione (ADEP) - Autonomous Province of Trento

This Chapter is based on:
Foladori P., Petrini S., Bruni L., Andreottola G. *Bacteria and photosynthetic cells in a photobioreactor treating real municipal wastewater: analysis and quantification using flow cytometry.* Algal Research, UNDER REVIEW.

Abstract

Wastewater born microalgal-bacterial consortia in closed photobioreactors (PBRs) have demonstrated high efficiency in pollutant removal, relying only on photosynthetic oxygenation. However, their qualitative and quantitative composition is still poorly understood.

In this paper, flow cytometry was extended to analyze a microalgal-bacterial consortium developed in a long-term PBR treating real municipal wastewater. A multi-step procedure was proposed to ensure the accuracy of the FCM analysis. Ultrasonication at specific applied energy of 90 kJ L^{-1} was identified as optimal for sample pre-treatment to recover the maximum number of bacteria and photosynthetic cells while avoiding their disruption. Fluorescent and scattering signals were used to distinguish and quantify microalgae and bacteria.

In the tested consortium, bacteria (marked green with SYBR-Green I) were 98% of total cells (on average 1.2E+12 cells/L) while microalgae (having red autofluorescence) accounted for only 2% of total cells (2.8E+10 cells/L). Microalgae were characterized by a biovolume 2 orders of magnitude larger than bacteria, resulting in a photosynthetic biomass quantitatively comparable to bacteria.

The proposed FCM approach represents a valuable tool with which to enhance knowledge about the composition and quantification of microorganisms in PBRs, which have not yet been fully understood.

12.1 Introduction

The treatment of municipal and industrial wastewater based on microalgal-bacterial consortia represents a promising sustainable solution to activated sludge. Microalgal photosynthesis represents a cost-effective means with which to produce the oxygen to support bacterial activity and at the same time sequestering the CO_2 produced by bacterial oxidation (Kang et al., 2018).

In the last years, microalgal-bacterial consortia have proved to be effective in the treatment of different types of wastewater without artificial aeration (Cai et al., 2013; Arcila and Buitrón, 2016; Wang Y. et al., 2016; Lee and Lei, 2019). Good removal efficiency of pollutants from municipal wastewater has been demon-

strated at a lab- and pilot-scale in closed photobioreactors (PBRs) (Gutzeit et al., 2005; Su et al., 2011; Ye et al., 2018b), usually operated as photo-sequencing batch reactors (Arcila and Buitrón, 2016; Wang L. et al., 2016). However, this technology is in its early stage of development (Molinuevo-Salces et al., 2019) and still little is known about the composition of consortia that naturally develop when treating real wastewater (Arango et al., 2016; Cho et al., 2017; He et al., 2013; Kang et al., 2018; Tsioptsias et al., 2016). The monitoring of the proportion of microorganisms in the consortia may be useful for interpreting changes in biomass characteristics (Luo et al., 2018) depending on design or operational conditions.

Microalgal-bacterial consortia are complex microcosms that consist of various eukaryotic microalgae and cyanobacteria coexisting with a large variety of bacteria, extracellular polymeric substances, colloids and inerts, embedded in flocs or granules (Su et al., 2011; Quijano et al., 2017; Chapter 6). Although several approaches have been applied to characterize these mixed communities in terms of concentration and abundance of different microorganisms, they remain only poorly understood. Microalgal-bacterial consortia have been characterized by means of physical, chemical or biological approaches (Perera et al., 2019).

Physical-chemical methods to assess biomass concentration, such as suspended solids and optical density measurements, permit only a gross estimation of biomass because inert and abiotic matter are included in the result. In addition, optical density and chlorophyll content only allow the estimation of photosynthetically active microorganisms, while bacteria cannot be detected.

Biological approaches that can be implemented without cultivation (such as epifluorescence microscopy, fluorescent-in-situ-hybridization, flow cytometry or metagenomics), provide more detailed information about the composition of the biomass.

Among these approaches, microscopy is a time-consuming and low-resolution analysis, especially when the quantification of abundance, size and biovolume of the microorganisms is required. Specific microbial groups can be identified

with high sensitivity and specificity, using fluorescent in situ hybridization (FISH) through rRNA-targeted fluorescently labelled oligonucleotide probes. However, the quantification of stained cells proves difficult in complex and dense aggregates such as microalgal-bacterial consortia.
Flow cytometry (FCM) is a powerful multi-parametric analysis that acquire light scattering and fluorescence of suspended particles when passing through a laser beam (Section Supplementary).
FCM has gained increasing attention in environmental microbiology and in the water sector (Safford and Bischel, 2019) thanks to its accuracy and also to the short analysis time. FCM can quantify 10^4-10^5 cells at a rate of 100-1000 cells per second with high accuracy and precision in the enumeration (Porter et al., 1997; Steen, 2000; Tracy et al., 2010) providing statistically representative results (Foladori et al., 2010b). FCM is suited to the analysis of photosynthetic microorganisms because they contain natural fluorescent pigments, such as chlorophylls and phycobilins (Peniuk et al., 2016), easily detectable as strong red or orange fluorescence without using fluorescent dyes (Hyka et al., 2013).
Compared to the '-Omics' approach, FCM analysis does not yield that deep level of species-specific information. However FCM is cheaper, faster and easier in the application, retrieving useful quantitative and qualitative data.

Since the 1990s, FCM has been widely applied in marine and aquatic microbiology to study phytoplankton (Sosik and Olson, 2007; Yentsch and Yentsch, 2008). Recently, FCM has been extended to microalgae cultures (Hyka et al., 2013; Peniuk et al., 2016; López-Rosales et al., 2016). However, there are few examples of FCM applied to microalgal consortia (Marchão et al., 2018) and microalgal-bacterial consortia, in particular treating synthetic wastewater (Vasseur et al., 2012; Luo et al., 2018).
For the simultaneous detection of microalgae and bacteria with FCM, Vasseur et al. (2012) exploited the red autofluorescence of photosynthetic cells and the green fluorescence of bacteria stained with SYBR-Green I. Luo et al. (2018) characterized the biomass composition and cell viability of a microalgal-bacterial consortium developed in a membrane PBR; before FCM analysis, samples were

pretreated by disaggregation with sonication for 5 minutes at 20 kHz (Luo et al., 2018). Vargas et al. (2016) measured with FCM the relative percentage of nitrifying bacteria and microalgae treating nitrogen-rich wastewater. However, no details about sample pretreatment were provided.
To the best of the authors' knowledge, an optimized FCM method to analyze the composition of a microalgal-bacterial consortia treating real wastewater has not yet been proposed.

FCM analysis needs a suspension of single cells and thus flocs or granules must be pre-treated properly (Hyka et al., 2013). However, biomass disaggregation should not cause cell damage. A suitable pre-treatment is represented by ultrasonication.
Ultrasonication covers a large variety of applications such as pre-treatment to disaggregate various matrices from food, to environment, to industry. Acoustic cavitation produced by sonication consists in the formation and collapse of microbubbles associated with extreme temperature and strong pressure gradients (Hua and Thompson, 2000; Gogate, 2002). The applied ultrasonic energy affects aggregate dispersion, microbial integrity and disruption. Investigations on microorganisms disaggregation have focused mainly on pure strains of bacteria or yeast while studies on mixed populations coexisting in complex matrices such as sludge or wastewater are rare (Falcioni et al., 2006). Therefore, further research is needed to optimize pretreatments to disaggregate complex consortia of microorganisms prior to FCM analysis. An effective pretreatment should make it possible to disperse the highest number of free cells in the bulk liquid but with a minimal risk of cell damage.

In this Chapter, for the first time FCM was extended to analyze a microalgal-bacterial consortium developed in a long-term PBR treating real wastewater (Chapter 6). In order to gain better understanding of the composition of these systems, the potential of FCM as a tool to quantify the absolute abundance of microalgae and bacteria was demonstrated.
A rigorous multi-step procedure easy to be applied, was proposed to ensure the accuracy of the FCM analysis. Pretreatment of samples with ultrasonication

was investigated in depth. Ultrasonication was optimized to disaggregate and disperse microalgal and bacterial in the bulk liquid, avoiding their disruption. The fluorescent and scattering signals recorded were used to distinguish and quantify microalgae and bacteria.

The FCM approach proposed is a valuable tool with to enhance knowledge about the composition and the quantification of microalgal-bacterial consortia since reliable procedures are still extremely scarce in the literature. FCM analysis could be applied as a monitoring method, improving knowledge about PBRs, which are in the early stage of development.

12.2 Materials and Methods

12.2.1 Outline of the FCM procedure

The entire FCM procedure is presented in Figure 12.1 while each step is described in detail from Section 12.2.2 to Section 12.2.6.
Briefly, the procedure comprises dilution, the pre-treatment of samples to disaggregate biomass flocs, and filtration prior to FCM analysis. Disaggregation was performed using ultrasonication (see Section 12.2.4), which has been widely applied in the literature to disperse coarse aggregates but has not yet been optimized for microalgal-bacterial consortia. The filtration at 20 μm was applied to prevent clogging in the nozzle of the flow cytometer. For FCM analysis, two aliquots were distinguished: (1) one aliquot was analyzed without staining in order to identify the number of autofluorescent cells (microalgae), and (2) a second aliquot was stained with SYBR-Green I to identify all microorganisms included (microalgae and bacteria). Comparing the number of cells in aliquots (1) and (2), the concentrations of microalgae and bacteria were estimated separately.

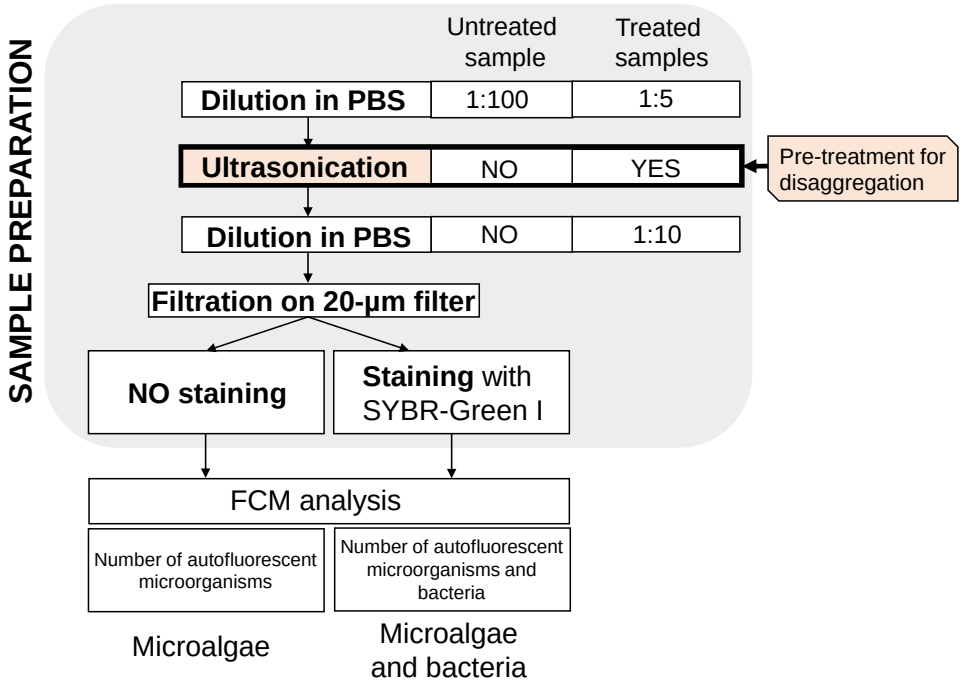

Figure 12.1 *Experimental procedure for the pre-treatment and the FCM analysis of the microalgal-bacterial consortium. PBS: Phosphate-Buffered-Saline solution*

12.2.2 Microalgal-bacterial consortium

The tested microalgal-bacterial consortium was collected from a lab-scale PBR operated as a sequencing batch reactor for more than two years. The operating condition has been described in a Chapter 6. The PBR was fed with real municipal wastewater collected after primary sedimentation at the full-scale WWTP of Trento Nord (Italy). Over the entire operating period the PBR guaranteed stable treatment removal performances and good effluent quality. The characterization of the influent and effluent wastewater is reported in Table 12.1.

Samples of mixed liquor (i.e. microalgal-bacterial consortium) were collected from the PBR for FCM analysis and processed within 1-2 h. Biomass concentration of the samples, measured as TSS (Total Suspended solids), was on average 2.2±0.2 g TSS/L. All the physical-chemical analyses indicated in Table 12.1

Parameter	**Influent real wastewater** [mg/L]	**Effluent** [mg/L]	**Removal efficiency** [%]
COD	258±163	68±9	66±17
TSS	119±102	40±46	65±30
NH_4^+-N	47.4±16.1	0.5±0.7	99±2
TN	55±21	16±8	69±17
TP	5.3±2.3	3.3±0.9	31±23

Table 12.1 *Influent and effluent wastewater and removal efficiency of the PBR (avg ± st.dev.). COD: Chemical Oxygen Demand; TSS: Total Suspended Solids; TN: Total Nitrogen; TP: Total Phosphorous.*

were conducted according to Standard Methods (APHA, 2012).

12.2.3 Sample preparation prior to FCM analysis

The samples were first diluted 1:5 v/v in Phosphate-Buffered-Saline solution (PBS, 3 g K_2HPO_4, 1 g KH_2PO_4 and 8.5 g NaCl per Liter; pH = 7.2) to obtain a volume of 100 mL. Then, the diluted samples underwent ultrasonication (Section 12.2.4), and were further diluted 1:10 v/v in PBS. Finally, 1-mL was filtered at 20-μm prior to FCM analysis. The final dilution of 1:50 v/v was considered optimal to reach a concentration of microorganisms of around 10^9-10^{10} cells/L, suitable for FCM analysis (Foladori et al., 2010b). The coarse filtration on 20-μm membranes (Celltrics, Sysmex Partec, Germany) was necessary to eliminate large particles and thus avoid clogging the nozzle of the flow cytometer.
An untreated sample was only diluted 1:100 v/v with PBS and filtered at 20 μm prior to analysis (Figure 12.1) and was associated with energy of sonication equal to zero.

12.2.4 Pre-treatment of ultrasonication

After the first dilution at 1:5 v/v in PBS, sonication was performed using a Branson 250 Digital Ultrasonifier (Emerson, USA) operating at 20 kHz. The sonotrode, with a tip diameter of 12.7 mm, was placed in the center of a beaker

containing the 100-mL sample. A cold water bath was used around the beaker to prevent heating of the sample during sonication.

To calculate the amount of ultrasound energy applied to the sample, the specific energy (E_s), expressed in kJ L^{-1}, was used as reference parameter. E_s was calculated considering the applied power (P, expressed in W), the time of sonication (t, in seconds) and the treated volume (V, in L), according to Eq 12.1.

$$E_s = \frac{P \cdot t}{V} \tag{12.1}$$

To define the ultrasonication level most suitable for dispersing aggregates, samples were sonicated at different E_s. Calculating E_s, instead of using only P or t, enables an immediate comparison among the results obtained in tests carried out at various level of applied power (P) and time (t). In this study, P from 18 to 88 W was applied (Figure 2). For each P, an initial volume of 100 mL was sonicated at increasing times of 20, 40, 60, 90, 120, 180, 240, 300 and 360 seconds (Figure 2). For each couple (P, t) the initial volume (V) was reduced by 1 mL, which was taken out for FCM analysis. To be noted is that this procedure produced 45 pre-treated samples with an E_s in the range 3-331 kJ L^{-1} (Figure 2), and only less than 150 mL of mixed liquor (microalgal-bacterial consortium) were wasted from the pilot-scale PBR.

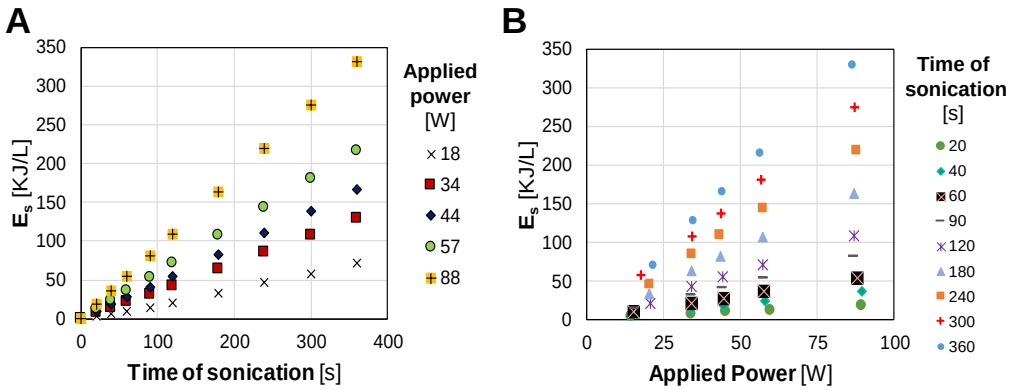

Figure 12.2 *Specific energy (E_s) applied to the samples varying (A) the time of sonication and (B) the power.*

12.2.5 Autofluorescence and fluorescent staining

After filtration at 20 μm (Figure 12.1), for each sample, two aliquots were processed as follows:

1) An unstained sample was immediately analyzed. Microalgae were detected thanks to the autofluorescence of their natural pigments;
2) A sample was stained with SYBR-Green I (SYBR-I; λ_{ex} = 495 nm, λ_{em} = 525 nm; Thermo Fisher Scientific, USA). An amount of 10 μL of dye, after dilution 1:30 v/v of commercial stock in dimethyl sulfoxide (DMSO, Merck, Germany), was added to 1 mL of the cell suspension containing about 10^9-10^{10} cells/mL and incubated at room temperature for 15 min in the dark, prior to analysis. SYBR-I is a DNA-specific fluorescent dye producing green fluorescence and it was used to detect bacteria.

12.2.6 Flow cytometry

FCM analyses were performed with an Apogee-A40 flow cytometer (Apogee Flow Systems, UK) equipped with an Argon laser (excitation wavelength at 488 nm). For each particle analyzed, two scattering signals and three fluorescent signals were collected:

- Forward Angle Light Scatter (FALS);
- Large Angle Light Scatter (LALS);
- green fluorescence (Channel FL1, λ=525 nm);
- orange fluorescence (Channel FL2, λ=575 nm);
- red fluorescence (Channel FL3, $\lambda \geq 610$ nm).

Data acquisition gates were set on green and red fluorescence distribution in order to eliminate the noise produced by non-fluorescent particles or debris. Signals were recorded with logarithmic gain. To avoid coincidence of particle counts, the event rate was kept below 1.5 μL/min. For each sample, the volume of a few μL was analyzed and events were recorded until at least 20,000 cells were enumerated. Cell concentration was recorded in events/μL and subsequently expressed as cells/L taking into account the final dilution of the sample,

according to its preparation. FCM data were analyzed using Apogee Histogram Software (Apogee Flow Systems, UK).

12.2.7 Epifluorescence microscopy

Microscopic observations were performed using a Nikon Labophot EFD-3 Microscope (Nikon, Japan) equipped with epifluorescence apparatus. Samples were exposed to: (i) bright-field, (ii) blue excitation at 450-490 nm to observe emission of green fluorescence at 520 nm; (iii) green excitation at 510-560 nm to observe emission of red fluorescence at 590 nm. Emission in the orange field was not examined because the microscope was not equipped with a specific band pass. Treated samples after sonication were observed to evaluate the degree of disintegration of microbial aggregates.

12.3 Results and Discussion

The terms “microalgae”, “photosynthetic microorganism” and “photosynthetic cells” were used as broad terms that include both eukaryotic microalgae and cyanobacteria. Likewise, the term “bacteria” referred to non-photosynthetic prokaryotic microorganisms, unless stated otherwise.

12.3.1 Microalgal-bacterial consortia flocs structure

The microscopic structure of the microalgal-bacterial consortium in PBR is shown in Figure 12.3. The image in bright field revealed dark green or brown flocs (with sizes from a few μm to 0.8 mm) composed of microalgae and bacteria embedded with organic and inorganic matter (Figure 12.3A). Filamentous microalgae represented the skeletal structure of the floc, as filamentous bacteria in activated sludge (Wanner and Grau, 1989).
Under epifluorescence microscopy, microalgae were characterized by red autofluorescence (under green excitation) linked to their pigment contents, such as chlorophylls and carotenoids (Figure 12.3B). Bacteria, which do not have natural fluorescence, were observed after staining the sample with the SYBR-I

dye, resulting in a bright green fluorescence when excited under blue light (Figure 12.3B). To be noted is that dyes with a red emission spectrum cannot be used for bacteria since red fluorescence may overlap with autofluorescence of microalgae (Hyka et al., 2013).

Optical and epifluorescence microscopy can provide insight into the morphology and composition of microalgal-bacterial consortia (Perera et al., 2019). However, to retrieve reliable quantitative information on the composition of the consortia, an extremely large number of cells should be analyzed for statistically representative results, resulting in a time-consuming analysis and tedious work for operators. Since microalgae and bacteria are embedded in flocs, the masking effect in dense clusters is another limitation. Moreover, microscopy does not enable the estimation of microalgal autofluorescence intensity, which has been gaining increasing importance in environmental monitoring because it is linked to the photosynthetic capacity (Simis et al., 2012).

FCM analysis overcomes some of the major limitations of optical microscopy. Therefore FCM may be a suitable tool for the quantitative and qualitative characterization of microalgal-bacterial consortia thanks to a time-saving and multiparametric analysis.

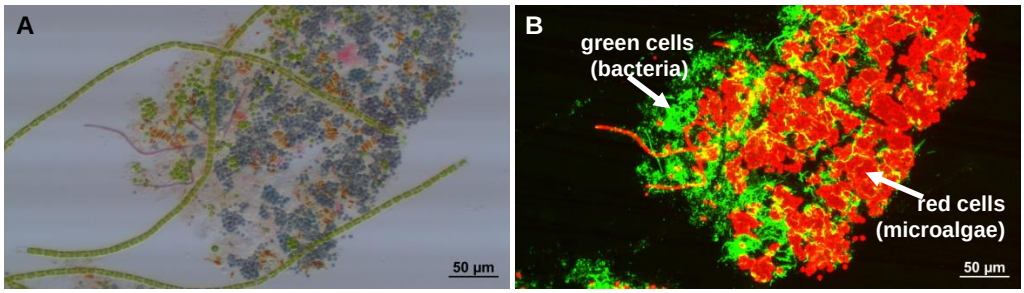

Figure 12.3 *Microalgal-bacterial consortium observed under: (A) bright field; (B) epifluorescence. Microalgae were characterized by red autofluorescence, while stained bacteria appeared green.*

12.3.2 Fluorescent signals to distinguish microalgae and bacteria with FCM

The presence of microalgae and bacteria in the tested consortium was evaluated by comparing the events recorded in the stained and unstained samples. FCM analyses of the samples pretreated at E_s of 90 kJ L^{-1} are shown in Figures 12.4, 12.5 and 12.6 because considered a representative example. As explained in Section 12.3.4, E_s of 90 kJ L^{-1} was identified as an optimal value for sonication to analyze the tested microalgal-bacterial consortium.

The events of the stained and unstained samples recorded in the red (FL3), orange (FL2) and green (FL1) channels, are overlapped in Figures 12.4A, 4B and 4C, respectively.

Red fluorescence (FL3) - In the unstained sample, a clear positive signal in red fluorescence (Figure 12.4A) was associated with photosynthetic microorganisms (eukaryotic microalgae and cyanobacteria). All photosynthetic cells contain chlorophyll *a* (Lee, 2008), which emits at 670 nm if excited at 480 nm (Marchão et al., 2018), and may also contain other pigments that emit in the red band (such as carotenoids). In the unstained sample, since bacteria are not fluorescent, they could not be detected and fall in the background.

In the stained sample a large amount of bacteria (1.2E+12 cells/L) emitted green fluorescence, while red (auto)fluorescent cells represented a minor part (2.3E+10 cells/L). Green fluorescent bacteria were not relevant (under the threshold) for FL3 because, since they were not red, bacteria fell in the background (Figure 12.4A).

Orange fluorescence (FL2) - In the unstained sample, a clear positive signal was also observed in orange fluorescence (Figure 12.4B). Comparing signals in FL3 and FL2, not all the red cells in FL3 were positive in FL2. A fraction of the red cells (25%) fell below the threshold of positive orange cells. In other words, the number of positive orange cells in FL2 was lower than positive red cells in FL3. The reason is that pigments such as phycoerythrin, which emits at 550-600 nm in the orange band (Dennis et al., 2011) are present in cyanobacteria but not in eukaryotic microalgae. To be noted is that these differences in pigmentation

could be used to discriminate eukaryotic microalgae and cyanobacteria according to their different auto-fluorescence.

Green fluorescence (FL1) - Positive events in FL1 were all the cells stained with SYBR-I (Figure 12.4C). Green events were mainly bacteria (1.2E+12 cells/L), which were two orders of magnitude more abundant than photosynthetic cells (2.3E+10 cells/L). In the unstained sample, cells did not have green autofluorescent and thus were not detected in FL1.

The cytograms in Figure 12.5 show simultaneously the red (on the vertical axis) and the green fluorescence (on the horizontal axis) of the cells. A thresholds was set in both red and green fluorescences to delimit a region in the FCM cytogram that includes instrument background (red and green below thresholds), which was excluded from the analysis.

In the unstained sample (Figure 12.5A) the emission of high red (auto)fluorescence made it possible to count the photosynthetic cells directly; bacteria did not appear because they were not fluorescent. In the dot plot of Figure 12.5A, the red dashed polygon identifies graphically the region of photosynthetic cells. Inside the demarked area, sub-groups of photosynthetic cells can be distinguished probably because of differences in fluorescent pigment contents.

In the stained sample (Figure 12.5B), total events (bacteria + photosynthetic cells) were counted. The emission of bacteria was bright green and not red, while photosynthetic cells appeared either red or green or both, depending on their capacity to adsorb SYBR-I. Photosynthetic cells included a large variety of microorganisms (eukaryotic microalgae, cyanobacteria, presented as both unicellular or filamentous cells), so that staining by SYBR-I may change significantly. For these reasons, due to the difficulty of delimiting in the cytogram an exclusive region for bacteria, their concentration was calculated as a difference between the total events counted in the stained sample, and photosynthetic cells counted in the unstained sample (Eq 12.2).

$$\text{Bacteria} = \text{Total event} - \text{Photosynthetic cells} \tag{12.2}$$

In the FCM analysis shown in Figure 12.5, total cells were 1.13E+12 cells/L and photosynthetic cells were 2.3E+10 cells/L (2% of total cells); thus, the concen-

tration of bacteria was 1.11E+12 cells/L (98% of total cells).

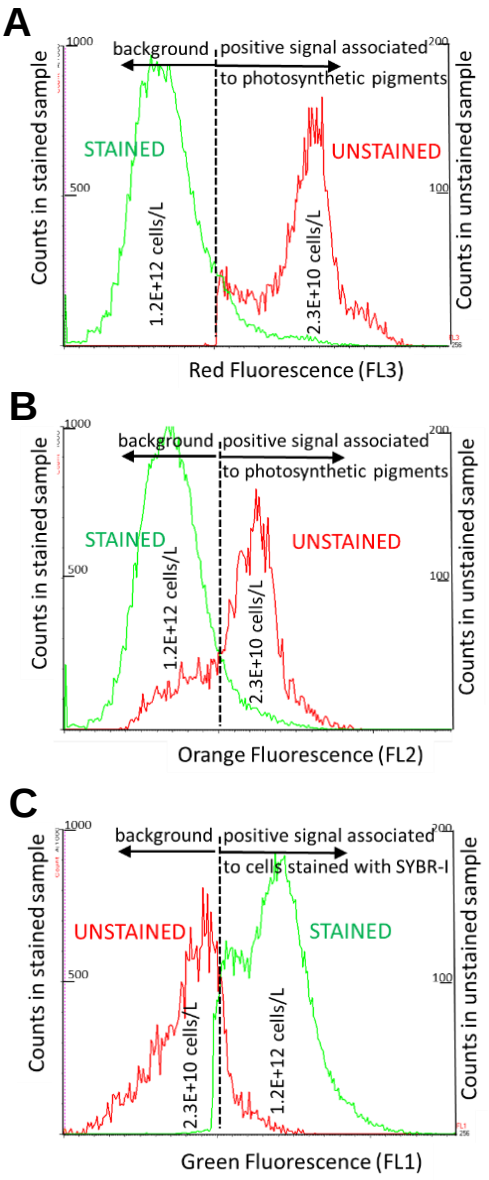

Figure 12.4 *Overlapping of (A) red, (B) orange and (C) green fluorescences in stained and unstained samples. Scales on vertical axes are different for the two samples. Absolute concentrations (integral of the histogram) are indicated. Stained and unstained samples were pretreated at E_s of 90 kJ L^{-1}.*

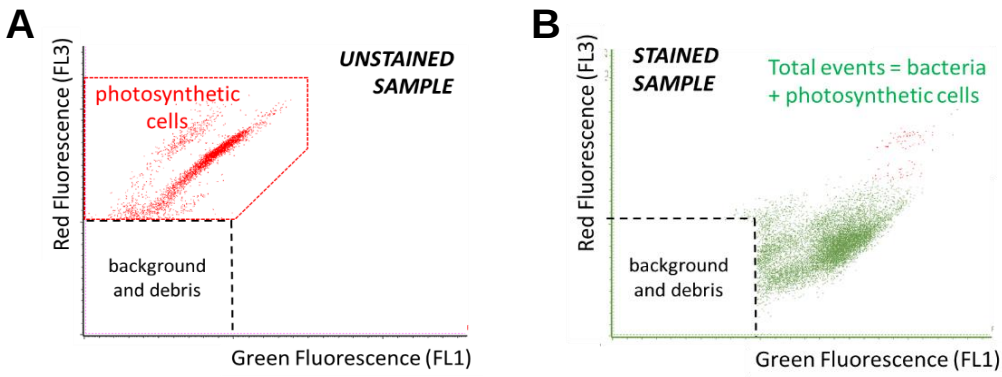

Figure 12.5 *FCM cytograms (dot plots) of the microalgal-bacterial consortium: (A) Unstained sample. The red dashed polygon delimits the region of photosynthetic cells; (B) Stained sample. Stained and unstained samples were pretreated at E_s of 90 kJ L^{-1}.*

12.3.3 Light scattering to distinguish microalgae and bacteria

As shown in the histograms in Figure 12.6, microalgae and bacteria produced significantly different signals of light scattering. Both histograms were gated on the green and red fluorescence, in order to eliminate the scattering originated by non-biotic particles or detritus presented in the microalgal-bacterial consortium.

FALS is the light scattering collected in the forward direction with respect to the incident laser beam and is related to the cellular size or biovolume (Salzman et al., 1990; Shapiro, 2003; Foladori et al., 2008). Therefore, FALS made it possible to distinguish the small bacteria from the large photosynthetic cells (Figure 12.6A), which may include a vast range of microalgal taxa.

FALS intensity was recorded with logarithmic scale that made it possible to compare graphically several order of magnitude of cell size. As shown in Figure 12.6A, FALS (on the horizontal axis) is expressed in arbitrary units and mapped onto 256 channels. In the FCM analysis shown in Figure 12.6A, the median channel of the FALS frequency distributions was 62 for bacteria and 193 for photosynthetic cells. Therefore, considering that FALS channels were logarithmics, the difference in biovolume among the two populations was very large (193-62=131 channels).

This result is in agreement with the expected biovolume of microalgae and bacteria in the literature. The average biovolume of bacteria in wastewater was 0.22 μm^3/cell in Vollertsen et al. (2001) on sizing bacteria under microscope. In activated sludge, Frølund et al. (1996) measured a mean biovolume of bacteria of 0.25 μm^3/cell. Similar results (0.23 μm^3/cell) were found with a FCM automated procedure applied to activated sludge (Foladori et al., 2008). With regards to the smallest unicellular microalgae, the biovolume of *Chlorella* is in the order of 30 μm^3, while the biovolume of *Synecococcus* is 20 μm^3 (Bellinger and Sigee, 2015). Cells of cyanobacteria are definitely smaller and the biovolume of *Prochlorococcus* (belonging to picoplankton) is less than 1 μm^3 (Bellinger and Sigee, 2015).

LALS is the light scattering collected at large solid angles and is affected by cell morphology, such as cytoplasmic granularity (Safford and Bischel, 2019). In the FCM analysis shown in Figure 12.6B, the median LALS channel was 49 for bacteria and 126 for photosynthetic cells. Although LALS values were referred to an arbitrary scale, they were significantly different, demonstrating the greater complexity in the cellular structure of photosynthetic cells in comparison to bacteria.

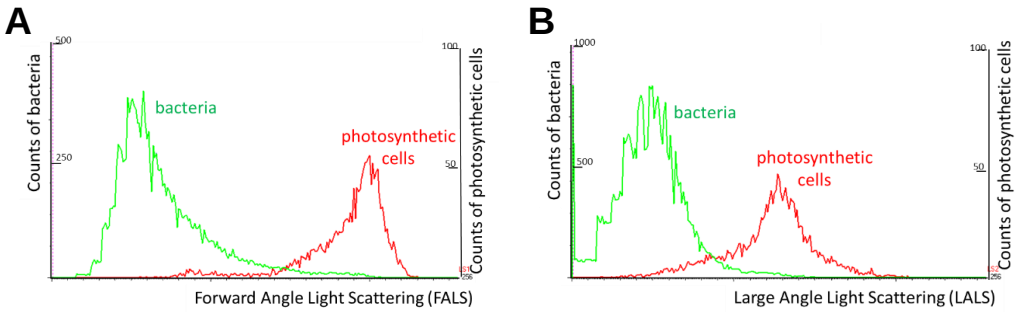

Figure 12.6 *Comparison of (A) FALS and (B) LALS in stained and unstained samples. Histograms were gated on the green and red fluorescence to distinguish bacteria and photosynthetic cells. Stained and unstained samples were pretreated at E_s of 90 kJ L^{-1}.*

12.3.4 How to estimate the concentration of cells in the microalgal-bacterial consortium

As shown in Figure 12.7, the pretreatment of the microalgal-bacterial consortium with sonication (E_s) made it possible to effectively disaggregate the flocs and thus increase the number of free single cells dispersed in the bulk liquid. Therefore, the amount of cells could be measured by FCM, which is a single-cell analysis. On the contrary, the microbial concentration in the untreated sample, containing large flocs of microalgae and bacteria, could not be directly quantified.

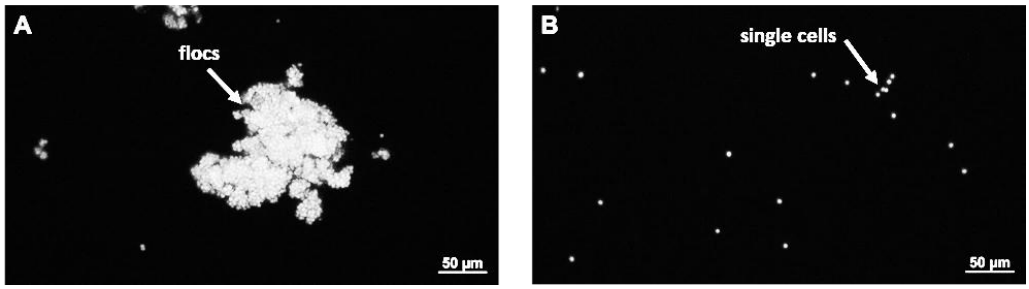

Figure 12.7 *Microscopic images of the microalgal-bacterial consortium (A) before and (B) after sonication at E_s = 90 kJ L^{-1}.*

The concentration of free bacteria and photosynthetic cells analyzed, depended on the specific energy applied (E_s) with sonication (Figure 12.8). After sonication, bacteria clumped in flocs were released free in the bulk liquid together with the photosynthetic cells. As shown in Figure 12.8A, the number of free cells increased with E_s. Fitting curves included in Figure 12.8A enable identification of the maximum cell density recorded for bacteria and photosynthetic microorganisms. The cell densities of the two groups were very different with 10^{10} cells/L for photosynthetic cells and 10^{12} cells/L for bacteria. Figures 12.8B and 12.8C show the average values and standard deviation of bacterial and photosynthetic cells recorded for classes of E_s, respectively. Flocs disaggregation at E_s up to 90-100 kJ L^{-1} enhanced notably the number of free total cells in the bulk liquid (Figure 12.8A). Floc size reduction of the treated samples

was directly observed under microscope (Figure 12.7) and also reported by other authors (Chu et al., 2001). For E_s higher than 90-100 kJ L^{-1}, the maximum number of disaggregated cells was achieved without compromising the cell integrity, as shown in Figure 12.8A, in which both fitting curves reached a plateau. Bacterial cell density was on average 1.2E+12 ± 4.9E+10 cells/L and remained statistically similar for E_s up to 180 kJ L^{-1} (Figure 12.8B), demonstrating high resistance of bacteria to sonication. Likewise, the maximum number of free photosynthetic cells was 2.8E+10 ± 2.3E+09 cells L^{-1} for E_s between 90 and 150 kJ L^{-1} (Figure 12.8C). The slight decrease of cell concentration at E_s higher than 150 kJ L^{-1} (Figure 12.8A) was due to the disruption of some cells, which were no longer detected by FCM.

Since the exact number of cells present in a microalgal-bacterial consortium is not known *a priori*, it is important to define a pretreatment method able to release the highest number of cells for subsequent enumeration by FCM. However, during the pretreatment of samples, a certain damage to some cells can not be excluded, especially for filamentous microorganisms. Therefore, a moderate E_s should be applied because it represents a compromise to obtain the highest concentration with a minimal risk of cell damage. For the microalgal-bacterial consortium tested an optimal (moderate) E_s was 90 kJ L^{-1} (Figure 12.8B-C). Interestingly, similar E_s values have been reported as optimal for dispersing activated sludge without extensive cell destruction. In particular Biggs and Lant (2000) indicated a E_s of 90 kJ L^{-1}, while Foladori et al. (2007) suggested E_s around 80 kJ L^{-1}.

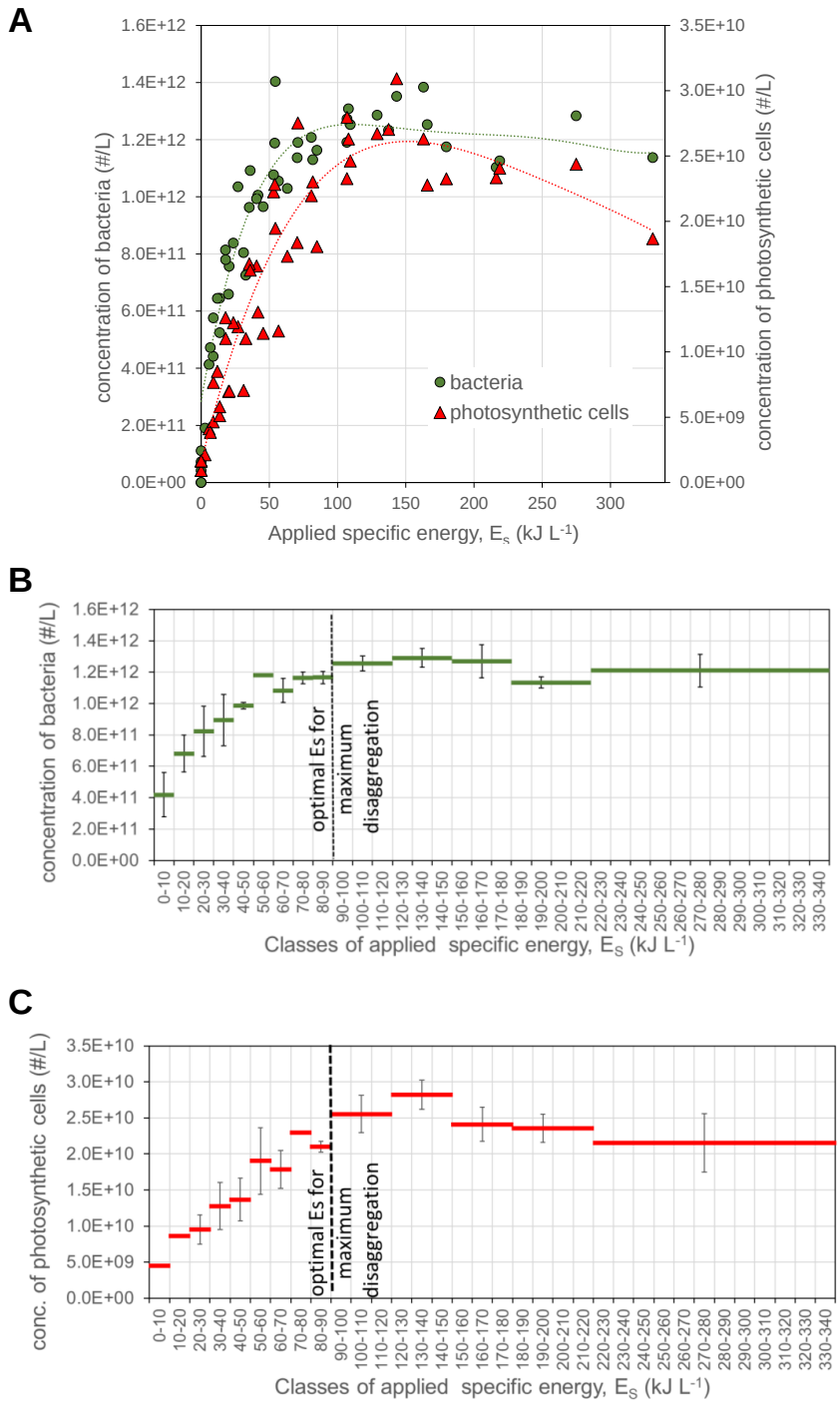

Figure 12.8 *(A) Dynamic of the concentration of bacteria and photosynthetic cells for increasing levels of E_s. Average values and standard deviation of (B) bacteria and (C) photosynthetic cells recorded for classes of E_s.*

12.3.5 Percentage of cells in the microalgal-bacterial consortium

The ratio between photosynthetic microorganisms and bacteria at increasing E_s values is shown in Figure 12.9. The ratio increased from 1 to 2 at increasing E_s (up to 90 kJ L^{-1}) due to progressive disaggregation of the consortium. Then, the ratio remained around 2 until E_s surpassed 250 kJ L^{-1}. At higher E_s values, the ratio decreased, indicating that the damage to microalgae prevailed over the damage to bacteria.

Although microalgae appeared weakly represented due to their low concentration, they were characterized by a large biovolume compared to bacteria (approximately 2 orders of magnitude larger, Figure 12.6A). Therefore, the resulting photosynthetic biomass was comparable to bacterial biomass since bacteria had a higher concentration but a lower biovolume.

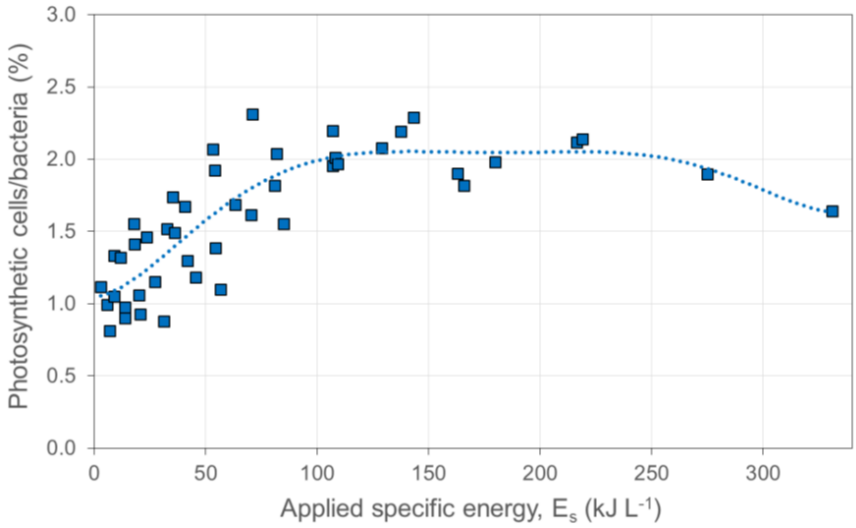

Figure 12.9 *Ratio (expressed as percentage) between photosynthetic microorganisms and bacteria at increasing applied specific energy (E_s).*

12.4 Conclusion

This study has proved the viability of FCM for qualitative and quantitative analysis of the composition of a microalgal-bacterial consortium in a PBR aimed at treating wastewater.

Microalgal-bacterial consortia are heterogeneous and complex matrices, so that the quantification of sub-groups of microorganisms should be not biased. Therefore, an optimal pretreatment protocol has been proposed to ensure the accuracy of the FCM analysis.

Sonication of the samples proved to be a suitable pretreatment to disperse aggregated cells in the bulk liquid. Although a certain damage to some cells during sonication may not be excluded, a moderate E_s level of 90 kJ L^{-1} was considered an optimal value for the quantification of microalgae and bacteria in the tested consortium.

Microalgae and bacteria were distinguished using light scattering and fluorescences (red associated with natural pigments in microalgae, green associated with nucleic acid-staining in bacteria) signals.

Bacteria were largely present in the consortium, amounting to 98% of total cells. However, microalgae, which represented only 2% of total cells, were characterized by a higher biovolume (2 orders of magnitude larger). Therefore, the amount of microalgal biomass could be considered in the same order of magnitude as the bacterial biomass. This would explain the high and stable removal treatment performance of the long-term PBR, in which bacterial activity was only sustained by photosynthetic oxygenation. However, further analyses are needed to refine the mass balance.

In conclusion, the multi-step procedure proposed could be included in monitoring procedures of PBRs. FCM could provide valuable information on the composition of the microalgal-bacterial consortia and detect anomalies with short analysis time (in the order of minutes).

Supplementary material

Principles of FCM

As shown in Figure S12.1, an aliquot of the sample (μL) is pumped in the flow cytometer to a focusing chamber in which suspended particles are forced to align in single file. Then, the stream of particles passes through a flow cell. In front of an interrogation point, a laser (or a light beam) strikes each particle, exciting the fluorescent one. For each particle detectors measure simultaneously: (i) light scattering in the forward and side directions, and (ii) two or more fluorescent signals. Then measurement are recorded and sent to a computer for display and further processing.

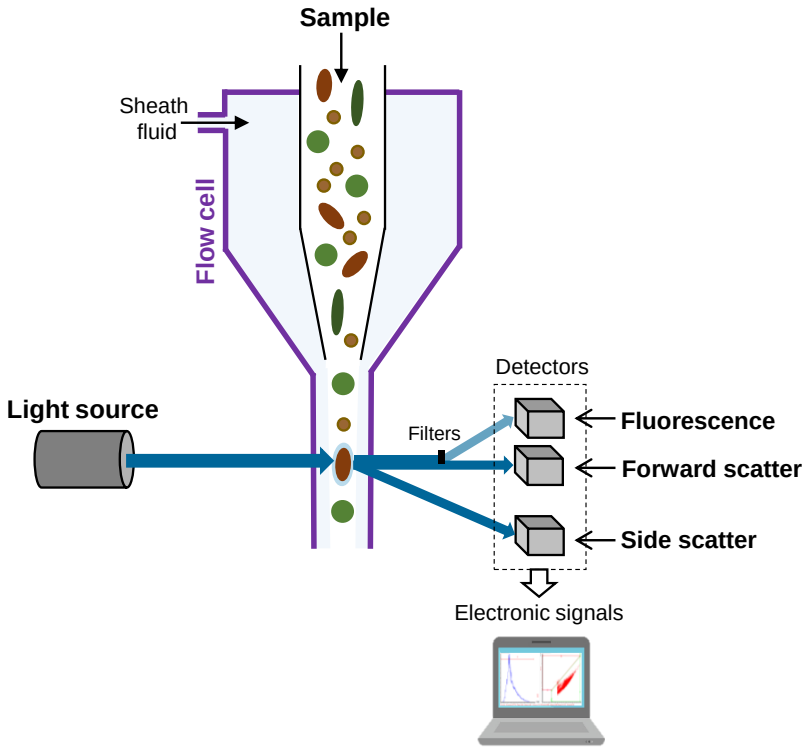

Figure S12.1 *Scheme of FCM analysis.*

CHAPTER 13

MICROBIAL COMMUNITY IN THE LONG-TERM PHOTOBIOREACTOR AND COMPARISON WITH ACTIVATED SLUDGE

This Chapter focuses on the composition and evolution of the microbial community developed in the long-term photobioreactor named Pilot (Chapter 6).
16S rRNA gene sequencing revealed that the bacterial community remained stable over 230 days of monitoring. The differences between the long-term bacterial community developed in the Pilot, and the activated sludge of the WWTP Trento Nord, were examined.
New environmental species associated to microalgal-bacterial consortia were discovered and are presented in Chapter 4.

This research was made in collaboration with the Department of Cellular, Computational and Integrative Biology (CIBIO) - University of Trento.

This Chapter is based on:
Petrini S., Masetti G., Foladori P., Beghini F., Armanini F., Segata N., Andreottola, G. *Microbial community evolution in a long-term photobioreactor operated at a lab-scale and comparison with activated sludge-based processes treating the same municipal wastewater at full-scale.* In preparation

Abstract

Microalgal-bacterial consortia represent a promising sustainable solution, alternative to activated sludge-based processes in the treatment of municipal wastewater. However, the microbiota that develops in photobioreactors (PBRs) is still largely unexplored.

In this study, high-throughput sequencing was applied to examine the microbial community composition of a PBR, its stability over a long period and the difference with activated sludge treating the same real municipal wastewater. Activated sludge samples were collected from the Conventional activated sludge line (CAS) and the Membrane Bioreactor line (MBR) of the full-scale wastewater treatment plant of Trento Nord (Italy).

Over time, PBR ensured high and stable removal efficiency of COD (66±17%) and ammonium (99±1%). Concurrently, the bacterial community did not show drastic shift in composition with *Proteobacteria* and *Cyanobacteria* as predominant phyla.

The microbiota in the influent wastewater partially persisted in all biological treatment units, suggesting an adaptation to operational conditions. In addition, the bacterial community in PBR differed in composition with CAS and MBR, which resulted very similar. Different operating conditions promoted the development of a specific PBR-associated microbiota, which varied from that of activated sludge.

13.1 Introduction

Anthropogenic activity produces large amounts of wastewater that can cause eutrophication, if directly discharged in water bodies. To prevent adverse environmental impact, wastewater should be properly treated before released. Activated sludge-based processes are implemented worldwide in wastewater treatment plants (WWTPs) as biological treatment to remove organic compounds and nutrients from wastewater (Wu et al., 2019). However, high costs for aeration (WRF and EPRI, 2013) and greenhouse-gas emissions have stimulated the development of alternative wastewater treatment technologies more sustainable (both economically and environmentally) than activated sludge (Gonçalves et al. 2017).

A promising solution to this issue is represented by the combination of microalgae (eukaryotic microalgae and prokaryotic cyanobacteria) and bacteria that have been proving to be effective for municipal wastewater treatment, relying only on photosynthetic oxygenation and thus without artificial aeration (Ramanan et al. 2016; Arcila and Buitrón 2017; Quijano et al., 2017; Wang et al. 2018). However, in view of the large-scale application of this technology, there are still some challenges to overcome (Molinuevo-Salces et al., 2019; de Jesús Martínez-Roldán and Ibarra-Berumen, 2019). Many types of photobioreactors (PBRs) and configurations have been tested. Most of the systems have been developed at a lab- and pilot-scale to treat usually synthetic or sterilized wastewater (Kang et al., 2018). To assess the stability of the treatment performance, PBRs should be fed with real wastewater and monitored in long-term studies. In this way, it would be possible to gain insight into the microbial community that spontaneously develop in PBRs fed with real municipal wastewater (He et al. 2013; Arango et al. 2016; Tsioptsias et al. 2016; Cho et al. 2017; Kang et al. 2018). Despite the recent advances in metagenomic technologies applied to environmental samples (Staley and Sadowsky, 2018), few studies have investigated the microbial composition of microalgal-bacterial consortia treating wastewater through DNA-based analyses (Mishra et al. 2019).

A long running pilot-scale photobioreactor (PBR) fed with real municipal wastewater (Chapter 6) was monitored over 8 months with the aim to assess (1) the treatment performance and (2) the microbial composition (bacterial composition and diversity) of the microalgal-bacterial consortium spontaneously developed in the system.
16S rRNA gene sequencing was performed on the PBR, the influent wastewater (WW) and activated sludge samples treating the same real municipal wastewater to characterize the residing bacterial population. Activated sludge samples were collected from the Conventional activated sludge line (CAS) and the Membrane Bioreactor line (MBR) of the full-scale WWTP Trento Nord (Trento, Italy). Activated sludge microbiota was used as benchmark. Alpha diversity and beta diversity were used to evaluate and compare the differences between the bac-

terial communities of PBR, WW, CAS and MBR. Microbiota composition and variations were assessed through bacteria relative abundances.

This work provides new insights into stable microalgal-bacterial consortia, their performances and their bacterial community diversity. To the best of the authors knowledge, this is the first time that the microbial composition of a microalgal-bacterial consortium spontaneously develop from real municipal wastewater, is characterized over a long-period of time.

13.2 Materials and Methods

13.2.1 Lab-scale photo-sequencing batch reactor (PBR)

The microalgal-bacterial consortium developed in a long-term lab-scale PBR (Figure 13.1A, Chapter 6), was monitored for a period of 231 days.
The PBR consisted of a cylindrical glass reactor (diameter 12 cm, height 20 cm; Colaver, Italy) with a working volume of 2L. The system was installed on February 2016 and was operated as a photo-sequencing batch reactor with a cycle of 48 h and a photoperiod of 16 h of light and 8 h of dark. The PBR was continuously fed with real municipal wastewater with an influent rate of 0.7 L/cycle that corresponded to an HRT (Hydraulic Retention Time) of 5.6 days. No pure strains of microalgae were inoculated, instead a consortium of microalgae and bacteria developed spontaneously. Total suspended solids (TSS) concentration in the PBR was on average 2.0±0.3 g TSS/L.
Light was provided by a LED lamp (8 led×0.5 W; Orion, Italy) that produced a light intensity of 30±5 μmol m^{-2} s^{-1}. No external aeration was provided thus oxygen was supplied only by photosynthesis. The reactor was not sealed off from atmosphere and no pH adjustment was performed.

13.2.2 Real municipal wastewater (WW)

The PBR was fed with real municipal wastewater (WW) collected form the Trento Nord WWTP (TN WWTP, Trento, Italy) after the primary treatment

(Figure 13.1A). No filtration of wastewater was performed so to allow resident microorganisms to enter the PBR.

13.2.3 Conventional activated sludge (CAS) and Membrane Bioreactor (MBR)

The samples were collected from the biological treatment units of the TN WWTP that operates on two parallel treatment lines (Figure 13.1A): Conventional activated sludge (CAS) and Membrane Bioreactor (MBR). The TN WWTP treats a population equivalent (PE) of around 100000 PE. 70% of the influent wastewater is treated by the CAS line while the remaining part is treated by the MBR line.

13.2.4 Collection of samples

Samples of the microalgal-bacterial consortium were collected from PBR for DNA extraction every 21 days between June 2017 and February 2018 (Figure 13.1B). In the same period WW samples, fed in the PBR, were collected every week for chemical characterization and for DNA extraction (Figure 13.1B). CAS and MBR samples were collected for DNA extraction one a week between December 2017 and February 2018 (Figure 13.1B). Samples were collected concomitantly with the samples for routine analysis performed by the plant manager company (Depurazione Trentino Centrale, DTC). Samples for DNA extraction were stored at -80°C before further processing.
Effluent wastewater from PBR was collected 2-3 times per week to monitor the treatment performance.

13.2.5 Analytical methods

Influent (WW) and effluent wastewater from PBR, were analyzed for chemical oxygen demand (COD), Total Kjeldahl Nitrogen (TKN), NH_4^+-N, NO_2^--N, NO_3^--N and total P (TP), according to Standard Methods (APHA, 2012). Total N (TN) was defined as the sum of TKN, NO_2^--N and NO_3^--N. TSS were measured

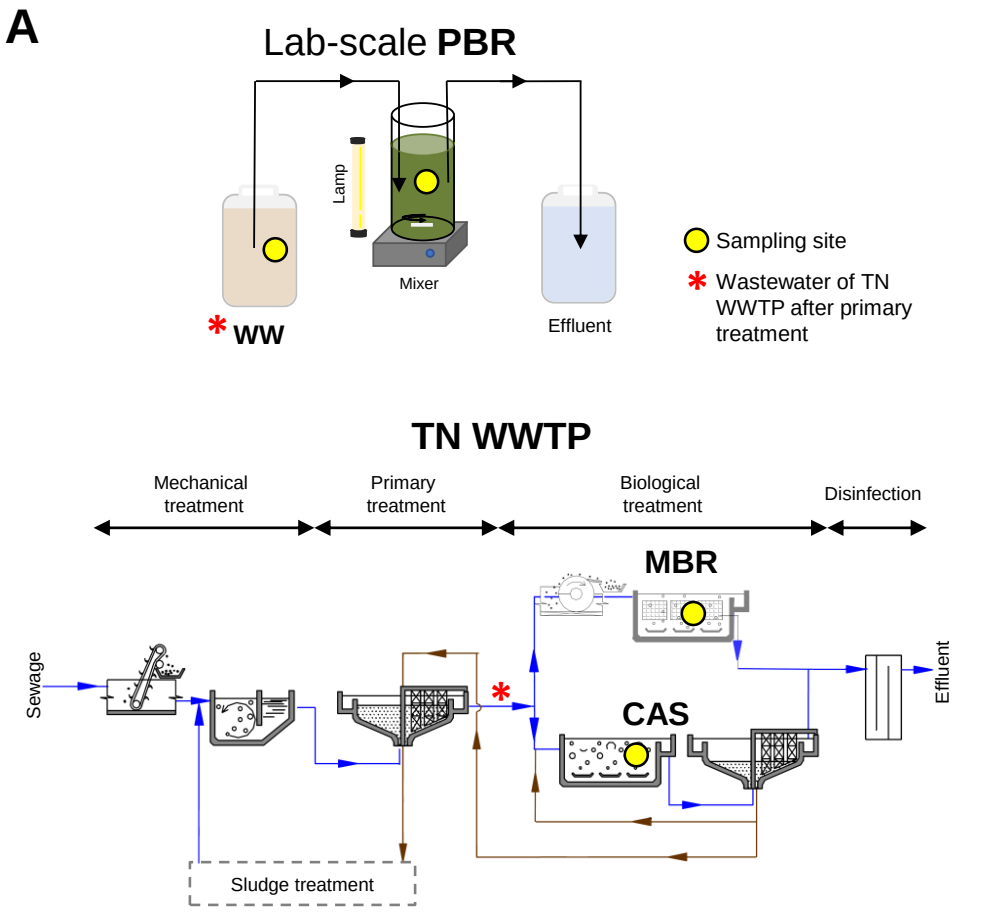

Figure 13.1 *(A) Scheme of PBR and of the water line of the TN WWTP. Yellow points indicate sampling sites. (B) Sample collection timepoints for DNA analysis. WW: Wastewater collected after primary treatment and fed in the PBR. PBR: Photo-sequencing batch reactor. CAS: Conventional activated sludge. MBR: Membrane Bioreactor.*

in the mixed liquor, according to APHA (APHA, 2012), to determine the biomass concentration in PBR.
The light intensity was measured as photosynthetically active radiation (PAR) with a SQ-520 quantum sensor (Apogee Instruments, USA).

13.2.6 DNA extraction and sequencing

DNA extraction was performed with DNeasy® PowerSoil® Kit (Qiagen, Germany). Samples were processed following the QIAGEN DNeasy® PowerSoil® Kit instructions except that (i) the PowerBead was filled with 1 ml of sample and (ii) the collection tube was centrifuged for 2, 1 and 1 minutes after adding Solution C3, C5 and C6, respectively.
16S rRNA gene sequencing was performed as described in Chapter 4, Section 4.2.6

13.2.7 16S rRNA gene sequencing processing and analysis

16S rRNA gene sequencing processing was performed as described in Chapter 4, Section 4.2.7. Differences in alpha diversity indices (considering all time points together) between PBR, CAS and MBR were assessed using a non-parametric Wilcoxon-Mann test. The trend of alpha diversity indices over-time was calculated through linear regression and the correlation was assessed with the Spearman's correlation coefficient. Beta-diversity was estimated from the Bray-Curtis dissimilarity matrix and it was represented in a Non-metric Dimensional Scaling (NMDS) plot.

13.3 Results and Discussion

13.3.1 PBR ensured stable removal efficiency of COD and TN

The average concentrations of the influent wastewater (Table 13.1) were in agreement with typical values expected in pre-settled municipal wastewater (Tchobanoglous et al. 2003).

The PBR was able to treat real municipal wastewater without artificial aeration. From June 2017 to February 2018, the PBR showed an average removal efficiency of 66±17%, 72±14% and 99±1% for COD, TN and NH_4^+-N (Table 13.1). The treatment process, sustained only by photosynthetic oxygenation, guaranteed average effluent COD and TN under EU discharge limit (EU Directive 91/271/EEC).
Despite the fluctuations of COD in the real influent wastewater (Figure 13.2A), PBR was characterized by low and stable effluent COD concentrations with an average of 68±10 mg/L (Table 13.1).
The main nitrogen removal mechanism was nitrification (Chapter 6), which ensured negligible effluent ammonium concentration resulting in an average removal efficiency of 99±1% (Table 13.1). Despite the almost complete ammonium removal, TN removal efficiency resulted of 72±14% on average because nitrate accumulated in the PBR due to nitrification. Since the system was not optimized for denitrification, nitrate removal fluctuated with time thus TN (Figure 13.2B). However, the average effluent TN resulted of 13±6 mg/L, under the discharge limit (EU Directive 91/271/EEC).
The PBR exhibited low removal efficiency of TP (40±15%) with an average effluent concentration of 2.8±0.7 mg P/L (Table 13.1). The low TP removal was linked to a limited biomass uptake, further investigations are needed to enhance biological phosphorus removal. To note, in the TN WWTP, phosphorus is removed through chemical precipitation.

The PBR treatment performance of COD and ammonium could be considered steady state over the monitored period because the system ensured high and stable removal efficiencies despite the fluctuations of the influent wastewater composition. It is generally accepted that a stable treatment process is a sign of a stable and healthy biological system that do not necessary imply a stable community composition but rather a stable presence of metabolic pathways (Gao et al., 2016; references therein).

Parameter	Influent wastewater [mg/L]	Effluent [mg/L]	Removal efficiency [%]
COD	234±89	68±10	66±17
TN	50±15	13±6	72±14
NH_4^+-N	41.0±12.7	0.4±0.7	99±1
TP	4.6±1.3	2.8±0.7	40±15

Table 13.1 *Characterization of influent and effluent wastewater and removal efficiency of the PBR between June 2017 and February 2018. (avg.±st.dev.).*

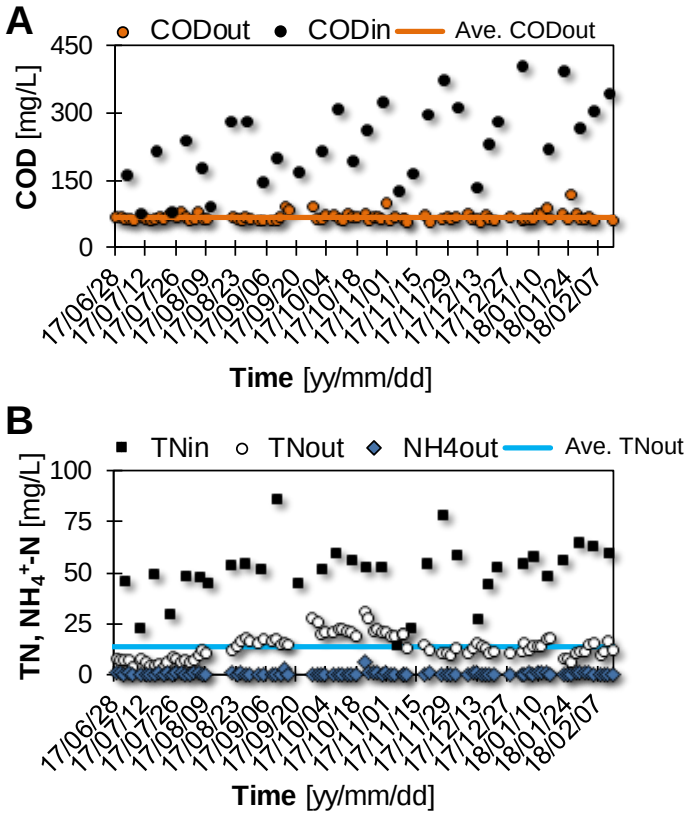

Figure 13.2 *Time course of influent (in) and effluent (out) concentrations of (A) COD and (B) Nitrogen forms from the PBR. Average effluent concentrations are represented with continuous lines.*

13.3.2 Bacterial communities' dynamics

16S rRNA gene amplicon sequencing was employed to investigate the community composition differences between a microalgal-bacterial consortium (i.e. PBR) and activated sludge (CAS and MBR), and their evolution over time. Activated sludge samples were collected form a real operating WWTP (TN WWTP) that received the municipal wastewater fed also in the PBR. To note, CAS and MBR, which are real operating reactors, treat the same influent wastewater but they are activated sludge-based processes that operates at different working conditions.
The influent wastewater microbiota (WW) was monitored to assess if influent microorganisms persisted in the biological treatment units and if it affected the composition of these engineered microcosms.
Total reads were 3,894,184 with a mean 40,564.417±14,627.790 counts/sample, ranging from min 309.00 (in negative-control sample library) to 71,375 max sample library.

13.3.2.1 Within-group diversity

Alpha diversity indices were calculated to examine species diversity in each group, considering all time points together (Figure 13.3A) and over time (Figure 13.3B).

WW was characterized by a lower richness (Chao1 = 3655.79±7.91 and number of observed OTUs = 2727.42±6.52) than CAS (Chao1 = 6089.89±6.94 and obsOTUs = 4525.73±6.23) and MBR (Chao1 = 5699.89±6.38 and obsOTUs = 4525.73±6.23), but comparable with PBR (Chao1 = 3865.13.89±5.47 and obsOTUs = 2961.67±4.9), considering all time points together. CAS (Shannon = 9.85±2.74 and Simpson = 0.99±2.85) and MBR (Shannon = 9.45±3.19 and Simpson = 0.99±3.90) showed the highest diversity indices followed by that of PBR (Shannon = 8.31±3.06 and Simpson = 0.97±7.06) and WW (Shannon = 8.31±3.06 and Simpson = 0.97±7.06).
As PBR, CAS and MBR were considered to as "steady state biomasses", we performed the nonparametric Wilcoxon-Mann test to assess significant differences

amongst them. Alpha diversity indices of PBR were significantly different from MBR (p in the order e-03) and even more from CAS (p = 5.5e-05). In PBR, the presence of microalgae and operational conditions very different from activated sludge-based processes (first and foremost HRT in the order of days, lower biomass concentration and presence of light) may have affected bacterial growth and adaptation. On the other hand, CAS and MBR alpha diversity indices were not significantly different suggesting that the different working condition of the activated sludge-based processes, did not affect the richness and the diversity of microbial communities treating the same influent wastewater. WW microbiome cannot be considered as a steady state biomass, since it is affected by the variability of the sewer where the conditions are not controlled as in biological treatment units.

As shown in Figure 13.3A, each group showed a stable richness over-time (Chao1 and observed OTUs). Differently, CAS, MBR and PBR tended to a lower diversity (Shannon and Simpson), while WW showed a significant increasing diversity (Shannon R=0.55, p<0.001 and Simpson R=0.61, p<0.001). PBR and WW samples were collected from June to February, while CAS and MBR only from December to February therefore time variations were observed for a more limited period.

As reported from several studies on real WWTPs (Griffin and Wells, 2017; Johnston et al., 2019), seasonal temperature fluctuations of the influent wastewater (WW) may have affected the diversity of WW, CAS and MBR. Since the lab-scale PBR was placed inside the lab at controlled temperature the effect of WW temperature on the PBR microbiota can be excluded. However, further investigations are needed to explain the opposite trend in biodiversity between WW and the steady state biomasses.

13.3.2.2 Between-group diversity

Beta diversity index was calculated with the Bray-Curtis dissimilarity matrix to reveal differences amongst bacterial communities.

Each group presented a clear spatial separation compared to each-other,

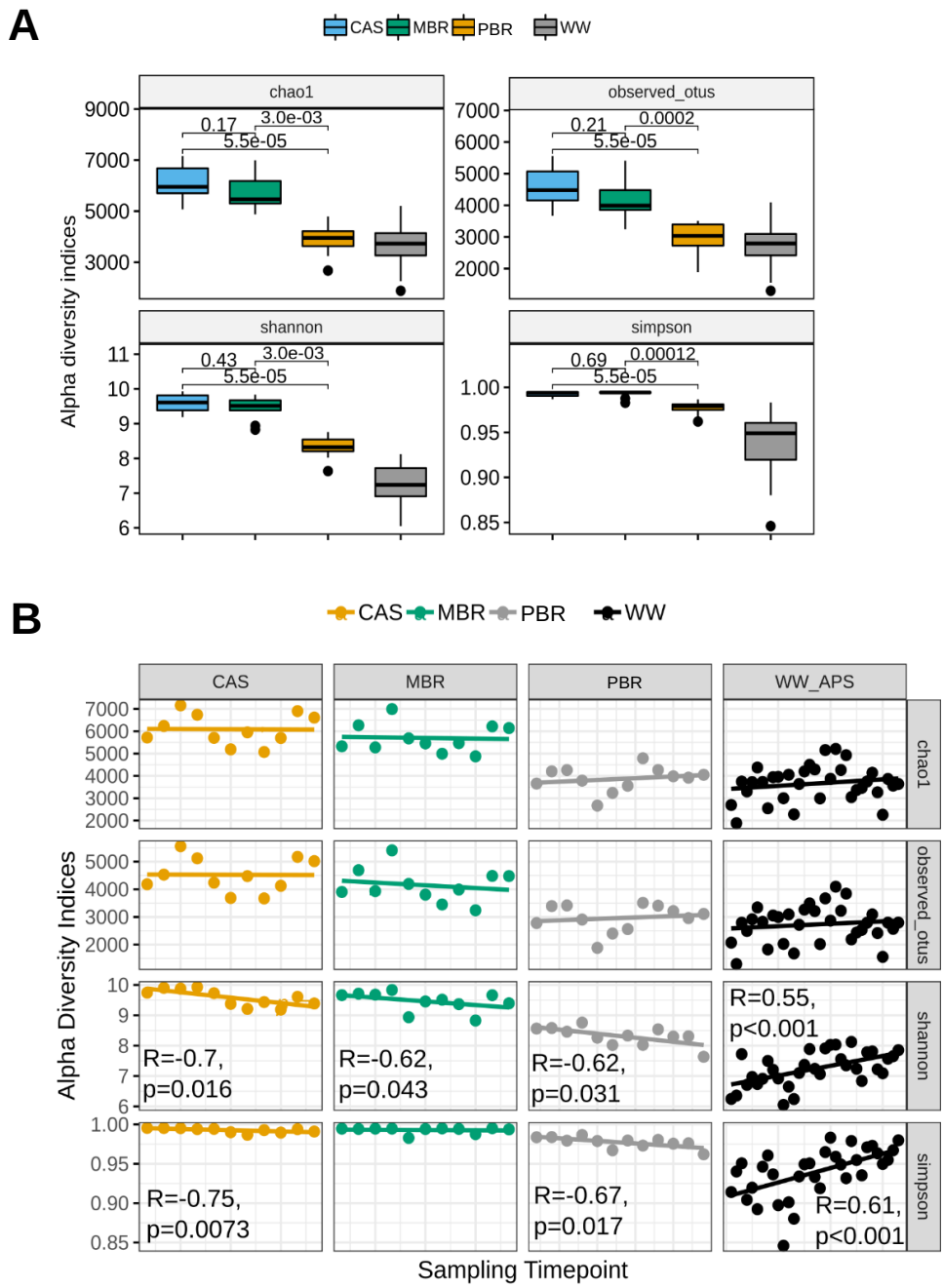

Figure 13.3 *(A) Alpha diversity indices in each group (A) considering all time points together. Differences between PBR, CAS and MBR were assessed using a non-parametric Wilcoxon-Mann test; (B) amongst time points modelled through a linear regression. Spearman's correlation coefficient (R) was used to assess the correlation between time and alpha diversity indices.*

with samples with-in groups clustering in closer proximity (Figure 13.4). WW samples were characterized by the higher variability while CAS and MBR samples relied very close to their own centroids. Two samples of PBR could be considered outliers with the respect to its centroid.
The closer proximity of the samples with-in CAS, MBR and PBR groups indicated that their microbial composition was stable over time. To note, PBR was monitored for a period of 8 months.
As shown in the NMDS plot (Figure 13.4), the influent microbial community (WW) was notably different from that of the communities established in the biological reactors (CAS, MBR, PBR). In addition, there was a clear spatial separation between PBR and the activated sludge-based reactors (CAS and MBR). CAS and MBR samples clustered in closer proximity with overlapping centroids. Therefore, the activated sludge in the reactors were composed by very similar microbial communities despite different operational conditions.
Taken together, this data indicates a stability in the community composition of the biological reactors and the great difference between the microalgal-bacterial consortium and activated sludge. Therefore, it emerges the importance to explore the composition of the PBR-associated microbiota and its functions.

13.3.3 Bacterial communities' composition

The bacterial community structures were analyzed to gain further insight into the microbiota differences (Figure 13.5). At the taxonomic level, 52 phyla and 747 genera were identified.

In all samples, *Proteobacteria* was the most abundant phylum ranging from a minimum average abundance of 36.8±6.6% in PBR to a maximum of 57.5±7.2% in WW. *Proteobacteria* in WW mostly belonged to the classes *Epsilonproteobacteria* (28.1±8.4%), *Gammaproteobacteria* (20.2±6.8%) and *Betaproteobacteria* (10.3±3.9%). *Betaproteobacteria* are involved in organic matter degradation and nutrient removal, and have been usually detected in real WWTP based on activated sludge processes (Nascimento et al. 2018; Cydzik-Kwiatkowska and Zielińska 2016). This class was the most abundant in PBR

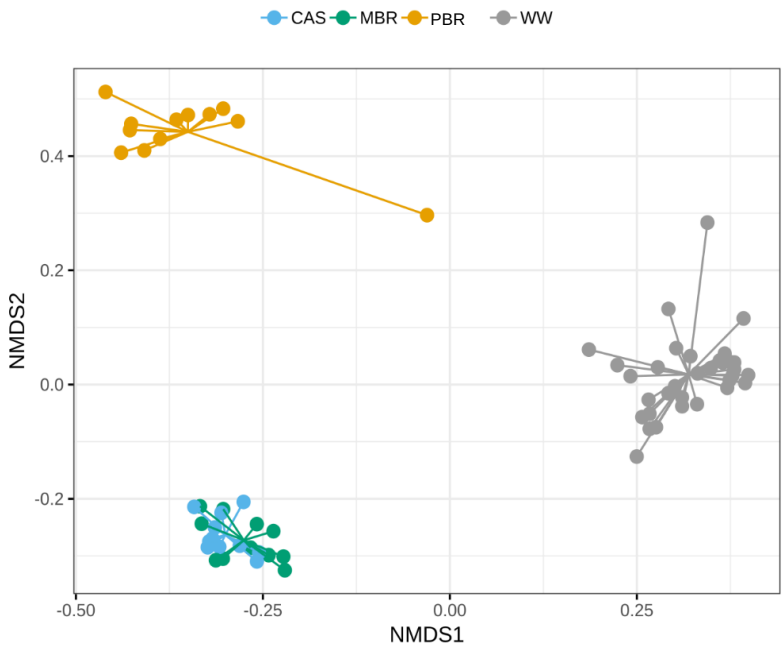

Figure 13.4 *Non-metric Dimensional Scaling (NMDS) plot based on Bray-Curtis dissimilarity matrix showing a spatial separation amongst groups.*

(18.1±6.6%) but also in CAS (24.0±2.2%) and MBR (24.9±2.0%) followed by *Alphaproteobacteria*, *Gammaproteobacteria* and *Deltaproteobacteria* at abundances lower than 9%, in agreement with other results on bacterial communities in activated sludge (Kim et al., 2019; Xue et al., 2019). *Epsilonproteobacteria* were negligible in all biological reactors. About WW, the other top abundant phyla were *Bacteroidetes* (22.6±4.0%), *Firmicutes* (8.4±2.9%), *Fusobacteria* (2.2±1.8%) and *Saccharibacteria* (1.7±1.6%) that represented, together with *Proteobacteria*, at least 92% of the bacterial community.

Firmicutes and *Fusobacteria* contain bacteria related to human and animal gut, sometimes reported as opportunistic pathogens (Rinninella et al., 2019). *Firmicutes* drastically reduced in CAS (2.6±0.7%) and MBR (3.0±1.0%) while were of a very low abundance in PBR. *Fusobacteria* were mostly absent in all biological reactors.

Bacteroidetes were the second most abundant phylum in CAS and MBR with

relative abundance of 20.0%-27.2% and 22.4%-32.0%, respectively, while it accounted only for 5.2%-11.4% in PBR. *Cyanobacterium* was the second most abundant phylum in PBR (8.5%-24.3%). The operating conditions of PBR, especially light availability, ensured the presence of *Cyanobacteria*, which were of a very low abundance in WW, CAS and MBR. *Cyanobacterium* represents the largest group of photosynthetic prokaryotes (Dvořák et al. 2017), its establishment in PBR demonstrates that microalgal-bacterial consortium can developed spontaneously from the influent wastewater and remain stable.
The bacterial community of PBR differed from CAS and MBR also for a higher abundance of *Planctomycetes*, *Parcubacteria*, *Chloroflexi*, *Gemmatimonadetes*, *Nitrospirae* and *Acidobacteria*. On the contrary *Actinobacteria*, *Verrucomicrobia* were more abundant in both CAS and MBR, while *Saccharibacteria*, *Gracilibacteria* were more abundant in CAS than MBR.
Saccharibacteria has been detected in activated sludge, although little is known about phylogeny and physiology. However, recent studies have shown that they play a role on organic substrate degradation and floc formation and stability (Kindaichi t al., 2016; Takenaka et al., 2018).
Acidobacteria, *Chlorobi*, *Chloroflexi* and *Gemmatimonadetes* phyla comprise phototrophic bacteria that exploit light as energy source for their metabolism, without producing oxygen (Zeng and Koblížek 2017). Despite these phyla were present in PBR, no genus related to phototrophic microorganisms was found.

The above results demonstrate that bacterial community of the biological reactors differed from WW suggesting an adaptation to operational conditions (Gao et al., 2016). CAS and MBR had similar bacteria composition, which has been considered typical of activated sludge also in other works (Gao et al. 2016; Zhang et al. 2017; Zhang et al. 2018; Xu et al. 2018; Kim et al. 2019). The most abundant phyla in PBR differed from activated sludge, especially *Cyanobacteria*.
Throughout the sampling period, the microbiota composition of each group did not show drastic change in bacterial population. About PBR, it was demonstrated that a microalgal-bacterial consortium can develop spontaneously and reach steady state condition. Therefore, it is possible to characterize the bacte-

rial composition and its metabolic potentials. Since there are only few studies available at the present, further in-depth analysis would be of interest in unravelling the composition of PBR-associated microbiota and its functions.

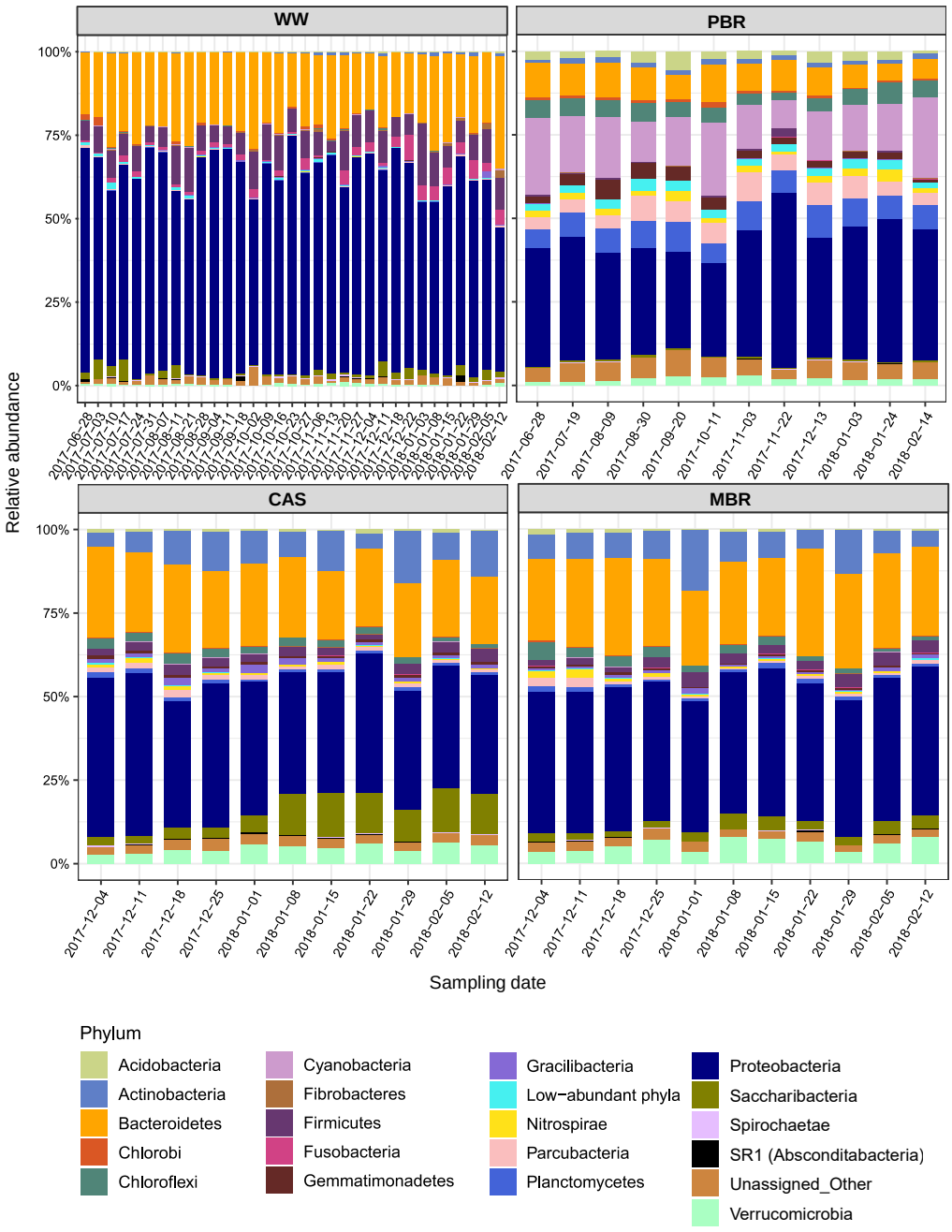

Figure 13.5 *Top-20 most abundant phyla distribution as percentage abundances in each group and per time points sampled. Low-abundant phyla were grouped together in the "Low-abundant phyla" group.*

CHAPTER 14

CONCLUSION

Microalgal-bacterial consortia represent a promising sustainable solution, alternative to activated sludge, in the secondary and tertiary treatment of municipal wastewater. The potentiality of this biological treatment relies on (free) photosynthetic oxygenation to replace mechanical aeration. However, this technology is in its early stage of development.
In view of the large-scale application, there are still some challenges to overcome in order to make microalgal-bacterial-based treatment competitive against activated sludge. To engineer the process, a certain gap of knowledge has emerged from the literature with respect to:

- Treatment of real municipal wastewater and removal performance in the long-term;
- Influence of the operational conditions on the treatment process;
- Development and stability of wastewater-born microbial community;
- Methods of investigation specifically design to characterize microalgal-bacterial consortia, both in terms of treatment performance and biomass composition.

To accomplish the research objectives (Section 2.8), closed photobioreactors, at a lab-scale, were installed and operated as sequencing-batch reactors. To note, the systems were exclusively fed with real municipal wastewater.

The results presented in Chapters 3, 4 and 5 showed that the initial inoculation of photobioreactors with pure microalgae strains is not necessary in systems aimed at treating real wastewater.
In fact, no significant differences were observed between the treatment performances of the two photobioreactors started-up with or without inoculation of *Chlorella vulgaris*. Moreover, the photosynthetic microorganisms were able to grow spontaneously. The bacterial population experienced an acclimation period (about a couple of months). Then, despite the initial presence of an inoculated microalgae, the microbiota adapted to the operational conditions and converged into a stable structure, different from the predominant bacteria present in the influent wastewater.
These findings confirm that wastewater microbiota is sufficient to start-up a photobioreactor. In view of the full-scale application, this means avoiding high sterilization cost of wastewater and initial inoculation of microalgae.

The long-term photo-sequencing batch reactor, called Pilot, proved the stability of microalgal-bacterial consortia to treat real municipal wastewater relying only on photosynthetic oxygenation (Chapter 6).
Over the entire experimentation, the system guaranteed high removal efficiency of COD, TKN and NH_4^+-N, with average values of 67±16%, 93±3% and 99±2%, respectively. The effluent concentration of COD and total nitrogen (on average) met the EU discharge limit (EU Directive 91/271/EEC). In addition, biomass aggregated in flocs ensured good settleability.
The stability of the treatment process enabled to characterize and optimized the Pilot performance, in particular:

- Chapter 7 showed the possibility to change the operational regime, exploiting light and dark periods (aerobic and anoxic conditions) to promote denitrification and thus enhance nitrogen removal. The operational conditions were also made with a view to energy saving;

- Real time monitoring with online sensors enabled to detect characteristic points along their profiles that revealed the complete ammonium oxida-

tion and the conclusion of the oxidation process.
Chapter 8 demonstrated that on-line monitoring is a useful tool to evaluate the conclusion of the wastewater treatment and thus to shorten the HRT. Reduce the HRT (and thus the footprint) is imperative for making microalgal-bacterial consortia more competitive than conventional activated sludge.
In the case of the Pilot, it emerged that the treatment was completed long before the end of the cycle. Therefore, the HRT of the Pilot (equal to 5.6 d) could be shortened more than 45%;

- Chapter 9 explores the limit of the Pilot. The effects of lower HRTs and outdoor condition on the removal efficiency were evaluated. Exploiting sunlight, the system ensured COD removal efficiency up to 75% at HRT of 1 d (applied load up to 330 mg COD L^{-1} d^{-1}), while the ammonium removal resulted limited at HRT of 1.4 d with a COD applied load higher than 150 mg COD L^{-1} d^{-1} that corresponded to a TKN applied load of about 50 mg N L^{-1} d^{-1}. To reduce the HRT and at the same time ensure nitrogen removal, photosynthetic oxidation should provide enough oxygen to sustain bacterial activity of both heterotrophs and nitrifiers.
In view of the full-scale application, for a sustainable and low-energy treatment, sunlight represents the cost-effective means to support (free) photosynthetic oxygenation, and thus should be exploit as light source.

High-throughput sequencing revealed that the bacterial community of the Pilot remained stable over 8 months of monitoring, with *Proteobacteria* and *Cyanobacteria* as predominant phyla (Chapter 13).
Interestingly, the microbial community of the photobioreactor resulted different from the activated sludge (collected from the full-scale wastewater treatment plant Trento Nord, Italy) treating the same real municipal wastewater. Different operating conditions promoted the development of a specific associated microbiota in the photobioreator. In fact, the use of shotgun metagenomics en-

abled the discovery of new environmental species presented in the microalgal-bacteria consortium (Chapter 4).
The results presented in Chapter 13 show that microalgal-bacterial consortium can develop spontaneously and reach steady state condition. Therefore, it is possible to characterize the bacterial composition and its metabolic potentials.

Experiments on ammonium removal rate in the Pilot (Chapter 6) highlighted that the specific ammonium removal rate was similar to activated sludge, however the volumetric rate was much lower due to the limited TSS concentration (3 times less than activated sludge). In view of the full-scale application, this results in a higher footprint compared to activated sludge.
In Chapter 10, the influence of the biomass concentration (measured as TSS) on the bacterial nitrification rate was explored. The results showed a solid-limited kinetic at low TSS concentrations and a light-limited kinetic at higher concentrations.
Assessment of the optimal TSS concentrations makes possible to concentrate the microbial biomass in a photobioreactor while ensuring high kinetics and a low footprint. Therefore, a standardize procedure to define the optimal TSS concentration in photobioreactors so as to guarantee the maximum ammonium removal rate, was proposed in Chapter 10.

Finally, advanced method of investigation, used in activated sludge, were extended to microalgal-bacterial consortia:

- An approach for respirometric tests was developed to monitor the global activity of microalgal-bacterial consortia under light and dark conditions. Kinetic and stoichiometric parameters were estimated for endogenous respiration, biodegradable COD oxidation and nitrification, of the microalgal-bacterial consortium developed in the Pilot. It emerged that the gross oxygen production rate of photosynthetic microorganisms, was just barely enough to cover the sum of the oxygen consumption rate for endogenous respiration, COD oxidation and ammonium oxidation. Thus, the treatment process may result oxygen limited at high applied load.
  The proposed comprehensive respirometric approach may serve as a

standard procedure to estimate parameters useful in the design of photobioreactors and essential to model microalgal-bacterial consortia;

- Flow cytometry was extended to analyze qualitatively and quantitatively microalgal-bacterial consortia.
  A multi-step procedure was proposed to ensure the accuracy of the FCM analysis thanks to an optimal sample pretreatment. Fluorescence and scattering signals were used to distinguish and quantify microalgae and bacteria. The microalgal-bacterial consortium developed in the Pilot was tested. FCM analysis revealed that bacteria were 98% of total cells. At the same time, microalgae, which accounted for only 2% of total cells, were characterized by a biovolume 2 orders of magnitude larger than bacteria, resulting in a photosynthetic biomass quantitatively comparable to bacteria. This would partially explain the high and stable removal treatment performance of the Pilot, in which bacterial activity was only sustained by photosynthetic oxygenation.
  The FCM approach proposed represents a valuable tool to enhance the knowledge about the composition and the quantification of microalgal-bacterial consortia. In addition, FCM analysis included in monitoring procedures of photobioreactors could detect anomalies with short analysis time (in the order of minutes).

The research project addressed many aspects and lay the foundation to apply a methodological research approach in the study of microalgal-bacterial consortia for wastewater treatment in view of the full-scale application of this promising technology.

Future works should:

- Test microalgal-bacterial consortia in photobioreactors at a pilot-scale to validate the operational consideration made in this research work;
- Exploit sunlight as solely light source, following the principles of sustainability and low-cost.

Indeed, further investigations are need to:

- Unravelling the composition of photobioreactor-associated microbiota and its functions;
- Clarify the phosphorous mechanisms removal;
- Implement a mathematical model with parameter based on experimental evidence;
- Valorized the biomass produced.

REFERENCES

Abinandan, S., Shanthakumar, S., 2015. Challenges and opportunities in application of microalgae (Chlorophyta) for wastewater treatment: A review. Renewable and Sustainable Energy Reviews, 52, 123-132. http://dx.doi.org/10.1016/j.rser.2015.07.086

Acién, F.G., Gómez-Serrano, C., Morales-Amaral, M.M., Fernández-Sevilla, J.M., Molina-Grima, E., 2016. Wastewater treatment using microalgae: how realistic a contribution might it be to significant urban wastewater treatment? Applied Microbiology and Biotechnology 100, 9013-9022. https://doi.org/10.1017/s00253-016-7835-7

Acién, F.G., Fernández-Sevilla, J.M., Molina-Grima, E., 2017. Microalgae: the basis of making sustainability. In: Case study of innovative projects - successful real cases. https://doi.org/10.5772/67930

Albertano, P., Congestri, R., Elliot Shubert, L.E., 1999. Cyanobacterial biofilms in sewage treatment plants along the Thyrrenian coast (Mediterranean Sea), Italy. Algological Studies/Archiv für Hydrobiologie 94,13-24. https://doi.org/10.1127/algol_stud/94/1999/13

Alcántara, C., Posadas, E., Guieysse, B., Muñoz, R., 2015. Microalgae-based wastewater treatment. In: Kim, S.K. (Ed.), Handbook of marine microalgae. Biotechnology Advances. Academic Press, London, pp. 439-455. https://doi.org/10.1016/B978-0-12-800776-1.00029-7

Allen, MB., 1952. The Cultivation of Myxophyceae. Archiv für Mikrobiologie 17, 34-53.

Álvarez-Díaz, P.D., Ruiz, J., Arbib, Z., Barragán, J., Garrido-Pérez, M.C., Perales, J.A., 2017. Freshwater microalgae selection for simultaneous wastewater nu-

trient removal and lipid production. Algal Research, 24, 477-485. http://dx.doi.org/10.1016/j.algal.2017.02.006

Åmand, L., Olsson, G., Carlsson, B., 2013. Aeration control - a review. Water Science and Technology 67, 2374-2398. https://doi.org/10.2166/wst.2013.139

Amin, S., Parker, M.S., Armbrust, E. V., 2012. Interactions between Diatoms and Bacteria. Microbiol. Mol. Biol. Rev. 76, 667-684. https://doi.org/10.1128/MMBR.00007-12

Anbalagan, A., Schwede, S., Lindberg, C., Nehrenheim, E., 2017. Influence of iron precipitated condition and light intensity on microalgae activated sludge based wastewater remediation. Chemosphere 168, 1523-1530. http://dx.doi.org/10.1016/j.chemosphere.2016.11.161

Andersen, R.A. 2005. Algal culturing techniques. Phycological Society of America. Elsevier academic press, Cambridge, Massachusetts, USA.

Andreottola, G., Foladori, P., Ragazzi, M., 2001. On-line control of a SBR system for nitrogen removal from industrial wastewater. Water Science and Technology 43, 93-100. https://doi.org/10.2166/wst.2001.0123

Anthonisen, A.C., Loehr, R.C., Prakasam, T.B.S., Srinath, E.G., 1976. Inhibition of nitrification by ammonia and nitrous acid. Journal of Water Pollution Control Federation 48, 835-852.

APHA, AWWA, WEF 2012. Standard Methods for the Examination of Water and Wastewater. 22th edn, American Public Health Association/American Water Works Association/Water Environment Federation, Washington DC, USA.

Arango, L., Cuervo, F.M., González-Sánchez, A., Buitrón, G., 2016. Effect of microalgae inoculation on the start-up of microalgae-bacteria systems treating municipal, piggery and digestate wastewaters. Water Science and Technology 73, 687-696. http://dx.doi.org/10.2166/wst.2015.544

Arcila, J.S., Buitrón, G., 2016. Microalgae-bacteria aggregates: effect of the

hydraulic retention time on the municipal wastewater treatment, biomass settleability and methane potential. Journal of Chemical Technology and Biotechnology 91, 2862-2870. http://dx.doi.org/10.1002/jctb.4901

Arcila, J.S., Buitrón, G., 2017. Influence of solar irradiance levels on the formation of microalgae-bacteria aggregates for municipal wastewater treatment. Algal Research, 27, 190-197. https://doi.org/10.1016/j.algal.2017.09.011

Ariede, M.B., Candido, T.M., Jacome, A.L.M., Robles Velasco, M.V., de Carvalho, J.C.M., Baby, A.R., 2017. Cosmetic attributes of algae - a review. Algal Research 25, 483-487. https://doi.org/10.1016/j.algal.2017.05.019

ASCE, 1993. Measurement of Oxygen Transfer in Clean Water, 2nd edn. American Society of Civil Engineers, New York, USA.

Azami, H., Sarrafzadeh, M.H., Mehrnia, M.R., 2012. Soluble microbial products (SMPs) release in activated sludge systems: a review. Iranian Journal of Environmental Health Science and Engineering 9, 30. http://dx.doi.org/10.1186/1735-2746-9-30

Barros, A., Gonçalves, A.L., Simões, M., Pires, J.C.M., 2015. Harvesting techniques applied to microalgae: A review. Renewable and Sustainable Energy Reviews 41, 1489-1500. https://doi.org/10.1016/j.rser.2014.09.037

Barsanti, L., Gualtieri, P., 2014. Algae: Anatomy, Biochemistry, and Biotechnology. Second Edition, CRC Press, Taylor and Francis, Boca Ratonm, USA.

Béchet, Q., Shilton, A., Guieysse, B., 2013. Modeling the effects of light and temperature on algae growth: State of the art and critical assessment for productivity prediction during outdoor cultivation. Biotechnology Advances 31, 1648-1663. http://dx.doi.org/10.1016/j.biotechadv.2013.08.014

Bellinger, E.G., Sigee, D.C., 2015. Biodiversity of mixed-species populations: microscope counts and biovolumes. In: Freshwater algae: identification, enumeration and use as bioindicators. 2nd edition. Wiley-Blackwell, Hoboken, New Jersey (USA).

Benjamini, Y., Hochberg, Y., 1995. Controlling the False Discovery Rate: A Practical and Powerful Approach to Multiple Testing. Journal of the Royal Statistical Society: Series B (Methodological) 57, 289-300. https://doi.org/10.1111/j.2517-6161.1995.tb02031.x

Bernaerts, T.M.M., Gheysen, L., Foubert, I., Hendrickx, M.E., Van Loey, A.M., 2019. The potential of microalgae and their biopolymers as structuring ingredients in food: a review Biotechnology Advances 37, 107419. https://doi.org/10.1016/j.biotechadv.2019.107419

Biggs, C.A., Lant, P.A., 2000. Activated sludge flocculation: on-line determination of floc size and the effect of shear. Water Research 34, 2542-2550. https://doi.org/10.1016/S0043-1354(99)00431-5

Bilad, M.R., Arafat, H.A., Vankelecom, I.F.J., 2014. Membrane technology in microalgae cultivation and harvesting:A review. Biotechnology Advances 32, 1283-1300. http://dx.doi.org/10.1016/j.biotechadv.2014.07.008

Blackburne R., Yuan Z., Keller J., 2008. Partial nitrification to nitrite using low dissolved oxygen concentration as the main selection factor. Biodegradation 19, 303-312. https://doi.org/10.1007/s10532-007-9136-4

Brennan, L., Owende, P., 2009. Biofuels from microalgae - A review of technologies for production, processing, and extractions of biofuels and co-products. Renewable and Sustainable Energy Reviews 14, 557-577. http://dx.doi.org/10.1016/j.rser.2009.10.009

Brindley, C., Acién, F.G., Fernandez-Sevilla, J.M., 2010. The oxygen evolution methodology affects photosynthetic rate measurements of microalgae in well-defined light regimes. Biotechnology and Bioengineering 106, 228-237. https:

//doi.org/10.1002/bit.22676

Cabanelas, I.T.D., Ruiz, J., Arbib, Z., Chinalia, F.A., Garrido-Pérez, C., Rogalla, F., Nascimento, I.A., Perales, J.A., 2013. Comparing the use of different domestic wastewaters for coupling microalgal production and nutrient removal. Bioresource Technology 131, 429-436. http://dx.doi.org/10.1016/j.biortech.2012.12.152

Cai, T., Park, S.Y., Li, Y., 2013 Nutrient recovery from wastewater streams by microalgae: Status and prospects. Renewable and Sustainable Energy Reviews 19, 360-369. http://dx.doi.org/10.1016/j.rser.2012.11.030

Cao, Y.S., 2011. Mass flow and energy efficiency of municipal wastewater treatment plants. IWA Publishing, London, UK.

Caporaso, J.G., Kuczynski, J., Stombaugh, J., Bittinger, K., Bushman, F.D., Costello, E.K., Fierer, N., Peña, A.G., Goodrich, J.K., Gordon, J.I., Huttley, G.A., Kelley, S.T., Knights, D., Koenig, J.E., Ley, R.E., Lozupone, C.A., McDonald, D., Muegge, B.D., Pirrung, M., Reeder, J., Sevinsky, J.R., Turnbaugh, P.J., Walters, W.A., Widmann, J., Yatsunenko, T., Zaneveld, J., Knight, R., 2010. QIIME allows analysis of high-throughput community sequencing data. Nature Methods 7, 335-336. https://doi.org/10.1038/nmeth.f.303

Cecchin, M., Benfatto, S., Griggio, F., Mori, A., Cazzaniga, S., Vitulo, N., Delledonne, M., Ballottari, M., 2018. Molecular basis of autotrophic vs mixotrophic growth in Chlorella sorokiniana. Scientific Reports 8, 6465-. https://doi.org/10.1038/s41598-018-24979-8

Chapman, R.L., 2013. Algae: the world's most important "plants"- an introduction. Mitigation and Adaptation Strategies for Global Change 18, 5-12. https://doi.org/10.1007/s11027-010-9255-9

Chew, K.W., Yap, J.Y., Show, P.L., Suan, N.H., Juan, J.C., Ling, T.C., Lee, D.J., Chang, J.S., 2017. Microalgae biorefinery: high value products perspectives. Bioresource Technology 229, 53-62.
http://dx.doi.org/10.1016/j.biortech.2017.01.006

Cho, H.U., Kim, Y.M., Park, J.M., 2017. Enhanced microalgal biomass and lipid production from a consortium of indigenous microalgae and bacteria present in municipal wastewater under gradually mixotrophic culture conditions. Bioresource Technology 228, 290-297. https://doi.org/10.1016/j.biortech.2016.12.094

Choi, O., Das, A., Yu, C.P., Hu, Z., 2010. Nitrifying bacterial growth inhibition in the presence of algae and cyanobacteria. Biotechnology and Bioengineering 107, 1004-1011. https://doi.org/10.1002/bit.22860

Christenson, L., Sims, R., 2011. Production and harvesting of microalgae for wastewater treatment, biofuels, and bioproducts. Biotechnology Advances 29, 686-702. http://dx.doi.org/10.1016/j.biotechadv.2011.05.015

Chu, C.P., Chang, B., Liao, G.S., Jean, D.S., Lee, D.J., 2001. Observations on changes in ultrasonically treated waste-activated sludge. Water Research 35, 1038-1046. https://doi.org/10.1016/S0043-1354(00)00338-9

Craggs, R.J. , Adey, W.H., Jessup, B.K., Oswald, W.J., 1996. A controlled stream mesocosm for tertiary treatment of sewage Ecological Engineering 6, 149-169.

Croft, M.T., Lawrence, A.D., Raux-Deery, E., Warren, M.J., Smith, A.G., 2005. Algae acquire vitamin B12 through a symbiotic relationship with bacteria. Nature 438, 90-93. https://doi.org/10.1038/nature04056

Cuellar-Bermudez, S.P., Aleman-Nava, G.S., Chandra, R., Garcia-Perez, J.S., Contreras-Angulo, J.R., Markou, G., Muylaert, K., Rittmann, B.E., Parra-Saldivar, R., 2017. Nutrients utilization and contaminants removal. A review of two approaches of algae and cyanobacteria in wastewater. Algal Research 24, 438-449. https://doi.org/10.1016/j.algal.2016.08.018

Cydzik-Kwiatkowska, A., Zielińska, M., 2016. Bacterial communities in full-scale wastewater treatment systems. World Journal of Microbiology and Biotechnology 32, 66. https://doi.org/10.1007/s11274-016-2012-9

Daims, H., 2014. The Family Nitrospiraceae, in: Rosenberg, E., DeLong, E.F.,

Lory, S., Stackebrandt, E., Thompson, F. (Eds.), The Prokaryotes. Springer Berlin Heidelberg, Berlin, Heidelberg, pp. 733-749.

De Godos, I., Arbid, Z., Lara, E., Cano, R., Muñoz, R., Rogalla, F., 2016. Wastewater treatment in algal systems. In: Novel Efficient Wastewater Treatment Processes (Considering Energetic, Economical and Environmental Aspects). IWA Publishing, London, UK.

de Jesús Martínez-Roldán, A., Ibarra-Berumen, J., 2019. Employment of Wastewater to Produce Microalgal Biomass as a Biorefinery Concept. In: Alam, A., Wang, Z., Microalgae Biotechnology for Development of Biofuel and Wastewater Treatment. Spring Nature Singapore. https://doi.org/10.1007/978-981-13-2264-8

Decostere, B., Janssens, N., Alvarado, A., Maere, T., Goethals, P., Van Hulle, S.W.H., Nopens, I., 2013. A combined respirometer-titrimeter for the determination of microalgae kinetics: Experimental data collection and modelling. Chemical Engineering Journal 222, 85-93.https://doi.org/10.1016/j.cej.2013.01.103

Decostere, B., Van Hulle, S.W.H., Duyck, M., Maere, T., Vervaeren, H., Nopens, I., 2014. The use of a combined respirometric-titrimetric setup to assess the effect of environmental conditions on micro-algal growth rate. Journal of Chemical Technology and Biotechnology 91, 248-256. https://doi.org/10.1002/jctb.4574

Decostere, B., De Craene, J., Van Hoey, S., Vervaeren, H., Nopens, I., Van Hulle, S., 2016. Validation of a microalgal growth model accounting with inorganic carbon and nutrient kinetics for wastewater treatment. Chemical Engineering Journal 285, 189-197. https://doi.org/10.1016/j.cej.2015.09.111

Delgadillo-Mirquez, L., Lopes, F., Taidi, B., Pareau, D., 2016. Nitrogen and phosphate removal from wastewater with a mixed microalgae and bacteria culture. Biotechnology Report, 11, 18-26. http://dx.doi.org/10.1016/

j.btre.2016.04.003

Deniz, I., García-Vaquero, M., Imamoglu, E., 2017. Trends in red biotechnology: Microalgae for pharmaceutical applications. In: Gonzalez-Fernandez, C., Muñoz, R., Microalgae-based biofuels and bioproducts. Woodhead Publishing Cambridge, UK.

Dennis, M.A., Landman, M., Wood, S.A., Hamilton, D., 2011. Application of flow cytometry for examining phytoplankton succession in two eutrophic lakes. Water Science Technology 64, 999-1008. https://doi.org/10.2166/wst.2011.099

Dineshbabu, G., Goswami, G., Kumar, R., Sinha, a., Das, D., 2019. Microalgae-nutritious, sustainable aqua- and animal feed source. Journal of Functional Foods 62, 103545. https://doi.org/10.1016/j.jff.2019.103545

Dutta, A., Sarkar, S., 2015. Sequencing batch reactor for wastewater treatment: recent advances. Current Pollution Reports 1, 177-190. https://doi.org/10.1007/s40726-015-0016-y

Dvořák, P., Casamatta, D.A., Hašler, P., Jahodářová, E., Norwich, A.R., Poulíčková, A., 2017. Diversity of the Cyanobacteria, in: Hallenbeck, P.C. (Ed.), Modern Topics in the Phototrophic Prokaryotes: Environmental and Applied Aspects. Springer International Publishing, Cham, Switzerland. pp. 3-46.

Edgar, R.C., 2010. Search and clustering orders of magnitude faster than BLAST. Bioinformatics 26, 2460-2461. https://doi.org/10.1093/bioinformatics/btq461

Eixler, S., Karsten, U., Selig, U., 2006. Phosphorus storage in *Chlorella vulgaris* (Trebouxiophyceae, Chlorophyta) cells and its dependence on phosphate supply. Phycologia 45, 53-60. https://doi.org/10.2216/04-79.1

Ekama, G.A., Wentzel, M.C., 2008. Nitrogen removal, in: biological wastewater treatment principles, modelling and design. IWA Publishing, London, UK. https://doi.org/10.2166/9781780401867

EU Directive 91/271/EEC (1991) Council Directive of 21 May 1991 concerning urban waste water treatment.

Eurostat, Statistics Explained: Electricity price statistics. http://ec.europa.eu/eurostat/statistics-explained/index.php/Electricity_price_statistics (Accessed 26 September 2017)

Falcioni, T., Manti, A., Boi, P., Canonico, B., Balsamo, M., Papa, S., 2006. Comparison of disruption procedures for enumeration of activated sludge floc bacteria by flow cytometry. Cytometry (Clinical Cytometry) 70B, 149-153. https://doi.org/10.1002/cyto.b.20097

Ferreira, A., Reis, A., Vidovic, S., Vladic, J., Gkelis, S., Melkonyan, L., Avetisova, G., Congestri, R., Acién, G., Muñoz, R., Collet, P., Gouveia, L., 2019. Combining Microalgae-Based Wastewater Treatment with Biofuel and Bio-Based Production in the Frame of a Biorefinery. In: Hallmann A., Rampelotto P. (eds) Grand Challenges in Algae Biotechnology. Grand Challenges in Biology and Biotechnology. Springer Nature, Cham, Switzerland. https://doi.org/10.1007/978-3-030-25233-5_9

Foladori, P., Bruni, L., Andreottola, G., Ziglio, G., 2007. Effects of sonication on bacteria viability in wastewater treatment plants evaluated by flow cytometry - Fecal indicators, wastewater and activated sludge. Water Research 41, 235-243. https://doi.org/10.1016/j.watres.2006.08.021

Foladori, P., Quaranta, A., Ziglio, G., 2008. Use of silica microspheres having refractive index similar to bacteria for conversion of flow cytometric forward light scatter into biovolume. Water Research 42, 3757-3766. https://doi.org/10.1016/j.watres.2008.06.026

Foladori, P., Andreottola, G., Ziglio, G., 2010a. Sludge Reduction Technologies in Wastewater Treatment Plants. London: IWA Publishing, 2010.

Foladori, P., Bruni, L., Tamburini, S., Ziglio, G., 2010b. Direct quantification of bacterial biomass in influent, effluent and activated sludge of wastewater treatment plants using flow cytometry. Water Research 44, 3807-3818. https:

//doi.org/10.1016/j.watres.2010.04.027

Foladori, P., Vaccari, M., Vitali, F., 2015. Energy audit in small wastewater treatment plants: methodology, energy consumption indicators, and lessons learned. Water Science and Technology 72, 1007-1015. http://dx.doi.org/10.2166/wst.2015.306

Frølund, B., Palmgren, R., Keiding, K., Nielsen, P.H., 1996. Extraction of extracellular polymers from activated sludge using a cation exchange resin. Water Research 30, 1749-1758. https://doi.org/10.1016/0043-1354(95)00323-1

Fuerst, J.A., Sagulenko, E., 2011. Beyond the bacterium: planctomycetes challenge our concepts of microbial structure and function. Nature Reviews Microbiology 9, 403-413. https://doi.org/10.1038/nrmicro2578

Gao, P., Xu, W., Sontag, P., Li, X., Xue, G., Liu, T., Sun, W., 2016. Correlating microbial community compositions with environmental factors in activated sludge from four full-scale municipal wastewater treatment plants in Shanghai, China. Applied Microbiology and Biotechnology 100, 4663-4673. https://doi.org/10.1007/s00253-016-7307-0

Gao, J., Zhu, J., Wang, M., Dong, W., 2018. Dominance and Growth Factors of Pseudanabaena sp. in Drinking Water Source Reservoirs, Southern China. Sustainability 10, 3936. https://doi.org/10.3390/su10113936

García, D., Alcántara, C., Blanco, S., Pérez, R., Bolado, S., Muñoz, R., 2017. Enhanced carbon, nitrogen and phosphorus removal from domestic wastewater in a novel anoxic-aerobic photobioreactor coupled with biogas upgrading. Chemical Engineering Journal 313, 424-434. http://dx.doi.org/10.1016/j.cej.2016.12.054

García, D., Posadas, E., Blanco, S., Acién, G., García-Encina, P., Bolado, S., Muñoz, R., 2018. Evaluation of the dynamics of microalgae population structure and process performance during piggery wastewater treatment in algal-bacterial photobioreactors. Bioresource Technology 248, 120-126. https:

//doi.org/10.1016/J.BIORTECH.2017.06.079

Geider, R.J., MacIntyre, H.L., Kana, T.M., 1998. A dynamic regulatory model of phytoplanktonic acclimation to light, nutrients, and temperature. Limnology Oceanography 43, 679-694. https://doi.org/10.4319/lo.1998.43.4.0679

Godos, I.D., Blanco, S., García-Encina, P.A., Becares, E., Muñoz, R., 2009. Long-term operation of high rate algal ponds for the bioremediation of piggery wastewaters at high loading rates. Bioresource Technology 100, 4332-4339. http://dx.doi.org/10.1016/j.biortech.2009.04.016

Gogate, P.R., 2002. Cavitation: an auxiliary technique in wastewater treatment schemes. Advances in Environmental Research 6, 335-358. https://doi.org/10.1016/S1093-0191(01)00067-3

Gonçalves, A.L., Pires, J.C.M., Simões, M., 2016. Wastewater polishing by consortia of *Chlorella vulgaris* and activated sludge native bacteria. Journal of Cleaner Production 133, 348-357. https://doi.org/10.1016/j.jclepro.2016.05.109

Gonçalves, A.L., Pires, J.C.M., Simões, M., 2017. A review on the use of microalgal consortia for wastewater treatment. Algal Research 24, 403-415. http://doi.org/10.1016/j.algal.2016.11.008

Gonçalves, A.L., Santos, F.M., Pires, J.C.M., 2019. Microalgal Consortia: From Wastewater Treatment to Bioenergy Production. In: Hallmann, A., Rampelotto, P., Grand Challenges in Algae Biotechnology. Grand Challenges in Biology and Biotechnology. Springer Nature Switzerland, Cham. https://doi.org/10.1007/978-3-030-25233-5_10

González-Fernández, C., Molinuevo-Salces, B., Cruz García-González, M., 2011. Nitrogen transformations under different conditions in open ponds by means of microalgae-bacteria consortium treating pig slurry. Bioresource Technology 102, 960-966. http://dx.doi.org/10.1016/j.biortech.2010.09.052

González-Fernández, C., Muñoz, R., 2017. Microalgae-Based Biofuels and Bioproducts. Woodhead Publishing, Elsevier 2017, Cambridge, UK.

Griffin, J., Wells, G., 2017. Regional synchrony in full-scale activated sludge bioreactors due to deterministic microbial community assembly. ISME Journal 11, 500-511. https://doi.org/10.1038/ismej.2016.121

Gupta, P.L., Choi, H.J., Pawar, R.R, Jung, S.P., Lee, S.M., 2016. Enhanced biomass production through optimization of carbon source and utilization of wastewater as a nutrient source. Journal of Environmental Management 184, 585-595. https://doi.org/10.1016/j.jenvman.2016.10.018

Gupta, S., Pawar, S.B., Pandey, R.A., 2019. Current practices and challenges in using microalgae for treatment of nutrient rich wastewater from agro-based industries. Science of the Total Environment 687, 1107-1126. https://doi.org/10.1016/j.scitotenv.2019.06.115

Gutzeit, G., Lorch, D., Weber, A., Engels, M., Neis, U., 2005. Bioflocculent algal-bacterial biomass improves low-cost wastewater treatment. Water Science and Technology 52, 9-18. https://doi.org/10.2166/wst.2005.0415

He, P.J., Mao, B., Lü, F., Shao, L.M., Lee, D.J., Chang, J.S., 2013. The combined effect of bacteria and *Chlorella vulgaris* on the treatment of municipal wastewaters. Bioresource Technology 146, 562-568. http://dx.doi.org/10.1016/j.biortech.2013.07.111

Henze, M., Gujer, W., Mino, T., Matsuo, T., van Loosdrecht, M.C.M., 2000. Activated Sludge Models ASM1, ASM2, ASM2d and ASM3. IWA Publishing, London, UK.

Henze, M., van Loosdrecht, M.C.M., Ekama, G.A., Brdjanovic, D., 2008. Biological Wastewater Treatment: Principles, Design and Modelling. IWA Publishing, London, UK. pp. 526.

Higgins, B.T., Gennity, I., Fitzgerald, P.S., Ceballos, S.J., Fiehn, O., VanderGheynst,

J.S., 2018. Algal-bacterial synergy in treatment of winery wastewater. npj Clean Water 1, 1-10. https://doi.org/10.1038/s41545-018-0005-y

Hu, Y., Hao, X., van Loosdrecht, M., Chen, H., 2017. Enrichment of highly settleable microalgal consortia in mixed cultures for effluent polishing and low-cost biomass production. Water Research 125, 11-22. http://dx.doi.org/10.1016/j.watres.2017.08.034

Hua, I., Thompson, J.E., 2000. Inactivation of Escherichia Coli by sonication at discrete ultrasonic frequencies. Water Research 34, 3888-3893. https://doi.org/10.1016/S0043-1354(00)00121-4

Huang, W., Li, B., Zhang, C., Zhang, Z., Lei, Z., Lu, B., Zhou, B., 2015. Effect of algae growth on aerobic granulation and nutrients removal from synthetic wastewater by using sequencing batch reactors. Bioresource Technology 179, 187-192. https://doi.org/10.1016/j.biortech.2014.12.024

Hyka, P., Lickova, S., Přibyl, P., Melzoch, K., Kovar, K., 2013. Flow cytometry for the development of biotechnological processes with microalgae. Biotechnology Advances 31, 2-16. https://doi.org/10.1016/j.biotechadv.2012.04.007

Iasimone, F., Panico, A., De Felice, V., Fantasma, F., Iorizzi, M., Pirozzi, F., 2018. Effect of light intensity and nutrients supply on microalgae cultivated in urban wastewater: Biomass production, lipids accumulation and settleability characteristics. Journal of Environmental Management 223, 1078-1085. https://doi.org/10.1016/j.jenvman.2018.07.024

Ippoliti, D., Gómez, C., del Mar Morales-Amaral, M., Pistocchi, R., Fernández-Sevilla, J.M., Gabriel, Acién, F., 2016. Modeling of photosynthesis and respiration rate for Isochrysis galbana (T-Iso) and its influence on the production of this strain. Biores. Technol. 203, 71-79. https://doi.org/10.1016/j.biortech.2015.12.050

Jaramillo, F., Orchard, M., Muñoz, C., Zamorano, M., Antileo, C., 2018. Advanced strategies to improve nitrification process in sequencing batch reac-

tors - a review. Journal of Environmental Management 218, 154-164. https://doi.org/10.1016/j.jenvman.2018.04.019

Johnston, J., LaPara, T., Behrens, S., 2019. Composition and Dynamics of the Activated Sludge Microbiome during Seasonal Nitrification Failure. Scientific Reports 9, 4565. https://doi.org/10.1038/s41598-019-40872-4

Judd, S.J., van den Broeke, L.J.P., Shurair, M., Kuti, Y., Znad, H., 2015. Algal remediation of CO2 and nutrient discharges: a review. Water Research 87, 356-366. http://dx.doi.org/10.1016/j.watres.2015.08.021

Kang, D.D., Froula, J., Egan, R., Wang, Z., 2015. MetaBAT, an efficient tool for accurately reconstructing single genomes from complex microbial communities. PeerJ 3, e1165. https://doi.org/10.7717/peerj.1165

Kang, D., Kim, K., Jang, Y., Moon, H., Ju, D., Jahng, D., 2018. Nutrient removal and community structure of wastewater-borne algal-bacterial consortia grown in raw wastewater with various wavelengths of light. International Biodeterioration and Biodegradation 126, 10-20. https://doi.org/10.1016/j.ibiod.2017.09.022

Karya, N.G.A.I., van der Steen, N.P., Lens, P.N.L., 2013. Photo-oxygenation to support nitrification in an algal-bacterial consortium treating artificial wastewater. Bioresource Technology 134, 244-250. http://dx.doi.org/10.1016/j.biortech.2013.02.005

Kennish, M.J., de Jonge, V.N., 2011. Chemical Introductions to the Systems: Diffuse and Nonpoint Source Pollution from Chemicals (Nutrients: Eutrophication). In: Kennish, M.J. and Elliott, M., Eds., Treatise on Estuarine and Coastal Science (Vol. 8, Human-Induced Problems (Uses and Abuses)), Elsevier, Oxford, UK. http://dx.doi.org/10.1016/b978-0-12-374711-2.00806-8

Khalil, Z.I., Asker, M.M., El-Sayed, S., Kobbia, I.A., 2010. Effect of pH on growth and biochemical of Donaliella and Chlorella. World Journal of Microbiology and Biotechnology 26, 1225-1231. https://doi.org/10.1016/j.

egypro.2014.12.064

Khan, M.I., Shin, J.H., Kim, J.D., 2018. The promising future of microalgae: current status, challenges, and optimization of a sustainable and renewable industry for biofuels, feed, and other products. Microbial Cell Factories 17, 1-21. https://doi.org/10.1186/s12934-018-0879-x

Kim, H., Hao, O.J., 2001. pH and oxidation-reduction potential control strategy for optimization of nitrogen removal in an alternating aerobic-anoxic system. Water Environ Research 73, 95-102. https://doi.org/10.2175/106143001X138741

Kim, Y.K., Yoo, K., Kim, M.S., Han, I., Lee, M., Kang, B.R., Lee, T.K., Park, J., 2019. The capacity of wastewater treatment plants drives bacterial community structure and its assembly. Scientific Report 9, 14809. https://doi.org/10.1038/s41598-019-50952-0

Kindaichi, T., Yamaoka, S., Uehara, R., Ozaki, N., Ohashi, A., Albertsen, M., Nielsen, P., Nielsen, J., 2016. Phylogenetic diversity and ecophysiology of Candidate phylum Saccharibacteria in activated sludge. FEMS Microbiology Ecology 92, fiw078. https://doi.org/10.1093/femsec/fiw078

Klindworth, A., Pruesse, E., Schweer, T., Peplies, J., Quast, C., Horn, M., Gl öckner, F.O., 2013. Evaluation of general 16S ribosomal RNA gene PCR primers for classical and next-generation sequencing-based diversity studies. Nucleic Acids Research 41, e1. https://doi.org/10.1093/nar/gks808

Kliphuis, A. M. J., Janssen, M., van den End, E.J., Martens, D.E., Wijffels, R.H., 2011. Light respiration in Chlorella sorokiniana. Journal of applied phycology 23, 935-947. https://doi.org/10.1007/s10811-010-9614-7

Kouzuma, A., Watanabe, K., 2015. Exploring the potential of algae/bacteria interactions. Current Opinion in Biotechnology 33, 125-129. https://doi.org/10.1016/j.copbio.2015.02.007

Krustok, I., Odlare, M., Shabiimam, M.A., Truu, J., Truu, M., Ligi, T., Nehren-

heim, E., 2015. Characterization of algal and microbial community growth in a wastewater treating batch photo-bioreactor inoculated with lake water. Algal Research 11, 421-427. https://doi.org/10.1016/j.algal.2015.02.005

Krustok, I., Odlare, M., Truu, J., Nehrenheim, E., 2016. Inhibition of nitrification in municipal wastewater-treating photobioreactors: Effect on algal growth and nutrient uptake. Bioresource Technology 202, 238-243. https://doi.org/10.1016/j.biortech.2015.12.020

Langdon, C., 1988. On the causes of interspecific differences in the growth-irradiance relationship for phytoplankton. II. A general review. Journal of Plankton Research 10, 1291-1312. http://dx.doi.org/10.1093/plankt/10.6.1291

Langmead, B., Salzberg, S.L., 2012. Fast gapped-read alignment with Bowtie 2. Nature Methods 9, 357-359. https://doi.org/10.1038/nmeth.1923

Le, T.T.H., Fettig, J., Meon, G., 2019. Kinetics and simulation of nitrification at various pH values of a polluted river in the tropics. Ecohydrology and Hydrobiology 19, 54-65. https://doi.org/10.1016/j.ecohyd.2018.06.006

Lee, A.K., Lewis, D.M., Ashman, P.J., 2010. Energy requirements and economic analysis of a full-scale microbial flocculation system for microalgal harvesting. Chemical Engineering Research and Design 88, 988-996. https://doi.org/10.1016/j.cherd.2010.01.036

Lee, C.G., Palsson, B., 1994. High-density algal photobioreactors using light-emitting diodes. Biotechnology and Bioengineering 44, 1161-1167. https://doi.org/10.1002/bit.260441002

Lee, C.S., Lee, S., Ko, S., Oh, H., Ahn, C., 2015. Effects of photoperiod on nutrient removal, biomass production, and algal-bacterial population dynamics in lab-scale photobioreactors treating municipal wastewater. Water Research 68, 680-691. http://dx.doi.org/10.1016/j.watres.2014.10.029

Lee R.E., 2008. Phycology. 4th edition, Cambridge University press, Cambridge, UK.

Lee, Y., Lei, Z., 2019. Microalgal-bacterial aggregates for wastewater treatment: A mini-review. Bioresource Technology Reports 8, 100199. https://doi.org/10.1016/j.biteb.2019.100199

Leong, W., Lim, J., Lam, M., Yoshimitsu, U., Ho, C., Ho, Y., 2018. Co-cultivation of activated sludge and microalgae for the simultaneous enhancements of nitrogen-rich wastewater bioremediation and lipid production. Journal of the Taiwan Institute of Chemical Engineers 87, 216-224. https://doi.org/10.1016/j.jtice.2018.03.038

Li, D., Liu, C.M., Luo, R., Sadakane, K., Lam, T.W., 2015. MEGAHIT: an ultra-fast single-node solution for large and complex metagenomics assembly via succinct de Bruijn graph. Bioinformatics 31, 1674-1676. https://doi.org/10.1093/bioinformatics/btv033

Li, K., Liu, Q., Fang, F., Luo, R., Lu, Q., Zhou, W., Juo, S.,Cheng, P., Liu, J., Addy, M., Chen, P., Chen, D., Ruan, R., 2019. Microalgae-based wastewater treatment for nutrients recovery: A review. Bioresource technology 291, 121934. https://doi.org/10.1016/j.biortech.2019.121934

Li, Y., Chen, Y., Chen, P., Min, M., Zhou, W., Martinez, B., Zhu, J., Ruan, R., 2011. Characterization of a microalga Chlorella sp. well adapted to highly concentrated municipal wastewater for nutrient removal and biodiesel production. Bioresource technology 102, 5138-5144. https://doi.org/10.1016/j.biortech.2011.01.091

Liu, J., Wua, Y., Wu, C., Muylaert, K., Vyverman, W., Yu, H.Q., Muñoz, R., Rittmann, B., 2017. Advanced nutrient removal from surface water by a consortium of attachedmicroalgae and bacteria: a review. Bioresource Technology 241, 1127-1137. http://dx.doi.org/10.1016/j.biortech.2017.06.054

Liu, L., Fan, H., Liu, Y., Liu, C., Huang, X., 2017. Development of algae-bacteria granular consortia in photo-sequencing batch reactor. Bioresource

Technology 232, 64-71. https://doi.org/10.1016/j.biortech.2017.02.025

Liu, L., Zhao, Y., Jiang, X., Wang, X., Liang, W., 2018. Lipid accumulation of Chlorella pyrenoidosa under mixotrophic cultivation using acetate and ammonium. Bioresource Technology 262, 342-346. https://doi.org/10.1016/j.biortech.2018.04.092

Liu, Y.Q., Lan, G.H., Zeng, P., 2015. Resistance and resilience of nitrifying bacteria in aerobic granules to pH shock. Letters in Applied Microbiology 61, 91-97. https://doi.org/10.1111/lam.12433

López-Rosales, L., García-Camacho, F., Sánchez-Mirón, A., Beato, E.M., Chisti, Y., Grima, E.M., 2016. Pilot-scale bubble column photobioreactor culture of a marine dinoflagellate microalga illuminated with light emission diodes. Bioresource Technology 216, 845-855. http://dx.doi.org/10.1016/j.biortech.2016.06.027

Ludwig, H.F, Oswald, W.J, Gotaas, H.B, Lynch, V., 1951. Algal symbiosis in oxidation ponds. 1. Growth characteristics of Euglena gracilis cultured in sewage. Sewage and Industrial Wastes 23, 1337-1354.

Luo, Y., Le-Clech, P., Henderson, R.K., 2017. Simultaneous microalgae cultivation and wastewater treatment in submerged membrane photobioreactors: A review. Algal Research 24, 425-437. https://doi.org/10.1016/j.algal.2016.10.026

Luo, Y., Le-Clech, P., Henderson, R.K., 2018. Assessment of membrane photobioreactor (MPBR) performance parameters and operating conditions. Water Research 138, 169-180. https://doi.org/10.1016/j.watres.2018.03.050

Luo, L., Dzakpasu, M., Yang, B., Zhang, W., Yang, Y., Wang, X.,C., 2019. A novel index of total oxygen demand for the comprehensive evaluation of energy consumption for urban wastewater treatment. Applied Energy 236, 253-261. https://doi.org/10.1016/j.apenergy.2018.11.101

Mamais, D., Noutsopoulos, C., Dimopoulou, A., Stasinakis, A., Lekkas, T.D., 2015. Wastewater treatment process impact on energy savings and greenhouse gas emissions. Water Science and Technology 71, 303-308. https://doi.org/10.2166/wst.2014.521

Manser, N.D., Wang, M., Ergas, S.J., Mihelcic, J.R., Mulder, A., van de Vossenberg, J., van Lier, J.B., van der Steen, P., 2016. Biological nitrogen removal in a photosequencing batch reactor with an algal-nitrifying bacterial consortium and anammox granules. Environmental Science and Technology Letters 3, 175-179. https://doi.org/10.1021/acs.estlett.6b00034

Mantikci, M., Hansen, J.L.S., Markager, S., 2017. Photosynthesis enhanced dark respiration in three marine phytoplankton species. Journal of Experimental Marine Biology and Ecology 497, 188-196. http://dx.doi.org/10.1016/j.jembe.2017.09.015

Marchão, L., da Silva, T.L., Gouveia, L., Reis, A., 2018. Microalgae-mediated brewery wastewater treatment: effect of dilution rate on nutrient removal rates, biomass biochemical composition, and cell physiology. Journal of Applied Phycology 30, 1583-1595. https://doi.org/10.1007/s10811-017-1374-1

Martín de la Vega, P.T., Martínez de Salazar, E., Jaramillo, M.A., Cros, J., 2012. New contributions to the ORP and DO time profile characterization to improve biological nutrient removal. Bioresource Technology 114, 160-167. http://dx.doi.org/10.1016/j.biortech.2012.03.039

Masella, A.P., Bartram, A.K., Truszkowski, J.M., Brown, D.G., Neufeld, J.D., 2012. PANDAseq: paired-end assembler for illumina sequences. BMC Bioinformatics 13, 31. https://doi.org/10.1186/1471-2105-13-31

Matamoros, V., Gutiérrez, R., Ferrer, I., García, J., Bayona, J.M., 2015. Capability of microalgae-based wastewater treatment systems to remove emerging organic contaminants: A pilot-scale study. Journal of Hazardous Materials 288, 34-42. http://dx.doi.org/10.1016/j.jhazmat.2015.02.002

Meng, F., Xi, L., Liu, D., Huang, W., Lei, Z., Zhang, Z., Huang, W., 2019. Ef-

fects of light intensity on oxygen distribution, lipid production and biological community of algal-bacterial granules in photo-sequencing batch reactors. Bioresource Technology 272, 473-481. https://doi.org/10.1016/j.biortech.2018.10.059

Mennaa, F.Z., Arbib, Z., Perales, J.A., 2015. Urban wastewater treatment by seven species of microalgae and an algal bloom: Biomass production, N and P removal kinetics and harvestability. Water Research 83, 42-51. http://dx.doi.org/10.1016/j.watres.2015.06.007

Mishra, A., Medhi, K., Malaviya, P., Thakur, I.,S., 2019. Omics approaches for microalgal applications: Prospects and challenges. Bioresource Technology 291, 121890. https://doi.org/10.1016/j.biortech.2019.121890

Molinuevo-Salces, B., García-González, M.C., González-Fernández, C., 2010. Performance comparison of two photobioreactors configurations (open and closed to the atmosphere) treating anaerobically degraded swine slurry. Bioresource Technology 101, 5144-5149.
https://doi.org/10.1016/j.biortech.2010.02.006

Molinuevo-Salces, B., Riaño, B., Hernández, D., Cruz Gracía-González, M., 2019. Microalgae and Wastewater Treatment: Advantages and Disadvantages. In: Alam, A., Wang, Z., Microalgae Biotechnology for Development of Biofuel and Wastewater Treatment. Spring Nature Singapore. https://doi.org/10.1007/978-981-13-2264-8

Morel, F.M.M., Hering, J.G., 1993. Principles and Applications of Aquatic Chemistry, John Wiley and Sons Inc, New York.

Mujtaba, G., Rizwan, M., Lee, K., 2017. Removal of nutrients and COD from wastewater using symbiotic co-culture of bacterium Pseudomonas putida and immobilized microalga *Chlorella vulgaris*. Journal of Industrial and Engineering Chemistry 49, 145-151. http://dx.doi.org/10.1016/j.jiec.2017.01.021

Mujtaba, G., Lee, K., 2017. Treatment of real wastewater using co-culture. Wa-

ter Research 120, 174-184. http://dx.doi.org/10.1016/j.watres.2017.04.078

Muñoz, R., Jacinto, M., Guieysse, B., Mattiasson, B., 2005. Combined carbon and nitrogen removal from acetonitrile using algal-bacterial bioreactors.Applied Microbiology and Biotechnology 67, 699-707. https://doi.org/10.1007/s00253-004-1811-3

Muñoz, R., Guieysse, B., 2006. Algal-bacterial processes for the treatment of hazardous contaminants: a review. Water Research 40, 2799-2815. http://dx.doi.org/10.1016/j.watres.2006.06.011

Muñoz, R., Alvarez, T., Muñoz, A., Terrazas, E., Guieysse, B., Mattiasson, B., 2006. Sequential removal of heavy metals ions and organic pollutants using an algal-bacterial consortium. Chemosphere 63, 903-911. https://doi.org/10.1016/j.chemosphere.2005.09.062

Myers, J., Cramer, M., 1948. Metabolic conditions in Chlorella. J. Gen. Physiol. 32, 103-110. http://dx.doi.org/10.1085/jgp.32.1.103

Najm, Y., Jeong, S., Leiknes, T., 2017. Nutrient utilization and oxygen production by *Chlorella vulgaris* in a hybrid membrane bioreactor and algal membrane photobioreactor system. Bioresource Technology 237, 64-71. http://dx.doi.org/10.1016/j.biortech.2017.02.057

Nascimento, A.L., Souza, A.J., Andrade, P.A.M., Andreote, F.D., Coscione, A.R., Oliveira, F.C., Regitano, J.B., 2018. Sewage Sludge Microbial Structures and Relations to Their Sources, Treatments, and Chemical Attributes. Frontiers in Microbiology 9, 1462. https://doi.org/10.3389/fmicb.2018.01462

Olsson, G., Nielsen, M.K., Jensen, A.L., Yuan, Z., 2005. Instrumentation, Control and Automation in Wastewater Systems. Scientific and Technical Report No. 15. IWA Publishing, London, UK.

Ondov, B.D., Treangen, T.J., Melsted, P., Mallonee, A.B., Bergman, N.H., Koren, S., Phillippy, A.M., 2016. Mash: fast genome and metagenome distance

estimation using MinHash. Genome Biology 17, 132. https://doi.org/10.1186/s13059-016-0997-x

Oswald, W.J., Gotaas, H.B., Ludwig, H.F., Lynch, V., 1953. Algae Symbiosis in Oxidation Ponds: III. Photosynthetic Oxygenation. Sewage Industrial Wastes 25, 692-705.

Pan, L.A., Zhang, L.H., Zhang, J., Gasol, J.M, Chao, M., 2005. On-board flow cytometric observation of picoplankton community structure in the East China Sea during the fall of different years. FEMS Microbiol Ecology 52, 243-253. https://doi.org/10.1016/j.femsec.2004.11.019

Park, J.B.K., Craggs, R.J., Shilton, A.N., 2011. Recycling algae to improve species control and harvest efficiency from a high rate algal pond. Water Research 45, 6637-6649. http://dx.doi.org/10.1016/j.watres.2011.09.042

Parks, D.H., Imelfort, M., Skennerton, C.T., Hugenholtz, P., Tyson, G.W., 2015. CheckM: assessing the quality of microbial genomes recovered from isolates, single cells, and metagenomes. Genome Research 25, 1043-1055. https://doi.org/10.1101/gr.186072.114

Pasolli, E., Asnicar, F., Manara, S., Zolfo, M., Karcher, N., Armanini, F., Beghini, F., Manghi, P., Tett, A., Ghensi, P., Collado, M.C., Rice, B.L., DuLong, C., Morgan, X.C., Golden, C.D., Quince, C., Huttenhower, C., Segata, N., 2019. Extensive Unexplored Human Microbiome Diversity Revealed by Over 150,000 Genomes from Metagenomes Spanning Age, Geography, and Lifestyle. Cell 176, 649-662. https://doi.org/10.1016/j.cell.2019.01.001

Pastore, M., Santaeufemia, S., Bertucco, A., Sforza, E., 2018. Light intensity affects the mixotrophic carbon exploitation in Chlorella protothecoides: consequences on microalgae-bacteria based wastewater treatment. Water Science and Technology 78, 1762-1771. https://doi.org/10.2166/wst.2018.462

Paul, E., Plisson-Saune, S., Mauret, M., Cantet, J., 1998. Process state eval-

uation of alternating oxic-anoxic activated sludge using ORP, pH and DO. Water Science and Technology 38 (3), 299-306.https://doi.org/10.1016/S0273-1223(98)00469-7

Peng, Y.Z., Maa, Y., Wang, S.Y., 2006. Improving nitrogen removal using online sensors in the A/O process. Biochemical Engineering Journal 31, 48-55. https://doi.org/10.1016/j.bej.2006.05.023

Peniuk, G.T., Schnurr, P.J., Allen, D.G., 2016. Identification and quantification of suspended algae and bacteria populations using flow cytometry: applications for algae biofuel and biochemical growth systems. Journal of Applied Phycology 28, 95-104. https://doi.org/10.1007/s10811-015-0569-6

Perera, I.A., Abinandan, S., Subashchandrabose, S.R., Venkateswarlu, K., Ravi, N., Mallavarapu, M., 2019. Advances in the technologies for studying consortia of bacteria and cyanobacteria/microalgae in wastewaters. Critical Reviews in Biotechnology 39, 709-731. https://doi.org/10.1080/07388551.2019.1597828

Porter, J., Deere, D., Hardman, M., Edwards, C., Pickup, R., 1997. Go with the flow - use of flow cytometry in environmental microbiology. FEMS Microbiology Ecology 24, 93-101. https://doi.org/10.1111/j.1574-6941.1997.tb00426.x

Posadas, E., García-Encina, P.A., Soltau, A., Domínguez, A., Díaz, I., Muñoz, R., 2013. Carbon and nutrient removal from centrates and domestic wastewater using algal-bacterial biofilm bioreactors. Bioresource Technology 139, 50-58. https://doi.org/10.1016/j.biortech.2014.03.057

Posadas, E., Bochon, S., Coca, M., García-González, M.C., García-Encina, P.A., Muñoz, R., 2014. Microalgae-based agro-industrial wastewater treatment: a preliminary screening of biodegradability. Journal of Applied Phycology 26, 2335-2345. https://doi.org/10.1007/s10811-014-0263-0

Posadas, E., del Mar Morales, M., Gomez, C., Acién, F.G., Muñoz, R., 2015. Influence of pH and CO_2 source on the performance of microalgae-based sec-

ondary domestic wastewater treatment in outdoors pilot raceways, Chemical Engineering Journal 265, 239-248. https://doi.org/10.1016/j.cej.2014.12.059.

Posadas, E., Alcántara, C., García-Encina, P.A., Gouveia, L., Guieysse, B., Norvill, Z., Acién, F.G., Markou, G., Congestri, R., Koreiviene, J., Muñoz, R., 2017. Microalgae cultivation in wastewater, in: Microalgae-Based Biofuels and Bioproducts: From Feedstock Cultivation to End-Products. pp. 67-91. https://doi.org/10.1016/B978-0-08-101023-5.00003-0

Powell, N., Shilton, A., Pratt, S., Chisti, Y., 2008. Factors influencing luxury uptake of phosphorus by microalgae in waste stabilization ponds. Environmental Science and Technology 42, 5958-5962. https://doi.org/10.1021/es703118s

Powell, N., Shilton, A., Chisti, Y., Pratt, S., 2009. Towards a luxury uptake process via microalgae - Defining the polyphosphate dynamics. Water Research 43, 4207-4213. http://dx.doi.org/10.1016/j.watres.2009.06.011

Prosser, J.I., Head, I.M., Stein, L.Y., 2014. The Family Nitrosomonadaceae, in: Rosenberg, E., DeLong, E.F., Lory, S., Stackebrandt, E., Thompson, F. (Eds.), The Prokaryotes: Alphaproteobacteria and Betaproteobacteria. Springer Berlin Heidelberg, Berlin, Heidelberg, pp. 901-918.

Pruesse E., Quast C., Knittel K., Fuchs B.M., Ludwig W., Peplies J., Glöckner, F.O. , 2007. SILVA: a comprehensive online resource for quality checked and aligned ribosomal RNA sequence data compatible with ARB. Nucleic Acids Research 35, 7188-7196. https://doi.org/10.1093/nar/gkm864

Quast, C., Pruesse, E., Yilmaz, P., Gerken, J., Schweer, T., Yarza, P., Peplies, J., Glöckner, F.O., 2013. The SILVA ribosomal RNA gene database project: improved data processing and web-based tools. Nucleic Acids Res. 41, D590-6. https://doi.org/10.1093/nar/gks1219

Quijano, G., Arcila, J.S., Buitrón, G., 2017. Microalgal-bacterial aggregates: Applications and perspectives for wastewater treatment. Biotechnology Ad-

vances 35, 772-781. http://dx.doi.org/10.1016/j.biotechadv.2017.07.003

Rada-Ariza, A.M., Lopez-Vazquez, C.M., van der Steen, N.P., Lens, P.N.L., 2017. Nitrfication by microalgal-bacterial consortia for ammonium removal in flat panel sequencing batch photo-bioreactors. Bioresource Technology 245, 81-89. https://doi.org/10.1016/j.biortech.2017.08.019

Ramanan, R., Kim, B.-H., Cho, D.-H., Oh, H.-M., Kim, H.-S., 2016. Algae-bacteria interactions: Evolution, ecology and emerging applications. Biotechnology Advances 34, 14-29. https://doi.org/10.1016/j.biotechadv.2015.12.003

Razzak, S.,A., Hossain, M.M., Lucky, R.A., Bassi, A.S., de Lasa, H., 2013. Integrated CO_2 capture, wastewater treatment and biofuel production by microalgae culturing - A review. Renewable and Sustainable Energy Reviews 27, 622-653. http://dx.doi.org/10.1016/j.rser.2013.05.063

Renuka, N. , Guldhe, A., Prasanna, R., Singh, P., Bux, F., 2018. Microalgae as multi-functional options in modern agriculture: current trends, prospects and challenges. Biotechnology Advances 36, 1255-1273. https://doi.org/10.1016/j.biotechadv.2018.04.004

Riaño, B., Hernández, D., García-González, M.C., 2012. Microalgal-based systems for wastewater treatment: effect of applied organic and nutrient loading rate on biomass composition. Ecological Engineering 49, 112-117. https://doi.org/10.1016/j.ecoleng.2012.08.021

Richmond, A.,2004. Handbook of microalgal culture: biotechnology and applied phycology. Blackwell Science Ltd, Oxford, UK.

Rinninella, E., Raoul, P., Cintoni, M., Franceschi, F., Miggiano, G.A.D., Gasbarrini, A., Mele, M.C., 2019. What is the Healthy Gut Microbiota Composition? A Changing Ecosystem across Age, Environment, Diet, and Diseases. Microorganisms 7, 14. https://doi.org/10.3390/microorganisms7010014

Rossi, S., Bellucci, M., Marazzi, F., Mezzanotte, V., Ficara, E., 2018. Activity assessment of microalgal-bacterial consortia based on respirometric tests. Water Science and Technology 78, 207-215. https://doi.org/10.2166/wst.2018.078

Rossi, S., Sforza, E., Pastore, M., Bellucci, M., Casagli, F., Marazzi, F., Ficara, E., 2020. Photo-respirometry to shed light on microalgae-bacteria consortia - a review. Reviews in Environmental Science and Bio/Technology 19, 43-72. https://doi.org/10.1007/s11157-020-09524-2

Ruiz-Martinez, A., Serralta, J., Seco, A., Ferrer, J., 2016. Behavior of mixed Chlorophyceae cultures under prolonged darkexposure. Respiration rate modeling. Ecologiacl Engineering 91, 265-269. http://dx.doi.org/10.1016/j.ecoleng.2016.02.025

Ryu, B.G., Kim, E.J., Kim, H.S., Kim, J., Choi, Y.E., Yang, J.W., 2014. Simultaneous treatment of municipal wastewater and biodiesel production by cultivation of *Chlorella vulgaris* with indigenous wastewater bacteria. Biotechnology and Bioprocess Engineering 19, 201-210. http://dx.doi.org/10.1007/s12257-013-0250-3

Safi, C., Zebib, B., Merah, O., Pontalier, P.Y., Vaca-Garcia, C., 2014. Morphology, composition, production, processing and applications of *Chlorella vulgaris*: A review. Renewable and Sustainable Energy Reviews 35, 265-278. https://doi.org/10.1016/j.rser.2014.04.007

Safford, H.R., Bischel, H.N., 2019. Flow cytometry applications in water treatment, distribution, and reuse: A review. Water Research 151, 110-133. https://doi.org/10.1016/j.watres.2018.12.016

Salzman, H.M., Singham, S.B., Johnston, R.G., Bohren, C.F., 1990. Light scattering and cytometry. In: Melamed NR et al. Flow cytometry and sorting. 2nd ed., Wiley, New York (USA) p. 81-107.

Saunders, A.M., Albertsen, M., Vollertsen, J., Nielsen, P.H., 2016. The activated sludge ecosystem contains a core community of abundant organisms.

ISME Journal 10, 11-20. https://doi.org/10.1038/ismej.2015.117

Sforza, E., Pastore, M., Spagni, A., Bertucco, A., 2018. Microalgae-bacteria gas exchange in wastewater: how mixotrophy may reduce the oxygen supply for bacteria. Environmental Science and Pollution Research 25, 28004-28014. https://doi.org/10.1007/s11356-018-2834-0

Sforza, E., Pastore, M., Barbera, E., Bertucco, A., 2019. Respirometry as a tool to quantify kinetic parameters of microalgal mixotrophic growth. Bioprocess and Biosystems Engineering 45, 839-851. https://doi.org/10.1007/s00449-019-02087-9

Shapiro, HM., 2013. Practical flow cytometry. Fourth Edition. Wiley-Liss, Inc New York, USA.

Shen, Y., Linville, J.L., Urgun-Demirtas, M., Mintz, M.M., Snyder, S.W., 2015. An overview of biogas production and utilization at full-scale wastewater treatment plants (WWTPs) in the United States: Challenges and opportunities towards energy-neutral WWTPs. Renewable and Sustainable Energy Reviews 50, 346-362. https://doi.org/10.1016/j.rser.2015.04.129

Simis S.G.H., Huot Y., Babin M., Seppälä J., Metsamaa L., 2012. Optimization of variable fluorescence measurements of phytoplankton communities with cyanobacteria. Photosynthesis Research 112, 13-30. https://doi.org/10.1007/s11120-012-9729-6.

Solimeno, A., García, J., 2017. Microalgae-bacteria models evolution: From microalgae steady-state to integrated microalgae-bacteria wastewater treatment models - A comparative review. Science of the Total Environment, 607-608, 1136-1150. http://dx.doi.org/10.1016/j.scitotenv.2017.07.114

Sosik, H.M., Olson, R.J., 2007. Automated taxonomic classification of phytoplankton sampled with imaging-in-flow cytometry. Limnology and Oceanography: Methods 5, 204-2 ḣttps://doi.org/10.4319/lom.2007.5.204

Spanjers, H., Vanrolleghem, P.A., Olsson, G., Dold, P.L., 1998. Respirometry in control of the activated sludge process: Principles. Scientific and Technical Report No. 7, IAWQ, London, UK

Spanjers, H., Vanrolleghem, P.A., 2016. Respirometry. In: Experimental Methods In Wastewater Treatment. van Loosdrecht, M.C.M., Nielsen, P.H., Lopez-Vazquez, C.M., Brdjanovic, D. IWA Publishing, London, UK.

Staley, C., Sadowsky, M., 2018. Practical considerations for sampling and data analysis in contemporary metagenomics-based environmental studies. Journal of Microbiological Methods 154, 14-18. https://doi.org/10.1016/j.mimet.2018.09.020

Steen, H.B., 2000. Flow cytometry of bacteria: glimpses from the past with a view to the future. Journal of Microbiological Methods 42, 65-74.https://doi.org/10.1016/S0167-7012(00)00177-9

Su, Y., Mennerich, A., Urban, B., 2011. Municipal wastewater treatment and biomass accumulation with a wastewater-born and settleable algal-bacterial culture. Water Research 45, 3351-3358. http://dx.doi.org/10.1016/j.watres.2011.03.046

Su, Y., Mennerich, A., Urban, B., 2012. Synergistic cooperation between wastewater-born algae and activated sludge for wastewater treatment: Influence of algae and sludge inoculation ratios. Bioresource Technology 150, 67-73. http://dx.doi.org/10.1016/j.biortech.2011.11.113

Subashchandrabose, S.R., Ramakrishnan, B., Megharaj, M., Venkateswarlu, K., Naidu, R., 2011. Consortia of cyanobacteria/microalgae and bacteria: Biotechnological potential. Biotechnology Advances 29, 896-907. https://doi.org/10.1016/j.biotechadv.2011.07.009

Suganya, T., Varman, M., Masjuki, H.H., Renganathan, S., 2016. Macroalgae and microalgae as a potential source for commercial applications along with biofuels production: A biorefinery approach. Renewable and Sustainable Energy Reviews 55, 909-941. http://dx.doi.org/10.1016/j.rser.2015.11.

026

Sullivan, A., Thomson, E.S., Stowe, E.L., 2018. Genomic and Physiological Analysis of a Novel Cyanobacterium, Pseudanabaena Strain Sr411, Isolated From the Susquehanna River. 13th Annual Susquehanna River Symposium "Science, Conservation, and Heritage" , 26-27th October 2018, Lewisburg (USA).

Sun, L., Zuo, W., Tian, Y., Zhang, J., Liu, J., Sun N., Li, J., 2019. Performance and microbial community analysis of an algal-activated sludge symbiotic system: Effect of activated sludge concentration. Journal of Environmental Sciences 76, 121-132. https://doi.org/10.1016/j.jes.2018.04.010

Sun, Y., Lu, M., Sun, Y., Chen, Z., Duan, H., Liu, D., 2019. Application and Evaluation of Energy Conservation Technologies in Wastewater Treatment Plants. Applied Sciences 9, 4501. https://doi.org/10.3390/app9214501

Sutherland, D.L., Turnbull, M.H., Broady, P.A., Craggs, R.J., 2014. Effects of two different nutrient loads on microalgal production, nutrient removal and photosynthetic efficiency in pilot-scale wastewater high rate algal ponds. Water Research 66, 53-62. https://doi.org/10.1016/j.watres.2014.08.010

Takenaka, R., Aoi, Y., Ozaki, N., Ohashi, A., Kindaichi, T., 2018. Specificities and Efficiencies of Primers Targeting Candidatus Phylum Saccharibacteria in Activated Sludge. Materials 11, 1129. https://doi.org/10.3390/ma11071129

Tang, B., Chen, Q., Bin, L., Huang, S., Zhang, W., Fu, F., Li, P., 2018. Insight into the microbial community and its succession of a coupling anaerobic-aerobic biofilm on semi-suspended bio-carriers. Bioresource Technology 247, 591-598. https://doi.org/10.1016/j.biortech.2017.09.147

Tang, T., Fadaei, H., Hu, Z., 2014. Rapid evaluation of algal and cyanobacterial activities through specific oxygen production rate measurement. Ecological Engineering 73, 439-445. http://dx.doi.org/10.1016/j.ecoleng.2014.09.095

Tanwar, P., Nandy, T., Ukey, P., Manekar, P., 2008. Correlating on-line monitoring parameters, pH, DO and ORP with nutrient removal in an intermittent cyclic process bioreactor system. Bioresource Technology 99, 7630-7635. http://dx.doi.org/10.1016/j.biortech.2008.02.004

Tchobanoglous, G., Burton, F.L., Stensel, H.D., 2003. Wastewater engineering: treatment and reuse. 4th ed., McGraw-Hill Metcalf and Eddy Inc., Boston.

Ting, H., Haifeng, L., Shanshan, M., Zhang, Y., Zhidan, L., Na, D., 2017. Progress in microalgae cultivation photobioreactors and applications in wastewater treatment: a review. International Journal of Agricultural and biological engineering 10, 1-29. http://dx.doi.org/10.3965/j.ijabe.20171001.2705

Tiron, O., Bumbac, C., Patroescu, I.V., Badescu, V.R., Postolache, C., 2015. Granular activated algae for wastewater treatment. Water Science and Technology 71, 832-839. http://dx.doi.org/10.2166/wst.2015.010

Tracy, B.P., Gaida, S.M., Papoutsakis, E.T., 2010. Flow cytometry for bacteria: enabling metabolic engineering, synthetic biology and the elucidation of complex phenotypes. Current Opinion in Biotechnology 21, 85-99. https://doi.org/10.1016/j.copbio.2010.02.006

Truong, D.T., Franzosa, E.A., Tickle, T.L., Scholz, M., Weingart, G., Pasolli, E., Tett, A., Huttenhower, C., Segata, N., 2015. MetaPhlAn2 for enhanced metagenomic taxonomic profiling. Nature Methods 12, 902-903. https://doi.org/10.1038/nmeth.3589

Tsioptsias, C., Lionta, G., Deligiannis, A., Samaras, P., 2016. Enhancement of the performance of a combined microalgae-activated sludge system for the treatment of high strength molasses wastewater. Journal of Environmental Management 183, 126-132. https://doi.org/10.1016/j.jenvman.2016.08.067

Udaiyappan , A.F.M., Hassan, H.A., Takriff, M.S., Abdullah, S.R.S., 2017. A review of the potentials, challenges and current status of microalgae biomass

applications in industrial wastewater treatment. Journal of Water Process Engineering 20, 8-21. https://doi.org/10.1016/j.jwpe.2017.09.006

Unnithan, V.V., Unc, A., Smith, G.B., 2014. Mini-review: a priori considerations for bacteria-algae interactions in algal biofuel systems receiving municipal wastewaters. Algal Research 4, 35-40. https://doi.org/10.1016/j.algal.2013.11.009

Valigore, J.M., Gostomski, P.A., Wareham, D.G., O'Sullivan, A.D., 2012. Effects of hydraulic and solids retention times on productivity and settleability of microbial (microalgal-bacterial) biomass grown on primary treated wastewater as a biofuel feedstock. Water Research 46, 2957-2964. https://doi.org/10.1016/j.watres.2012.03.023

Van Den Hende, S., Vervaeren, H., Saveyn,H., Maes, G., Boon, N., 2011. Microalgal bacterial floc properties are improved by a balanced inorganic/organic carbon ratio. Biotechnology and Bioengineering 108, 549-558. https://doi.org/10.1002/bit.22985

Van Den Hende, S., Carré, E., Cocaud, E., Beelen, V., Boon, N., Vervaeren, H., 2014. Treatment of industrial wastewaters by microalgal bacterial flocs in sequencing batch reactors. Bioresource Technology 161, 245-254. http://dx.doi.org/10.1016/j.biortech.2014.03.057

Van Den Hende, S., Beelen, V., Julien, L., Lefoulon, A., Vanhoucke, T., Coolsaet, C., Sonnenholzner, S., Vervaeren, H., Rousseau, D.P.L., 2016. Technical potential of microalgal bacterial floc raceway ponds treating food-industry effluents while producing microalgal bacterial biomass: An outdoor pilot-scale study. Bioresource Technology 218, 969-979. https://doi.org/10.1016/j.biortech.2016.07.065

Van Den Hende, S., Rodrigues, A., Hamaekers, H., Sonnenholzner, S., Vervaeren, H., Boon, N., 2017. Microalgal bacterial flocs treating paper mill effluent: A sunlight-based approach for removing carbon, nitrogen, phosphorus, and calcium. New Biotechnology 39, 1-10.http://dx.doi.org/10.1016/j.

nbt.2017.03.004

Vanrolleghem, P.A., Spanjers, H., Petersen, B., Ginestet, P., Takacs, I., 1999. Estimating (combinations of) activated sludge Model No.1 parameters and components by respirometry. Water Science and Technology 39, 195-214. https://doi.org/10.2166/wst.1999.0042

Vargas, G., Donoso-Bravo, A., Vergara, C., Ruiz-Filippi, G., 2016. Assessment of microalgae and nitrifiers activity in a consortium in a continuous operation and the effect of oxygen depletion. Electronic Journal of Biotechnology 23, 63-68.https://doi.org/10.1016/j.ejbt.2016.08.002

Vasseur, C., Bougaran, G., Garnier, M., Hamelin, J., Leboulanger, C., Le Chevanton, M., Mostajir,B., Sialve, B., Steyer, J.P., Fouilland, E., 2012. Carbon conversion efficiency and population dynamics of a marine algae-bacteria consortium growing on simplified synthetic digestate: First step in a bioprocess coupling algal production and anaerobic digestion. Bioresource Technology 119, 79-87. https://doi.org/10.1016/j.biortech.2012.05.128

Vergara, C., Muñoz, R., Campos, J.L., Seeger, M., Jeison, D., 2016. Influence of light intensity on bacterial nitrifying activity in algal bacterial photobioreactors and its implications for microalgae-based wastewater treatment. International Biodeterioration and Biodegradation 114, 116-121. https://doi.org/10.1016/j.ibiod.2016.06.006

Vo, H.N.P., Ngo, H.H., Guo, W., Nguyen, T.M.H., Liu, Y., Liu, Y., Nguyen, D.D., Chang, S.W., 2019. A critical review on designs and applications of microalgae-based photobioreactors for pollutants treatment Science of the Total Environment 651, 1549-1568. https://doi.org/10.1016/j.scitotenv.2018.09.282

Vollertsen, J., Jahn, A., Nielsen, J.L., Hvitved-Jacobsen, T., Nielsen P.H., 2001. Comparison of methods for determination of microbial biomass in wastewater. Water Research 35, 1649-1658. https://doi.org/10.1016/S0043-1354(00)00450-4

Vu, L., Loh, K., 2016. Symbiotic hollow fiber membrane photobioreactor for microalgal growth and bacterial wastewater treatment. Bioresource Technology 219, 261-269. http://dx.doi.org/10.1016/j.biortech.2016.07.105

Vulsteke, E., Van Den Hende, S., Bourez, L., Capoen, H., Rousseau, D.P.L., Albrecht, J., 2017. Economic feasibility of microalgal bacterial floc production for wastewater treatment and biomass valorization: A detailed up-to-dateanalysis of up-scaled pilot results. Bioresource Technology 224, 118-129. http://dx.doi.org/10.1016/j.biortech.2016.11.090

Wagner, D., Valverde-Perez, B., Sæbø, M., de la Sotilla, M., Van Wagenen, J., Smets, B.F., Plosz, B., 2016. Towards a consensus-based biokinetic model for green microalgae - The ASM-A. Water Research 103, 485-499. http://dx.doi.org/10.1016/j.watres.2016.07.026.

Wang, M., Yang, H., Ergas, S.J., van der Steen, P., 2015. A novel shortcut nitrogen removal process using an algal-bacterial consortium in a photo-sequencing batch reactor (PSBR). Water Research 87, 38-48. http://dx.doi.org/10.1016/j.watres.2015.09.016

Wang, L., Liu, J., Zhao, Q., Wei, W., Sun, Y., 2016. Comparative study of wastewater treatment and nutrient recycle via activated sludge, microalgae and combination systems. Bioresource Technology 211, 1-5. http://dx.doi.org/10.1016/j.biortech.2016.03.048

Wang, Y., Ho, S., Cheng, C., Guo, W., Nagarajan, D., Ren, N., Lee, D., Chang, J., 2016. Perspectives on the feasibility of using microalgae for industrial wastewater treatment. Bioresource Technology 222, 485-497. http://dx.doi.org/10.1016/j.biortech.2016.09.106

Wang, M., Keeley, R., Zalivina, N., Halfhide, T., Scott, K., Zhang, Q., van der Steen, P., Ergas, S.J., 2018. Advances in algal-prokaryotic wastewater treatment: a review of nitrogen transformations, reactor configurations and molecular tools. Journal of Environmental Management 217, 845-57. https://doi.org/10.

1016/j.jenvman.2018.04.021

Wanner, J., Grau, P., 1989. Identification of filamentous microorganisms from activated sludge: A compromise between wishes, needs and possibilities. Water Research 23, 883-891. https://doi.org/10.1016/0043-1354(89)90013-4

WRF, EPRI, 2013. Electricity Use and Management in the Municipal Water Supply and Wastewater Industries. Water Research Foundation (WRF), Electric Power Research Institute (EPRI).

Wu, L., Ning, D., Zhang, B., Li, Y., Zhang, P., Shan, X., Zhang, Q., Brown, M.R., Li, Z., Van Nostrand, J.D., Ling, F., Xiao, N., Zhang, Y., Vierheilig, J., Wells, G.F., Yang, Y., Deng, Y., Tu, Q., Wang, A., Global Water Microbiome Consortium, Zhang, T., He, Z., Keller, J., Nielsen, P.H., Alvarez, P.J.J., Criddle, C.S., Wagner, M., Tiedje, J.M., He, Q., Curtis, T.P., Stahl, D.A., Alvarez-Cohen, L., Rittmann, B.E., Wen, X., Zhou, J., 2019. Global diversity and biogeography of bacterial communities in wastewater treatment plants. Nature Microbiology 4, 1183-1195. https://doi.org/10.1038/s41564-019-0426-5

Xie, X., Huang, A., Gu, W., Zang, Z., Pan, G., Gao, S., He, L., Zhang, B., Niu, J., Lin, A., Wang, G., 2016. Photorespiration participates in the assimilation of acetate in Chlorella sorokiniana under high light. New Phytologist 209, 987-998, https://doi.org/10.1111/nph.13659

Xu, L., Weathers, P.J., Xiong, X.R., Liu, C.Z., 2009. Microalgal bioreactors: Challenges and opportunities. Engineering in Life Sciences 9, 178-189. https://doi.org/10.1002/elsc.200800111

Xu, S., Yao, J., Ainiwaer, M., Hong, Y., Zhang, Y., 2018. Analysis of Bacterial Community Structure of Activated Sludge from Wastewater Treatment Plants in Winter. Biomed Research International 2018, 8278970. https://doi.org/10.1155/2018/8278970

Xue, J., Schmitz, B.W., Caton, K., Zhang, B., Zabaleta, J., Garai, J., Taylor, C.M., Romanchishina, T., Gerba, C.P., Pepper, I.L., Sherchan, S.P., 2019. Assessing the

spatial and temporal variability of bacterial communities in two Bardenpho wastewater treatment systems via Illumina MiSeq sequencing. Science of Total Environment 657, 1543-1552. https://doi.org/10.1016/j.scitotenv.2018.12.141

Ye, J., Liang, J., Wang, L., Markou, G., 2018a. The mechanism of enhanced wastewater nitrogen removal by photo-sequencing batch reactors based on comprehensive analysis of system dynamics within a cycle. Bioresource Technology 260, 256-263. https://doi.org/10.1016/j.biortech.2018.03.132

Ye, J., Liang, J., Wang, L., Markou, G., Jia, Q., 2018b. Operation optimization of a photo-sequencing batch reactor for wastewater treatment: Study on influencing factors and impact on symbiotic microbial ecology. Bioresource Technology 252, 7-13. https://doi.org/10.1016/j.biortech.2017.12.086

Ye, L., Zhang, T., 2013. Bacterial communities in different sections of a municipal wastewater treatment plant revealed by 16S rDNA 454 pyrosequencing. Applied Microbiology and Biotechnology 97, 2681-2690. https://doi.org/10.1007/s00253-012-4082-4

Yentsch, C.S., Yentsch, C.M., 2008. Single cell analysis in biological oceanography and its evolutionary implications. Journal of Plankton Research 30, 107-117. https://doi.org/10.1093/plankt/fbm092

Zanetti, L., Frison, N., Nota, E., Tomizioli, M., Bolzonella, D., Fatone, F., 2012. Progress in real-time control applied to biological nitrogen removal from wastewater. A short-review. Desalination 286, 1-7. http://dx.doi.org/10.1016/j.desal.2011.11.056

Zeng, Y., Koblížek, M., 2017. Phototrophic Gemmatimonadetes: A New Purple Branch on the Bacterial Tree of Life, in: Hallenbeck, P.C. (Ed.), Modern Topics in the Phototrophic Prokaryotes: Environmental and Applied Aspects. Springer International Publishing, Cham, Switzerland. pp. 163-192.

Zhang, B., Xu, X., Zhu, L., 2017. Structure and function of the microbial

consortia of activated sludge in typical municipal wastewater treatment plants in winter. Scientific Reports 7, 17930. https://doi.org/10.1038/s41598-017-17743-x

Zhang, B., Xu, X., Zhu, L., 2018. Activated sludge bacterial communities of typical wastewater treatment plants: distinct genera identification and metabolic potential differential analysis. AMB Express 8, 184. https://doi.org/10.1186/s13568-018-0714-0

Zhang, Q.H., Yang, W.N., Ngo, H.H., Guo, W.S., Jin, P.K., Mawuli Dzakpasu, Yang S.J., Wang, Q., Wang, X.C., Ao, D., 2016. Current status of urban wastewater treatment plants in China. Environment International 92-93, 11-22. https://doi.org/10.1016/j.envint.2016.03.024

Zhang, Y., Su, H., Zhong, Y., Zhang, C., Shen, Z., Sang, W., Yan, G., Zhou, X., 2012. The effect of bacterial contamination on the heterotrophic cultivation of Chlorella pyrenoidosa in wastewater from the production of soybean products. Water Research 46, 5509-5516. http://dx.doi.org/10.1016/j.watres.2012.07.025

Zhang, T., Shao, M.F., Ye, L., 2012. 454 Pyrosequencing reveals bacterial diversity of activated sludge from 14 sewage treatment plants. ISME Journal 6, 1137-1147. https://doi.org/10.1038/ismej.2011.188

Ziglio, G., Andreottola, G., Foladori, P., Ragazzi, M., 2001. Experimental validation of a single-OUR method for wastewater RBCOD characterisation. Water Science and Technology 43, 119-126. https://doi.org/10.2166/wst.2001.0674

RESEARCH OUTPUTS AND RELEVANT WORKS

Papers in peer-reviewed journals

- Foladori, P., Petrini, S., Andreottola, G., 2018. *Evolution of real municipal wastewater treatment in photobioreactors and microalgae-bacteria consortia using real-time parameters.* Chemical Engineering Journal 345, 507-516. https://doi.org/10.1016/j.cej.2018.03.178;
- Foladori, P., Petrini, S., Nessenzia, M., Andreottola, G., 2018. *Enhanced nitrogen removal and energy saving in a microalgal-bacterial consortium treating real municipal wastewater.* Water Science and Technology 78, 174-182. https://doi.org/10.2166/wst.2018.094;
- Petrini, S., Foladori, P., Andreottola, G., 2018. *Lab-scale investigation on the role of microalgae towards a sustainable treatment of real municipal wastewater.* Water science and technology 78, 1726-1732. https://doi.org/10.2166/wst.2018.453;
- Foladori, P., Petrini, S., Andreottola, G., 2020. *How suspended solids concentration affects nitrification rate in microalgal-bacterial photobioreactors without external aeration.* Heliyon 6, e03088. https://doi.org/10.1016/j.heliyon.2019.e03088;
- Petrini, S., Foladori, P., Beghini, F., Armanini, F., Segata, N., Andreottola, G., 2020. *How inoculation affects the development and the performances of microalgal-bacterial consortia treating real municipal wastewater.* Journal of Environmental Management 263, 110427. https://doi.org/10.1016/j.jenvman.2020.110427;

Submitted:

- Petrini, S., Foladori, P., Donati, L., Andreottola, G. *Comprehensive respirometric approach to assess photosynthetic, heterotrophic and nitrifying*

activity in microalgal-bacterial consortia treating real municipal wastewater. Biochemical Engineering Journal, **under review**;

- Foladori, P., Petrini, S., Bruni, L., Andreottola, G. *Bacteria and photosynthetic cells in a photobioreactor treating real municipal wastewater: analysis and quantification using flow cytometry*. Algal Research, **under review**;
- Petrini, S., Foladori P., Bruni, L., Andreottola G. *The role of initial microalgal inoculation on the start-up of photobioreactors treating real wastewater, and its outcome in the long term: A flow cytometry investigation.* Bioresource Technology Reports, **under review**;

Oral presentations

- Petrini, S., Foladori, P., 2017. *Microalgae: A way towards a sustainable wastewater treatment. What about micropollutant removal?* International and Interdisciplinary Euregio Conference "Water as natural resource in a changing environment: quality, threats and sustainable use", Free University of Bozen, Bozen (Italy), 12 December 2017;
- Petrini, S., Foladori, P., 2018. *Microalgae as a key factor for a sustainable treatment of real municipal wastewater*. 10th Eastern European Young Water Professionals Conference, Zagreb (Croatia), 7-12 May 2018.

Proceedings

- Petrini, S., Foladori, P., Bruni, L., 2017. *Shifting of a microalgae-bacteria consortium during the treatment of real municipal wastewater in a photobioreactor*. XXXV Conferenza nazionale di citometria, Paestum (Italy), 3-6 October 2017;
- Petrini, S., Foladori, P., 2018. *Microalgae as a key factor for a sustainable treatment of real municipal wastewater*. Full-paper for the 10th Eastern European Young Water Professionals Conference, Zagreb (Croatia), 7-12 May 2018.

Posters

- Petrini, S., 2017. *Depurazione o biorefinery?* Poster presented at Place-

ment Day 2017 of the Department of Civil, Environmental and Mechanical Engineering of the University of Trento, Trento (Italy), 03 March 2017;

- Petrini, S., Foladori, P., Armanini, F., Beghini, F., Segata, N., Andreottola, G., 2019. *Nutrient removal and microbial community analysis of a stable microalgal-bacterial consortium treating real municipal wastewater*. Poster presented at the 16th IWA Leading Edge Conference on Water and Wastewater Technologies, Edinburgh (UK), 10-14 June 2019;
- Petrini, S., Foladori, P., Bruni, L., Andreottola, G., 2019. *Performances and microbial evolution in a microalgal-bacterial consortium treating real municipal wastewater*. Poster presented at the IWA Conference on Algal Technologies and Stabilization Ponds for Wastewater Treatment and Resource Recovery (IWAlgae2019), Valladolid (Spain), 1-2 July 2019;
- Petrini, S., Foladori, P., Andreottola, G., 2019. *Enhanced monitoring of a microalgal-bacteria consortium treating real wastewater: respirometry and kinetics*. Poster presented at the IWA Conference on Algal Technologies and Stabilization Ponds for Wastewater Treatment and Resource Recovery (IWAlgae2019), Valladolid (Spain), 1-2 July 2019.

Co-supervisor of Master thesis

- Pacini Andrea, A.Y. 2015-2016. Improving the efficiency of a microalgal-bacterial consortium for municipal wastewater treatment (Original title: Efficientamento di un consorzio di microalghe e batteri nel trattamento dei reflui civili). Supervisor: Prof. Foladori Paola;
- Gallerani Giorgio, A.Y. 2016-2017. Removal of pharmaceuticals from wastewaters: biological treatments with low energy consumption and environmental impact (Original title: Rimozione di farmaci dai reflui: trattamenti biologici a basso consumo energetico ed impatto ambientale). Supervisor: Prof. Foladori Paola;
- Nessenzia Mirco, A.Y. 2016-2017. Combination of bacteria and microalgae for wastewater treatment with low energy consumption (Orginal title: Combinazione di batteri e microalghe per la depurazione dei reflui urbani a bassa energia). Supervisor: Prof. Foladori Paola;

- Carlini Giorgia, A.Y. 2017-2018. Modeling of a photobioreactor for wastewater treatment (Original title: Modellazione di un fotobioreattore per il trattamento delle acque reflue). Supervisor: Prof. Foladori Paola;
- Donati Lorenza, A.Y. 2017-2018. Application of respirometry for the kinetic characterization of photobioreactors (Original title: Applicazione della respirometria per la caratterizzazione cinetica dei fotobioreattori). Supervisor: Prof. Foladori Paola;
- Notaro Silvia, A.Y. 2017-2018. Development of a microbial fuel cell with porous anode and cathode with oxygenic biomass (Original title: Sviluppo di una microbial fuel cell con anodo poroso e catodo a biomassa ossigenica). Supervisors: Prof. Foladori Paola and Prof. Della Volpe Claudio;
- Zambonardi Alberto, A.Y. 2017-2018. Optimization of a lab-scale photobioreactor for wastewater treatment (Original title: Ottimizzazione di un fotobioreattore a scala di laboratorio per il trattamento di acque reflue). Supervisor: Prof. Foladori Paola;
- Ferrari Alberto, A.Y. 2018-2019. Wastewater tretment and electrical parameters of an "algal microbial fuel cell" (Original title: Trattamento di acque reflue e parametri elettrici in una "algal microbial fuel cell"). Supervisors: Prof. Foladori Paola and Prof. Della Volpe Claudio;
- Ferraro Alessandro, A.Y. 2018-2019. Investigation on the maximum performance of a photobioreactor treating wastewater (Original title: Indagine sulle prestazioni massime di un fotobioreattore per il trattamento di acque reflue). Supervisor: Prof. Foladori Paola.

In progress:

- Gallina Umberto. Respirometric investigation on microalgal-bacterial consortia treating wastewater (Original title: Indagini respirometriche su consorzi di batteri e microalghe per la depurazione dei reflui). Supervisor: Prof. Foladori Paola.

ACKNOWLEDGEMENTS

I wish to show my gratitude to my supervisors, Prof. Foladori and Prof. Andreottola for providing guidance and feedback throughout this project.

I would like to thank Prof. Molina-Grima and Prof. Ergas for reviewing my Thesis and for their comments and suggestions.

I would also like to extend my thanks to Roberta for her generous support (beyond the technical one!). I cannot forget to thank Laura, not only for her help in doing the biological analysis (microscopic observations were each time a surprise!) but also for her encouragement (You and Carla were my supportive club!).

I would like to acknowledge Prof. Claudio Della Volpe for his warm encouragement and his esteem for me.

Thanks to Giulia who was very supportive and helped in analyzing the metagenomics analysis (it was a pleasure to work in team with you).

I would like to recognize and acknowledge the precious contribution of the master students that I had the chance to work with (except the proofreading of your thesis!).

A warm thank to my "PhD colleagues" of XXXII cycle (Marina first of all and Mich, Ale and Andrea) for sharing the hard times (Sari!!!) and the moments of fun (ufficio pause in memoriam). Thanks to the lunch club at 13.00 o' clock (or at 12.30, if someone was starving!).

Thanks to my friends, the "Trento" friends and the longtime friends (gli amici del paesello!).

My biggest thanks to my family for all the support you have shown me throughout these years (even if you still do not completely understand what I was doing!).

Last but not least, I wish to acknowledge the great love of Lorenzo who has been extraordinarily tolerant and supportive. You kept me going on. This work would not have been possible without your presence.

High costs for aeration, greenhouse-gas emissions and excess sludge disposal have entailed a paradigm shift in the wastewater treatment. Microalgal-bacterial-based wastewater treatments have gained increasing attention because of their potential in energy demand reduction and biomass resource recovery. In particular, photosynthetic oxygenation is combined with bacterial activity to treat wastewater avoiding external artificial aeration. To optimize the technology in order to become more competitive than activated sludge, an in-depth investigation about the treatment performance and the microbiology interactions under real operational condition is needed.

This work focused on the study of wastewater-borne microalgal-bacterial consortia treating real municipal wastewater. The main objectives were to: (i) Understand the removal mechanisms and the influence of operational conditions to optimize the process; (ii) Analyze the microbial community.

At first, a photo-sequencing batch reactor (PSBR), called Pilot, was started up and continuously monitored for two years to analyze the evolution of the treatment performance and of the biomass composition. At the same time, other two lab-scale PSBRs were installed to evaluate if microalgal inoculation is essential to start up a consortium. Samples of these consortia were collected over a period of one year and analyzed through microscopic observations, flow cytometry and metagenomics, to investigate the microbial structure and diversity.

A second part of the research focused on the optimization of the Pilot to explore its limit in view of the scale-up of the system. In addition, respirometry was adapted to test microalgal-bacterial consortia to estimate the removal kinetic parameters for future modelling.

The research project addressed many aspects and lay the foundation to apply a methodological research approach to scale-up this promising technology.

Serena Petrini is an Environmental Engineer. She was born on December 1991 in Jesi (Italy). She received her Batchelor degree in Civil and Environmental Engineering from Polytechnic University of Marche (Ancona) in 2013. She gained her Master degree in Environmental and Land Engineering form University of Trento in 2016.

In 2016, Serena Petrini started her PhD research at the University of Trento under the supervision of Prof. Dr. Eng. Gianni Andreottola and Prof. Dr. Eng. Paola Foladori, at the Department of Civil, Environmental and Mechanical Engineering. She worked in the Sanitary Engineering research group (LISA). Her principal research focused on wastewater treatment based on microalgal-bacterial consortia.